Energy Efficiency in Wireless Sensor Networks: Transmission Protocols and Performance Evaluation

Lakshmikanth Guntupalli

Energy Efficiency in Wireless Sensor Networks: Transmission Protocols and Performance Evaluation

Doctoral Dissertation for the Degree *Philosophiae Doctor (PhD)* at the Faculty of Engineering and Science, Specialisation in Information and Communication Technology

University of Agder
Faculty of Engineering and Science
2016

Doctoral Dissertation at the University of Agder 135
ISSN: 1504-9272
ISBN: 978-82-7117-828-4

Printed by Wittusen & Jensen
Oslo

Summary

Energy efficiency is one of the major goals for achieving green wireless communications. The recent growth in ubiquitous wireless connections and multimedia applications demands higher energy efficiency for wireless communications. As a part of this picture, wireless sensor networks (WSNs) need to be more energy efficient since the battery capacity of nodes in such networks is limited in the absence of energy harvesting sources.

In general, an energy efficient protocol should perform as few as possible operations when delivering user information successfully across the network. Energy efficient data transmission schemes could utilize network resources more effectively to lower down the energy consumption level. In this dissertation research, we focus on improving energy efficiency for data transmission and medium access control (MAC) protocols in WSNs. While energy consumption is inevitable for transmitting and receiving data in a WSN, the other typical and dominant energy consumption activities are idle listening, overhearing, and retransmissions due to unsuccessful transmission attempts. An energy efficient MAC protocol conserves energy by minimizing all these auxiliary operations in order to prolong network lifetime. On the other hand, balanced energy consumption among nodes which mitigates energy hole across a WSN also helps to extend network lifetime.

In this context, we propose two cooperative transmission (CT) based energy balancing MAC protocols for the purpose of WSN lifetime prolongation. The first one is an asynchronous cooperative transmission MAC protocol, in which nodes generate their own wakeup schedules based on their level number in a WSN topology. The second one is a receiver initiated cooperative transmission MAC protocol in which the CT is initiated by a relay node. It is demonstrated that both proposed CT MAC protocols are able to achieve significantly extended network lifetime.

In addition, an energy conserving sleeping mechanism for synchronous duty cycling MAC protocols is also proposed in this thesis. It is an event-triggered sleeping (ETS) mechanism, which triggers the sleep mode of a node based on the incoming traffic pattern to that node. The ETS mechanism eliminates overhearing in a WSN and achieves higher energy efficiency.

Furthermore, we apply packet aggregation at the MAC layer in WSNs

for achieving more energy efficient data transmission. In aggregated packet transmission (APT), multiple packets are transmitted as a batch in a frame within a single duty cycle instead of transmitting merely one packet per cycle. Numerical results demonstrate that APT achieves higher throughput and shorter delay, in addition to higher energy efficiency.

To evaluate the performance of the proposed MAC protocols and transmission schemes, we develop discrete time Markov chain (DTMC) models and verify them by comparing the results obtained from both analysis and discrete-event based simulations. The analytical and simulation results match precisely with each other, confirming the effectiveness of the proposed protocols and schemes as well as the accuracy of the developed models.

Preface

This dissertation is a result of the research work carried out at the Department of Information and Communication Technology (ICT), University of Agder (UiA), Campus Grimstad, Norway, from January 2012 to May 2016. My main supervisor has been Professor Frank Y. Li, University of Agder, and my co-supervisor has been Professor Jorge Martinez-Bauset, Universitat Politècnica de València (UPV). From March 2013 to June 2013, I visited the UPV, Spain as a research scholar, hosted by Professor Jorge Martinez-Bauset. From September 2013 to January 2014, I was a visiting researcher at Georgia Institute of Technology (GATECH), USA. My host professor at GATECH was Professor Mary Ann Weitnauer.

My visits to UPV and GATECH were coordinated or financed by the European Commission under the 7th Framework Program (FP7) through the Security, Services, Networking, and Performance of Next Generation IP-Based Multimedia Wireless Networks Project under Grant Agreement Number 247083.

Production note: LaTeX has been adopted as the tool for writing this dissertation, as well as the papers produced during my PhD study. The mathematical calculations and simulation results are obtained by using MATLAB and SMPL.

Acknowledgements

Foremost, I would like to express my profound gratitude to my main supervisor, Professor Frank Y. Li. Without his dedicated guidance and support, this dissertation would not have been possible. With his vision, enthusiasm, and responsibility to students, Dr. Li exemplifies to me how to behave as a researcher and a teacher. During these past four years, he has been an inspiring mentor, not only for my research but also for my personal development.

Heartfelt thanks to my co-supervisor Professor Jorge Martinez-Bauset for his insightful guidance and enormous help that led to fruitful research results. He hosted my research visit to UPV. He has been so hospitable to me, not only during but also far beyond my stay in Valenica. I am really grateful to both of my supervisors for their patience and consistent encouragement which guided me through the whole PhD study period. Special thanks to Professor Mary Ann Weitnauer for providing me an opportunity to visit GATECH which has been a lifetime learning experience for me. I greatly appreciate Dr. Weitnauer's invaluable comments and suggestions which improved the quality of my research work. I extend my thanks to other co-authors in my papers for their contributions.

The facilities provided by UiA helped me to conduct my research efficiently. I wish to thank Professors Frank Reichert and Andreas Prinz for their administrative support. I appreciate the assistance provided by the PhD coordinators at the Faculty of Engineering and Science, UiA, Mrs. Emma Elisabeth Horneman and Mrs. Tonje Sti.

I am grateful to Vimala Srinivas, one of my PhD fellow colleagues, and her family for their hospitality. They treated me like a family member. For sure it mitigated my homesickness. I would also like to thank my office-mates Indika Balapuwaduge, Mohammed Abomhara and Huihui Yang for their co-operation. I enjoyed very much working in this office. I appreciate all the

nice dinners we had at Abomhara's home along with technical, cultural, and political discussions. I am thankful to other PhD colleagues Parvaneh, Hossain and their families, Meisam, Mehdi, and friends Astri, Tomm Laurendz for their friendship and sociability.

Last but not least, I express my deep respect and intense gratitude to my parents for their love, blessings, understanding and moral support. I am also grateful to Venkata Narasimharao Yaramasu and Nitin Goel who motivated me to pursue a PhD degree.

Lakshmikanth Guntupalli
May 2016
Grimstad, Norway

Dedicated to my parents

Nageswara Rao and Mary

List of Publications

The author of this dissertation is the first author or a principal contributor of all the papers listed below. Papers A-E in the first set of the following list are selected to represent the main research achievements and are reproduced as Part II of this dissertation. Papers listed in the second set are complementary to the main focus.

Papers Included in the Dissertation

Paper A Lakshmikanth Guntupalli, Jian Lin, Mary Ann Weitnauer, and Frank Y. Li, "ACT-MAC: An Asynchronous Cooperative Transmission MAC Protocol for WSNs," *in Proc. IEEE International Conference on Communications (ICC) Workshop on Energy Efficiency in Wireless Networks and Wireless Networks for Energy Efficiency (E2Nets)*, Sydney, Australia, 10-14 June 2014.

Paper B Lakshmikanth Guntupalli, Frank Y. Li, and Jorge Martinez-Bauset, "Event-Triggered Sleeping for Synchronous DC MAC in WSNs: Mechanism and DTMC Modeling," *IEEE Global Communications Conference (GLOBECOM)*, Washington, DC, USA, 4-8 December 2016 (accepted).

Paper C Lakshmikanth Guntupalli, Jorge Martinez-Bauset, Frank Y. Li, and Mary Ann Weitnauer, "An Aggregated Packet Transmission in Duty-Cycled WSNs: Modeling and Performance Evaluation," *IEEE Transactions on Vehicular Technology*, Early access available in IEEE Xplore, March 2016, DOI:10.1109/TVT.2016.2536686.

Paper D Jorge Martinez-Bauset, Lakshmikanth Guntupalli, and Frank Y. Li, "Performance Analysis of Synchronous Duty-Cycled MAC Protocols," *IEEE Wireless Communications Letters (WCL)*, vol. 4, no. 5, pp 469-472, October 2015.

Paper E Lakshmikanth Guntupalli and Frank Y. Li, "DTMC Modeling for Performance Evaluation of DW-MAC in Wireless Sensor Networks," in Proc. *IEEE Wireless Communications and Networking Conference (WCNC)*, Doha, Qatar, 3-6 April 2016.

Other Papers

Paper F Lakshmikanth Guntupalli, Frank Y. Li, and Xiaohu Ge, "EECDC-MAC: An Energy Efficient Cooperative Duty Cycle MAC Protocol," in *Proc. IEEE/IFIP Wireless Days (WD)*, Dublin, Ireland, 21-23 November 2012.

Paper G Lakshmikanth Guntupalli, Jorge Martinez-Bauset, and Frank Y. Li, "Modeling Cooperative Transmission for Synchronous MAC Protocols in Duty-Cycled WSNs," *IEEE International Conference on Communications (ICC)*, Paris, France, 21-25 May 2017. To be submitted (A draft version is attached in Appendix A).

Paper H Lakshmikanth Guntupalli, Jorge Martinez-Bauset, and Frank Y. Li, "Performance of Duty-Cycled WSN with Aggregated Packet Transmission in Error-Prone Wireless Links". To be submitted to a journal (A draft version is attached in Appendix B).

Contents

List of Figures

List of Tables

Abbreviations

1D	One Dimensional
2D	Two Dimensional
3D	Three Dimensional
4D	Four Dimensional
3G	Third Generation
4G	Fourth Generation
5G	Fifth Generation
ACK	Acknowledgment
ACT-MAC	Asynchronous Cooperative Transmission MAC
AG-MAC	Aggregation MAC
APT	Aggregated Packet Transmission
BA	Beacon of Acknowledgment
BC	Beacon for Cooperation
BE	Beacon with Residual Energy Information
BU	Beacon with Prediction Update
CCT	Concurrent Cooperative Transmission
CDC-MAC	Cooperative Duty Cycling MAC
CN	Cooperating Node
CPT	Control Packet Triggered
CSMA/CA	Carrier Sense Multiple Access with Collision Avoidance
CT	Cooperative Transmission
CT-D	Cooperative Transmission Decision
CTMC	Continuous Time Markov Chain
CTS	Clear To Send
CW	Contention Window
D2D	Device-to-Device
DC	Duty Cycling

DCF	Distributed Coordination Function
DES	Discrete-Event Simulation
DIFS	DCF Inter Frame Space
DTMC	Discrete Time Markov Chain
DW-MAC	Demand Wakeup MAC
E-F	Error-Free
EH	Energy Harvesting
E-P	Error-Prone
ETS	Event-Triggered Sleeping
FER	Frame Error Rate
FIFO	First In First Out
IoT	Internet-of-Things
ICT	Information and Communications Technology
IP	Internet Protocol
JAM	Joint Aggregation and MAC
LBA	Lifetime Balanced Aggregation
LCG	Linear Congruential Generator
LMAC	Lightweight Medium Access
MAC	Medium Access Control
MPT	Multiple Packet Transmission
MRC	Maximum Ratio Combining
NCT	Non-CT
NS2	Network Simulator 2
OSC-MAC	On-demand Scheduling Cooperative MAC
PRS	Pseudo Random Sequence
PW-MAC	Predictive Wakeup MAC
REACT	Residual Energy Activated Cooperative Transmission
RICT-MAC	Receiver Initiated Cooperative Transmission MAC
RI-MAC	Receiver Initiated MAC
RLN	Relay Node
RN	Reference Node
RTS	Request To Send
SCP-MAC	Scheduled Channel Polling MAC
SCT-MAC	Scheduling Cooperative Transmission MAC
SPT	Single Packet Transmission

S-MAC	Sensor MAC
TDCT	Time Division Cooperative Transmission
TDMA	Time Division Multiple Access
TDMA-ASAP	TDMA Scheduling with Adaptive Slot-Stealing and Parallelism
TRAMA	Traffic-Adaptive Medium Access
WBAN	Wireless Body Area Network
Wi-Fi	Wireless Fidelity
WLAN	Wireless Local Area Network
WSN	Wireless Sensor Network
WuR	Wake-up Radio
X-MAC	Short Preamble MAC

Part I

Chapter 1

Introduction

In this chapter, the diversity of wireless communications is introduced and the importance of green communications is highlighted. The motivation of this dissertation work is presented along with the background information about the research topics. Furthermore, the objectives and methodologies are explained and how the dissertation is organized is also outlined.

1.1 Wireless Communications

Wireless communication technologies such as mobile, cellular, ad hoc and sensor networks have been widely deployed in diverse fields thanks to their access flexibility as well as ubiquitous computing and communication capability. Mobile networks provide easy channel access to terminals at various locations and speeds [1]. Today, mobile devices have become probably the most popular tools for information exchange among people as well as among machines or devices using e.g., third or fourth generation (3G or 4G) cellular networks, wireless fidelity (Wi-Fi) and Bluetooth. Fourth generation (4G) wireless cellular networks can support data rates of up to 1 Gbps with low mobility like nomadic/local wireless access, and up to 100 Mbps with high mobility such as mobile access on vehicles. The upcoming fifth generation (5G) network is expected to achieve 1000 times higher data rate than the system capacity of 4G [2]. In addition to voice traffic, the demand for rich multimedia services with faster Internet access via mobile phones is steadily increasing [3]. To meet the demand for wireless broadband connections in

4G/5G cellular networks, Device-to-Device (D2D) communication can serve as a *complementary* solution, and it may improve spectrum utilization efficiently [4]. By reusing the spectrum of cellular networks, two D2D users can form a direct data link over the licensed or unlicensed band without connecting via a base station and the core network [5].

In parallel to this trend, wireless sensor networks (WSNs) are being deployed for monitoring, detection and target tracking applications [6]. Similarly, wireless body area networks (WBANs) [7], which typically consist of a collection of low-power, miniaturized, lightweight devices with wireless communication capabilities operated in the proximity of a human body, are also emerging. These devices can be placed in, on, or around the body, and are often wireless sensor nodes that can monitor human body functions and the characteristics of the surrounding environment. Recently, the Internet-of-Things (IoT) through which a huge number of devices are connected via typically wireless sensors are gaining popularity for building smart cities, homes, transportation of goods, etc [8]. The WSN/IoT technology can play an essential role in other domains of our daily life as well, from healthcare, industrial automation, to emergency response to disasters, shopping, etc [9].

In brief, the wireless industry has experienced explosive growth during the past few decades and it continues to grow rapidly. Therefore, the rising energy concern due to the ubiquity of energy consuming wireless devices has ignited an acute interest in the development and deployment of energy efficient, eco-friendly wireless communication systems.

1.2 Green Wireless Communications

Climate change including global warming is imposing ecological as well as economical challenges around the globe. The effect of climate change is estimated as losing global gross domestic product by 5% in a year and this loss may raise to 20% in the future [10]. Moreover, the level of global green house gas emissions such as carbon dioxide (CO_2) is increasing every year [11]. The information and communications technology (ICT) sector has its share of $2 \sim 3\%$ in overall emissions [12]. Furthermore, it is predicted that this contribution can become 10% in $5 \sim 10$ years [13] and that the footprint

will be almost doubled from 2007 to 2020 [10]. As a part of the ICT industry, wireless and mobile communications also have their role in this process. It is estimated that the energy consumed by various wireless networks and devices such as cellular, Wi-Fi, ad hoc and sensor networks, will be increased by approximately 20% per year [14].

On the other hand, green wireless communications focus on limiting the green house gas emissions by communication and networking technologies. In fact, green communication eliminated 376 million metric tons of carbon in 2008 and by 2013 it can reduce 1.2 billion metric tons [10]. Furthermore, it is estimated [10] that green ICT can achieve $23 \sim 30\%$ reduction of the current global emissions. Since ICT is well incorporated into other fields such as embedded and industrial control systems, greening through ICT is also expected to achieve 15% reduction of the total energy consumption by 2020 [15].

Therefore in this era represented by very high data rate and prodigious traffic demand, green wireless communication has become more popular and important than ever before. It has indeed become an essential requirement for the design of future wireless communications systems. The evolution of green wireless communications calls for a paradigm shift for system design across all protocol stack layers [16]. At any layer, a protocol can be made greener by minimizing the operations required to deliver information successfully in the network. A protocol could also be optimized so that it enhances the energy efficient operation of the network elements [17] in order to diminish the energy consumption level by a communication network [18]. In this dissertation research, we concentrate on energy efficiency at the medium access control (MAC) layer in WSNs.

1.3 Energy Consumption in WSNs

WSNs contain many small-size sensor nodes with limited processing power and battery capacity. Owing to the features such as portability, low-cost and ease of establishment, WSNs support many applications. In typical WSN applications, nodes sense data from a field under observation and transmit them to a sink via one or multiple hops. In a large-scale WSN, all nodes

may form a tree topology with the sink as the destination [19]. Then, the relay nodes forward data in a hop-by-hop fashion. The sink node sends the received information to a data collection center where the data is analyzed with respect to various parameters of interest. All nodes need to consume energy in order to perform data collection and transmission tasks. Eventually, all nodes deplete their batteries. Therefore, it is clear that the lifetime of a sensor node in a WSN depends on the capacity of its battery, as well as how energy is consumed [20]. However, without energy harvesting (EH) the battery capacity is fixed and limited. In some applications like hostile environment monitoring, replacing node batteries might not be feasible or is too costly [21]. Therefore, developing protocols for achieving energy efficiency is of high importance for the design of WSNs.

Generally, energy consumption activities are coordinated by MAC protocols [22]. Therefore, a MAC protocol plays a vital role for network lifetime prolongation. The primary energy consumption sources in a WSN are idle listening, overhearing, and retransmissions due to unsuccessful transmissions, in addition to data transmission and reception [23]. Among these activities, *Idle listening occurs in a network when a node does not have any packets to send or receive but it is still listening to channel*. However, the duration of this idle listening depends on the MAC protocol adopted. Similarly, *overhearing happens when a node receives a packet which is not destined to it*. Collision of packets also consumes extra energy since those lost packets need to be retransmitted. An energy efficient MAC protocol reduces redundant energy consumption by avoiding additional activities rather than information exchange.

1.4 Motivation and Research Questions

Energy efficiency in sensor networks can be achieved by two ways. First, by employing the protocols or algorithms which are designed with minimal operations in order to consume energy as low as possible. Second, by making energy consumption rates at different parts of the network balanced or almost balanced. Ideally, all nodes throughout the network should have almost the same lifetime. Otherwise some parts of the network may deplete

sooner than the others, making the network disconnected. If any critical parts of the network run out of battery earlier, it may lead to mal-function of the entire network, even though the other parts of the network still have a certain amount of residual energy.

As far as energy efficiency at the MAC layer for WSNs is concerned, duty cycling (DC) appears as a popular energy conserving mechanism by letting nodes sleep for a certain period of time in a duty cycle. However, there are still open issues towards the development of energy efficient MAC protocols in order to meet the requirements towards green wireless communications. In addition, emerging technologies and communication strategies pose new challenges in the design of MAC protocols. Motivated by the fact that the research at the MAC layer is one of the most important and active areas in the WSN research community, this PhD dissertation makes an effort to address some of these challenges. More specifically, this thesis addresses the following research questions.

- Question 1: In a WSN, balanced energy consumption is expected to be maintained so that nodes deplete their battery ideally at the same time. In that case, how can energy consumption at different nodes be balanced in order to prolong the network lifetime of a WSN?

- Question 2: DC does reduce energy consumption caused by idle listening. However, how to conserve energy consumption by mitigating other problems such as overhearing occurred at the MAC layer in DC MAC protocols?

- Question 3: Transmission of a packet *alone* consumes comparatively higher energy, due to the control overhead needed to transfer that single packet. Then, how can we improve energy efficiency for packet transmission with minimal overhead in MAC protocols?

- Question 4: How to develop accurate analytical models to analyze the performance of energy efficient MAC protocols and transmission schemes? Furthermore, how to verify the accuracy of the developed models?

1.5 Objectives and Methodologies

One major objective of green wireless communications is to achieve higher energy efficiency while maintaining the quality of other performance parameters. Although energy efficiency can be achieved by minimizing the activities performed across all layers, the scope of this dissertation is limited mainly to the MAC layer. Thus the primary goal of this dissertation is to propose protocols and mechanisms which can reduce energy consumption by addressing the above mentioned research questions and to assess their performance analytically and via simulations. More specifically,

- Aim 1: To develop a MAC protocol which mitigates energy hole in WSNs. To do so, an exploration of the reasons for occurring energy hole in a WSN is required. With that knowledge, a new method which can postpone the occurrence of an energy hole will be proposed.

- Aim 2: To develop an adaptive sleeping mechanism to avoid the occurrence of overhearing happened in MAC protocols. For achieving this goal, the knowledge on the pattern of the arriving traffic into a network is needed. Then, a protocol which allows nodes sleep earlier (or longer) according to the arriving rate of the incoming traffic would help.

- Aim 3: To develop a data transmission scheme with minimal overhead in MAC protocols. This transmission scheme should be more energy efficient and perform well with respect to the other performance metrics such as throughput and delay.

- Aim 4: To develop novel and accurate analytical models to analyze the performance of the proposed MAC protocols and transmission schemes. The accuracy of the developed models should also be verified.

The developed protocols and mechanisms are evaluated through both mathematical analysis and computer simulations. For mathematical analysis, discrete time Markov chain (DTMC) modeling is performed. For simulations, SMPL [24] , which is a *C* based discrete event simulator is adopted in this study. The performance metrics introduced to evaluate the performance of the designed mechanisms and protocols are energy consumption, lifetime, energy efficiency, throughput, delay, etc.

1.6 Thesis Organization

The dissertation is divided into two parts. Part I contains an overview of the work carried out throughout this PhD study and Part II includes a collection of five published or accepted papers, which are mentioned in the list of publications.

The rest of Part I is organized as follows.

- Chapter II presents different MAC mechanisms and introduces two novel cooperative transmission MAC protocols, one asynchronous and another receiver initiated for the purpose of energy hole mitigation. Furthermore it introduces briefly an adaptive traffic event-triggered sleeping (ETS) mechanism for synchronous DC MAC protocols.
- Chapter III introduces various data transmission schemes such as single packet transmission (SPT) and aggregated packet transmission (APT). Moreover, it categorizes different methods for packet aggregation.
- Chapter IV summarizes three categories of performance evaluation methods along with a comparison between the developed mathematical models and the existing ones.
- Chapter V concludes the dissertation and discusses potential future directions to continue the research work.

Chapter 2

Energy Efficient MAC Protocols

This chapter presents different categories of WSN MAC protocols and reviews the literature under each category. Furthermore, it explains the energy hole and overhearing problems in WSNs. The design of energy efficient MAC protocols for solving these problems in WSNs is also outlined.

2.1 Medium Access Control in WSNs

MAC provides rules for channel access by nodes covered in the same access network. This section provides an overview of existing MAC protocols for WSNs, categorized in Fig. 2.1. Briefly, existing MAC protocols can be classified mainly into two groups: contention-free and contention-based. Competition occurs for channel access among nodes following the same contention-based protocol. In contrast, in contention-free protocols, channel access by each node is dedicated and controlled by a central controller.

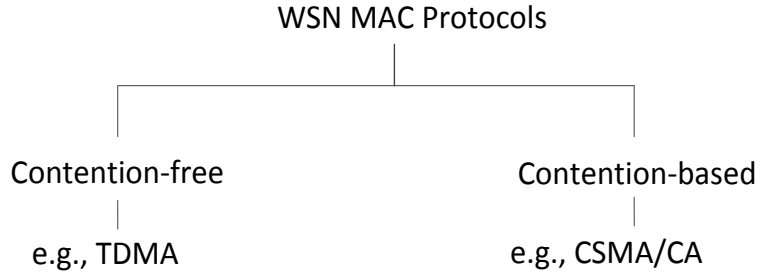

Figure 2.1: Classification of existing MAC protocols.

2.1.1 Contention-free MAC Protocols

Contention-free MAC protocols allocate medium resources such as time or frequency to a node without overlapping with other nodes'. Thus, contention and collisions are avoided. A popular category of contention-free MAC protocols is time division multiple access (TDMA). In TDMA MAC, the wireless medium is divided into many small time slots with fixed duration as shown in Fig. 2.2 and each slot is allocated to one station. In this figure, Slot 1 is dedicated to Node A, Slot 2 is reserved for Node C while Slot 3 is allocated to Node B. Consequently, zero collision probability is ensured and each node transmits user data in its corresponding slot. The benefits obtained from a TDMA MAC protocol are scheduled transmission and zero collisions. However, TDMA based protocols appear to be inefficient in case of bursty data traffic. For instance, since every slot is reserved exclusively to one node, other nodes are not allowed to access that slot. If the owner of the slot does not have any data packets to send, then the slot would be wasted. To avoid unnecessary energy consumption, a receiving node may turn off its radio when no transmission is detected at the starting instant of a slot. Another disadvantage of TDMA is that the coordination of slots requires precise synchronization among all nodes, which is difficult in WSNs. Consequently, the achieved throughput and energy efficiency could be lower along with longer delay. Examples of TDMA based protocols in WSNs include traffic-adaptive medium access protocol (TRAMA) [25], TDMA scheduling with adaptive slot-stealing and parallelism (TDMA-ASAP) [26], lightweight medium access protocol (LMAC) [27].

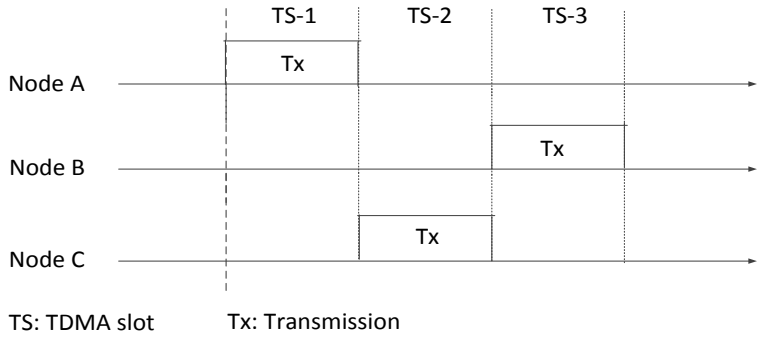

Figure 2.2: Operation of a TDMA-based MAC protocol with three slots.

2.1.2 Contention-based MAC Protocols

In contention-based MAC protocols, sensor nodes contend for medium access before data transmission. Typically, the carrier sense multiple access with collision avoidance (CSMA/CA) [28] mechanism is adopted in order to resolve contention in a WSN. The basic principle of CSMA/CA is illustrated in Fig. 2.3. When a node intends to transmit, it performs carrier sensing to check the availability of the medium. If it detects that the channel is idle and has been idle for distributed coordination function (DCF) inter frame space (DIFS), then the node can start its transmission by sending a request to send (RTS) packet after a random backoff time. A data packet is transmitted afterwards when a clear to send (CTS) packet from the intended receiver is received. For instance, Nodes A, B and C in Fig. 2.3 are competing for access and each node has chosen its backoff duration. As shown in the figure, Node A is the winner since it has taken the shortest backoff time and the other nodes have selected longer backoff times. Consequently, the medium is occupied by Node A. Note that a collision occurs when the smallest backoff time is selected by two or more nodes. In that case, packet transmission would be unsuccessful even if the channel is error-free.

CSMA/CA is designed to be simple and flexible and it does not require additional information from the rest of the network for transmitting data. The CSMA/CA based protocols and transmission schemes are popular in both academia and industries. Hence, the scope of this thesis work is bounded to contention-based MAC protocols.

Many contention-based MAC protocols have been proposed in the literature. However, which type suits better depends on the application scenario.

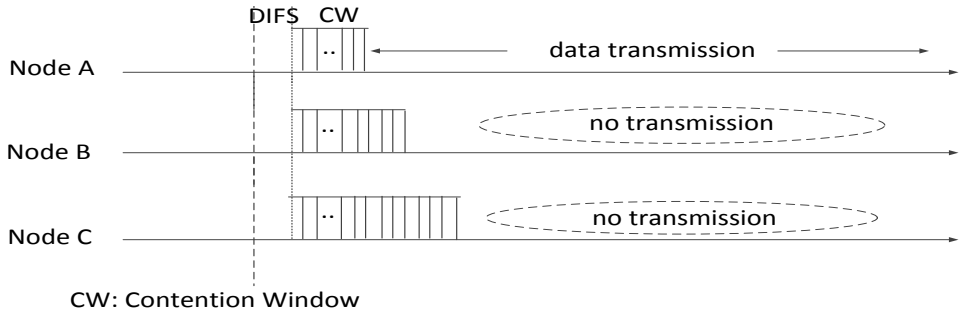

Figure 2.3: Operation of a contention-based MAC protocol with competition.

2.2 Duty Cycling MAC Protocols

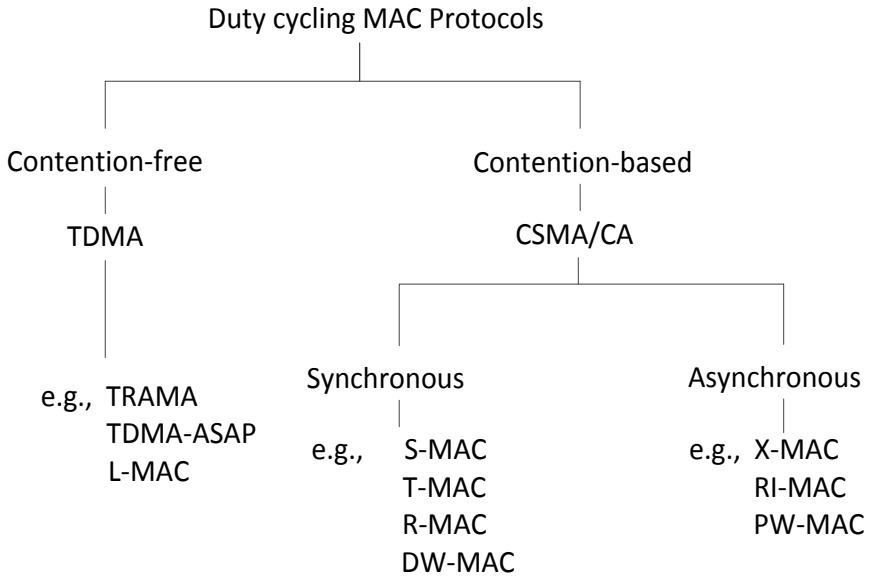

Figure 2.4: Classification of existing duty cycling MAC protocols.

Duty cycling [29] is introduced for the purpose of energy saving coordinated by a MAC protocol. Following DC, nodes are active for certain duration and in sleep in the remaining period of a duty cycle. In other words, a cycle contains an *active* period and a *sleep* period. In the *active* period, the radio transceiver of a node is *ON* and it may transmit and receive data, whereas in the *sleep* period it is *OFF* and no transmission can be performed. Therefore, by allowing nodes sleep, DC reduces idle listening and conserves energy. For that reason, DC is widely employed in WSN MAC protocols.

The contention-free and contention-based categories summarized in Sec.2.1 apply also to DC MAC protocols. Moreover, these protocols can be categorized based on the way how transmission opportunities are obtained and according to the sleep-awake schedules. In one category, the transmission opportunity is provided in a network by configuring a fixed time slot to each node. Accordingly, competition among nodes is avoided. This class of protocols belongs contention-free DC MAC protocols [21]. Another category is contention-based, meaning that competition among nodes is expected in order to obtain a transmission opportunity [21].

Furthermore, based on the sleep-awake schedules of nodes in a WSN, DC MAC protocols can also be classified into synchronous and asynchronous

protocols [22]. In synchronous MAC protocols, the wake-up schedules for all nodes in a WSN are synchronized, meaning that nodes wake up at the same time and compete for channel access, whereas the nodes in asynchronous MAC protocols follow their own schedules to wake up and sleep.

2.2.1 Synchronous MAC Protocols

Data exchange is possible only when both the transmitting and the receiving sensor nodes are awake at the same time. Therefore, in synchronous MAC protocols, all nodes synchronize their wake-up times with their neighboring nodes. This synchronization enables neighboring nodes to wake up at the scheduled time instant, as depicted in Fig. 2.5. Furthermore, periodic wake-up and sleep avoid idle listening and reduce energy consumption. In order to facilitate this synchronization, a part of the *active* period, which is referred to as a *sync* period, is allocated. The remaining part of an *active* period is referred to as the *data* period and it is used for data exchange. Thus, a cycle in synchronous MAC protocols is composed of a *sync*, a *data* and a *sleep* period consecutively, as shown in Fig. 2.5.

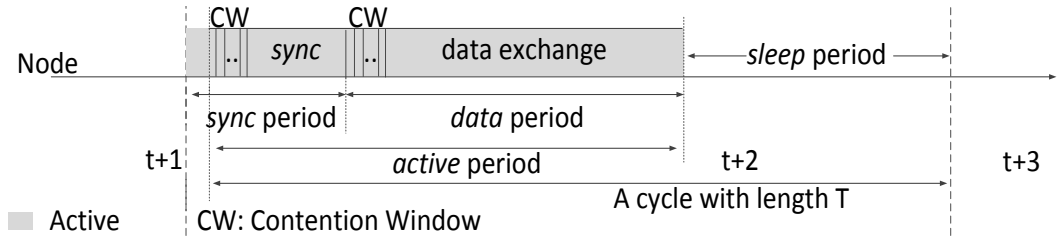

Figure 2.5: Duty cycle of a synchronous MAC protocol.

Note that the contention mechanism is performed before transmitting either *SYNC* or *DATA* packets. Among all contending nodes, the nodes that lost competition enter the *sleep* period *right after* hearing the data transmission initiation, whereas the winning node goes to sleep *after finishing* the transmission, as depicted in Fig. 2.6.

As illustrated in this figure, Nodes A, B and C are contending for channel access through selected backoff times. During Cycle t+2, Node A is the winner since it is *the only node that has selected the shortest backoff*, and it transmits its packet successfully. Generally, when multiple nodes compete with each other, the same backoff time could be selected by two or more

nodes. In Cycle t+3 Nodes A and B have picked the same smallest backoff time. Consequently a collision occurred and a transmission opportunity is wasted. Note that the backoff value chosen by Node C is larger. For next competition it has to *reset*[1] *its timer for the new cycle* after hearing a collision or a transmission. Similarly, all nodes follow the same process in forthcoming cycles as well. Sensor MAC (S-MAC) [23] and demand wakeup MAC (DW-MAC) [30] are two representative examples among many available synchronous DC MAC protocols.

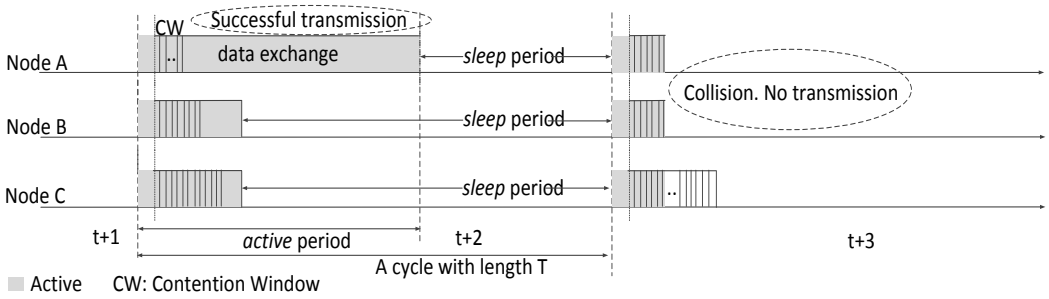

Figure 2.6: Operation of a contention-based MAC protocol with a synchronized wake-up schedule.

S-MAC is a synchronous protocol which introduces periodic listen and sleep periods to reduce idle listening. The length of the listening and sleeping duration is determined according to different application scenarios. All nodes are free to determine their own listen/sleep schedules. S-MAC adopts the RTS/CTS handshake to avoid collisions and overhearing. DW-MAC is another synchronous protocol in which the sending and receiving nodes agree to wake up at a specific time instant through the exchange of synchronization messages. However, a common drawback of S-MAC and DW-MAC is the need for synchronization and for the maintenance of multiple schedules.

2.2.2 Asynchronous MAC Protocols

In contrast, nodes in asynchronous MAC protocols do not need to synchronize with other nodes' wake-up schedules and each node follows its own schedule. However, to transmit *data* to the any other node, it is compulsory that the receiving node is also active at that time. Therefore, if a node has

[1] In contrast, the Wi-Fi nodes freeze their backoff timers in such a case and apply the exponential backoff algorithm in the next transmission contention if the current transmission fails.

packets to send, it wakes up and *has to keep awake* until the receiving node wakes up. When it knows that the receiver is ready to receive, it delivers the packet. Note that competition is required in case that two or more nodes have packets to transmit.

Figure 2.7 illustrates the duty cycle operation of an asynchronous MAC protocol. As shown in the figure, the sending node waits until the receiver wakes up to exchange *DATA*. In case that the receiver wakes up prior to the sender does, it can either wait until it detects the sender being awake or it goes to sleep after a predefined duration, as illustrated in Fig. 2.7. Which mode to adopt is completely dependent on the employed MAC handshake procedure. No matter which mode is employed, either the sender or the receiver needs to spend time for idle listening, leading to significant energy consumption. On the other hand, a benefit obtained by this category of MAC protocols is shorter delay. Popular asynchronous MAC protocols among the available ones are receiver initiated MAC (RI-MAC) [31] and predictive wakeup MAC (PW-MAC) [32].

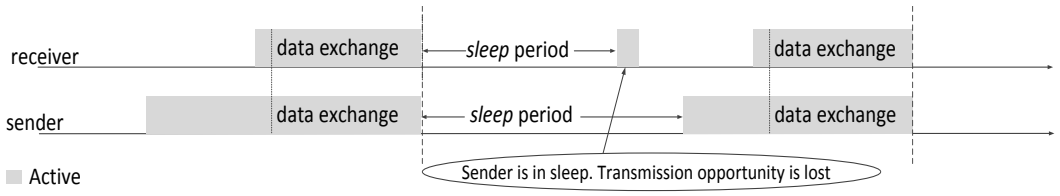

Figure 2.7: Duty cycle of an asynchronous MAC protocol.

RI-MAC is an asynchronous duty cycle MAC protocol in which the transmission is always initiated by a receiver. In RI-MAC, each node follows its own wake-up schedule. When the receiving node wakes up, it broadcasts a beacon to request for data transmission on the channel. The sending node sends the data after the beacon is received. Although RI-MAC could achieve high energy efficiency, a disadvantage is that the sender must keep awake until it receives a beacon from the receiver before transmission. On the other hand, if the sender does not wake up early enough, it loses the beacon. PW-MAC is another asynchronous duty cycle MAC protocol which introduces an independently generated pseudo-random sequence to control each node's wake-up times. In PW-MAC, a sender predicts the wake-up time of a receiver from the receiver's pseudo-random schedule generator. In a MAC protocol

with optimal energy efficiency, the sender and the receiver should wake up at the same time when there is a packet to send. They transfer a packet successfully, and both immediately go back to sleep right after transmission. PW-MAC achieves higher energy efficiency at both the receiver and the sender.

2.3 The Energy Hole Problem

In typical WSN applications, nodes sense data from the field of observation and transmit them towards a sink node. In such a WSN, nodes typically form a tree topology with the sink acting as the destination. Each source node collects data and sends it to the sink node via intermediate relaying nodes by packet forwarding. In this process, all the parent (intermediate) nodes in the direction towards the sink need to relay data received from their child (transmitting) nodes. In case that a parent node has multiple child nodes, it needs to forward more packets to the destination node. Consequently, this heavily burdened node consumes energy at a faster rate when compared with the other nodes in the network [33], as shown in Fig. 2.8. As a result, this node would be the first node in the network which depletes its battery. If the relay node is the closest node to the sink, for instance Node R in Fig. 2.8, then the network would be disconnected if this relay node is not functioning. This phenomenon is referred to as *the energy hole problem* in WSNs.

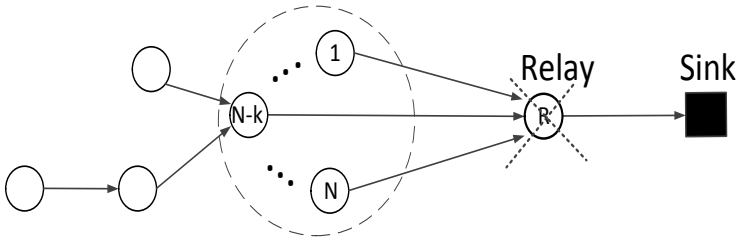

Figure 2.8: Energy hole illustration: R depletes earlier, leading to network disconnection.

2.3.1 Existing Energy Hole Mitigation Techniques

Cooperative transmission (CT) has been proven as an efficient technique to mitigate energy hole through energy balancing [34]. Combining CT and duty cycling can further enhance the longevity of a WSN. The residual energy

activated cooperative transmission (REACT) forwarding protocol proposed in [35] triggers a CT when a node on the primary route towards the sink has higher residual energy than the next-hop node (a parent node) along the route. A sending node and its cooperating neighboring nodes transmit the packet independently over the same wireless channel. A transmission by multiple nodes at the same time extends the transmission range [35]. As a result, a far away node can receive the packet with sufficient signal strength and decodes it properly. Consequently, the heavily burdened node, R, is protected, as illustrated in Fig. 2.9. Although [35] demonstrated that this approach exhibited significant benefit, it assumed a highly idealized MAC protocol and did not consider duty cycling. Existing MAC protocols which utilize the CT concept include scheduling cooperative MAC (SCT-MAC) [36], cooperative duty cycling MAC (CDC-MAC) [37] and on-demand scheduling cooperative MAC (OSC-MAC) [38].

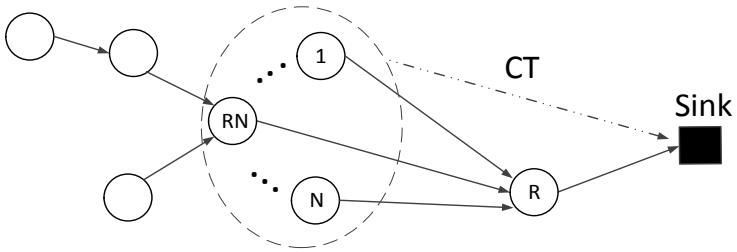

Figure 2.9: CT delivers a packet directly to a two-hop away node, hopping over R.

2.3.2 An Asynchronous CT MAC Protocol

Although existing MAC protocols in the literature are able to mitigate energy hole, there is still room for further energy reduction improvement and to prolong network lifetime. Paper A in Part II of the dissertation proposes an asynchronous CT MAC protocol, referred to as the ACT-MAC protocol, to address the same energy hole problem. It achieves longer lifetime than the existing protocols do.

The ACT-MAC protocol employs a pseudo-random number generator to produce the duration of a cycle. The considered WSN is divided into different levels and each level is assigned a number. The seed of this pseudo-random number generator is the level number of a node. Thus it is an asynchronous

CT MAC protocol. It is assumed that every node knows its number of level based on the network topology. Then, any node can initiate CT with its two-hop away parent node using the level-based wake-up schedules. It is demonstrated that ACT-MAC is able to extend network lifetime since it consumes lower energy by avoiding the synchronization procedure which is needed in many other CT MAC protocols.

2.3.3 A Receiver Initiated CT MAC Protocol

Most synchronous CT MAC protocols follow a sender initiated CT, leading to a longer synchronization period. Energy efficiency can be further increased by employing a scheme with a shorter synchronization period. Appendix A in Part II of this thesis proposes a receiver initiated CT MAC protocol, referred to as the RICT-MAC protocol, which introduces a short duration for synchronization. We show that it mitigates energy hole effectively with lower energy consumption and achieves extended lifetime in comparison with two existing protocols.

According to the RICT-MAC protocol, the relay, i.e., the receiving node, initiates CT. Since the relay node can reach both the transmitting node (a child node of the relay) and the node to which it is forwarding the packet to (a parent node of the relay), it requires fewer number of synchronization messages to handle CT based transmissions.

2.4 The Overhearing Problem

In a network or a network cluster with multiple nodes, all nodes that have packets to transmit contend for channel access in order to send their packets to a single cluster-head or the sink node. Collision may happen when two or more nodes contend with each other and retransmission is needed if collision happens. Correspondingly, higher energy is consumed.

In other words, the channel is successfully accessed when only one node wins the contention. The RTS or CTS packet in CSMA/CA informs the other neighboring nodes that it is going to transmit or receive and how long the frame exchange will last. Upon overhearing one of these control packets, the other nodes go to sleep. This sleeping mechanism is hereafter referred

to as a control packet triggered (CPT) sleeping mechanism [28], [23]. In CPT, a node that does not have any packets to send still needs to wait until it overhears a control packet before going to sleep. For example, when no node is active in a network, all nodes need to be awake for the whole duration of the data period, leading to high energy consumption.

2.4.1 An Event-Triggered Sleeping Mechanism

To address the overhearing problem occurring in CPT, an event-triggered sleeping mechanism is proposed in Paper B in Part II of the dissertation. The main idea of the ETS mechanism is to allow nodes that do not have any packet to send sleep *right after the sync period* without participating in medium access contention. Accordingly, such a node can sleep longer for the rest of the same cycle and it consequently saves energy. The ETS mechanism applies to any synchronous DC protocols and suits ideally for WSNs with low traffic rate, for instance, in event triggered monitoring and surveillance applications.

2.5 Chapter Summary

This chapter presents an overview of various MAC protocols existing in the literature. We explain also the effect of energy hole in a WSN and how a node wastes its energy due to overhearing. Furthermore, the main ideas of the proposed protocols, i.e., ACT-MAC in Paper A and the ETS mechanism in Paper B are outlined. A draft version of the paper containing RICT-MAC is attached as Appendix A since it has not been published yet at the time of this thesis submission. Both the proposed protocols and the sleeping mechanism achieve higher energy efficiency when compared with existing solutions.

Chapter 3

Energy Efficient Data Transmission

This chapter explains how data transmission is performed in association with a MAC protocol in duty-cycled WSNs. It discusses also the effect of different methods for energy efficient data[2] transmission. In the thesis, we focus solely on data transmission, not on the frame structure of a packet or a frame.

3.1 Single Packet Transmission

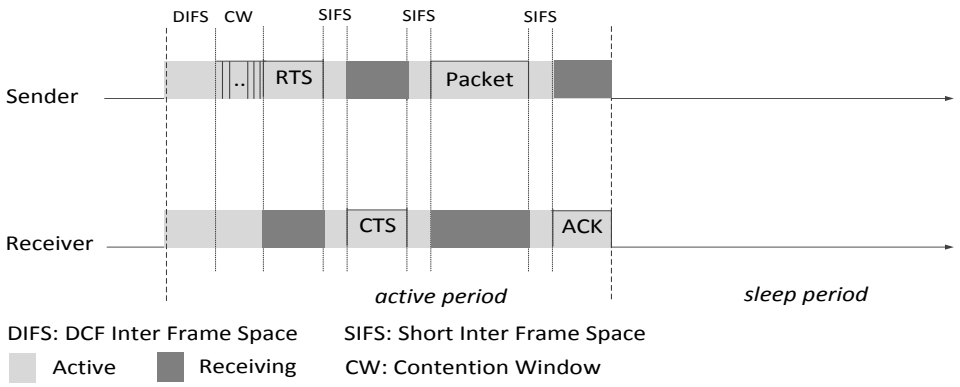

Figure 3.1: Illustration of a single packet transmission based on CSMA/CA.

In duty-cycled WSNs, nodes switch off their radio transceivers in the sleep period. This implies that the packets arrived in the sleep period cannot be transmitted immediately. Instead, these pending packets will be buffered in a queue. Consequently, this procedure may result in a longer delay since the

[2]Throughout this thesis, data represents general data, packet indicates a specific single packet and frame represents a batch of packets which are aggregated together for transmission.

sleep period is typically much longer than the active period. Usually, during the active period of each cycle, nodes communicate with their neighbors and transmit or receive merely one data packet [23]. Hereafter this transmission mode is referred to as single packet transmission (SPT).

As an example for SPT in CSMA/CA based MAC protocols, the corresponding operation is illustrated in Fig. 3.1. The senders first contend for medium access by selecting their backoff times after DIFS, as shown in the figure. The channel is successfully accessed when only one node wins a contention. Once gaining channel access, both the winning node and the receiving nodes perform a handshake procedure prior to packet transmission following the same CSMA/CA as shown in the initial phase of the active period. The sender transmits first an RTS packet to the receiving node. The receiver responds with CTS saying that it is ready to receive the packet after a short inter frame space (SIFS). Then the data packet is transmitted by the sender. Upon receiving the acknowledgment message from the receiver, both nodes go to sleep immediately and wake up again in the next cycle.

3.2 Aggregated Packet Transmission

In aggregated packet transmission (APT), a batch of packets are transmitted together as a *frame*. APT is also performed similar to SPT as illustrated in Fig. 1. When the receiving node replies with CTS, then the sending node transmits in this case a frame consisting *a batch of packets*. Clearly, throughput would be increased and delay could be shortened by transmitting multiple

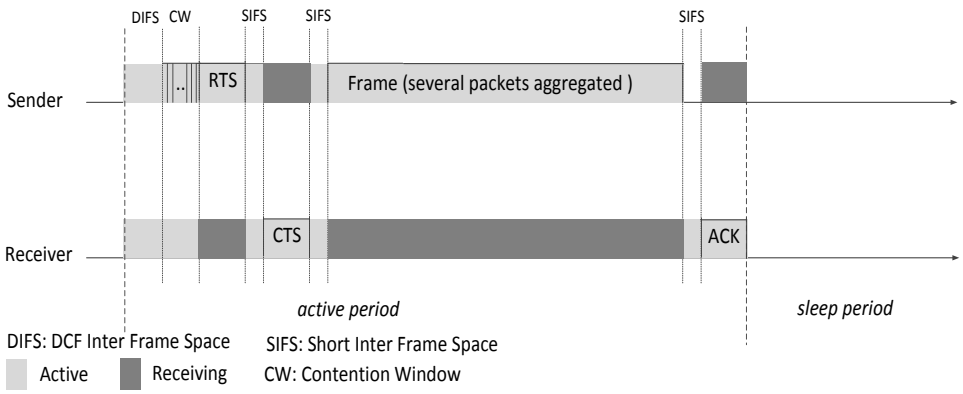

Figure 3.2: Illustration of a aggregated packet transmission based on CSMA/CA.

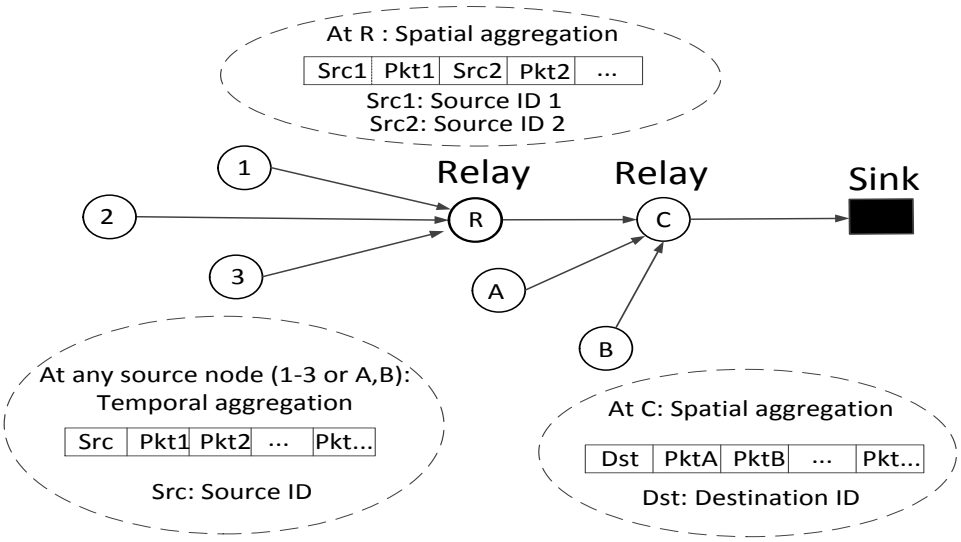

Figure 3.3: Illustration of packet aggregation at different nodes in a WSN.

aggregated packets as a batch. Energy efficiency would also be improved, because the control overhead to send an aggregated frame is the same as the one required in case of SPT.

Generally all source nodes in a WSN send their packets towards a single sink node via intermediate nodes. In such networks, aggregation can be performed at either/both a source node or/and at a relay node. If a source node aggregates multiple self-generated (sensed) packets, then *temporal aggregation* is performed. Temporal aggregation means that a node selects typically one type of traffic from its sensed or received data and it combines multiple packets of the same type into a frame. Then the aggregated frame contains the same source ID, as shown in Fig. 3.3. On the other hand, when an intermediate node applies aggregation, it applies usually *spatial aggregation*. Spatial aggregation is meant that the relay or intermediate node assembles packets from different sources into a frame which are destined to the same destination ID, as illustrated in Fig. 3.3. As shown in this figure, Nodes 1-3 or A, B aggregate packets in the time domain while relays R and C aggregate packets received from Nodes 1-3 and A, B in the space domain respectively. Since the frame structure details inside a frame are not an aspect of interest in the context of this thesis work, we consider only temporal aggregation for performance evaluation of APT.

The aggregated transmission of packets in wireless networks has already been investigated in many earlier studies. In [39], a packet aggregation scheme

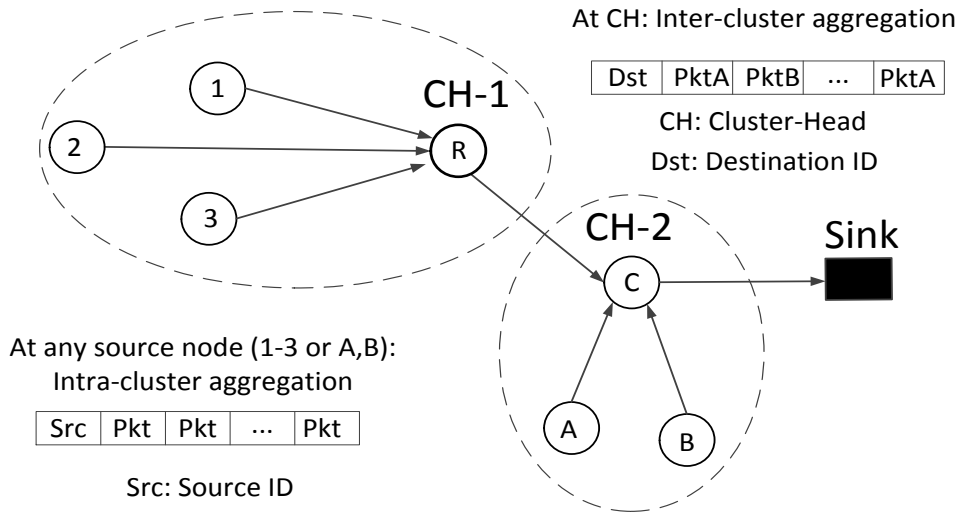

Figure 3.4: Illustration of aggregation at cluster-heads in a WSN.

was analyzed for the packet reservation multiple access (PRMA) protocol in cellular networks. Packet aggregation was implemented and evaluated in [40] for wireless local area network (WLAN). However, how packet aggregation works in duty-cycled WSNs and how to evaluate the performance of packet aggregation in such networks remain as an unanswered question.

3.3 Aggregation from a Protocol Stack Perspective

3.3.1 Aggregation at the Network Layer

A majority of the published works dealing with packet aggregation in WSNs studied packet aggregation via simulations or test-beds. The starting point of these studies is that the data sensed by a group of neighboring nodes is somewhat spatial-correlated or/and redundant, and that unprocessed transmission is likely to waste energy and degrade network performance. Keeping this point in mind, many studies concentrated on packet aggregation at the network layer [41]. That is, the data which is routed across multiple clusters is aggregated. In this case, it is usually cluster-heads that perform inter-cluster aggregation before forwarding packets towards the sink, as shown in Fig. 3.4. Various aspects are taken into account in these studies, like the selection of the cluster-heads that participate in the routing of the information towards the sink; the construction of the shortest path; the design of a scheduling algo-

rithm that produces collision-free medium access; etc. A recent survey paper [42] provides a comprehensive overview on this topic. Although not from an analytical perspective, packet enlargement (aggregation) was considered in [43]. The authors therein proposed an algorithm to adjust packet length dynamically in order to minimize packet error rate in adverse radio link environments and evaluated it in a test-bed.

3.3.2 Aggregation at the MAC Layer

On the other hand, aggregation may happen inside a cluster by either a member node or the cluster-head. For intra-cluster aggregation, temporal aggregation suits better for aggregating packets. Moreover, intra-cluster aggregation is performed at the MAC layer and it further saves energy in many realistic scenarios by perfroming aggregation at this layer. It has already been showed that DC MAC protocols conserve energy. Intuitively, combining both DC and aggregation may further increase energy efficiency and extend network lifetime. In the literature, only few aggregation based MAC protocols are available, for instance aggregation MAC (AG-MAC) [44], lifetime balanced aggregation (LBA) [45] and joint aggregation and MAC (JAM) [46]. However, their aggregation schemes are protocol or application specific, meaning that they may not be applicable to another MAC protocol or in another application.

3.4 Aggregation: Static versus Dynamic

One of the benefits with packet aggregation is that higher energy efficiency can be achieved. However, taking necessary actions and reacting in an efficient way might not be easy in critical applications if the aggregated packets are not delivered in a timely manner. Furthermore, higher data rate is also expected for achieving satisfactory performance in mission critical applications [47]. Therefore, a packet aggregation scheme should also consider the quality for other performance metrics such as delay and throughput.

For any node that intends to perform APT, aggregation can be done in two ways.

- *Static aggregation*: it waits until a required number of packets, X, arrived into the queue and then transmits these X packets as a *batch*.
- *Dynamic aggregation*: It aggregates all available packets Y in the queue, if $Y < X$, and transmits a frame consisting of these Y packets once a transmission opportunity arises; Otherwise, it aggregates and transmits X packets, and the remaining packets are kept in the buffer.

Intuitively, static aggregation seems to be more energy efficient. However it may degrade throughput and increase delay. This is due to the fact that there would not be any transmission in some cycles until a specified number of packets have arrived to a node if static aggregation is employed. On the other hand, dynamic aggregation improves the performance with respect to all metrics. This is because that the number of packets aggregated is dynamically adjusted in each operation cycle based on the traffic arriving to a node. Therefore, we propose and evaluate a dynamic aggregation scheme in Paper C in Part II of this thesis.

3.5 Chapter Summary

In summary, this chapter discusses transmission schemes in WSNs and explains the benefits of aggregated packet transmission. Furthermore, it explains different techniques to aggregate packets at the MAC layer and justifies the reasons for investigating dynamic APT in Paper C.

Chapter 4

Performance Evaluation

Once a protocol or scheme is designed, its performance should be evaluated extensively and independently by different means. Analysis and comparison with existing proposals can give an insight on the performance and identify the weaknesses of the studied schemes. Based on this evaluation, enhancements to existing schemes and new methods can be proposed. This chapter discusses various techniques to evaluate the performance of a protocol or mechanism with a focus on three categories of popular tools for performance evaluation.

4.1 Performance Evaluation Methods

In general, the performance of any MAC protocol can be evaluated by analytical models, computer simulations and/or real-life field measurements [48]. If the results from any two of these three methods match with each other, then these results are considered to be convincing or/and accurate. The most commonly studied performance metrics in WSNs include energy consumption, network lifetime, energy efficiency, throughput and delay.

4.1.1 Real-life Experiments based on Testbeds

The implementation of a protocol in real-life WSN environment needs the deployment of the protocol to all nodes in a given network. To do so, every node must be programmed individually. Such a network requires also data collection and analysis tools.

For a small- or medium-scale WSN, testbed appears as a popular alternative to conduct real-life experiments [49]. Testbeds allow us to verify and assess various algorithms, schemes, and generally new techniques in a close-to-reality manner. Many WSN testbeds are available in the market, such as SCALE [50], MoteLab [51], TWIST [52], SWAT [53], and Mirage [54].

A testbed must be programmed based on an operating system (OS) to execute the required sensing, processing and communication functions. One of the most popular operating systems is tiny micro-threading operating system (TinyOS) [55]. It is an open-source embedded OS and uses nesC as the programming language. TinyOS includes all software modules to perform data sensing, storage, routing and communication. Other operating systems also exist, for example, CONTIKI [56], MANTIS [57], and SOS [58].

However, field measurement based studies are often time consuming and budget constraint. Therefore more analysis or simulation based studies are reported in the literature.

4.1.2 Simulations

Simulation imitates the physical behavior of a network consisting of various sizes of node population via software and it is carried out typically on *one computer*. Usually, simulation based studies need to make assumptions regarding traffic conditions, network topologies and channel environments. Moreover, simulators with data interpretation and visualization packages save our time and help us avoid human made errors in data processing. Simulations can be performed in three distinct ways: discrete-event, continuous, and Monte Carlo [58].

Discrete-event simulation (DES) emulates a system that tracks changes in the system at particular points in time. The system which is to be simulated contains a set of events and a set of state variables. The values of the state variables are changing based on the occurred events, i.e., how states change over time is reflected in DES. A DES program builds a system using the state variables and simulates it using the events to evaluate the system behavior [59]. A system with a number of customers, e.g., packets in an Internet protocol (IP) network arriving and waiting for services, is a typical scenario for DES simulations.

Continuous simulation mimics a system which changes its state continuously over time [60]. This type of system can be described in terms of equations, specifically in differential equations. Then, continuous simulation solves this system using different numerical methods, like the Runge-Kutta method [61].

Monte Carlo simulation reveals the behavior of a system with uncertainty [62]. In such a model, no representation of the time domain is required. Monte Carlo simulations are performed by obtaining statistical relationships between the output values obtained from one or multiple input variables provided to the system. The decisions are then made based on statistical analysis. Basically, this simulation method is based on repetitive trials. It performs so called what-if analysis and is widely used in risk analysis and many other scientific fields.

In WSNs, packets are sensed by a node and stored in its queue. When a transmission opportunity arises, the packets are delivered towards the destination. In this sense, packets are the customers waiting for their service, i.e., transmission. Therefore, discrete-event simulations are more popular for performance evaluation in WSNs. There are many simulation tools available for WSN performance evaluation, like TinyOS based simulator TOSSIM [63], C++ based simulators OMNET++ [64], QualNeT [65], network simulator NS2 [66], network simulator NS3 [66], and C based simulator SMPL [24]. In the past, NS2 was popular and now NS3 is becoming more popular in the wireless networking research community. For the evaluation of queuing networks, a C based discrete-event simulator, SMPL, has also been proven as an excellent tool.

Since this thesis mainly focuses on the queuing analysis of sensor networks with nodes having finite queue capacity, discrete-event simulations suit better. For our simulations, SMPL is adopted as the simulation platform.

4.1.3 Mathematical Analysis

Analytical models provide more insights into the performance of a protocol or an algorithm. They can also mutually validate the results obtained from simulations and testbed experiments.

Furthermore, mathematical modeling can serve as a powerful tool for un-

derstanding the intricacies of WSN behavior. Developing mathematical models to evaluate performance parameters is usually more tractable for assessing the overall behavior of a protocol. However, when developing a mathematical model to evaluate or emulate a real-world phenomenon, it is important to represent the scenario properly and to configure parameters as realistic as possible.

In general, for modeling network behavior, stochastic process analyses with Markov chains [67] and PetriNets [68] based on queuing theory are the major tools. Analytical models can also be used to solve a variety of optimization problems based on game theory [69]. Evaluating the performance of communication networks by Markov chains is a popular approach as its effectiveness has been proven in countless studies. Therefore, Markov models are used to evaluate the protocols and schemes proposed in this dissertation.

4.2 Markov Chain Models

Markov chain models perform numerical analysis related to the probability of being in a given state in a system. Generally, a Markov model contains different states. According to the behavior of a system, transitions among states occur. Markov models rely on the memory-less property, meaning that the probability that the system arrives into a future state depends *only* on the current state, regardless of its presence in any earlier states. From the model, the amount of time spent in each state by the system as well as the expected number of transitions among states are obtained. These probabilities are needed to calculate the performance metrics of a studied system.

4.2.1 CTMC

A continuous time Markov chain (CTMC) is a stochastic process with a countable state space in which the time spent in a state (the holding time) is distributed exponentially. When the holding time expires, the process transits from one state to another state and this transition is independent of the previous transitions. Then the transitions in CTMC occur at a rate corresponding to the exponential distribution of the holding time. Thus each transition is represented with an event rate, either the arrival rate or the service rate. As

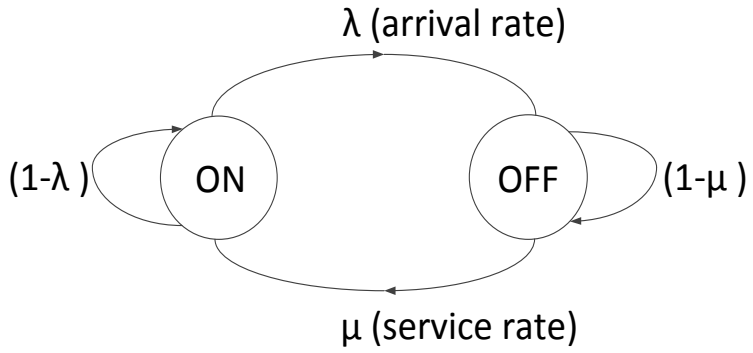

Figure 4.1: Illustration of a two-state CTMC ON-OFF model.

an example, a two-state ON-OFF model is shown in Fig. 4.1. At any state, the sum of the outgoing rates is equal to the sum of all the incoming rates. Moreover, the stationary distributions, π, can be determined as the solutions of the equations given bellow,

$$\pi \boldsymbol{Q} = \mathbf{0}, \quad \pi \boldsymbol{e} = 1, \tag{4.2.1}$$

where $\boldsymbol{Q}$ is the transition rate matrix, $\boldsymbol{e}$ is the column vector of ones, and $\mathbf{0}$ is the row vector of zeros.

4.2.2 DTMC

A stochastic process is a discrete time Markov chain (DTMC) which contains a finite state space and within the space a state change (transition) occurs with a probability independent of the previous transitions. An example of a two-state DTMC is shown in Fig. 4.2. The DTMC changes to a new state at each time step and it stays in the same state until the next time step. These transitions depend on the probability of occurring events such as arrivals and departures. For a given state in a DTMC, the summation of the exit transition probabilities is equal to 1 and the state stationary distributions, π, are obtained by solving the following equations,

$$\pi \boldsymbol{P} = \pi, \quad \pi \boldsymbol{e} = 1, \tag{4.2.2}$$

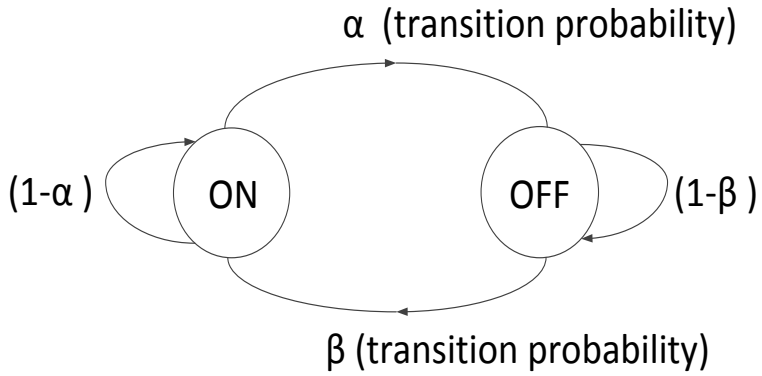

Figure 4.2: Illustration of a two-state ON-OFF DTMC model.

where $\boldsymbol{P}$ is the transition probability matrix, $\boldsymbol{e}$ and $\mathbf{1}$ have the same meaning as presented in CTMC.

4.3 DTMC Modeling of MAC Protocols in WSNs

In synchronous DC MAC protocols employed in WSNs, nodes are synchronized to wake up at the same time. Then, nodes which have packets to send contend for data transmission according to CSMA/CA. The winning node transmits and the other nodes go to sleep. In the next cycle, all nodes wake up again following the same procedure for data transmission. In this cycle, all nodes need to select a new backoff value, i.e., all the backoff timers are reset at each cycle of operation. DTMC modeling is a popular tool to model synchronous DC MAC protocols in WSNs.

Note that only the nodes which have packets to transmit compete for channel access and these nodes are considered as active nodes. At the beginning of each cycle, all *active* nodes generate a random backoff time uniformly from window $\{0, W-1\}$. If the smallest backoff time is selected by *only one* node, then that node wins channel access and reserves the medium for data exchange. If a node selects a backoff time which is not the smallest one, it loses the competition and waits until the next cycle to compete again. In case that two or more nodes select the same smallest backoff time, there will be a collision. Consider that $N \geq 1$ nodes are contending with each other and a node is randomly selected as a reference node (RN). In the example illustrated in Fig. 4.3, the RN is the winner in Cycle $t+1$.

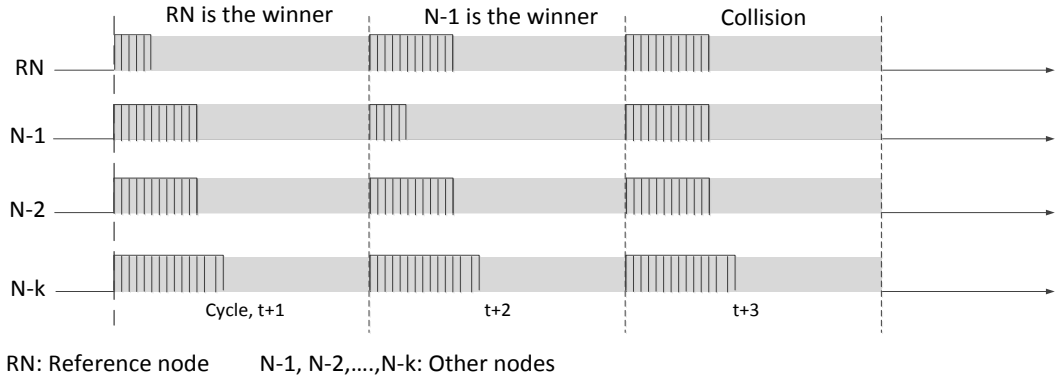

Figure 4.3: Illustration of the backoff process for channel access competition.

When the RN is contending with other k, where $0 \leq k \leq N-1$, active nodes, the probabilities that the RN transmits a packet successfully, $P_{s,k}$; it transmits a packet (successfully or collided), $P_{sf,k}$; and the transmission failed (collided), $P_{f,k}$, are given respectively by

$$P_{s,k} = \sum_{i=0}^{W-1} \frac{1}{W} \left(\frac{W-1-i}{W} \right)^k , \tag{4.3.1}$$

$$P_{sf,k} = \sum_{i=0}^{W-1} \frac{1}{W} \left(\frac{W-1}{W} \right)^k , \tag{4.3.2}$$

$$P_{f,k} = P_{sf,k} - P_{s,k} . \tag{4.3.3}$$

These three expressions constitute the basis for developing the DTMC models for performance evaluation of the proposed protocols and transmission schemes in this thesis.

4.3.1 Dimensionality of the DTMC Models: Factors Considered

Using the probabilities, $P_{s,k}$, $P_{sf,k}$ and $P_{f,k}$, various DTMC models can be developed for analyzing CSMA/CA based DC MAC protocols in WSNs. In each model, it might not be required to include all of the above probabilities. Which factors to consider decides the number of dimensions needed in a

model. Generally, the dimensions considered in our DTMC modeling are the following

- Number of packets in the queue of the RN;
- Number of nodes in the studied network or cluster;
- Number of retransmissions allowed for each packet or frame;
- The channel is considered as error-free or not.

4.3.2 Existing Models versus the Developed

To clarify the difference between our models and the existing models, let i be the the number of packets found at the queue of the RN, k be the number of *active* nodes in the network and r be the number of retransmissions experienced by the packet at the head of the queue of the node. If only one parameter is modeled, we need only one dimension (1D) in a model and refer it to as 1D DTMC. Similarly, if a combination of two parameters is included, then the model is a 2D DTMC. In other words, a 3D DTMC model includes all the aforementioned three parameters when the channel is assumed to be error-free.

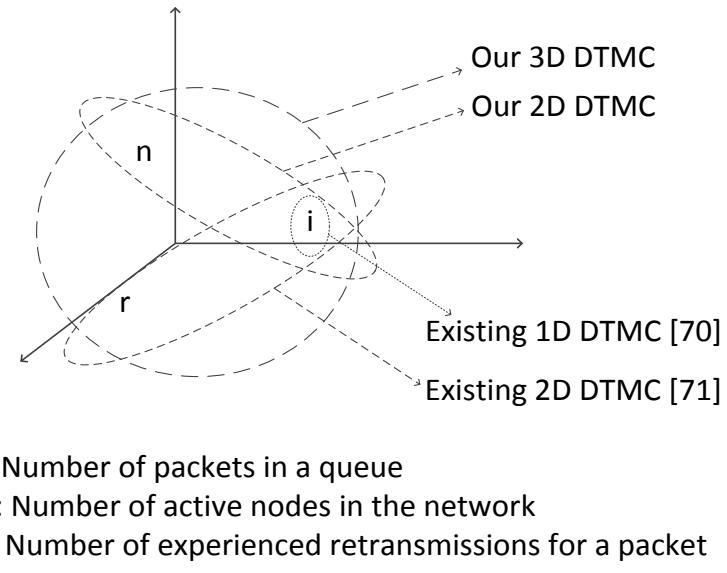

Figure 4.4: Illustration of the DTMC models for DC MAC protocols: Existing versus ours.

The distinction between the models proposed in Papers B-E and the DTMC models for DC MAC protocols available in the literature is illustrated in

Fig. 4.4. A 1D DTMC studied in [70] considered only i. The previous 2D DTMCs in [71] and [72] modeled both i and r. In contrast, a new 1D DTMC with respect to k is proposed in Paper D of this thesis and it is iteratively operated with the 1D DTMC with respect to i [70], We demonstrate that it improves the accuracy of the models. A similar model has been developed for evaluating multiple packet transmission based on DW-MAC in Paper E in Part II of this thesis. As such, novel 2D DTMCs are defined by (i,k) in Papers B, C and Appendix A, and these models are different from existing combinations in [71] and [72]. This 2D DTMC is developed to evaluate SPT, APT and CT in Papers B, C and Appendix A respectively. In addition, a 3D DTMC is developed by a triplet (i,k,r) to evaluate APT in Paper C. In the same paper, we have also introduced briefly a 4D DTMC which contains channel condition as the fourth dimension. More detailed descriptions about the developed 4D DTMC and the closed-form expressions for performance parameters are presented in Appendix B, as this new result has not been submitted for publication yet as of this thesis submission.

4.4 Chapter Summary

This chapter gives an overview on the performance evaluation methods used for performance evaluation in general as well as of the work carried out in this thesis. Three categories of methods for performance evaluation of any system are outlined, i.e., real-life experiments, simulations, and mathematical analysis. Popular tools available in each category of these methods are also listed in this chapter.

Papers B-E contain performance evaluation based on discrete-event simulations and DTMC models. The numerical results obtained from the simulations under various network configurations and conditions precisely match with the ones obtained through analytical models, confirming that the developed DTMC models are able to predict accurately the behavior of the proposed protocols and schemes.

Chapter 5

Conclusions and Future Work

This final chapter summarizes the whole dissertation work. It points out also a few future directions to continue the research work relevant to energy efficient data transmission in WSNs.

5.1 Conclusions

After reviewing many state-of-the-art MAC protocols and energy efficient data transmission operations in the literature, we identified that energy exhaustion in WSNs was mainly caused by energy hole, idle listening and overhearing. In order to tackle these problems, this thesis work proposed MAC protocols, transmission schemes and sleeping mechanisms with a focus on energy efficient data transmission in WSNs. Basically, all the proposed techniques are able to diminish unnecessary energy consumption and extend network lifetime. Moreover, we developed DTMC models which emulated the behavior of the schemes and validated the accuracy of these models by discrete-event based simulations.

5.2 Contributions

This dissertation research advances the state-of-the-art with respect to three main aspects of WSNs towards green wireless communications: MAC protocol design; data transmission; and mathematical modeling of DC WSNs. In brief, the contributions are listed as follows.

- As a part of energy efficient MAC protocol design, a novel asynchronous CT MAC protocol, ACT-MAC, has been proposed and the performance is compared with another CT MAC protocol, SCT-MAC. The ACT-MAC protocol can be applied to large-scale WSNs as it is based on the level number of a node. It is shown that ACT-MAC extends the network lifetime by saving energy consumption without the need for node synchronization.

- A receiver initiated cooperative transmission MAC protocol has been proposed to extend network lifetime. The proposed RICT-MAC protocol is a synchronous DC MAC protocol and its performance is compared with another CT MAC protocol, SCT-MAC, and a non-CT protocol, DW-MAC. It is proven that RICT achieves higher energy efficiency and a longer network lifetime thanks to the feature that CT is initiated by the relay node.

- A user traffic triggered sleeping mechanism, ETS, has been proposed to improve energy efficiency in synchronous DC MAC protocols. When a node has a packet to send, it competes and possibly transmits the packet. However, in case that no traffic is arriving to a node or no event is detected by a node, the node remains asleep in ETS. Thus, ETS could save energy especially at low traffic load conditions and achieves higher energy efficiency.

- Packet aggregation has been shown as an energy efficient data transmission scheme, since the same control overhead as in SPT is required to send a frame containing a batch of packets which are aggregated. Since multiple packets are transmitted in a single duty cycle, APT maintains higher energy efficiency and achieves shorter delay.

- The performance of the proposed MAC protocols and schemes is evaluated by the developed DTMC models and the performed discrete-event based simulations. The coincidence of the analytical and simulation results demonstrates the effectiveness of the proposed schemes and mechanisms, as well as the accuracy of the developed models.

5.3 Future Work

This thesis research concentrated mainly on the MAC layer for data transmission in WSNs. Protocols and mechanisms were proposed and their performance was evaluated to examine performance metrics relevant to green communications. Beyond the research questions and the efforts reported in this dissertation, a few further directions within the studied area can still be envisaged. For instance, new technologies in the WSN area such as energy harvested WSNs [73], wake-up radio (WuR) [74] and IoT [8] are currently emerging and these emerging communication paradigms require indeed novel protocols and mechanisms. Among various potential topics, this dissertation work can be continued in the following directions.

- The thesis work has proposed independently a cooperative MAC protocol which could extend network lifetime and an aggregated packet transmission scheme which could increase energy efficiency. A new DTMC model could be developed to evaluate the performance of a CT mechanism jointly operating with APT at the MAC layer.

- Combining energy harvesting with DC can obviously extend network lifetime and possibly increase energy efficiency. Therefore there is a need for developing DC protocols for EH enabled WSNs, investigating how to achieve energy efficiency in the presence of both battery powered and harvested energy.

- Recently, WuR appears as an emerging trend in the field of WSNs. Basically, wake-up radios are the transceivers that have the capability of waking up neighboring nodes at an extremely lower power consumption level than that of the main radio. This feature brings forward new requirements and challenges in designing selective wake-up aware protocols for WuR enabled WSNs. Clearly, designing MAC protocols for data transmission in such WSNs is an important and fertile direction of our future work.

- IoT is an emerging technology that is tightly coupled with WSNs. The IoT enables physical objects, such as vehicles, phones, appliances, goods, etc., to communicate directly or over multiple hops with the help of

sensors connected to the future global Internet. In other words, IoT makes these objects smarter by taking the advantage of extremely low power and ubiquitous computing capabilities of the IoT sensors. Definitely, new protocols are required for communication compatibility between these heterogeneous devices and correspondingly their performance needs to be evaluated.

REFERENCES

[1] B. Kim, Y. Cho, and J. Hong, "AWNIS: Energy-efficient adaptive wireless network interface selection for industrial mobile devices," *IEEE Trans. Ind. Informat.*, vol. 10, no. 1, pp. 714–729, Feb. 2014.

[2] C. Wang, F. Haider, X. Gao, X. You, Y. Yang, D. Yuan, H. Aggoune, H. Haas, S. Fletcher, and E. Hepsaydir, "Cellular architecture and key technologies for 5G wireless communication networks," *IEEE Commun. Mag.*, vol. 52, no. 2, pp. 122–130, Feb. 2014.

[3] M. Agiwal, A. Roy, and N. Saxena, "Next generation 5G wireless networks: A comprehensive survey," *IEEE Commun. Surveys Tuts.*, Early access available in IEEE Xplore, DOI:10.1109/COMST.2016.2532458, Feb. 2016.

[4] G. Wu, C. Yang, S. Li, and G. Y. Li, "Recent advances in energy-efficient networks and their application in 5G systems," *IEEE Wireless Commun.*, vol. 22, no. 2, pp. 145–151, Apr. 2015.

[5] Y. Zhang, E. Pan, L. Song, W. Saad, Z. Dawy, and Z. Han, "Social network aware device-to-device communication in wireless networks," *IEEE Trans. Wireless Commun.*, vol. 14, no. 1, pp. 177–190, Jan. 2015.

[6] I. F. Akyildiz, W. Su, Y. Sankarasubramaniam, and E. Cayirci, "Wireless sensor networks: A survey," *Comput. Netw.*, vol. 38, no. 4, pp. 393–422, IEEE, Dec. 2002.

[7] R. Cavallari, F. Martelli, R. Rosini, C. Buratti, and R. Verdone, "A survey on wireless body area networks: Technologies and design challenges," *IEEE Commun. Surveys Tuts.*, vol. 16, no. 3, pp. 1635–1657, Aug. 2014.

[8] M. R. Palattella, M. Dohler, Al. Grieco, G. Rizzo, J. Torsner, T. Engel, and L. Ladid, "Internet of Things in the 5G era: Enablers, architecture, and business models," *IEEE J. Sel. Areas Commun.*, vol. 34, no. 3, pp. 510–527, Mar. 2016.

[9] A. Al-Fuqaha, M. Guizani, M. Mohammadi, M. Aledhari, and M. Ayyash, "Internet of Things: A survey on enabling technologies, protocols and applications," *IEEE Commun. Surveys Tuts.*, vol. 17, no. 4, pp. 2347–2376, Nov. 2015.

[10] SMART 2020, "Enabling the low carbon economy in the information age,", Available at http://www.smart2020.org/publications/, (accessed on 12 May 2016.

[11] J. Malmodin, Å. Moberg, D. Lundén, G. Finnveden, and N. Lövehagen, "Greenhouse gas emissions and operational electricity use in the ICT and entertainment & media sectors," *Journal of Ind. Ecol.*, vol. 14, no. 5, pp. 770–790, Wiley Online Library, Nov. 2010.

[12] N. Han, Y. Chung, and M. Jo, "Green data centers for cloud-assisted mobile ad hoc networks in 5G," *IEEE Network*, vol. 29, no. 2, pp. 70–76, Apr. 2015.

[13] L. Chen, W. Wang, A. Anpalagan, A. V. Vasilakos, K. Illanko, H. Wang, and M. Naeem, "Green cooperative cognitive communication and networking: A new paradigm for wireless networks," *Mobile Nets. and Apps.*, vol. 18, no. 4, pp. 524–534, Apr. 2013.

[14] A. Fehske, G. Fettweis, J. Malmodin, and G. Biczók, "The global footprint of mobile communications: The ecological and economic perspective," *IEEE Commun. Mag.*, vol. 49, no. 8, pp. 55–62, Aug. 2011.

[15] K. Sierszecki, T. Mikkonen, M. Steffens, T. Fogdal, and J. Savolainen, "Green software: Greening what and how much?," *IEEE Software*, vol. 31, no. 3, pp. 64–68, Apr. 2014.

[16] D. Feng, C. Jiang, G. Lim, L. J. Cimini, G. Feng, and G. Y. Li, "A survey of energy-efficient wireless communications," *IEEE Commun. Surveys Tuts.*, vol. 15, no. 1, pp. 167–178, IEEE, Feb. 2013.

[17] G. Y. Li, Z. Xu, C. Xiong, C. Yang, S. Zhang, Y. Chen, and S. Xu, "Energy-efficient wireless communications: Tutorial, survey, and open issues," *IEEE Wireless Commun.*, vol. 18, no. 6, pp. 28–35, Dec. 2011.

[18] T. Chen, Y. Yang, H. Zhang, H. Kim, and K. Horneman, "Network energy saving technologies for green wireless access networks," *IEEE Wireless Commun.*, vol. 18, no. 5, pp. 30–38, Oct. 2011.

[19] A. A. K. Somappa, K. Øvsthus, and L. M. Kristensen, "An industrial perspective on wireless sensor networks-a survey of requirements, protocols, and challenges," *IEEE Commun. Surveys Tuts.*, vol. 16, no. 3, pp. 1391–1412, Aug. 2014.

[20] L. M. Borges, F. J. Velez, and A. S. Lebres, "Survey on the characterization and classification of wireless sensor network applications," *IEEE Commun. Surveys Tuts.*, vol. 16, no. 4, pp. 1860–1890, Nov. 2014.

[21] T. Kim, I. H. Kim, Y. Sun, and Z. Y. Jin, "Physical layer and medium access control design in energy efficient sensor networks: An overview," *IEEE Trans. Ind. Informat.*, vol. 11, no. 1, pp. 2–15, Feb. 2015.

[22] P. Huang, L. Xiao, S. Soltani, M. W. Mutka, and N. Xi, "The evolution of MAC protocols in wireless sensor networks: A survey," *IEEE Commun. Surveys Tuts.*, vol. 15, no. 1, pp. 101–120, Feb. 2013.

[23] W. Ye, J. Heidemann, and D. Estrin, "Medium access control with coordinated adaptive sleeping for wireless sensor networks," *IEEE/ACM Trans. Net.*, vol. 12, no. 3, pp. 493–506, June 2004.

[24] M. H. MacDougal, *Simulating Computer Systems Techniques and Tools*. The MIT Press, 1987.

[25] V. Rajendran, K. Obraczka, and J. J. Garcia-Luna-Aceves, "Energy-efficient, collision-free medium access control for wireless sensor networks," *Wireless Networks*, vol. 12, no. 1, pp. 63–78, Springer-Verlag New York, Inc., Feb. 2006.

[26] S. Gobriel, D. Mosse, and R. Cleric, "TDMA-ASAP: Sensor network TDMA scheduling with adaptive slot-stealing and parallelism," in *Proc. IEEE ICDCS*, June 2009.

[27] L. F. W. V. Hoesel and P. J. M. Havinga, "A lightweight medium access protocol (LMAC) for wireless sensor networks: Reducing preamble

transmissions and transceiver state switches," in *Proc. INSS*, Society of Instrument and Control Engineers (SICE), June 2004.

[28] B. P. Crow, I. Widjaja, J. G. Kim, and P. T. Sakai, "IEEE 802.11 wireless local area networks," *IEEE Commun. Mag.*, vol. 35, no. 9, pp. 116–126, Nov. 1997.

[29] J. Wang, Z. Cao, X. Mao, and Y. Liu, "Sleep in the Dins: Insomnia therapy for duty-cycled sensor networks," in *Proc. IEEE INFOCOM*, Apr. 2014.

[30] Y. Sun, S. Du, O. Gurewitz, and D. B. Johnson, "DW-MAC: A low latency, energy efficient demand-wakeup MAC protocol for wireless sensor networks," in *Proc. ACM MobiHoc*, May 2008.

[31] Y. Sun, O. Gurewitz, and D. B. Johnson, "RI-MAC: A receiver-initiated asynchronous duty cycle MAC protocol for dynamic traffic loads in wireless sensor networks," in *Proc. ACM SenSys*, Nov. 2008.

[32] L. Tang, Y. Sun, O. Gurewitz, and D. B. Johnson, "PW-MAC: An energy-efficient predictive-wakeup MAC protocol for wireless sensor networks," in *Proc. IEEE INFOCOM*, Apr. 2011.

[33] J. Ren, Y. Zhang, K. Zhang, A. Liu, J. Chen, and X. Shen, "Lifetime and energy hole evolution analysis in data-athering wireless sensor networks," *IEEE Trans. Ind. Informat.*, vol. 12, no. 2, pp. 788–800, Apr. 2016.

[34] J. Lin, H. Jung, Y. J. Chang, J. W. Jung, and M. A. Weitnauer, "On cooperative transmission range extension in multi-hop wireless ad-hoc and sensor networks: A review," *Ad Hoc Netw.*, vol. 29, pp. 117–134, June 2015.

[35] J. W. Jung and M. A. Ingram, "Residual-energy-activated cooperative transmission (REACT) to avoid the energy hole," in *Proc. IEEE ICC Workshops*, May 2010.

[36] J. Lin and M. A. Ingram, "SCT-MAC: A scheduling duty cycle MAC protocol for cooperative wireless sensor network," in *Proc. IEEE ICC*, June 2012.

[37] H. Jiao, M. A. Ingram, and F. Y. Li, "A cooperative lifetime extension MAC protocol in duty cycle enabled wireless sensor networks," in *Proc. IEEE MILCOM*, Nov. 2011.

[38] Jian Lin and Mary Ann Ingram, "OSC-MAC: Duty cycle scheduling and cooperation in multi-hop wireless sensor networks," in *Proc. IEEE WCNC*, Apr. 2013.

[39] Q. Zhang, V. B. Iversen, and F. H. P. Fitzek, "Throughput and delay performance analysis of packet aggregation scheme for PRMA," in *Proc. IEEE PIMRC*, Sept. 2007.

[40] T. Li, Q. Ni, D. Malone, D. Leith, Y. Xiao, and T. Turletti, "Aggregation with fragment retransmission for very high-speed WLANs," *IEEE/ACM Trans. on Netw.*, vol. 17, no. 2, pp. 591–604, Apr. 2009.

[41] E. Fasolo, M. Rossi, J. Widmer, and M. Zorzi, "In-network aggregation techniques for wireless sensor networks: a survey," *IEEE Wireless Commun.*, vol. 14, no. 2, pp. 70–87, May 2007.

[42] M. Bagaa, Y. Challal, A. Ksentini, A. Derhab, and N. Badache, "Data aggregation scheduling algorithms in wireless sensor networks: Solutions and challenges," *IEEE Commun. Surveys Tuts.*, vol. 16, no. 3, pp. 1339–1368, Third Quarter 2014.

[43] W. Dong, C. Chen, X. Liu, Y. He, Y. Liu, J. Bu, and X. Xu, "Dynamic packet length control in wireless sensor networks," *IEEE Trans. Wireless Commun.*, vol. 13, no. 3, pp. 1172–1181, Mar. 2014.

[44] K. Nguyen, U. Meis, and Y. Ji, "An energy efficient, high throughput mac protocol using packet aggregation," in *Proc. IEEE GLOBECOM Workshops*, IEEE, Dec. 2011.

[45] Z. Li, Y. Peng, D. Qiao, and W. Zhang, "LBA: Lifetime balanced data aggregation in low duty cycle sensor networks," in *Proc. of INFOCOM*, Mar. 2012.

[46] Z. Li, Y. Peng, D. Qiao, and W. Zhang, "Joint aggregation and MAC design to prolong sensor network lifetime," in *Proc. IEEE ICNP*, Oct. 2013.

[47] P. Suriyachai, U. Roedig, and A. Scott, "A survey of MAC protocols for mission-critical applications in wireless sensor networks," *IEEE Commun. Surveys Tuts.*, vol. 14, no. 2, pp. 240–264, May 2012.

[48] G. Z. Papadopoulos, K. Kritsis, A. Gallais, P. Chatzimisios, and T. Noël, "Performance evaluation methods in ad hoc and wireless sensor networks: A literature study," *IEEE Commun. Mag.*, vol. 54, no. 1, pp. 122–128, Jan. 2016.

[49] J. Horneber and A. Hergenröder, "A survey on testbeds and experimentation environments for wireless sensor networks," *IEEE Commun. Surveys Tuts.*, vol. 16, no. 4, pp. 1820–1838, Fourth Quarter 2014.

[50] A. Cerpa, N. Busek, and D. Estrin, "SCALE: A tool for simple connectivity assessment in lossy environments," *CENS Tech. Rep.*, Available at http://www.eecs.harvard.edu/ mdw/course/cs263/papers/scale-tr03.pdf., 2003.

[51] G. Werner-Allen, P. Swieskowski, and M. Welsh, "Motelab: A wireless sensor network testbed," in *Proc. IEEE IPSN*, Apr. 2005.

[52] V. Handziski, A. Köpke, A. Willig, and A. Wolisz, "TWIST: A scalable and reconfigurable testbed for wireless indoor experiments with sensor networks," in *Proc. ACM MobiHoc Workshop Multi-hop Ad Hoc Networks: From Theory to Reality*, May 2006.

[53] K. Srinivasan, M. A. Kazandjieva, M. Jain, E. Kim, and P. Levis, "SWAT: Enabling wireless network measurements," in *Proc. ACM SenSys*, Nov. 2008.

[54] B. N. Chun, P. Buonadonna, A. AuYoung, C. Ng, D. C. Parkes, J. Shneidman, A. C Snoeren, and A. Vahdat, "Mirage: A microeconomic resource allocation system for sensornet testbeds," in *Proc. IEEE EmNetS*, May 2005.

[55] J. Hill, R. Szewczyk, A. Woo, S. Hollar, D. Culler, and K. Pister, "System architecture directions for networked sensors," in *ACM SIGPLAN Notices*, Nov. 2000, vol. 35, pp. 93–104.

[56] A. Dunkels, B. Grönvall, and T. Voigt, "Contiki-a lightweight and flexible operating system for tiny networked sensors," in *Proc. IEEE LCN*, Nov. 2004.

[57] S. Bhatti, J. Carlson, H. Dai, J. Deng, J. Rose, A. Sheth, B. Shucker, C. Gruenwald, A. Torgerson, and R. Han, "MANTIS OS: An embedded multithreaded operating system for wireless micro sensor platforms," *Mobile Netw. Appl.*, vol. 10, no. 4, pp. 563–579, Springer-Verlag New York, Inc., Aug. 2005.

[58] M. Shapiro, Y. Gourbant, S. Habert, L. Mosseri, M. Ruffin, and C. Valot, "SOS: An object-oriented operating system - assessment and perspectives," *Comput. Syst.*, vol. 2, no. 4, pp. 287–337, Dec. 1989.

[59] A. H. Buss, "A tutorial on discrete-event modeling with simulation graphs," in *Proc. Winter Sim. Conf.*, Dec. 1995.

[60] T. B. Brito, E. F. C. Trevisan, and R. C. Botter, "A conceptual comparison between discrete and continuous simulation to motivate the hybrid simulation methodology," in *Proc. Winter Sim. Conf.*, Dec. 2011.

[61] J. Butcher, "A history of Runge-Kutta methods," *Appl. Numer. Math.*, vol. 20, no. 3, pp. 247–260, 1996.

[62] S. Raychaudhuri, "Introduction to Monte Carlo simulation," in *Proc. Winter Sim. Conf.*, Dec. 2008.

[63] P. Levis, N. Lee, M. Welsh, and D. Culler, "TOSSIM: Accurate and scalable simulation of entire TinyOS applications," in *Proc. ACM SenSys*, Nov. 2003.

[64] A. Varga and R. Hornig, "An overview of the OMNeT++ simulation environment," in *Proc. ICST SMUTools*, Mar. 2008.

[65] Scalable Network Technologies. Inc., "QualNet simulator,", 2012.

[66] T. Issariyakul and E. Hossain, *Introduction to Network Simulator NS2*. Springer Science & Business Media, 2011.

[67] W. J. Stewart, *Probability, Markov Chains, Queues, and Simulation: The Mathematical Basis of Performance Modeling*. Princeton University Press, 2009.

[68] M. A. Marsan, "Stochastic Petri nets: An elementary introduction," *Advances in Petri Nets*, pp. 1–29, June 1990.

[69] T. AlSkaif, M. G. Zapata, and B. Bellalta, "Game theory for energy efficiency in wireless sensor networks: Latest trends," *J. Netw. Comput. Appl.*, vol. 54, pp. 33–61, Aug. 2015.

[70] O. Yang and W. Heinzelman, "Modeling and performance analysis for duty-cycled MAC protocols in wireless sensor networks," *IEEE Trans. Mobile Comput.*, vol. 11, no. 6, pp. 905–921, June 2012.

[71] O. Yang and W. Heinzelman, "Modeling and throughput analysis for S-MAC with a finite queue capacity," in *Proc. IEEE ISSNIP*, Dec. 2009.

[72] F. Tong, L. Zheng, M. Ahmadi, M. Li, and J. Pan, "Modeling and analyzing duty-cycling, pipelined-scheduling MACs for linear sensor networks," *IEEE Trans. Veh. Technol.*, vol. 65, no. 4, pp. 2608–2620, Apr. 2016.

[73] M.-L. Ku, W. Li, Y. Chen, and K. J. R. Liu, "Advances in energy harvesting communications: Past, present, and future challenges," *IEEE Commun. Surveys Tuts.*, Early access available in IEEE Xplore, DOI:10.1109/COMST.2016.2532458, Nov. 2015.

[74] J. Oller, I. Demirkol, J. Casademont, J. Paradells, G. U. Gamm, and L. Reindl, "Has time come to switch from duty-cycled MAC protocols to wake-up radio for wireless sensor networks?," *IEEE/ACM Trans. Netw.*, vol. 24, no. 2, pp. 674–687, Apr. 2016.

Part II

Paper A

Title:	ACT-MAC: An Asynchronous Cooperative Transmission MAC Protocol for WSNs
Authors:	Lakshmikanth Guntupalli†, Jian Lin‡, Mary Ann Weitnauer‡, and Frank Y. Li†
Affiliation:	†Dept. of Information and Communication Technology, University of Agder (UiA), N-4898 Grimstad, Norway ‡School of Electrical and Computer Engineering, Georgia Institute of Technology (GATECH), Atlanta, GA 30332-0250, USA
Conference:	*IEEE International Conference on Communication (ICC) Workshop on Energy Efficiency in Wireless Networks and Wireless Networks for Energy Efficiency (E2Nets)*, June 2014
Copyright ©:	IEEE

ACT-MAC: An Asynchronous Cooperative Transmission MAC Protocol for WSNs

Lakshmikanth Guntupalli, Jian Lin, Mary Ann Weitnauer, and Frank Y. Li

***Abstract* — Duty cycling (DC) has been proven to be an efficient mechanism to reduce energy consumption in wireless sensor networks (WSNs). On the other hand, cooperative transmission (CT) enables longer range transmission to hop over an energy-hole node, resulting in more balanced energy consumption among nodes. In the literature, there exist few CT MAC protocols for DC operated WSNs and these protocols rely on fixed cycle length. In this paper, we propose a novel variable cycle length protocol, namely asynchronous cooperative transmission medium access control (ACT-MAC), which contains both features of reducing the unnecessary idle listening by DC and mitigating the energy-hole by making use of CT. The proposed protocol employs a pseudo random sequence (PRS) generator to produce the variable length cycles. Numerical results show the ACT-MAC protocol's superiority over the existing protocols in terms of network longevity and the energy efficiency.**

I. INTRODUCTION

Avoiding unnecessary energy consumption in order to maximize network lifetime is an essential design principle in battery operated wireless sensor networks (WSNs). Duty cycling (DC) saves energy by allowing sensor nodes to turn their radio on and off periodically. Many medium access control (MAC) protocols [1] - [5] have been proposed to adopt DC to prolong the lifetime of WSNs.

Existing duty cycle MAC protocols proposed for WSNs can be categorized as synchronous and asynchronous protocols. Sensor-MAC (S-MAC) [1], scheduled channel polling MAC (SCP-MAC) [2] and demand-wakeup MAC (DW-MAC) [3] represent synchronous protocols, which typically exchange data during the common active period. A disadvantage of these protocols is that they require precise synchronization, causing more control overhead. A short preamble MAC protocol for duty cycled WSNs (X-MAC) [4]

and receiver initiated MAC (RI-MAC) [5] are asynchronous duty cycle MAC protocols in which each node has its own independent duty cycle schedule. In these protocols, a node which has a packet to transmit wakes up and stays awake until it hears from the receiver. This waiting duration may bring significant latency for packet delivery.

On the other hand, the *energy-hole* is a known problem in multi-hop WSNs in which an intermediate node that is carrying heavier traffic has to consume more energy and consequently exhausts earlier [6]. If this node is the only node connecting two parts of a network, then the network partition occurs as a result of an energy-hole. Generally, the nodes near the sink are heavily burdened and are prone to the energy-hole. To alleviate this problem, cooperative transmission (CT) [7] can be activated [8]. The residual energy activated cooperative transmission (REACT) forwarding protocol proposed in [9] relies on the residual energy information of the nodes to trigger CT. When a parent node has lower residual energy compared with the child node on the route, the child node initiates CT. To perform the CT, the source node collaborates with its neighboring nodes and the collaborators transmit the packet on independent channels toward the destination over a longer distance to reach a two-hop away receiver [7]. As a consequence, the parent node with lower residual energy level is protected. To take advantage of range extension and for energy-hole avoidance, a few MAC protocols which combine both DC and CT have been proposed based on REACT. Among those MAC protocols, CDC-MAC [10] and EECDC-MAC [11] employ concurrent CT (CCT), whereas time division CT (TDCT) is used in SCT-MAC [12] and OSC-MAC [13]. However, these protocols rely on a fixed cycle length.

In this paper, we propose a duty cycling CT MAC protocol with a *variable cycle length*, which is generated by a pseudo random sequence (PRS) generator. The designed protocol is a CT protocol, because it mitigates the energy-hole by using CT. This protocol is an asynchronous MAC protocol, since all nodes maintain their own schedules based on a seed. Correspondingly, we refer to this proposed protocol as an asynchronous CT MAC (ACT-MAC) protocol. PRS is not completely random due to its periodic property [14]. Furthermore, regardless of the number of times the seed is used as an input, the generator produces the same sequence. Therefore, when a node knows the seed number of the receiving node, then it can deduce all the wakeup times

of its receiver in a computationally efficient way. A novel feature of ACT-MAC is the introduction of the *level number* of the node as its seed; meaning that all the sibling nodes contain the same schedule. Moreover, once it has its level number, it automatically knows the level number of its parent node. Therefore, a node can know the wakeup slots of the receiving nodes and wake up at the same time, avoiding idle listening, which is a primary energy consumption factor. Furthermore, exchange of any extra control messages is not required to get another node's schedule. In fact, some existing MAC protocols make use of PRS to generate the schedules [14]. However, those are not CT MAC protocols. We evaluate the performance of the proposed ACT-MAC using both CCT and TDCT schemes. We further compare it with an energy efficient predictive wakeup MAC protocol (PW-MAC) [14], which is also a PRS based protocol. Moreover, we also compare ACT-MAC with SCT-MAC due to the similar feature of selecting the cooperators from the same collision domain.

The rest of this paper is organized as follows. The network model and protocol design consideration are presented in Sec. II. In Sec. III, we present ACT-MAC design in detail. Energy consumption analysis is presented in Sec. IV. Then the system performance is evaluated and compared with other MAC protocols in Sec. V. Finally the paper is concluded in Sec. VI.

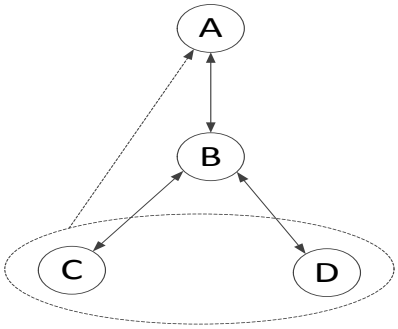

Figure A.1: Network model [11]: A WSN in which C and D may transmit to A directly to diminish energy-hole using CT.

II. Network Model and Protocol Design Considerations

We adopt the same network model from [11] as shown in Fig. A.1. The lowest level nodes are C, D etc., with a parent Node B and two-hop away

parent Node A. Here, we consider Node A as the sink and assume that it is also duty cycling but powered continuously. When the child nodes transmit packets, the parent node forwards them to the sink node. In such a case, the parent node B consumes more energy and dies earlier than the child nodes do. Then the energy-hole occurs and the network is disconnected.

Using CT, Nodes C and D avoid the energy-hole by sending the data to Node A directly. How CCT reaches a two-hop away parent node is demonstrated experimentally in [15] using non-coherent processing. Note that CCT can be performed only when at least two cooperating nodes are active in a common interval. In our design, this is possible since all cooperating nodes are chosen from the same level and wake up during the same pseudo random intervals. In order to produce the same schedules with a seed, it is required to install the same PRS generators at all nodes in the network. The level number for each node is given by the sink node during the network initialization phase.

III. ACT-MAC DESIGN

The basic principle of ACT-MAC is to generate the level number based pseudo random interval wakeup times. Besides, it activates CT for data transmission, if necessary. Similar to the other CT MAC protocols, ACT-MAC utilizes REACT forwarding technique to make the CT or non-CT decision. As in our earlier contribution EECDC-MAC [11], we modify REACT slightly in ACT-MAC. That is, we allow the initiation of CT when the nodes are with equal energy levels to ensure more balanced energy consumption of the receiving node. Therefore, in ACT-MAC, *if the remaining energy of the receiving node E_{rr} is greater than the sending node's remaining energy E_{rs}, then non-CT will be executed otherwise CT is performed*.

During network initialization, the level number is distributed by the sink node. We consider that the sink node is at the highest level. The sink assumes its own level as 0 and broadcasts to its child nodes. Then this number will be increased by 1 at each network level. When the child nodes broadcast their levels, the parent node receives it and knows that it has a child. If a node does not hear anything from any child nodes, then it is the lowest level node in the network. Hence in Fig. A.1, the level numbers of the Nodes A, B are 0 and 1 respectively and the remaining nodes, i.e., C and D, belong to Level 2.

After receiving the level number, nodes generate wakeup schedules and start duty cycling. How the schedules are produced and the rendezvous for CT is achieved are discussed in the following subsections.

A. PRS Based Duty Cycling

The PRS can be generated in many ways. However, for comparison purpose, we consider the linear congruential generator (LCG) which is adopted in PW-MAC [14]. Correspondingly, in ACT-MAC, the LCG generates the sequence of cycle lengths according to

$$X_{n+1} = (\alpha.X_n + \beta)\, mod\, M\,. \tag{A.1}$$

This generator produces the uniformly distributed pseudo random numbers in the range of [0, M-1]. Note that the cycle length generated by (A.1) varies for each iteration. Here, X_n is the previous cycle length and becomes the seed for generating the current cycle length X_{n+1}. The constants, α, β are the multiplier and increment values respectively, and can be set to any integer number between 0 and M-1. Taking X_0 as the initial seed, the combinations of X_0, α, β and M values produce different sequences. ACT-MAC allocates common α, β and M to all nodes, but X_0 is their level number.

Using the level number, a node is able to predict the wakeup schedules of all other levels in the network. A node is awake during its own slot to receive the DATA from child and follows its parent schedule for transmission. Note that, for a parent node, it does not need to calculate the schedule of its child nodes. Furthermore, the child nodes generate all the higher level node's schedules to wake up for CT. In the considered network, all the Level 2 nodes use Node B's schedule for data transmission. Since 2 is the lowest level, they do not wakeup in their own slots in order to save energy. Moreover, they use Node A's schedule when CT is performed.

B. Asynchronous Cooperative Transmission

ACT-MAC uses a receiver initiated approach for data transmission, which is similar to other asynchronous MAC protocols such as RI-MAC and PW-MAC. An advantage of this beacon based receiver initiated (RI) method is that it reduces the duty cycle at the receiver. A benefit of using the predictive wakeup (PW) mechanism is that it makes a reduction in duty cycle at the sender side. Therefore, combining both RI and PW achieves higher energy

efficiency. Thus, in ACT-MAC, when a sender has a packet to transmit, it wakes up at the receiver's wakeup slot and avoids unnecessary idle listening by the sender. Fig. A.2 shows the duty cycles of all nodes in the network. In the figure, the slot in which the non-CT transmission occurs is *non-CT* (NCT) slot. A *CT-decision* (CT-D) is a regular non-CT slot, but in which the CT decision is made. A slot where the actual CT transmission occurs is referred to as a CT slot. The rest of this subsection discusses the operations performed in each of the above mentioned slots.

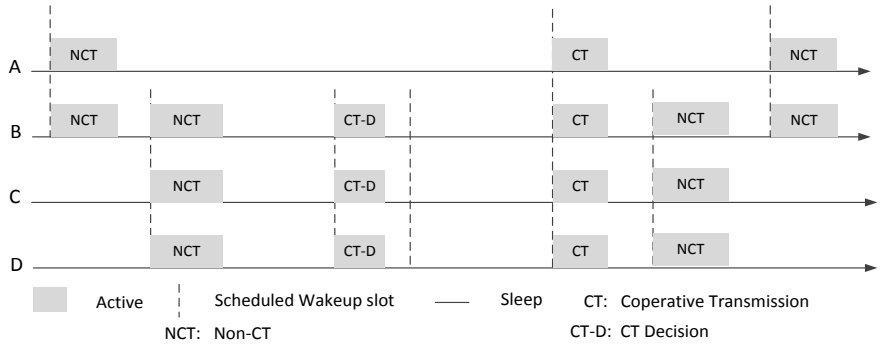

Figure A.2: Duty cycle of receiver and cooperator nodes in ACT-MAC.

To initiate transmission, Receiver B from Fig. A.1, sends a beacon with its residual energy information (BE). Then the sending nodes, e.g., C and D in the same figure, receive BE and compare the energy value with their own energy levels. After CT or non-CT decision is made, those nodes compete for channel access to transmit the DATA frame. For non-CT, DATA is transmitted within the same wakeup slot after the decision is taken. Whereas for CT, the decision is made in the CT-decision slot and DATA is transmitted in the CT slot. Remember that the non-CT slots between CT-decision and CT slot are not used for data transmission as shown in Fig. A.2. Furthermore, ACT-MAC allows only one packet transmission in a CT slot. Consequently, it may produce a significant delay. On the other hand, it achieves remarkable energy efficiency. For that reason, our ACT-MAC protocol applies better to delay tolerant sensor applications such as habitat monitoring [12]. To transmit the DATA in CT, ACT-MAC adopts either the CCT or the TDCT scheme. To perform CCT, the CT initiator node multicasts DATA to helpers as the first step. Then, both nodes perform the concurrent transmission after a SIFS interval. Whereas in TDCT, the CT initiator node broadcasts the

DATA frame first. Then the cooperating node retransmits it again to the two-hop-away parent node. Thus, the main difference between these two schemes is that the CT initiator node transmits the DATA twice in CCT and once in TDCT. To decode the incoming DATA, the two-hop parent node uses Maximum Ratio Combining (MRC) [12]. The MAC procedures for both schemes are described in the following paragraphs as shown in Figures 3-6 in both CT-decision and CT slots.

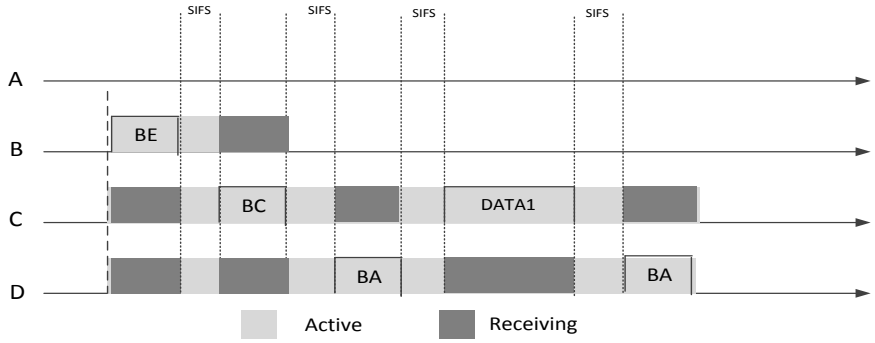

Figure A.3: CT-D slot for CCT in ACT-MAC.

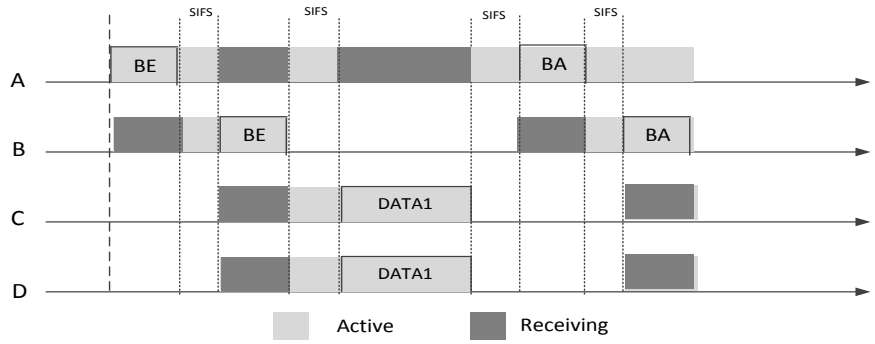

Figure A.4: CCT in ACT-MAC.

1) CT Decision Slot: When the winning node, for example Node C, decides to transmit the DATA using CT, it broadcasts a beacon for cooperation (BC) message. Upon receiving the BC, the cooperator Node D replies with a beacon of acknowledgment (BA) while the receiving node B goes to sleep. Fig. A.3 shows the steps performed in CT-decision slot for CCT. As shown in the figure, in response to the BA, Node C sends the DATA packet to Node D. After the helping node replies with BA, both nodes go to sleep and wake up again at the CT slot. In case of TDCT from Fig. A.5, Node C sends BC and Node D replies with BA and both nodes go to sleep.

2) CT Slot: After this CT agreement, all nodes wake up at Node A's active slot. Similarly, the beacon transmission procedure is followed by Node A as well. In its designated wakeup slot, Node A sends a BE to the sending nodes via Node B. Note that Nodes C and D delay their wakeup time by the duration of BE to avoid idle listening. Similarly, Node B is allowed to sleep for the duration of (2DATA + 2SIFS) to eliminate the unnecessary energy consumption. However, this node needs to wake up again to forward the BA from Node A to its child node. In case of CCT from Fig. A.4, nodes C and D transmit the DATA at the same time. For TDCT, however, Node C broadcasts DATA first as shown in Fig. A.6. Then Nodes D sends it again after a SIFS interval.

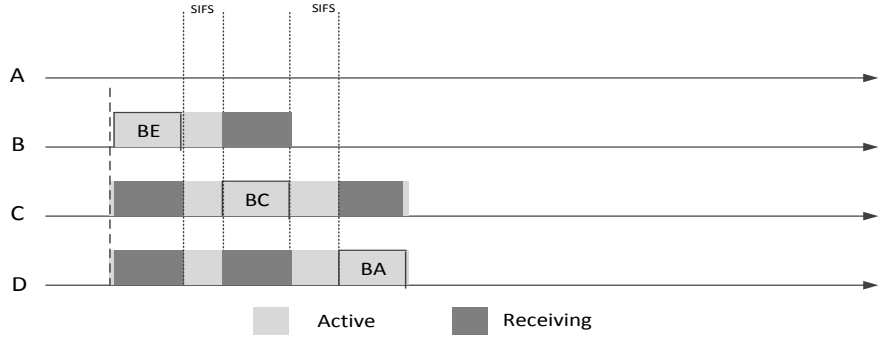

Figure A.5: CT-D slot for TDCT in ACT-MAC.

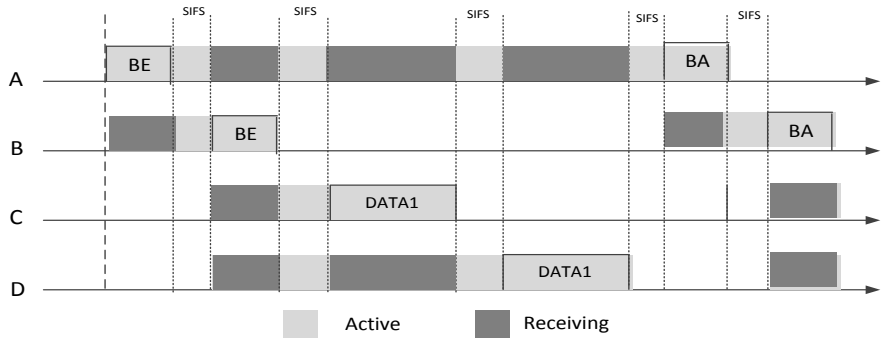

Figure A.6: TDCT in ACT-MAC.

3) non-CT Slot: For non-CT transmission, as shown in Fig. A.7, Node C sends its DATA first. Meanwhile, the other node sleeps for the duration of (DATA+ BA + 2SIFS). Then, it wakes up and applies the backoff scheme for its data transmission. In the non-CT phase, a node goes to sleep after the DATA frame is sent in current cycle and wakes up in the next cycle.

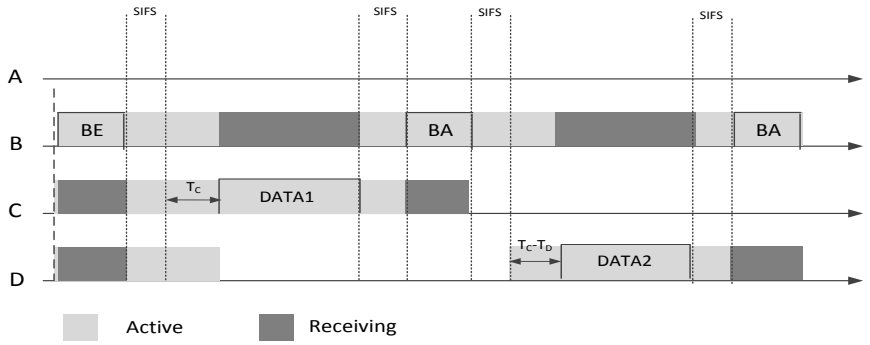

Figure A.7: Non-CT within the same wakeup slot in ACT-MAC.

C. Prediction Error Correction

To handle the clock-drift during the network operation, we follow the same *on demand prediction error correction mechanism* as mentioned in PW-MAC. In this method, the sender requests an update periodically by setting a flag in the DATA frame. Then the receiver replies with a beacon including update in addition to the acknowledgment. We refer to this beacon as beacon with prediction update (BU). Based on the provided information, the sending node adjusts its wakeup time in order to synchronize with the receiving node active slot. In PW-MAC, this BU contains the seed of receiver (2 bytes), the time difference between sender and receiver (4 bytes), and the last wakeup time of receiver (4 bytes). However, ACT-MAC does not require having the seed in BU, since it is already known.

IV. Energy Consumption Analysis

We analyze the energy performance of ACT-MAC in this section. The analysis is based on the two hop network model described in Sec. II where each node generates packets of fixed size at a variable length pseudo random interval T_{cycle}. In this analysis, we focus on the energy consumed by the radio and the energy spent by the other components such as CPU or sensors is not included in our calculation.

Consider five radio states: transmitting, receiving, listening, idle and sleeping; each drawing the power of P_{tx}, P_{rx}, P_{listen}, P_{idle} and P_{sleep} respectively. The radio transition costs from one state to another state are ignored, since the ON periods for data transfer are assumed to be long enough to render transition costs negligible. The energy consumption of the radio is determined by how much time it spends in the transmitting, receiving, listening, idle

Table A.1: Networking Parameters

Parameter	*Meaning*	*Value*
P_{tx}	Power in transmitting	31.2 mW
P_{rx}	Power in receiving	22.2 mW
P_{listen}	Power in listening	22.2 mW
P_{idle}	Power in idle state	22.2 mW
P_{sleep}	Power in sleeping	33 μW
T_{cs}	Average carrier sense time	7 mW
T_B	Time to T_x/R_x a byte	4163 μs
T_{sifs}	SIFS time slot	5 ms
L_{data}	Data packet length	Varying
L_{be}	Beacon length	10 bytes
$L_{ba/bc}$	Ack/cooperation beacon length	8 bytes
T_{data}	$L_{data}T_B$	Varying
T_{be}	$L_{be}T_B$	8.32 ms
$T_{ba/bc}$	$L_{ba/bc}T_B$	5.82 ms
N_c	Number of cooperator nodes	2

and sleeping modes denoted as T_{tx}, T_{rx}, T_{listen}, T_{idle} and T_{sleep} respectively. The time with radio being asleep is simply sleep time and is given by

$$T_{sleep} = T_{cycle} - T_{tx} - T_{rx} - T_{listen} - T_{idle}. \tag{A.2}$$

In order to compare our results with that of the other earlier protocols, we keep all the terms and the typical values based on the Mica2 radio (Chipcon CC1000 [3]) as listed in Table A.1. For ACT-MAC, the energy consumption, per node, is the sum of the energy spent in each state:

$$\begin{aligned} E &= E_{cs} + E_{tx} + E_{rx} + E_{idle} + E_{sleep} \\ &= P_{listen}T_{cs} + P_{tx}T_{tx} + P_{rx}T_{rx} + P_{idle}T_{idle} + P_{sleep}T_{sleep}\,. \end{aligned} \tag{A.3}$$

Note that the node has to perform carrier sensing before transmitting any packet. Furthermore, an interval of SIFS is maintained between any two consecutive transmissions. This calculation is done for two schemes: CCT and TDCT, since CT in ACT-MAC is performed in one of these schemes. Remember that the receiving node, i.e., the parent node, consumes the same energy in TDCT as it does in CCT during the CT period. However, the energy consumed by a CT initiator node in CCT is higher than it does in TDCT.

The energy consumed by a node in each slot can be calculated from the corresponding figures. For example, the energy consumption by the CT initiator, Node C in Fig. A.1, in a CT cycle is derived below.

In the CT-decision slot, the initiating node, has to receive one BE message and broadcasts the BC. After receiving the cooperating node's reply with the BA, it multicasts the DATA packet as shown Fig. A.3. During the CT slot shown in Fig. A.4, it sends the same data packet again following the CCT in cooperation with cooperators. Of course, it should receive a BE from the sink node via its parent node. After the completion of data transmission, the node receives the ACK message for the sent DATA. Then,

$$\begin{aligned} T_{tx} = T_{bc} + 2T_{data}\,, \quad T_{rx} = 2T_{be} + 3T_{ba}\,, \quad T_{idle} = 5T_{sifs}\,, \\ T_{sleep} = T_{cycle} - T_{cs} - (T_{bc} + 2T_{data}) - (2T_{be} + 3T_{ba}) - 5T_{sifs}\,. \end{aligned} \tag{A.4}$$

Substituting (A.4) into (A.3), the energy consumed by Node C as a CT intiating node in CT is obtained by,

$$\begin{aligned} E_{nodect} = {} & P_{listen}T_{cs} + P_{tx}(T_{bc} + 2T_{data}) \\ & + P_{rx}(2T_{be} + 3T_{ba}) + P_{idle}(5T_{sifs}) \\ & + P_{sleep}(T_{cycle} - T_{cs} - T_{bc} - 2T_{data} - 2T_{be} - 3T_{ba} - 5T_{sifs}). \end{aligned} \tag{A.5}$$

Similarly, the parent node's energy consumption can be obtained from Fig. A.3 and Fig. A.4. The energy spent by the parent and CT initiating node in TDCT can be calculated from Fig. A.5 and Fig. A.6. Moreover, the energy consumed by both parent and CT initiating nodes in non-CT can be estimated from Fig. A.7.

V. Performance Evaluation

To demonstrate the efficacy of the proposed protocol, the results for ACT-MAC are compared with PW-MAC and SCT-MAC. The results presented in this section are evaluated using MATLAB based on the analysis in Sec. IV. We use the same LCG to evaluate the performance of PW-MAC. The generated cycle lengths are in between 1 and 9 seconds. The values of α, β are cofigured as 1 and 2 respectively. However, according to the design of

PW-MAC, a BU has to contain all the values α, β, M and X0 of the receiver node, and as mentioned in [14], 10 bytes is required in addition to the base beacon size of 6 bytes [5]. Hence, the BU size in PW-MAC is 16 bytes. In ACT-MAC, we add 4 bytes to include the residual energy information in a BE. Thus, the BE size in the proposed protocol is 10 bytes, while the BU size is 18 bytes as explained in Sec. II. However, the BA size is same in both protocols and is 8 bytes [5]. In order to compare our protocol with others, SCT-MAC is evaluated using the mean of the produced pseudo random sequence and the other information required is taken from [12]. The SH packet in SCT-MAC works similar to the beacon in our protocol. However, the size is 14 bytes since it contains a number of CT and non-CT reservations in the current cycle. Moreover, we have neglected the energy consumption in the initialization phase for all studied protocols.

A. Comparing with Asynchronous MAC Protocol

Fig. A.8 illustrates the lifetimes of Nodes B, C and D in Fig. A.1 for the two studied asynchronous protocols. The first observation is that the lifetime of the parent node is shorter when compared with its child nodes in PW-MAC and both child nodes have the same lifetime. This is obvious since the PW-MAC's parent node is heavily loaded in serving both of its children as a non-CT protocol, and the child nodes share the same load. ACT-MAC exhibits the advantage of CT clearly in the nodal lifetime. The energy is balanced among the parent and initiating nodes and they exhaust at the same time. In this paper, we adopt the network lifetime definition as the lifetime of the first exhausted node. Accordingly, from the network lifetime point of view, ACT with CCT scheme has achieved 151.55% longer network lifetime when compared with the PW-MAC protocol.

B. Comparing CT Schemes

To analyze the energy balancing nature further, ACT-MAC, is evaluated using the TDCT scheme also. Fig. A.8 shows the lifetime comparison of both CCT and TDCT schemes for ACT-MAC. In this figure, CCT exhibits the superiority in terms of balancing the node energy consumption in comparison with the TDCT scheme. Remember that, protecting the energy constraint node by CT is achieved at the cost of consuming more energy of the other nodes. This fact is confirmed when TDCT is used. In TDCT, the cooperator node spends energy in transmitting the packet again to the sink node after re-

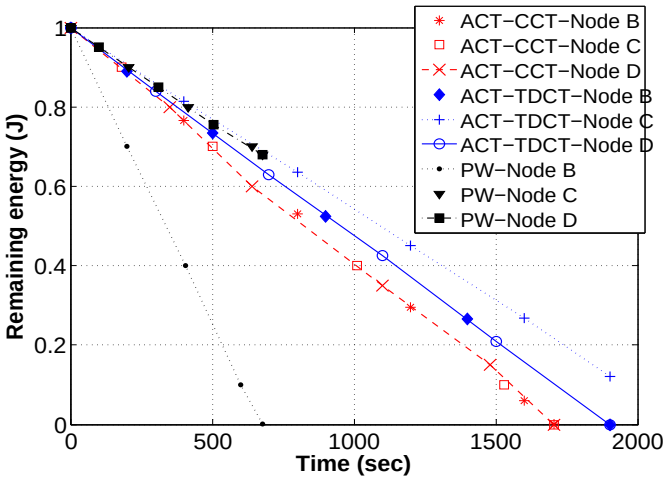

Figure A.8: Lifetime comparison of ACT-MAC and PW-MAC protocols.

ceiving it from the CT initiating node. Whereas the CT source node transmits the packet only once. So, it consumes lower energy than the helping node. This energy difference creates the imbalance in the nodal lifetime when CT is used more often. Since in CCT the energy expenses are shared among the CT source and cooperating nodes almost equally, CCT achieves more balanced energy consumption. Nonetheless, TDCT has achieved 9% longer network lifetime.

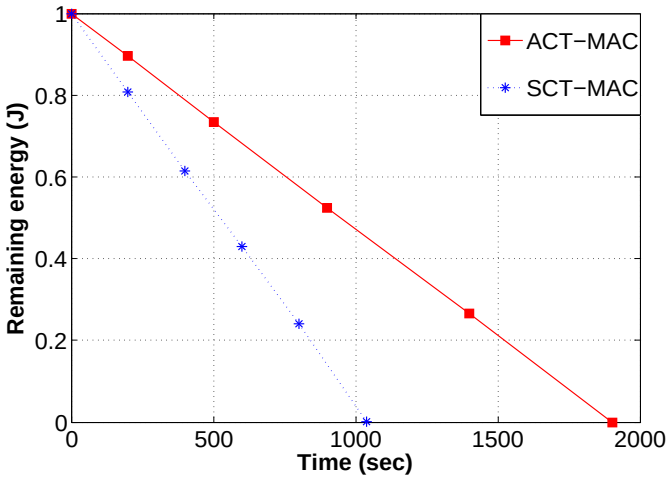

Figure A.9: Lifetime comparison of ACT-MAC (with TDCT) and SCT-MAC.

C. Comparing with the SCT MAC Protocol

We further compare ACT-MAC with the SCT-MAC protocol. In order to compare them fairly, we use TDCT in ACT-MAC here, since SCT-MAC is also based on TDCT. Fig. A.9 represents the lifetime of parent nodes of

the ACT and SCT- MAC protocols, which is the network lifetime of TDCT. Again, ACT-MAC achieves 81.714% longer lifetime over SCT-MAC. This shorter lifetime for the SCT protocol is due to the synchronization overhead.

D. Comparing Energy Efficiency

In this study, we define energy efficiency as the number of successfully delivered information bits per consumed joule of energy. The number of bits delivered during the network lifetime by these three protocols per unit joule energy with different packet sizes is shown in Fig. A.10. The packet size is varied from 50 bytes to 250 bytes considering the maximum packet size supported by CC1000 radios [3]. Clearly the energy efficiency is increased with larger packet size for all these three protocols. Furthermore, more bits are transmitted by ACT-MAC per unit joule of energy due to longer lifetime. The percentage increase in ACT-MAC's energy efficiency with DATA packet size is illustrated in Table A.2. When the packet size is 100 bytes, ACT-MAC has 21.66% and 51.18% higher energy efficiency compared with SCT-MAC and PW-MAC respectively.

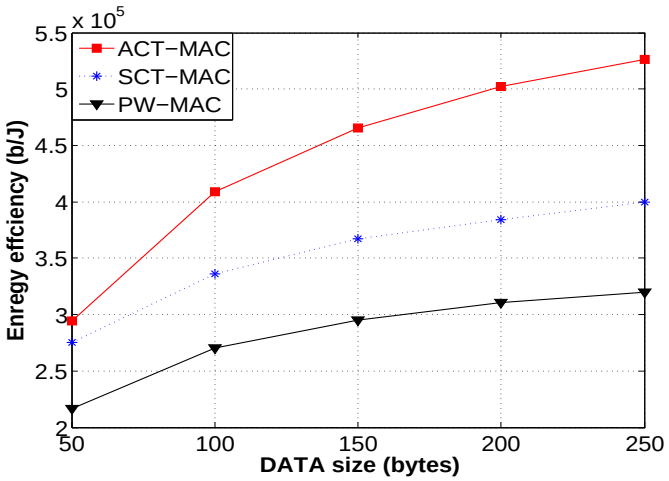

Figure A.10: Energy efficiency comparison of the ACT-MAC, SCT-MAC and PW-MAC protocols.

V. CONCLUSIONS

In this paper, we have presented ACT-MAC, an asynchronous cooperative transmission (CT) MAC protocol for duty cycling (DC) WSNs. The pro-

Table A.2: Percentage Increase in ACT-MAC's Energy Efficiency When Compared to SCT-MAC and PW-MAC Protocols

L_{data} (bytes)	50	100	150	200	250
SCT-MAC	6.97	21.66	26.79	30.38	31.50
PW-MAC	35.79	51.18	57.72	61.85	64.37

posed protocol employs a pseudo random generator to schedule the wakeup slots of all nodes based on their level numbers. This feature makes the proposed protocol asynchronous. Using the level number as the initial seed, this protocol integrates CT with asynchronous DC. The results demonstrate that the energy consumption levels of sensor nodes are evenly distributed in the network by using ACT-MAC. Furthermore, due to the absence of synchronization overhead, ACT-MAC could achieve longer lifetime. Consequently, higher energy efficiency is achieved when compared with the synchronous SCT-MAC protocol. Finally, since the scheduling is based on a level number, ACT-MAC is expected to apply to large scale WSNs.

REFERENCES

[1] W. Ye, J. Heidemann, and D. Estrin, "Medium access control with coordinated adaptive sleeping for wireless sensor networks," IEEE/ACM Transactions on Networking, vol. 13, no. 3, June 2004.

[2] W. Ye, F. Silva, and J. Heidemann, "Ultra-low duty cycle MAC with scheduled channel polling," in Proc. of ACM SenSys, Boulder, Colorado, USA, Nov. 2006.

[3] Y. Sun, S. Du, O. Gurewitz, and D. B. Johnson, "DWMAC: A low latency, energy efficient demand-wakeup MAC protocol for wireless sensor networks", in Proc. ACM MobiHoc, Hong Kong, May 2008.

[4] M. Buettner, G. V. Yee, E. Anderson, R. Han, "X-MAC: a short preamble MAC protocol for duty-cycled wireless sensor networks," in Proc. of ACM SenSys, Boulder, Colorado, USA, Nov. 2006.

[5] Y. Sun, O. Gurewitz, and D. B. Johnson, "RI-MAC: A receiver initiated asynchronous duty cycle MAC protocol for dynamic traffic loads

in wireless sensor networks," in Proc. of ACM SenSys, Raleigh, NC, USA, Nov. 2008.

[6] J. Li and P. Mohapatra, "An analytical model for the energy hole problem in many-to-one sensor networks," in Proc. IEEE VTC 2005-Fall, Dallas, TX, USA, Sept. 2005.

[7] J. N. Laneman, D. N. C. Tse, and G. W. Wornell, "Cooperative diversity in wireless networks: Efficient protocols and outage behavior," IEEE Transactions on Information Theory, vol. 50, no. 12, pp. 3062-3080, 2004.

[8] J. W. Jung and M. A. Weitnauer, "On using cooperative routing for lifetime optimization of multi-hop wireless sensor networks: analysis and guidelines," IEEE Transactions on Communications, Vol. 61, No. 8, pp. 3413 - 3423, May 2013.

[9] J. W. Jung and M. A. Ingram, "Residual-Energy-Activated Cooperative Transmission (REACT) to avoid the energy hole," in Proc. of IEEE ICC Workshop on Cooperative and Cognitive Mobile Networks (CoCoNet3), Cape Town, South Africa, May 2010.

[10] H. Jiao, M.A. Ingram and F.Y. Li, "A cooperative lifetime extension MAC protocol in duty cycle enabled wireless sensor networks," in Proc. of IEEE MILCOM, Baltimore, MD, USA, 7-10 Nov. 2011.

[11] L. Guntupalli, F. Y. Li, X. Ge, "EECDC-MAC: An energy efficient cooperative duty cycle MAC protocol," in Proc of IEEE/IFIP Wireless Days, Dublin, Ireland, Nov. 2012.

[12] J. Lin and M. A. Ingram, "SCT-MAC: A scheduling duty cycle MAC protocol for cooperative wireless sensor network", in Proc. IEEE ICC, Ottawa, Canada, June 2012.

[13] J. Lin and M. A. Ingram, "OSC-MAC: Duty cycle scheduling and cooperation in multi-hop wireless sensor networks", in Proc. of IEEE WCNC, Shanghai, China, April 2013.

[14] L. Tang, Y. Sun, O. Gurewitz and D. B. Johnson, “PW-MAC: An energy-efficient prediction-wakeup MAC protocol for wireless sensor networks", in Proc. of IEEE INFOCOM, Shanghai, China, April 2011.

[15] H. Jung, Y. J. Chang, and M. A. Ingram, “Experimental range extension of concurrent cooperative transmission in indoor environments at 2.4 GHz,” in Proc. of IEEE MILCOM, San Jose, CA, USA, Nov. 2010.

Paper B

Title:	Event-Triggered Sleeping for Synchronous DC MAC in WSNs: Mechanism and DTMC Modeling
Authors:	Lakshmikanth Guntupalli†, Frank Y. Li†, and Jorge Martinez-Bauset‡
Affiliation:	†Dept. of Information and Communication Technology, University of Agder (UiA), N-4898 Grimstad, Norway ‡Dept. of Communications, Universitat Politècnica de València (UPV), 46022 València, Spain
Conference:	*IEEE Global Communications Conference (GLOBECOM)*, December 2016 (accepted)
Copyright ©:	IEEE

An Event-Triggered Sleeping for Synchronous DC MAC in WSNs: Mechanism and DTMC Modeling

Lakshmikanth Guntupalli, Frank Y. Li, and Jorge Martinez-Bauset

Abstract — **Overhearing and idle listening are two primary sources for unnecessary energy consumption in wireless sensor networks. Although introducing duty cycling in medium access control (MAC) reduces idle listening, it cannot avoid overhearing in a network with multiple contending nodes. In this paper, we propose an event-triggered sleeping (ETS) mechanism for synchronous duty-cycled (DC) MAC protocols in order to avoid overhearing when a node is not active. This ETS mechanism applies to any synchronous DC MAC protocols and makes them more energy efficient. Furthermore, we develop a two dimensional discrete time Markov chain model to evaluate the performance of the proposed ETS mechanism by integrating it to a popular synchronous DC MAC protocol namely sensor-MAC. Using the developed model, energy consumption, energy efficiency and network lifetime are calculated. Numerical results obtained through both analytical model and discrete-event simulations demonstrate the effectiveness of the ETS mechanism, represented by lower energy consumption, higher energy efficiency and longer lifetime when compared with the conventional control packet triggered sleeping mechanism.**

I. INTRODUCTION

Wireless sensor networks (WSNs) support a wide range of applications including event detection, monitoring, target tracking, etc [1]. The lifetime of a sensor node in such WSNs depends on the capacity of its battery as well as how energy is consumed. Clearly, the battery capacity is fixed and cannot be recharged without energy harvesting. In some applications such as hostile environment monitoring, replacing node batteries might not be feasible or is too costly. Therefore, an energy consumption efficient medium access control (MAC) protocol plays an important role for network lifetime prolongation since the energy consumption activities are determined by MAC. An energy

efficient MAC protocol reduces unnecessary energy consumption by avoiding idle listening and/or overhearing experienced by nodes. For instance, idle listening can be minimized by employing a duty-cycled (DC) MAC protocol which allows nodes sleep for a while when no activities are needed in order to conserve energy. On the other hand, wake-up radio has emerged in recent years as an efficient technique for reducing energy consumption in WSNs [2].

For DC enabled WSNs, synchronous MAC has been a popular category for MAC design [3] [4]. With such MAC protocols, nodes are aligned to wake up and sleep periodically according to a predefined schedule. This schedule is exchanged among neighboring nodes when they are awake in the specified duration, regarded as a *sync* period. Data exchange is then performed in the following *data* period, after which a *sleep* period starts. The whole duration consisting of a successive *sync*, *data* and *sleep* period forms one *cycle*. Synchronization is done in the *sync* period and then nodes compete for medium access and perform data exchange during the *data* period. The duration of the sleep period for each node varies, depending on it wins medium access competition or not. A winning node goes to sleep after completing its transmission, and a node which lost access competition starts to sleep earlier after it receives a control packet indicating that another node has started to transmit. In all synchronous DC MAC protocols including Sensor-MAC (S-MAC) [3], a node initiates a data packet transmission using control packets, but those control packets are named differently in various protocols. The duty cycling principle adopted in the synchronous DC protocols mitigates idle listening, but could not avoid overhearing in the *data* period, as explained in the following sub-section.

A. Problem Statement

Typically in synchronous DC enabled WSNs, nodes follow the carrier sense multiple access with collision avoidance (CSMA/CA) mechanism for packet transmission during the *data* period. In a network or a network cluster with multiple nodes, all nodes that have packets to transmit contend for channel access in order to send their packets to a single cluster-head or a sink node. However, only one node wins channel access and transmits first a control packet, i.e., the request to send (RTS) packet in CSMA/CA, informing the other neighboring nodes that it is going to transmit. Upon overhearing this control packet, the other nodes go to sleep. This sleeping mechanism

is hereafter referred to as control packet triggered (CPT) sleeping mechanism. *In CPT, an inactive node, i.e., a node that does not have any packets to send, still needs to wait until it overhears a control packet before going to sleep*. For example, when no node is active in a network, all nodes need to be awake for the whole duration of the *data* period, leading to high energy consumption.

B. Contributions

In this paper, we propose an event-triggered sleeping (ETS) mechanism to address the overhearing problem occurring in CPT. The main idea of the ETS mechanism is to allow nodes that do not have a packet to send sleep right after the *sync* period without participating in medium access contention. Thus, such a node can sleep longer for the rest of the same cycle, and it consequently saves energy. The ETS mechanism applies to any synchronous DC protocols and suits ideally for WSN scenarios with low traffic rate, for instance in event-triggered monitoring and surveillance applications.

To evaluate the performance of ETS, we develop a two dimensional (2D) discrete time Markov chain (DTMC) model to analyze ETS operating jointly with S-MAC protocol. This 2D DTMC tracks the evolution of both the number of packets in the buffer of a node and the number of active nodes in the cluster. Different from the existing one dimensional DTMCs considering only the number of packets in a queue [5] or obtaining the distribution of active nodes from another additional DTMC [6], the developed 2D DTMC determines the distributions for both the number of packets and the number active nodes. Using the obtained distributions, energy consumption, energy efficiency and the lifetime of a node are calculated. Moreover, the 2D DTMC model results are validated through discrete-event simulations.

The rest of the paper is organized as follows. In Sec. II, we present the network model and the details of ETS along with an overview of S-MAC. Sec. III describes the proposed 2D DTMC model, followed by the energy consumption analysis in Sec. IV. Numerical results are demonstrated in Sec. V, before the paper is concluded in Sec. VI.

II. Scenario and Event-Triggered Sleeping

This section presents the operation of ETS over S-MAC and the network scenario along with assumptions.

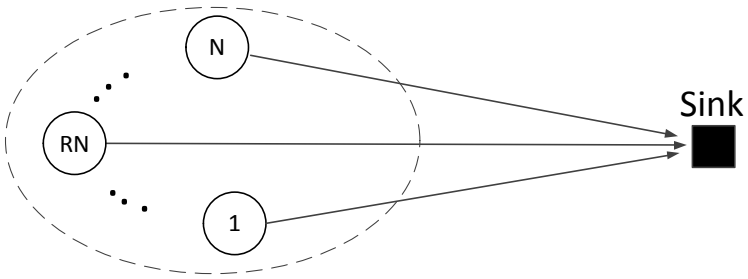

Figure B.1: A WSN with multiple contending nodes and a sink.

A. Sensor Network Scenario

In typical WSN applications, nodes collect data from a sensing field and transmit them to a sink. Within such a scenario, we consider a cluster of N sensor nodes, each with a queue capacity of Q packets. Nodes sense activities around them and generate packets according to the Poisson distribution. The neighboring nodes send their packets towards one common destination, the *sink*, over an error-free channel by competing with each other, as shown in Fig. B.1. Nodes containing packets to transmit are regarded as active nodes and the other are inactive ones. For analysis convenience, we select one of the N nodes arbitrarily and refer to it as the reference node (RN). Hereafter, *DATA*, *SYNC*, *RTS* and *CTS* represent packets and the different parts of a cycle are denoted as *sleep*, *sync*, and *data* respectively.

B. ETS Operation in S-MAC

Consider that nodes in a WSN may stay as inactive in some cycles and become active in other cycles. ETS lets all inactive nodes sleep immediately after the *sync* period in order to save energy. However, both active and inactive nodes have to wake up in every *sync* period to maintain each other synchronized. Fig. B.2 illustrates the operation of S-MAC with a comparison of the ETS and CPT sleeping mechanisms. In ETS, an inactive node does not participate in medium access competition and therefore its sleep period becomes longer, as shown in the figure. In CPT, instead, an inactive node has to wait until an RTS packet is received before it goes to sleep. Note however that *only active nodes compete for channel access in both mechanisms*. Assume that the RN is the winner of the contention among N nodes inside one cluster. After gaining channel access, the RN transmits an *RTS* to the sink. This *RTS* control packet triggers all other active nodes to go to sleep.

For channel access, all *active* nodes generate a random backoff time uni-

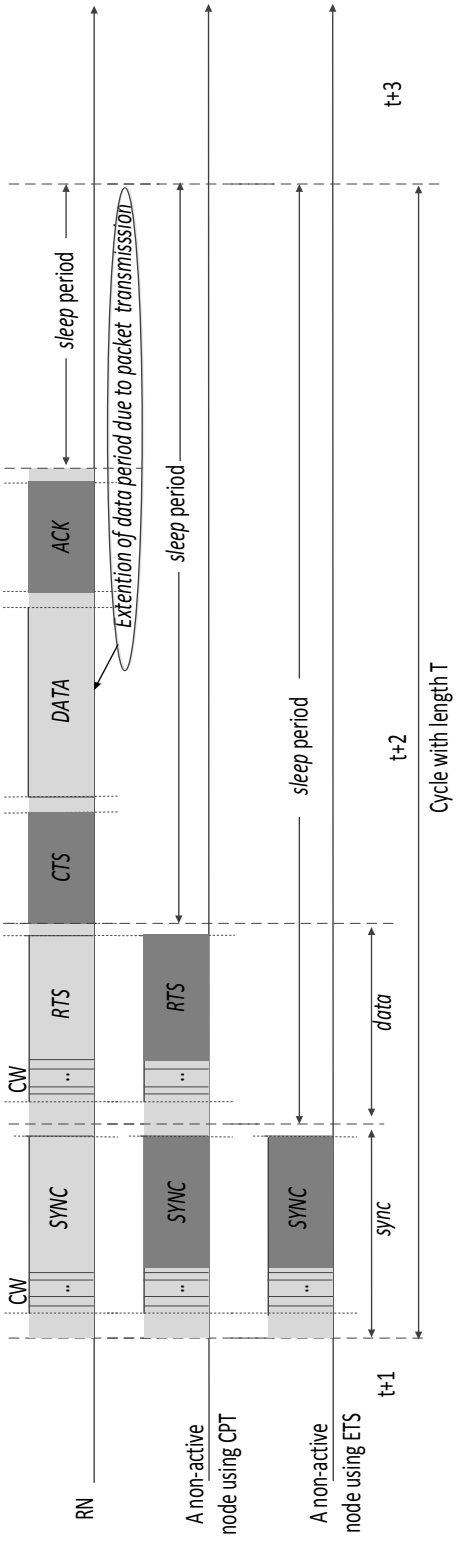

Figure B.2: Operation of S-MAC with ETS and CPT. In ETS, a non-active node goes to sleep right after the *sync* period. In CPT, a non-active node which lost channel access contention starts to sleep after the *data* period. The spaces without symbols are inter frame spaces.

formly from window $\{0, W-1\}$ in the beginning of every *data* period. If the smallest backoff time is selected by only one node, then that node wins channel access and reserves the medium for *DATA* transmission in the corresponding *sleep* period. If a node selects a backoff time which is not the smallest one, it loses the competition and waits until the next *data* period to compete again. In case that two or more nodes select the same smallest backoff time, there will be a collision.

Consider $k+1$ active nodes including the RN in a cycle. When the RN is contending with other k, where $0 \leq k \leq N-1$, nodes, the probabilities that the RN transmits a packet successfully, $P_{s,k}$, transmits a packet (successfully or collided), $P_{sf,k}$, and failed (collided), $P_{f,k}$, are given by $P_{s,k} = \sum_{i=0}^{W-1} \frac{1}{W} \left(\frac{W-1-i}{W} \right)^k$, $P_{sf,k} = \sum_{i=0}^{W-1} \frac{1}{W} \left(\frac{W-i}{W} \right)^k$, $P_{f,k} = P_{sf,k} - P_{s,k}$ respectively. Correspondingly the average successful backoff time is determined by $BT_{s,k} = \frac{1}{P_{s,k}} \sum_{i=0}^{W-1} i \cdot \frac{1}{W} \left(\frac{W-1-i}{W} \right)^k$, while the unsuccessful one becomes $BT_{f,k} = \sum_{i=0}^{W-1} i \cdot \left[\left(\frac{W-i}{W} \right)^k - \left(\frac{W-1-i}{W} \right)^k \right]$.

III. A 2D DTMC Model for ETS

A state in the 2D DTMC is represented by (i,k), where i is the number of packets in the queue of the RN, $i \leq Q$, and k is the number of active nodes other than the RN in the network, $k \leq K = N-1$. Express the probability of arriving i packets to a node with an arrival rate of λ in a cycle of length T as $A_i = (\lambda T)^i \cdot e^{-\lambda T}/i!$. Then the probability of arriving i or more packets is $A_{\geq i} = 1 - \sum_{j=0}^{i-1} A_j$. When k nodes compete in a cycle, the probability of transmitting a packet successfully is $S_k = kP_{s,k-1}$ and the probability for a collision is $\widehat{S}_k = 1 - S_k$. Furthermore, when there is a successful transmission, the probability that a node's queue becomes empty is $P_e = P_s A_0 \pi_1 / P_s (1-\pi_0)$ and $\widehat{P}_e = 1 - P_e$ is the probability that it remains non-empty, where P_s is the probability of successful transmission, π_0 and π_1 are the stationary probabilities that the node's queue has '0' and '1' packet, respectively. Consider $B_k(l) = \binom{l}{k} \widehat{A}^k A_0^{l-k}$ as the probability that k out of l nodes which have their queues empty to receive packets in a cycle, where $\widehat{A} = 1 - A_0$. Then, $P_{(i,k),(j,l)}$ is the transition probability from State (i,k) to State (j,l). The transition probabilities of the proposed 2D DTMC are given in Table B.1.

Table B.1: Transition Probabilities of the DTMC Model for S-MAC enabled with ETS

$P_{(0,0),(j,l)} = B_l(K)\cdot A_j;\ 0 \le j \le Q-1,\ 0 \le l \le K,$	No active nodes. Transitions occur due to new arrivals	$P_{(0,0),(Q,l)} = B_l(K)\cdot A_{\ge Q};\ 0 \le l \le K.$
$P_{(0,k),(j,l)} = S_k \cdot P_e \cdot B_{l-k+1}(K-k)\cdot A_j$ $+S_k\cdot \widehat{P}_e \cdot B_{l-k}(K-k)\cdot A_j;$ $+\widehat{S}_k \cdot B_{l-k}(K-k)\cdot A_j;$ $0 \le j \le Q-1,\ 1 \le k \le l \le K-1,$	RN is a non-active node. Transitions caused by other active nodes	$P_{(0,k),(Q,l)} = S_k \cdot P_e \cdot B_{l-k+1}(K-k)\cdot A_{\ge Q}$ $+S_k\cdot \widehat{P}_e \cdot B_{l-k}(K-k)\cdot A_{\ge Q};$ $+\widehat{S}_k \cdot B_{l-k}(K-k)\cdot A_{\ge Q};$ $1 \le k \le l \le K-1,$
$P_{(0,k),(j,k-1)} = S_k \cdot P_e \cdot B_0(K-k)\cdot A_j;$ $0 \le j \le Q-1,\ 1 \le k \le K,$		$P_{(0,k),(Q,k-1)} = S_k \cdot P_e \cdot B_0(K-k)\cdot A_{\ge Q};\ 1 \le k \le K,$
$P_{(0,k),(j,K)} = S_k \cdot \widehat{P}_e \cdot B_{K-k}(K-k)\cdot A_j;$ $+\widehat{S}_k \cdot B_{K-k}(K-k)\cdot A_j;$ $0 \le j \le Q-1,\ 1 \le k \le K,$		$P_{(0,k),(Q,K)} = S_k \cdot \widehat{P}_e \cdot B_{K-k}(K-k)\cdot A_{\ge Q};$ $+\widehat{S}_k \cdot B_{K-k}(K-k)\cdot A_{\ge Q};$ $1 \le k \le K.$
$P_{(i,0),(j,l)} = P_{s,0}\cdot B_l(K)\cdot A_{j-i+1}$ $+(1-P_{s,0})\cdot B_l(K)\cdot A_{j-i};$ $1 \le i \le j \le Q-1,\ 0 \le l \le K,$	RN is the only active node	$P_{(i,0),(Q,l)} = P_{s,0}\cdot B_l(K)\cdot A_{\ge Q-i+1}$ $+(1-P_{s,0})\cdot B_l(K)\cdot A_{\ge Q-i};$ $1 \le i \le Q,\ 0 \le l \le K,$
$P_{(i,k),(j,l)} = P_{s,k}\cdot B_{l-k}(K-k)\cdot A_{j-i+1}$ $+kP_{s,k}\cdot P_e \cdot B_{l-k+1}(K-k)\cdot A_{j-i}$ $+kP_{s,k}\cdot \widehat{P}_e \cdot B_{l-k}(K-k)\cdot A_{j-i}$ $+\widehat{S}_{k+1}\cdot B_{l-k}(K-k)\cdot A_{j-i};$ $1 \le i \le j \le Q-1,\ 1 \le k \le l \le K-1,$	Transitions owing to multiple contending nodes	$P_{(i,k),(Q,l)} = P_{s,k}\cdot B_{l-k}(K-k)\cdot A_{\ge Q-i+1}$ $+kP_{s,k}\cdot P_e \cdot B_{l-k+1}(K-k)\cdot A_{\ge Q-i}$ $+kP_{s,k}\cdot \widehat{P}_e \cdot B_{l-k}(K-k)\cdot A_{\ge Q-i}$ $+\widehat{S}_{k+1}\cdot B_{l-k}(K-k)\cdot A_{\ge Q-i};$ $1 \le i \le Q,\ 1 \le k \le l \le K-1,$
$P_{(i,k),(j,K)} = P_{s,k}\cdot B_{K-k}(K-k)\cdot A_{j-i+1}$ $+kP_{s,k}\cdot \widehat{P}_e \cdot B_{K-k}(K-k)\cdot A_{j-i}$ $+\widehat{S}_{k+1}\cdot B_{K-k}(K-k)\cdot A_{j-i};$ $1 \le i \le j \le Q-1,\ 1 \le k \le K,$		$P_{(i,k),(Q,K)} = P_{s,k}\cdot B_{K-k}(K-k)\cdot A_{\ge Q-i+1}$ $+kP_{s,k}\cdot \widehat{P}_e \cdot B_{K-k}(K-k)\cdot A_{\ge Q-i}$ $+\widehat{S}_{k+1}\cdot B_{K-k}(K-k)\cdot A_{\ge Q-i};$ $1 \le i \le Q,\ 1 \le k \le K,$
$P_{(i,k),(j,k-1)} = kP_{s,k}\cdot P_e \cdot B_0(K-k)\cdot A_{j-i}$ $1 \le i \le j \le Q-1,\ 1 \le k \le K,$		$P_{(i,k),(Q,k-1)} = kP_{s,k}\cdot P_e \cdot B_0(K-k)\cdot A_{\ge Q-i}$ $1 \le i \le Q,\ 1 \le k \le K,$
$P_{(i,k),(i-1,l)} = P_{s,k}\cdot B_{l-k}(K-k)\cdot A_0;$ $1 \le i \le Q,\ 0 \le k \le l \le K,$		
$P_{(i,k),(i-1,l)} = 0;\ 1 \le i \le Q,\ 1 \le k \le K,\ l < k,$ $P_{(i,k),(j,l)} = 0,\ 0 \le i \le j \le Q,\ 2 \le k \le K,\ l < k-1,$	Impossible transitions	$P_{(i,k),(j,l)} = 0;\ 2 \le i \le Q,\ j < i-1,\ 0 \le k \le l \le K,$ $P_{(i,k),(j,k-1)} = 0;\ 1 \le i \le Q,\ j < i,\ 1 \le k \le K.$

The solution of this 2D DTMC is obtained by solving the following linear equations

$$\boldsymbol{\pi P} = \boldsymbol{\pi}\,, \quad \boldsymbol{\pi e} = \mathbf{1}\,, \tag{B.1}$$

where $\boldsymbol{\pi}$ is the stationary distribution, $\boldsymbol{P}$ is the transition probability matrix, whose elements are defined in Table B.1, and $\boldsymbol{e}$ is a column vector of ones. By using the stationary probabilities $\pi_i = \sum_{k=0}^{K} \pi(i,k)$ obtained from (B.1), the probability of successful transmission can be calculated as

$$P_s = \frac{1}{G} \sum_{i=1}^{Q} \sum_{k=0}^{K} \pi\,(i,k) \cdot P_{s,k}\,, \tag{B.2}$$

where $G = \sum_{i=1}^{Q} \sum_{k=0}^{K} \pi\,(i,k)$. By iteratively solving the set of equations (B.1) and (C.7), P_s at a fixed-point can be obtained.

IV. Energy Consumption Analysis

In this section, we calculate the average energy consumed by the RN in a cycle according to S-MAC when ETS is employed. Hereafter, t_{DATA}, t_{SYNC}, t_{RTS} and t_{ACK} denote the packet transmission duration, and T_{sleep}, T_{sync} and T_{data} represent the duration of each corresponding period in a cycle.

As described in Sec. II, each cycle contains a *sync*, *data* and *sleep* period. We adopt a synchronization process similar to the one used in [5], in which a node transmits one *SYNC* packet every N_{sc} cycles, and receives one packet per cycle in the remaining $N_{sc} - 1$ cycles. Accordingly, the energy consumed by the RN node in the *sync* period is given by,

$$\begin{aligned} E_{sc} = {} & \frac{1}{N_{sc}} \cdot \left[(t_{SYNC} \cdot P_{tx} + (T_{sync} - t_{SYNC}) \cdot P_{rx}) \right] \\ & + \frac{N_{sc} - 1}{N_{sc}} \cdot (T_{sync} \cdot P_{rx})\,, \end{aligned} \tag{B.3}$$

where P_{tx} and P_{rx} are the transmission and reception power levels respectively.

The energy consumption for ETS during the *data* period is calculated only when the RN is active. In the following analysis, we assume that $k+1$ nodes are active, meaning that the RN is active and it contends with other k active nodes. The probability that the RN is active among $k+1$ active nodes is

$q_{1,k} = (k+1)/N$. Then the RN may transmit a *DATA* packet successfully, or failed (due to collision), or just overhears another node's transmission (lost contention). Accordingly, the energy consumption in these three situations is calculated respectively as

$$\begin{aligned} E_{txs,k} &= (t_{RTS} + t_{DATA}) \cdot P_{tx} + (t_{CTS} + t_{ACK}) \cdot P_{rx}\,, \\ E_{txf} &= t_{RTS} \cdot P_{tx} + t_{CTS} \cdot P_{rx}\,, \\ E_{oh} &= t_{RTS} \cdot P_{rx}\,. \end{aligned} \tag{B.4}$$

Furthermore, if the RN lost the contention, the other nodes might be successful with a probability $q_{2,k} = q_{1,k} k P_{s,k}$ or unsuccessful with a probability $q_{3,k} = (1 - q_{1,k} k P_{s,k} - (1 - q_{1,k}) k P_{s,k} - q_{1,k} k P_{sf,k})$, conditioned on the RN being active. Then, the average energy consumed by the RN during the *data* period of a cycle when it contends with other k nodes, $k \geq 1$, is obtained by

$$\begin{aligned} E_{d,k+1} = {} & q_{1,k} P_{s,k} \left[E_{txs,k} + \left(4D_p + BT_{s,k}\right) \cdot P_{rx} \right] \\ & + q_{1,k} P_{f,k} \left[E_{txf} + \left(2D_p + BT_{f,k}\right) \cdot P_{rx} \right] \\ & + q_{2,k} \left[E_{oh} + \left(D_p + BT_{s,k}\right) \cdot P_{rx} \right] \\ & + q_{3,k} \left[E_{oh} + \left(D_p + BT_{f,k}\right) \cdot P_{rx} \right], \end{aligned} \tag{B.5}$$

where D_p is the one-way propagation delay. Note that the above terms in $E_{d,k+1}$ calculation correspond to the RN energy consumption due to: a successfully transmission; a collision; overhearing a successful transmission by the active nodes other than the RN; and overhearing a failed transmission by nodes other than the RN, respectively. $E_{d,1} = q_{1,0} \cdot [E_{txs,0} + (4D_p + (W-1)/2) \cdot P_{rx}]$ while $E_{d,0} = 0$ since an inactive node sleeps in the *data* period. Therefore the average energy consumed by the RN during the the *data* period of a cycle is given by,

$$E_d = \sum_{k=0}^{N} E_{d,k} \cdot \pi'_k \tag{B.6}$$

where π'_k is the stationary probability of finding k active nodes in the network and can be determined by, $\pi'_k = \sum_{i=1}^{Q} \pi(i, k-1) + \pi(0,k)$ for $1 \leq k \leq N-1$. Note that $\pi'_0 = \pi(0,0)$, and $\pi'_N = \sum_{i=1}^{Q} \pi(i, N-1)$, respectively.

The average energy consumed by the RN during the *sleep* period of a cycle is given by,

$$\begin{aligned} E_{sl,k+1} = {} & q_{1,k}P_{s,k} \cdot \left[\left(T - T_{sync} - T_{d,s,k}\right) \cdot P_{sl}\right] \\ & + q_{1,k}P_{f,k} \cdot \left[\left(T - T_{sync} - T_{d,f,k}\right) \cdot P_{sl}\right] \\ & + q_{2,k}P_{s,k} \left[\left(T - T_{sync} - T_{d,os,k}\right) \cdot P_{sl}\right] \\ & + q_{3,k} \cdot \left[\left(T - T_{sync} - T_{d,of,k}\right) \cdot P_{sl}\right], \end{aligned} \tag{B.7}$$

where $T_{d,s,k} = t_{RTS} + t_{DATA} + t_{CTS} + t_{ACK} + 4D_p + BT_{s,k}$, $T_{d,f,k} = t_{RTS} + t_{CTS} + 2D_p + BT_{f,k}$, $T_{d,os,k} = t_{RTS} + D_p + BT_{s,k}$, and $T_{d,of,k} = t_{RTS} + D_p + BT_{f,k}$. These terms represent the duration of the *data* period corresponding to the terms included in (AppxB.9). $E_{sl,1} = q_{1,0} \cdot \left[\left(T - T_{sync} - T_{d,s,0}\right) \cdot P_{sl}\right]$ and $E_{sl,0} = [(T - T_{sync}) \cdot P_{sl}]$, where $T_{d,s,0} = t_{RTS} + t_{DATA} + t_{CTS} + t_{ACK} + 4D_p + (W-1)/2$.

As explained in [5], a node does not go to sleep and would keep awake during the *sleep* period of N_{sc} consecutive cycles to avoid missing *SYNC* packets from its neighboring nodes. This process happens in one of N_{aw} sets of cycles. The energy consumed in such an awake cycle, $E_{aw,k}$, can be obtained by replacing P_{sl} with P_{rx} in (B.7) since the RN keeps listening to the channel. Then, the average energy consumed during the *sleep* period of a cycle is obtained by

$$E_{s,k} = \frac{E_{sl,k} \cdot N_{sc} \cdot (N_{aw} - 1) + E_{aw,k} \cdot N_{sc}}{N_{sc} \cdot N_{aw}}. \tag{B.8}$$

Similar to how E_d is obtained in (B.6), the average energy consumption during the *sleep* period of a cycle, E_s, is obtained using the same equation by substituting $E_{d,k}$ with $E_{s,k}$ in (B.6). Finally, the total average energy consumed by the RN in a cycle is obtained by

$$E = E_{sc} + E_d + E_s. \tag{B.9}$$

Accordingly, the lifetime of the RN can be determined as

$$LT = \frac{E_{initial}}{E} \text{ cycles}. \tag{B.10}$$

Furthermore, the average number of bytes successfully transmitted per total

average energy consumed in a cycle by the RN, or the energy efficiency, denoted by ξ, is given by

$$\xi = \left(\frac{\eta \cdot S}{E}\right), \tag{B.11}$$

where S is size of the transmitted packet in bytes and η is the number of successfully transmitted packets in a cycle and can be determined as $\eta = \sum_{i=1}^{Q}\sum_{k=0}^{K}\pi(i,k)\cdot P_{s,k}$.

Note that the energy consumption when a non-active node follows CPT as proposed in original S-MAC can be obtained by incorporating the following modifications in (AppxB.9) and (B.7). $q_{2,k} = [kq_{1,k} + (k+1)\left(1-q_{1,k}\right)]\cdot P_{s,k}$, $q_{3,k} = 1 - q_{2,k} - q_{1,k}P_{sf,k}$, $E_{d,0} = (t_{RTS} + W + D_p)\cdot P_{rx}$ and its corresponding duration.

V. Simulations and Numerical Results

In this section, we evaluate and compare the performance of the ETS and CPT sleeping mechanisms operated on the S-MAC protocol. The considered performance metrics, i.e., average energy consumption, lifetime and energy efficiency of a node are obtained through both the developed DTMC model and discrete-event simulations. The simulation results are reported as the average values over $5\cdot 10^6$ cycles.

The network illustrated in Fig. B.1 is adopted in our evaluation, configured as: number of nodes $N \in (5,6\ldots,20)$; queue length of a node $Q = 10$ with $E_{initial} = 1$ J; size of the *DATA* packet $S = 50$ bytes; *DATA* arrival rate $\lambda \in [0.5, 1.5]$ packet/s; and for the *sync* period, $N_{sc} = 10$, $N_{aw} = 40$. Furthermore, S-MAC is configured with 50% duty cycle. The other MAC parameters are taken from [5]. The transmission, reception and sleep power levels are $P_{tx} = 52$ mW, $P_{rx} = 59$ mW and $P_{sl} = 3\,\mu$W [7] respectively. The network performance is evaluated by varying the number of nodes N or packet arrival rate λ while keeping the other parameters fixed at $\lambda = 1.1$ packet/s or $N = 15$ respectively.

A. Energy Consumption and Lifetime

It is obvious that the packet arrival rate will affect the number of cycles in which a node remains active or inactive. In Fig. B.3, we evaluate both mechanisms with different traffic arrival rates varying from 0.5 to 1.5 packet/s with

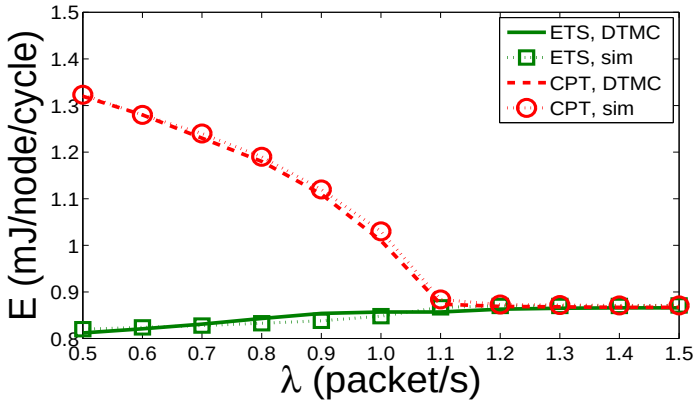

Figure B.3: Average energy consumed by the RN per cycle as the packet arrival rate varies, given that $N = 15$.

a granularity interval of 0.1 packet/s. The figure clearly demonstrates the superiority of the ETS mechanism in a network with light traffic. When $\lambda < 1.1$ packet/s, nodes in the network are inactive during many or even most of the cycles and then can sleep in the *data* period when ETS is employed. Consequently, a node saves a substantial amount of energy. Whereas in CPT, all nodes regardless of whether they have packets in their queue or not have to wake up and keep listening to the channel until an RTS packet is received. Thereby, a node consumes a large amount of energy caused by overhearing. With the increase in packet generation rate, the network will eventually be saturated after $\lambda \geq 1.1$ packet/s. When saturated, (almost) all nodes in the network become active and contend for channel access in every cycle. Then, energy consumption stabilizes and both mechanisms show the same performance.

Traffic congestion in a network can be caused by either injecting higher traffic loads to all nodes or increasing the node population. Configuring λ to 1.1 packet/s which is the saturation point, we examine the performance of ETS by increasing the network size from 5 to 20 at a granularity level of 1. Clearly, fewer number of nodes with a constant λ generate lighter traffic in the network. Furthermore, due to less competition, the probability of obtaining channel access for a node is higher. Then, a node can transmit packets successfully with a higher probability, meaning it is less likely that node will continue to be active in the next cycle. Therefore, with a lower node population, nodes following ETS consume lower energy. The same level of

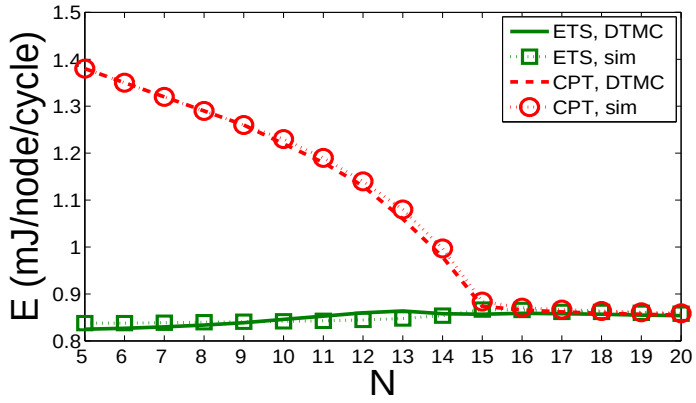

Figure B.4: Average energy consumed by the RN per cycle as the number of nodes varies, given that $\lambda = 1.1$ packet/s.

energy consumption is maintained for both mechanisms after the network is congested, as shown in Fig. B.4. Again, a CPT node consumes higher energy because of its dependence on receiving an RTS packet to enter into the *sleep* period. The competition increases when more nodes join the network. Then, a node stays active in many cycles and consecutively the level of energy consumed by a node using CPT decreases until the saturation point. After $N = 15$, nodes stay active in all cycles and the energy consumption level remains stable for both ETS and CPT.

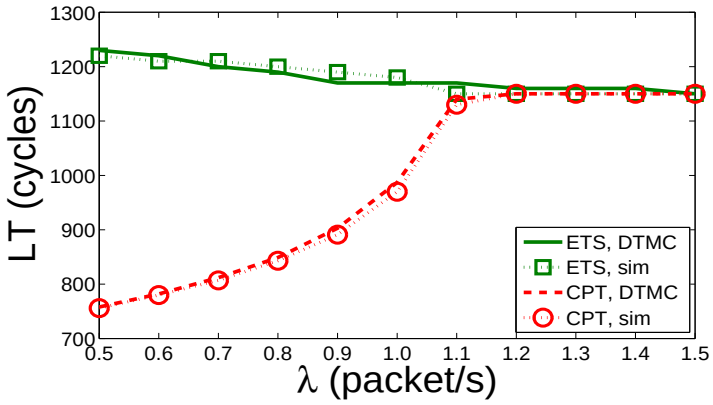

Figure B.5: Lifetime of the RN as the packet arrival rate varies, given that $N = 15$.

Correspondingly, the obtained node lifetimes with the same configurations are presented in Fig. B.5 and Fig. B.6 respectively. Obviously, lower energy consumption leads to longer node lifetime. As observed, ETS achieves approximately 65% longer lifetime at $N = 5$ in Fig. B.6 and at $\lambda = 0.5$

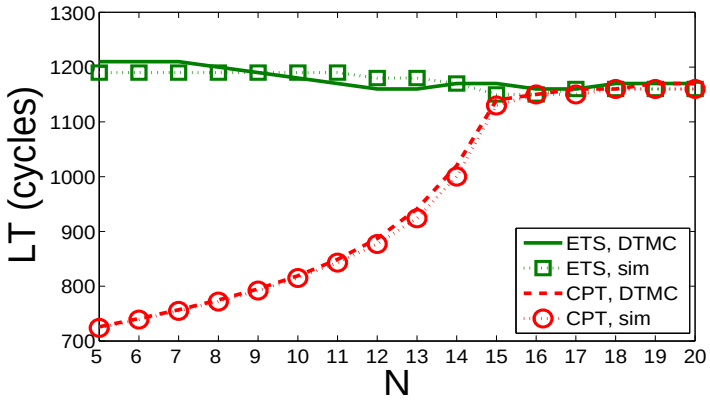

Figure B.6: Lifetime of the RN as the number of nodes varies, given that $\lambda = 1.1$ packet/s.

packet/s in Fig. B.5, in comparison with its CPT counterpart. Consequently the network lifetime which is very much relevant to node lifetime is also extended.

B. Energy Efficiency

As defined, the energy efficiency of a node, ξ, depends on the average number of bytes transmitted successfully by that node as well as the total average energy consumption, E, in a cycle. With both configurations, we observe that ξ behaves similarly for ETS and CPT once the network is saturated.

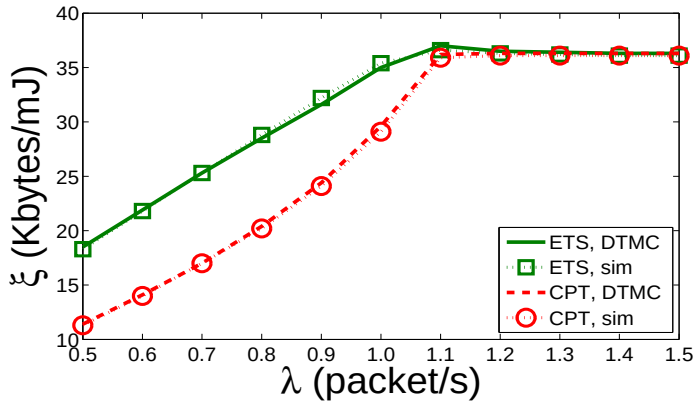

Figure B.7: Energy efficiency of the RN as the packet arrival rate varies, given that $N = 15$.

Within the non-saturation regions, however, ETS achieves much higher energy efficiency than CPT does. As shown in Fig. B.7 with a fixed network size and variable packet arrivals, ξ increases monotonically in both mechanisms, but ETS achieves approximately 65% higher efficiency. This is because

that the number of packets successfully transmitted by both mechanisms is at a constant level while much lower energy consumption per cycle is achieved in ETS. Similarly, in the constant arrival rate and variable network size case, ETS maintains a high level of stability in ξ as illustrated in Fig. B.8, since the consumed energy per cycle, E, is low and almost stable for ETS (shown in Fig. B.4). When there are more nodes in the network after $N = 15$, ξ decays drastically in both ETS and CPT owing to the decrement of number of successfully transmitted packets by a node per cycle.

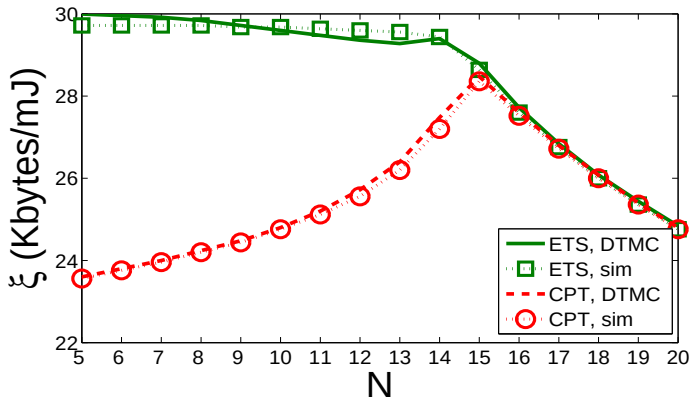

Figure B.8: Energy efficiency of the RN as the number of nodes varies, given that $\lambda = 1.1$ packet/s.

VI. CONCLUSIONS

In this paper, we proposed an event-triggered sleeping mechanism to mitigate energy consumption caused by overhearing in prevailing control packet triggered sleeping mechanisms for synchronous duty cycle MAC protocols. Furthermore, a two dimensional DTMC model is developed to evaluate both the ETS and CPT mechanisms operated on S-MAC and closed-form expressions for calculating energy consumption, lifetime and energy efficiency are derived. The obtained analytical and discrete-event simulation results match precisely for both mechanisms. It is demonstrated that the proposed ETS mechanism achieves about 65% longer lifetime and 65% higher energy efficiency under light traffic conditions when compared with the legacy CPT mechanism and both mechanisms achieve the same performance when the network is saturated.

REFERENCES

[1] P. Huang, L. Xiao, S. Soltani, M. W. Mutka, and N. Xi, "The evolution of MAC protocols in wireless sensor networks: A survey", *IEEE Commun. Surveys Tut.* vol. 15, no. 1, pp. 101-120, First Quarter 2013.

[2] J. Oller, I. Demirkol, J. Casademont, J. Paradells, G. Ulrich Gamm, and L. Reindl, "Has time come to switch from duty-cycled MAC protocols to wake-up radio for wireless sensor networks?", *IEEE/ACM Trans. Netw.*, vol. 24, no. 2, pp. 674-687, Apr. 2016.

[3] W. Ye, J. Heidemann, and D. Estrin, "Medium access control with coordinated adaptive sleeping for wireless sensor networks", *IEEE/ACM Trans. Netw.*, vol. 12, no. 3, pp. 493-506, Jun. 2004.

[4] C. Liu, P. Huang, and L. Xiao, "TAS-MAC: A traffic-adaptive synchronous MAC protocol for wireless sensor networks", *ACM Trans. Sen. Netw.*, vol. 12, no. 1, pp. 1-30, Feb. 2016.

[5] O. Yang and W. Heinzelman, "Modeling and performance analysis for duty-cycled MAC protocols in wireless sensor networks", *IEEE Trans. Mobile Comput.*, vol. 11, no. 6, pp. 905-921, Jun. 2012.

[6] J. Martinez-Bauset, L. Guntupalli, and F. Y. Li, "Performance analysis of synchronous duty-cycled MAC protocols", *IEEE Wireless Commun. Lett.*, vol. 4, no. 5, pp. 469-472, Oct. 2015.

[7] MICAz Data Sheet, available at `http://edge.rit.edu/edge/P08208/public/Controls_Files/MICaZ-DataSheet.pdf`, 2016.

Paper C

Title:	An Aggregated Packet Transmission in Duty-Cycled WSNs: Modeling and Performance Evaluation
Authors:	Lakshmikanth Guntupalli†, Jorge Martinez-Bauset‡, Frank Y. Li†, and Mary Ann Weitnauer*
Affiliation:	†Dept. of Information and Communication Technology, University of Agder (UiA), N-4898 Grimstad, Norway ‡Dept. of Communications, Universitat Politècnica de València (UPV), 46022 València, Spain *School of Electrical and Computer Engineering, Georgia Institute of Technology (GATECH), Atlanta, GA 30332-0250, USA
Journal:	*IEEE Transactions on Vehicular Technology (TVT)*, Early Access Available in IEEE Xplore, March 2016, DOI:10.1109/TVT.2016.2536686
Copyright ©:	IEEE

Aggregated Packet Transmission in Duty-Cycled WSNs: Modeling and Performance Evaluation

Lakshmikanth Guntupalli, Jorge Martinez-Bauset, Frank Y. Li, and Mary Ann Weitnauer

***Abstract* — Duty cycling (DC) is a popular technique for energy conservation in wireless sensor networks that allows nodes to wake up and sleep periodically. Typically, a single packet transmission (SPT) occurs per cycle, leading to possibly long delay. With aggregated packet transmission (APT), nodes transmit a batch of packets in a single cycle. The potential benefits brought by an APT scheme include shorter delay, higher throughput and higher energy efficiency. In the literature, different analytical models have been proposed to evaluate the performance of SPT schemes. However, no analytical models for the APT mode on synchronous DC medium access control mechanisms exist. In this paper, we first develop a three-dimensional (3D) discrete time Markov chain (DTMC) model to evaluate the performance of an APT scheme with packet retransmission enabled. The proposed model captures the dynamics of the state of the queue of nodes and the retransmission status, as well as the evolution of the number of active nodes in the network, i.e., nodes with a non-empty queue. We then study the number of retransmissions needed to transmit a packet successfully. Based on the observations, we develop another less complex DTMC model with infinite retransmissions which embodies only two dimensions. Furthermore, we extend the 3D model into a four-dimensional model by considering error-prone channel conditions. The proposed models are adopted to determine packet delay, throughput, packet loss, energy consumption, and energy efficiency. Furthermore the analytical models are validated through discrete-event based simulations. Numerical results show that an APT scheme achieves substantially better performance than its SPT counterpart in terms of delay, throughput, packet loss and energy efficiency, and that the developed analytical models reveal precisely the behavior of the APT scheme.**

Keywords—Duty-cycled wireless sensor networks, discrete time Markov chain model, packet aggregation, performance evaluation.

I. INTRODUCTION

One of the goals for designing medium access control (MAC) protocols in energy constrained wireless sensor networks (WSNs) is to achieve higher energy efficiency. Among the proposed energy efficient techniques, duty cycling (DC) is employed in many existing MAC protocols. By following DC, nodes turn their radios *on* and *off* periodically to avoid idle listening in order to save energy consumption. Sensor-MAC (S-MAC) [1] is a benchmark example for synchronous DC MAC protocols. In S-MAC, nodes transmit or receive only *one DATA* packet per cycle. This transmission scheme is referred to hereafter as single packet transmission (SPT). Since only one packet is transmitted per cycle, packets stored in the queue might need to wait a long time before being delivered. On the other hand, in many WSN applications, timely data delivery is required for event-driven scenarios. For example, in fire detection scenarios, alarms should be alerted in real-time so that urgent actions can take place prior to the occurrence of a disaster. Furthermore, an appropriate decision can be taken when accurate data is available and better accuracy can be achieved with higher data rate.

In order to boost data rate and minimize delay in WSNs, packet aggregation, in which a batch of packets are transmitted together, has been proposed as a pragmatic approach. Packet aggregation is a feasible technique for WSNs since all packets are typically addressed to one node, i.e., the sink node [2]. Aggregated data transmission helps to increase the probability that a node transmits a packet successfully, since queues are emptied faster when multiple packets are transmitted together, and correspondingly the mean number of contending nodes per cycle decreases [3]. Packet aggregation may also bring other benefits like shorter delay and higher energy efficiency. Indeed, many data aggregation schemes have been proposed for the purpose of energy saving, delay reduction, collision avoidance, or more accurate data transmission [4]. However, very few analytical models exist for performance evaluation of aggregated data transmission in WSNs.

In this paper, we adopt the concept of packet aggregation and propose an analytical model to evaluate the performance of an aggregated packet trans-

mission (APT) scheme. This scheme operates in WSNs with a synchronous DC MAC protocol like S-MAC. We refer to the set of consecutive packets in the buffer of a node that will be transmitted together in the same cycle as a $frame$. The maximum number of packets aggregated in a frame is constrained by the maximum frame length of the wireless link, as well as the number of packets in the queue.

We develop first a three-dimensional (3D) discrete-time Markov chain (DTMC) to model the time evolution of the state of a node in a WSN, where nodes have finite queue capacity and operate according to S-MAC. One of the three state elements is dedicated to track the number of retransmissions experienced by the frame at the head of the queue of the node. We analyze accordingly the number of retransmissions required to successfully transmit a frame in an error-free channel, where losses only occur due to collisions in the channel. Based on the results of the 3D DTMC, we observe that, in many configurations, 99.999% of the frames are successfully delivered after at most two retransmissions. Therefore, by configuring the maximum retransmission counter in the nodes to two or larger, we might achieve zero or close-to-zero packet loss. Correspondingly, we propose a simpler two-dimensional (2D) DTMC model that allows infinite retransmissions to evaluate the performance of the APT scheme. Clearly, the state of a node in this model omits the element dedicated to retransmissions. We observe that this model is applicable to many realistic scenarios where initial packet transmission failures are finally recovered by retransmissions.

On the other hand, although the error-free channel assumption has been extensively adopted in the literature [5, 6, 7], it is more realistic to consider that wireless channels are intrinsically error-prone. Accordingly, we further develop a four-dimensional (4D) model by defining multiple *loss* and *non-loss* states to characterize error-prone wireless channels, and integrate them into the the 3D model. This modeling approach captures both first- and second-order statistics with sufficient accuracy, which is considered an adequate characterization of the wireless link for practical scenarios. Using the proposed models, different performance parameters are studied, like average packet delay, throughput, average energy consumption per cycle, and energy efficiency.

The rest of this paper is structured as follows. Section II reviews the

related work and Section III describes the network model. In Section IV, we present both the 3D and 2D DTMC models in details. The expressions for performance parameters are deduced in Section V. The performance of the APT and SPT schemes is compared in Section VI. Furthermore, the 4D model is presented in Section VII, before the paper is concluded in Section VIII.

II. Related Work and Contributions

Among the analytical models proposed to analyze the performance of carrier sense multiple access with collision avoidance (CSMA/CA) MAC protocols, the model proposed in [5] is a popular one. It is based on a DTMC that captures the behavior of an individual node contending for channel access. The primary assumptions of the model are: error-free channel, the collision probability of a station when it attempts to transmit is independent of its state, and nodes operate in the saturation mode. These assumptions make the model simple, yet quite accurate. Since then, Bianchi's model has been extensively studied, refined and extended to different scenarios. See for example [8] and their references.

Most of the models based on Bianchi's approach do not keep track of the number of packets in the queue of the node, and therefore they cannot be applied to an APT MAC mechanism like the one studied here. When a node employing APT wins access to the medium, the number of packets in the queue must be known to define the size of the frame. If this information is not known, the time evolution of the system cannot be modeled with precision.

Exceptions exist. For example, the 3D DTMC model proposed in [6] extends the model in [5] with a new dimension to keep track of the state of the queue. However, there is another important reason that makes previous models not directly applicable for evaluating the performance of synchronous DC MAC protocols like S-MAC, since the backoff timers designed therein are reset at each cycle [7].

A continuous time Markov chain (CTMC) with exponentially distributed times in the *active* and *sleep* states was developed to model the behavior of sensor nodes with finite queue capacity in [9]. Clearly when nodes have random cycle duration, the synchronization of node schedules becomes a tedious

and energy consuming task. Another model for analyzing S-MAC was proposed in [10], based on an $M/G/1$ model. However, it requires that packet arrivals follow a Poisson process and that each node has an infinite buffer.

Provided the synchronous nature of S-MAC, modeling S-MAC based WSNs using a DTMC seems to be a natural option. To model the evolution with time of the state of a generic node in the network, a one-dimensional (1D) DTMC model supporting a general packet arrival distribution per cycle, finite queue and zero packet retransmissions was proposed in [7]. The same authors proposed in [11] a 2D model to analyze the impact of packet retransmissions. However, the models in [7] and [11] were developed based on the assumption that the probability that a node is active is independent of the other nodes being active. Nodes are active, and contend for channel access, if their queues are non-empty.

We argue that some degree of dependence occurs among nodes in practice. This is because the probability of successful transmission of a node depends on the number of active nodes in the network, and this number varies over time depending on the state of the other nodes. For a WSN employing S-MAC, we compared in [12] a model that considers nodes as mutually independent with another model that incorporates the dependence among nodes. The study concludes that substantially more accurate results can be obtained when dependence is incorporated into the model.

In this paper, we propose a 3D DTMC that incorporates the dependency among nodes in the network. To clarify the difference between our model and the previous models, let (i) be the state of the 1D DTMC studied in [7], where i is the number of packets found at the queue of a node. Also, let (i,r) be the state of the previous 2D DTMCs [11], [13], where i has the same definition and r is the number of retransmissions experienced by the packet at the head of the queue of the node. In contrast, the state of the proposed 3D DTMC is defined by a triplet (i,k,r), where k keeps track of the number of *active* nodes in the network. The state of our 2D DTMC is defined by (i,k), where the r element has been omitted, and it is therefore different from the previous 2D DTMCs in [11], [13]. It is furthermore worth mentioning that all aforementioned models were developed for the SPT scheme without considering packet aggregation.

When data is sensed by a group of neighboring nodes, it tends to be some-

what space-correlated and redundant. Then unprocessed transmission of such data is likely to waste energy and degrade network performance. Correspondingly, packet aggregation in WSNs has been proposed, mainly from a routing perspective [14, 15, 16, 17, 18]. That is, cluster-heads perform the processing and aggregation of intra-cluster and inter-cluster information, before it is forwarded towards the sink. For example in [16] the authors obtained an approximated closed-form expression for end-to-end delay when data aggregation was enabled in a generic multi-hop WSN. Nonetheless, the above aggregation schemes for WSNs do not consider any specific MAC layer protocol.

Currently, there exist only a few MAC protocols that integrate data aggregation in WSNs. Among them, aggregation MAC (AG-MAC) [19] is a synchronous DC MAC protocol. A joint aggregation and MAC (JAM) [20] scheme was proposed for RI-MAC [21] as another asynchronous DC MAC protocol. Moreover, a lifetime balanced data aggregation scheme was proposed for DC WSNs in [22]. However, these studies have been carried out largely by simulations or test-bed based experiments.

In this paper, we aim at modeling analytically the performance of packet aggregation at the MAC layer and the intra-cluster level. To the best of our knowledge, this paper is the first attempt to develop analytical models for MAC level packet aggregation in synchronous duty-cycled WSNs. In summary, the main contributions of this paper are as follows:

- We propose a novel modeling approach to evaluate the performance of an aggregated packet transmission scheme that operates in WSNs with finite capacity queue running on a synchronous DC MAC protocol like S-MAC. A salient feature of the proposed analytical model is that it handles the dependence that occurs among nodes in practice by keeping track of the number of active nodes in the network. This makes the proposed model substantially more accurate than the other models that assume mutual independence among nodes [12].

- A 3D DTMC is proposed to model the time evolution of the state of a node with finite retransmissions. To reduce the complexity of the 3D DTMC, a less complex 2D DTMC allowing infinite retransmissions is developed as an alternative model for scenarios where a vast majority

of frames that arrive with error can be recovered by retransmissions. In addition to the 2D and 3D models which are built based on an error-free channel assumption, a 4D model which integrates error-prone channel conditions into the 3D model is also developed.

- The proposed models apply to both APT and SPT schemes. In that sense, it can be considered as a generalization of the analytical models proposed for the SPT scheme like [7], [12]. Note also that in the studied APT scheme the size of a frame may change randomly from cycle to cycle, as described with more detail in Algorithm 1 of the next section.
- Closed-form expressions for calculating mean packet delay, throughput, packet loss probability, energy consumption, and energy efficiency are obtained based on the proposed models. Furthermore, the analytical model has been shown to be very accurate, when compared with discrete-event based simulations.

III. NETWORK MODEL

In this section, we give a brief description of the operation of S-MAC, introduce the network scenario and the assumptions of the study, and provide expressions that model the access to the medium of nodes in a WSN operated on S-MAC.

A. Brief Description of S-MAC

In S-MAC the time is partitioned into cycles of equal length T, and each cycle contains an *active* and a *sleep* period. The *active* period is further divided into two parts: the *sync* period of fixed length T_{sync}, where *SYNC* packets are exchanged, and the *data* period, where *DATA* packets are exchanged. Throughout this paper, we use capital letters to represent the type of a packet. For example, *DATA*, *SYNC* and *RTS* are the packets. Conversely, we use lowercase letters to represent the different parts of a cycle: *active*, *sleep*, *sync* and *data*.

In a *sync* period, every node chooses a sleep-awake schedule and exchanges it with its neighbors using *SYNC* packets. These packets include the address of the sender and the time of its next *active* period initiation. With this information, nodes are able to coordinate to wake up at the same time at the beginning of the next cycle. In the considered network, all nodes are

awake at the start of a *sync* period and might broadcast a *SYNC* packet. To this end they follow a CSMA/CA mechanism for contention-based channel access. It is based on generating a random backoff time and performing a carrier sensing procedure. If the channel is idle when the backoff timer expires, then the node transmits the SYNC packet.

Refer to a set of N_{sc} consecutive cycles as an *update* super-cycle. As in [7], we assume for simplicity that nodes transmit one *SYNC* packet every N_{sc} cycles, i.e., one packet per *update* super-cycle, and it might receive one *SYNC* packet per cycle in the remaining $N_{sc} - 1$ cycles.

In order to avoid missing *SYNC* packets from neighboring nodes, from now and then a node keeps awake for the whole cycle. As these cycles are different from the *normal* cycles which include both *active* and *sleep* periods, we refer to them as *awake* cycles. Define a hyper-cycle as a set of N_{aw} *update* super-cycles, i.e., $N_{aw} \cdot N_{sc}$ consecutive cycles. We assume that a node follows *awake* cycles during a complete super-cycle (N_{sc} consecutive cycles), while it follows *normal* cycles during the other $N_{aw} - 1$ *update* super-cycles of the hyper-cycle. The characteristics of *normal* and *awake* cycles will be later used to determine the average energy consumed by a node.

Nodes might transmit a *DATA* packet during the *data* period using a CSMA/CA mechanism for contention-based channel access. To this end, they generate new backoff times at each *data* period initiation and perform carrier sense. If the channel is idle when the backoff timer expires, then the node can transmit the *DATA* packet using an RTS/CTS/DATA/ACK handshake. When a winning node receives *CTS* in response to its previous *RTS*, it transmits one *DATA* frame. In S-MAC, a node goes to *sleep* until the beginning of next *sync* period when: i) it loses the contention (hears a busy medium before its backoff time expires); ii) it encounters an *RTS* collision or *CTS* is lost; and iii) after the reception of an *ACK* as a response to a successful frame transmission. Recall that each *sync* period is followed by a *data* (*listen*) period. For further details on S-MAC please refer to [1].

B. Network Scenario and Assumptions

Consider a cluster of N sensor nodes that transmit packets towards a single destination node, i.e., the *sink*, as shown in Figure C.1. For convenience, we select one of the N nodes arbitrarily, and refer to it as the reference node (RN). We assume that the sink node behaves as a packet absorption node,

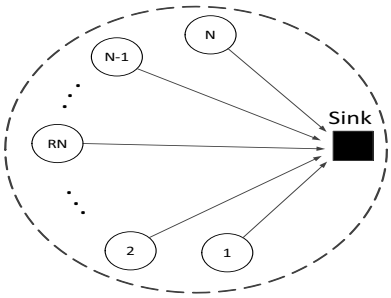

Figure C.1: A network model where all nodes are reachable within one hop and send DATA frames to a single sink.

i.e., it only receives packets (it never transmits). All nodes are one hop away from each other forming a *single-cell* cluster, but multiple clusters together may form a larger network.

A node is capable of buffering a finite number, Q, of packets, and it serves them according to a first in first out (FIFO) discipline. A node performs packet aggregation based on the number of packets accumulated in its queue. A set of packets aggregated according to the following rule will be referred to as a *frame*. The transmission of a frame by the RN happens when it wins the contention for medium access. If the number of packets in its queue is smaller than the maximum allowed frame size F, then a frame containing all the packets in the queue is transmitted. However, if the number of packets in its queue is greater than or equal to F, then a frame containing F packets is transmitted. If the transmission is successful, then the number of packets in the queue of the RN is decremented by the frame size.

For clarity, the packet aggregation scheme is described in Algorithm 1. Note that the APT scheme presented here is not a MAC protocol itself, but it is a possible mode for the operation of S-MAC. That is, to obtain channel access, the RN has to contend with other nodes according to S-MAC as explained before. Observe that the proposed APT scheme is general and it is applicable to any synchronous DC MAC protocol as well.

The operation of S-MAC with APT is illustrated in Figure C.2. In the figure, the RN wins the contention in the cycle and a frame is sent to the sink node. As in conventional SPT S-MAC scenarios, all other active nodes go to sleep after receiving *RTS* from the RN. Therefore, for these nodes the *data* period lasts merely until the reception of *RTS*. However, the duration of the *data* period for the RN depends on the transmitted frame size. Observe

Algorithm 1: Aggregated Packet Transmission by the RN

```
1  begin
2      input:
3      i = Number of packets in the queue of a node
4      F = Maximum size of a frame
5      output:
6      f = Number of packets aggregated in the frame
7      q = Number of packets left in the queue after frame transmission
8      if the RN wins medium access then
9          if i ≤ F then
10             transmit i packets in the frame, f = i, q = 0;
11         end
12         else if i > F then
13             transmit F packets, f = F, q = i − F;
14         end
15     end
16 end
```

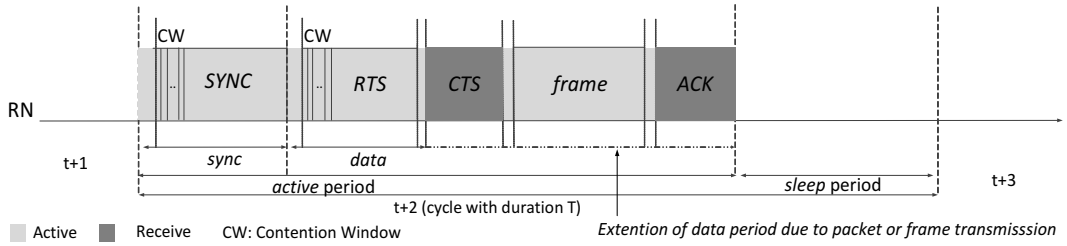

Figure C.2: Operation of S-MAC, where each cycle consists of an *active* period and a *sleep* period. The *active* period is further divided into *sync* and *data* periods.

that the duration of the *data* period is constrained by the length of the cycle and therefore, it must be shorter than or equal to $T - T_{sync}$. This provides an upper bound for the maximum allowed frame size F. A node drops a frame when the number of consecutive retransmissions of the same frame reaches the maximum number of allowed retransmissions, R.

Note also that, as the buffer has finite capacity, packet loss due to buffer overflow might happen when packets arrive and find a full buffer. During overflow episodes, some degree of selective packet discarding must occur at the nodes to give priority to the most important information. Once such imperative information is selected, nodes will deploy retransmissions in order to achieve a loss free transfer across the network.

In this study, we assume that: i) all nodes contain the same initial energy; ii) the channel is error-free (for 2D and 3D models), or error-prone (for 4D model); iii) transmission failure happens either only due to collision in the

medium (for 2D and 3D models) or due to both collision and channel failure (for 4D model); iv) packets arrive to the buffer of a node following a renewal arrival process, and the number of packets that arrive per cycle is characterized by independent and identically distributed random variables. For simplicity, we assume that the number of packets that arrive to a buffer follow a discrete Poisson distribution of mean λT, where λ is the packet arrival rate and T is the cycle duration.

C. Access to the Medium

According to the operation of S-MAC, at each cycle, nodes with a non-empty queue generate a random backoff time taken from $\{0, W-1\}$. When the RN is active, it transmits a frame successfully when the other contending nodes select backoff times longer than the one selected by the RN. A frame transmitted by the RN will fail (collide) when the RN and one or more of the other contending nodes select the same backoff time, and this backoff time is the smallest among all contending nodes. If the backoff time generated by the RN is not the smallest one among those generated by the other contending nodes, then two outcomes are possible: either another node is able to transmit successfully, or other nodes collide while transmitting. Nodes that lose contention (because they hear a busy medium before their backoff time expires) or encounter an *RTS* collision, go to sleep until the *sync* period of the next cycle.

Consider a cycle where the RN is active and denote by k, $0 \leq k \leq N-1$, the number of nodes that are also active in the same cycle in addition to the RN. Let $P_{s,k}$, $P_{sf,k}$ and $P_{f,k}$ be the probabilities that the RN transmits a frame successfully, transmits a frame (successfully or with collision), and it transmits with failure (collision) when contending with other k nodes. Then,

$$\begin{aligned} P_{s,k} &= \sum_{i=0}^{W-1} \frac{1}{W} \left(\frac{W-1-i}{W} \right)^k , \\ P_{sf,k} &= \sum_{i=0}^{W-1} \frac{1}{W} \left(\frac{W-i}{W} \right)^k , \\ P_{f,k} &= P_{sf,k} - P_{s,k} = \frac{1}{W} . \end{aligned} \tag{C.1}$$

$P_{s,k}$ is the probability that the RN selects a backoff value from $\{0, W-1\}$ and

the other k nodes choose a larger value. $P_{sf,k}$ and $P_{f,k}$ can be described in similar terms.

At a first glance, it might seem counter-intuitive that $P_{f,k} = 1/W$, and it is therefore independent of k. A simple example that might help to clarify this fact is provided next. For $k = \infty$, an infinite number of nodes will select backoff time 0, an infinite number of nodes will select backoff time 1, and so on. The RN collides *only* when it selects backoff time 0. Clearly, other selections will result in other nodes colliding but not the RN, as the RN will detect that the channel is busy while performing carrier sense, and it will go to sleep until next cycle. The RN selects backoff time 0 with probability $1/W$.

Conditioned on a successful or unsuccessful packet transmission by the RN when contending with other k nodes, the average backoff times are given by,

$$BT_{s,k} = \frac{1}{P_{s,k}} \sum_{i=0}^{W-1} i \cdot \frac{1}{W} \left(\frac{W-1-i}{W} \right)^k ,$$
$$BT_{f,k} = \sum_{i=0}^{W-1} i \cdot \left[\left(\frac{W-i}{W} \right)^k - \left(\frac{W-1-i}{W} \right)^k \right] . \tag{C.2}$$

IV. DTMC WITH FINITE/INFINITE RETRANSMISSIONS

In this section, we develop first a 3D DTMC model for APT based on the S-MAC protocol with finite retransmissions and then a 2D DTMC model based on infinite retransmissions. The notation adopted throughout the paper is defined in Table C.1.

A. 3D DTMC for APT with Finite Retransmissions

A state in the proposed DTMC is represented by (i,k,r), where i is the number of packets in the queue of the RN, $i \leq Q$, k is the number of active nodes in the network other than the RN, $k \leq K = N-1$, and r is the number of retransmissions experienced by the frame at the head of the queue of the RN, $r \leq R$.

The transition probabilities of this DTMC are defined in Table C.2. Note that when the transition between two states is not possible, its transition probability is zero. For brevity, zero transition probabilities are not shown in the

Table C.1: Notation for DTMC Models.

Symbol	Explanation
T	Duration of a cycle
N	Number of nodes in the network
Q	Queue capacity in packets
W	Contention window size
K	Maximum number of active nodes in the network other than the RN, $K = N-1$
R	Maximum number of frame retransmissions
λ	DATA packet arrival rate at the node buffer
A_i	Probability of i packets arriving in a cycle, $A_i = e^{-\lambda T}(\lambda T)^i/i!$
$A_{\geq i}$	Probability of i or more packets arriving in a cycle, $A_{\geq i} = 1 - \sum A_j$ where $j = 0 \ldots i-1$
$\widehat{A}$	$1 - A_0$, where A_0 is the probability of no packet arrivals in a cycle
$B_k(K)$	Probability that k nodes, out of K that have their queues empty, receive packets in a cycle, $B_k(K) = \binom{K}{k}\widehat{A}^k A_0^{K-k}$
S_k	Probability that an active node transmits a frame successfully in a cycle where k nodes contend, $S_k = kP_{s,k-1}$
$\widehat{S}_k$	$1 - S_k$
$\widehat{T}_k$	Probability that the RN does not transmit when contending with other k nodes and two or more of the other nodes collide, $1-(k+1)P_{s,k} - P_{f,k}$
F	Maximum frame size that a node can transmit (in packets)
π_i	Stationary probability of finding a node with i packets in the queue. See (C.6)(C.8).
α	Number of packets aggregated for transmission when node is in state i, $\alpha = min(i,F)$
P_s	Average probability that an active node transmits a frame successfully in a random cycle. See (C.5)(C.7).
P_e	Probability that the queue of an active node becomes empty conditioned on a successful transmission. See (C.4).
$\widehat{P}_e$	$1 - P_e$

Table C.2: Transition Probabilities of the 3D DTMC Model for S-MAC-APT with Finite Retransmissions

No active node exists. Transitions occur due to new arrivals	
$P_{(0,0,0),(j,l,0)} = B_l(K)\cdot A_j;\ 0 \le j < Q,\ 0 \le l \le K,$	$P_{(0,0,0),(Q,l,0)} = B_l(K)\cdot A_{\ge Q};\ 0 \le l \le K.$
No packets in the queue of the RN, i.e., no transmissions by the RN. Transitions are caused by the other k active nodes	
$P_{(0,k,0),(j,l,0)} = S_k\cdot P_e\cdot B_{l-k+1}(K-k)\cdot A_j + S_k\cdot \widehat{P}_e\cdot B_{l-k}(K-k)\cdot A_j + \widehat{S}_k\cdot B_{l-k}(K-k)\cdot A_j;\ 0 \le j < Q,\ 1 \le k \le l < K,$	$P_{(0,k,0),(Q,l,0)} = S_k\cdot P_e\cdot B_{l-k+1}(K-k)\cdot A_{\ge Q} + S_k\cdot \widehat{P}_e\cdot B_{l-k}(K-k)\cdot A_{\ge Q} + \widehat{S}_k\cdot B_{l-k}(K-k)\cdot A_{\ge Q};\ 1 \le k \le l < K,$
$P_{(0,k,0),(j,K,0)} = S_k\cdot \widehat{P}_e\cdot B_{K-k}(K-k)\cdot A_j + \widehat{S}_k\cdot B_{K-k}(K-k)\cdot A_j;\ 0 \le j < Q,\ 1 \le k \le K,$	$P_{(0,k,0),(Q,K,0)} = S_k\cdot \widehat{P}_e\cdot B_{K-k}(K-k)\cdot A_{\ge Q} + \widehat{S}_k\cdot B_{K-k}(K-k)\cdot A_{\ge Q};\ 1 \le k \le K,$
$P_{(0,k,0),(j,k-1,0)} = S_k\cdot P_e\cdot B_0(K-k)\cdot A_j;\ 0 \le j < Q,\ 1 \le k \le K,$	$P_{(0,k,0),(Q,k-1,0)} = S_k\cdot P_e\cdot B_0(K-k)\cdot A_{\ge Q};\ 1 \le k \le K.$
$k+1$ nodes including the RN are active. Successful transmission by the RN in its first attempt or by any other node	
$P_{(i,k,0),(j,l,0)} = P_{s,k}\cdot B_{l-k}(K-k)\cdot A_j;\ 1 \le i \le F,\ 0 \le j \le i-1,\ 0 \le k \le l \le K,$	$P_{(i,k,0),(j,l,0)} = P_{s,k}\cdot B_{l-k}(K-k)\cdot A_{j-i+F};\ F+1 \le i \le Q,\ i-F \le j \le i-1,\ 0 \le k \le l \le K,$
$P_{(i,k,0),(j,l,0)} = P_{s,k}\cdot B_{l-k}(K-k)\cdot A_{j-i+\alpha} + kP_{s,k}\cdot P_e\cdot B_{l-k+1}(K-k)\cdot A_{j-i} + kP_{s,k}\cdot \widehat{P}_e\cdot B_{l-k}(K-k)\cdot A_{j-i} + \widehat{T}_k\cdot B_{l-k}(K-k)\cdot A_{j-i};\ 1 \le i \le j < Q,\ 1 \le k \le l < K,$	$P_{(i,k,0),(Q,l,0)} = P_{s,k}\cdot B_{l-k}(K-k)\cdot A_{\ge Q-i+\alpha} + kP_{s,k}\cdot P_e\cdot B_{l-k+1}(K-k)\cdot A_{\ge Q-i} + kP_{s,k}\cdot \widehat{P}_e\cdot B_{l-k}(K-k)\cdot A_{\ge Q-i} + \widehat{T}_k\cdot B_{l-k}(K-k)\cdot A_{\ge Q-i};\ 1 \le i \le Q,\ 1 \le k \le l < K,$
$P_{(i,k,0),(j,K,0)} = P_{s,k}\cdot B_{K-k}(K-k)\cdot A_{j-i+\alpha} + kP_{s,k}\cdot \widehat{P}_e\cdot B_{K-k}(K-k)\cdot A_{j-i} + \widehat{T}_k\cdot B_{l-k}(K-k)\cdot A_{j-i};\ 1 \le i \le j < Q,\ 1 \le k \le K,$	$P_{(i,k,0),(Q,K,0)} = P_{s,k}\cdot B_{K-k}(K-k)\cdot A_{\ge Q-i+\alpha} + kP_{s,k}\cdot \widehat{P}_e\cdot B_{K-k}(K-k)\cdot A_{\ge Q-i} + \widehat{T}_k\cdot B_{l-k}(K-k)\cdot A_{\ge Q-i};\ 1 \le i \le Q,\ 1 \le k \le K.$
$k+1$ nodes including the RN are active. Successful transmission by the RN after r failed attempts	
$P_{(i,k,r),(j,l,0)} = P_{s,k}\cdot B_{l-k}(K-k)\cdot A_j;\ 1 \le i \le F,\ 0 \le j \le i-1,\ 0 \le k \le l < K,\ 0 \le r \le R,$	$P_{(i,k,r),(j,l,0)} = P_{s,k}\cdot B_{l-k}(K-k)\cdot A_{j-i+F};\ F+1 \le i \le Q,\ i-F \le j \le i-1,\ 0 \le k \le l \le K,\ 0 \le r \le R,$
$P_{(i,k,r),(j,l,0)} = P_{s,k}\cdot B_{l-k}(K-k)\cdot A_{j-i+\alpha};\ 1 \le i \le j < Q,\ 0 \le k \le l \le K,\ 0 \le r < R,$	$P_{(i,k,r),(Q,l,0)} = P_{s,k}\cdot B_{l-k}(K-k)\cdot A_{\ge Q-i+\alpha};\ 1 \le i \le Q,\ 0 \le k \le l \le K,\ 0 \le r < R,$
$k+1$ nodes including the RN are active. Failed transmission by the RN	
$P_{(i,k,r),(j,l,r+1)} = P_{f,k}\cdot B_{l-k}(K-k)\cdot A_{j-i};\ 1 \le i \le j < Q,\ 0 \le k \le l \le K,\ 0 \le r < R,$	$P_{(i,k,r),(Q,l,r+1)} = P_{f,k}\cdot B_{l-k}(K-k)\cdot A_{\ge Q-i};\ 1 \le i \le Q,\ 0 \le k \le l \le K,\ 0 \le r < R.$
$P_{(i,k,R),(j,l,0)} = P_{sf,k}\cdot B_{l-k}(K-k)\cdot A_{j-i+\alpha};\ 1 \le i \le Q,\ i-\alpha \le j < Q,\ 0 \le k \le l \le K,$	$P_{(i,k,R),(Q,l,0)} = P_{sf,k}\cdot B_{l-k}(K-k)\cdot A_{\ge Q-i+\alpha};\ 1 \le i \le Q,\ 0 \le k \le l \le K.$
$k+1$ nodes including the RN are active. The RN loses access contention	
$P_{(i,k,r),(j,l,r)} = kP_{s,k}\cdot P_e\cdot B_{l-k+1}(K-k)\cdot A_{j-i} + kP_{s,k}\cdot \widehat{P}_e\cdot B_{l-k}(K-k)\cdot A_{j-i} + \widehat{T}_k\cdot B_{l-k}(K-k)\cdot A_{j-i};\ 1 \le i \le j < Q,\ 1 \le k < K,\ 0 \le r \le R,$	$P_{(i,k,r),(Q,l,r)} = kP_{s,k}\cdot P_e\cdot B_{l-k+1}(K-k)\cdot A_{\ge Q-i} + kP_{s,k}\cdot \widehat{P}_e\cdot B_{l-k}(K-k)\cdot A_{\ge Q-i} + \widehat{T}_k\cdot B_{l-k}(K-k)\cdot A_{\ge Q-i};\ 1 \le i \le Q,\ 1 \le k < K,\ 0 \le r \le R,$
$P_{(i,K,r),(j,K,r)} = KP_{s,K}\cdot \widehat{P}_e\cdot B_{K-K}(K-K)\cdot A_{j-i} + \widehat{T}_K\cdot B_{K-K}(K-K)\cdot A_{j-i};\ 1 \le i \le j < Q,\ 0 \le r \le R,$	$P_{(i,K,r),(Q,K,r)} = KP_{s,K}\cdot \widehat{P}_e\cdot B_{K-K}(K-K)\cdot A_{\ge Q-i} + \widehat{T}_K\cdot B_{K-K}(K-K)\cdot A_{\ge Q-i};\ 1 \le i \le Q,\ 0 \le r \le R,$
$P_{(i,k,r),(j,k-1,r)} = kP_{s,k}\cdot P_e\cdot B_0(K-k)\cdot A_{j-i};\ 1 \le i \le j < Q,\ 1 \le k \le K,\ 0 \le r \le R,$	$P_{(i,k,r),(Q,k-1,r)} = kP_{s,k}\cdot P_e\cdot B_0(K-k)\cdot A_{\ge Q-i};\ 1 \le i \le Q,\ 1 \le k \le K,\ 0 \le r \le R.$

table. As an example, we explain $P_{(i,k,0),(j,l,0)}$, i.e., the transition probability from State $(i,k,0)$ to State $(j,l,0)$. It is given by,

$$\begin{aligned} P_{(i,k,0),(j,l,0)} &= P_{s,k} \cdot B_{l-k}(K-k) \cdot A_{j-i+\alpha} \\ &+ kP_{s,k} \cdot P_e \cdot B_{l-k+1}(K-k) \cdot A_{j-i} \\ &+ kP_{s,k} \cdot \widehat{P}_e \cdot B_{l-k}(K-k) \cdot A_{j-i} \\ &+ \widehat{T}_k \cdot B_{l-k}(K-k) \cdot A_{j-i}\,. \\ & i-\alpha \leq j < Q\,,\ 0 \leq l-k \leq l\,,\ l < K\,. \end{aligned}$$

The first term defines the probability that the RN wins the contention, it transmits a frame composed of $\alpha = min(i,F)$ packets, it receives $j-i+\alpha$ packets and $l-k$ nodes out of the $K-k$ inactive ones become active. The second term defines the probability that an active node different from the RN wins the contention, it transmits a frame successfully and its buffer becomes empty (P_e), and therefore the node becomes inactive, $l-k+1$ nodes out of the $K-k$ inactive ones become active, and the RN receives $j-i$ packets. The third term defines the probability that an active node different from the RN wins the contention, it transmits a frame successfully but its buffer does not become empty ($\widehat{P}_e$), $l-k$ nodes out of the $K-k$ inactive ones become active, and the RN receives $j-i$ packets. Lastly, the fourth term defines the probability that the RN does not transmit when contending with other k nodes and two or more of the other nodes collide ($\widehat{T}_k$), $l-k$ nodes out of the $K-k$ inactive ones become active, and the RN receives $j-i$ packets. Note that in the last term it is assumed that, for any of the nodes that collide, the probability that it discards a frame and becomes inactive is negligible.

The solution of this aperiodic and irreducible DTMC is obtained by solving the set of linear equations

$$\boldsymbol{\pi P} = \boldsymbol{\pi}\,, \quad \boldsymbol{\pi e} = \mathbf{1}\,, \tag{C.3}$$

where $\boldsymbol{\pi}$ is the stationary distribution, $\boldsymbol{P}$ is the transition probability matrix, whose elements are defined in Table C.2, and $\boldsymbol{e}$ is a column vector of ones. The elements of the distribution $\boldsymbol{\pi}$ are $\pi(i,k,r)$, i.e., the fraction of cycles

where the RN is in State (i,k,r). To determine

$$P_e = \frac{P_s A_0 \sum_{i=1}^{F} \pi_i}{P_s (1-\pi_0)}, \tag{C.4}$$

the stationary distribution $\boldsymbol{\pi}$ is required, where P_s is the average probability that an active node transmits a frame successfully in a random cycle conditioned on being active, and π_i is the stationary probability of finding i packets in the queue of a node. Note that P_e is a conditional probability. Its denominator is the fraction of cycles where the RN transmits a frame successfully. While its numerator is the fraction of cycles where the RN successfully transmits a frame that empties the buffer and no additional packets arrive. P_s and π_i can be determined by

$$P_s = \frac{1}{G} \sum_{i=1}^{Q} \sum_{k=0}^{K} \sum_{r=0}^{R} \pi(i,k,r) \cdot P_{s,k}, \tag{C.5}$$

$$\pi_i = \sum_{k=0}^{K} \sum_{r=0}^{R} \pi(i,k,r), \tag{C.6}$$

where $G = \sum_{i=1}^{Q} \sum_{k=0}^{K} \sum_{r=0}^{R} \pi(i,k,r)$.

By solving the set of equations (C.3), $\boldsymbol{\pi}(P_s)$ can be determined for a given P_s. Then, a new $P_s(\boldsymbol{\pi})$ can be obtained from (C.5) for a given $\boldsymbol{\pi}$. Denote by P_s the solution of this fixed-point equation, i.e., the value of $P_s(\boldsymbol{\pi})$ at the fixed-point. Note that the stationary distribution for the 3D DTMC that defines the operation of the SPT scheme with finite retransmissions can be readily obtained by setting $F = 1$.

Note that finding a good estimation for the distribution of the number of active nodes in a cycle is crucial to determine with precision P_s, the stationary distribution $\boldsymbol{\pi}$, and the performance parameters defined later in Section V. In [12] we compared the accuracy of different performance parameters obtained when two different approaches are used to characterize the number of active nodes in a cycle. That is, i) when it is assumed that nodes become active independently, as done for example in [7], [11], and the number of active nodes in a cycle follows a binomial distribution; and ii) when the number of active nodes in the network is represented in the network state vector and evolves from cycle to cycle, as done in the model proposed here. The

study concludes that substantially more accurate results are obtained when the second approach is adopted.

B. 2D DTMC for APT with Infinite Retransmissions

The main objective of the proposed 3D DTMC model is to evaluate the performance of a WSN that employs an APT scheme on a synchronous DC MAC when frame retransmissions are enabled. As it will be shown later in Section VI, a vast majority of the frames require at most two retransmissions to achieve a successful transmission. Therefore, the same performance would be observed by setting $R \geq 2$. This observation motivated us to develop a simpler 2D DTMC model to evaluate the performance of APT with infinite retransmissions.

We adopt the same notation used for the 3D DTMC, except that the dimension related to the number of retransmissions, r, is omitted. A state in the 2D DTMC is represented by (i,k), where i is the number of packets in the queue of the RN, $i \leq Q$, and k is the number of active nodes other than the RN in the network, $k \leq K = N-1$. Then, $P_{(i,k),(j,l)}$ is the transition probability from State (i,k) to State (j,l).

The transition probabilities of the proposed 2D DTMC are given in Table C.3. In the table, the first row defines transitions caused only by new arrivals when the RN has an empty queue and no other node is active. The second row describes transmissions made by the other nodes while the RN has an empty queue. The third and fourth rows define RN's transmissions in cycles where there is no other active node and when there are other active nodes respectively. Lastly, the fifth row defines transitions that are not possible.

The stationary distribution can be determined by solving the set of linear equations (C.3), where the transition probability matrix $\boldsymbol{P}$ is now defined in Table C.3. As in the 3D DTMC, P_s is found as the solution of a fixed-point equation where

$$P_s = \frac{1}{G} \sum_{i=1}^{Q} \sum_{k=0}^{K} \pi\,(i,k) \cdot P_{s,k}\,, \tag{C.7}$$

$$\pi_i = \sum_{k=0}^{K} \pi(i,k)\,, \tag{C.8}$$

Table C.3: Transition Probabilities of the 2D DTMC Model for S-MAC-APT with Infinite Retransmissions

No active node exists. Transitions occur due to new arrivals	
$P_{(0,0),(j,l)} = B_l(K)\cdot A_j;\ 0 \le j < Q,\ 0 \le l \le K,$	$P_{(0,0),(Q,l)} = B_l(K)\cdot A_{\ge Q};\ 0 \le l \le K.$
No packets in the queue of the RN, i.e., no transmissions by the RN. Transitions are caused by the other k active nodes	
$P_{(0,k),(j,l)} = S_k\cdot P_e\cdot B_{l-k+1}(K-k)\cdot A_j + S_k\cdot \widehat{P}_e\cdot B_{l-k}(K-k)\cdot A_j + \widehat{S}_k\cdot B_{l-k}(K-k)\cdot A_j;\ 0 \le j < Q,\ 1 \le k \le l < K,$	$P_{(0,k),(Q,l)} = S_k\cdot P_e\cdot B_{l-k+1}(K-k)\cdot A_{\ge Q} + S_k\cdot \widehat{P}_e\cdot B_{l-k}(K-k)\cdot A_{\ge Q} + \widehat{S}_k\cdot B_{l-k}(K-k)\cdot A_{\ge Q};\ 1 \le k \le l < K,$
$P_{(0,k),(j,K)} = S_k\cdot \widehat{P}_e\cdot B_{K-k}(K-k)\cdot A_j + \widehat{S}_k\cdot B_{K-k}(K-k)\cdot A_j;\ 0 \le j < Q,\ 1 \le k \le K,$	$P_{(0,k),(Q,K)} = S_k\cdot \widehat{P}_e\cdot B_{K-k}(K-k)\cdot A_{\ge Q} + \widehat{S}_k\cdot B_{K-k}(K-k)\cdot A_{\ge Q};\ 1 \le k \le K.$
$P_{(0,k),(0,k-1)} = S_k\cdot P_e\cdot B_0(K-k)\cdot A_j;\ 0 \le j < Q,\ 1 \le k \le K,$	$P_{(0,k),(Q,k-1)} = S_k\cdot P_e\cdot B_0(K-k)\cdot A_{\ge Q};\ 1 \le k \le K,$
The RN is the only active node	
$P_{(i,0),(j,l)} = P_{s,0}\cdot B_l(K)\cdot A_j\ 1 \le i \le F,\ 0 \le j \le i-1,\ 0 \le l \le K,$	$P_{(i,0),(j,l)} = P_{s,0}\cdot B_l(K)\cdot A_{j-i+F}\ F+1 \le i \le Q,\ i-F \le j \le i-1,\ 0 \le l \le K,$
$P_{(i,0),(j,l)} = P_{s,0}\cdot B_l(K)\cdot A_{j-i+\alpha}\ 1 \le i \le j < Q,\ 0 \le l \le K,$	$P_{(i,0),(Q,l)} = P_{s,0}\cdot B_l(K)\cdot A_{\ge Q-i+\alpha}\ 1 \le i \le Q,\ 0 \le k \le K.$
Contention: transitions are caused by $k+1$ active nodes including the RN	
$P_{(i,k),(j,l)} = P_{s,k}\cdot B_{l-k}(K-k)\cdot A_j\ 1 \le i \le F,\ 0 \le j \le i-1,\ 0 \le k \le l < K,$	$P_{(i,k),(j,l)} = P_{s,k}\cdot B_{l-k}(K-k)\cdot A_{j-i+F}\ F+1 \le i \le Q,\ i-F \le j \le i-1,\ 0 \le k \le l \le K,$
$P_{(i,k),(j,l)} = P_{s,k}\cdot B_{l-k}(K-k)\cdot A_{j-i+\alpha} + kP_{s,k}\cdot P_e\cdot B_{l-k+1}(K-k)\cdot A_{j-i} + kP_{s,k}\cdot \widehat{P}_e\cdot B_{l-k}(K-k)\cdot A_{j-i} + \widehat{S}_{k+1}\cdot B_{l-k}(K-k)\cdot A_{j-i};\ 1 \le i \le j < Q,\ 1 \le k \le l < K,$	$P_{(i,k),(Q,l)} = P_{s,k}\cdot B_{l-k}(K-k)\cdot A_{\ge Q-i+\alpha} + kP_{s,k}\cdot P_e\cdot B_{l-k+1}(K-k)\cdot A_{\ge Q-i} + kP_{s,k}\cdot \widehat{P}_e\cdot B_{l-k}(K-k)\cdot A_{\ge Q-i} + \widehat{S}_{k+1}\cdot B_{l-k}(K-k)\cdot A_{\ge Q-i};\ 1 \le i \le Q,\ 1 \le k \le l < K,$
$P_{(i,k),(j,K)} = P_{s,k}\cdot B_{K-k}(K-k)\cdot A_{j-i+\alpha} + kP_{s,k}\cdot \widehat{P}_e\cdot B_{K-k}(K-k)\cdot A_{j-i} + \widehat{S}_{k+1}\cdot B_{K-k}(K-k)\cdot A_{j-i};\ 1 \le i \le j < Q,\ 1 \le k \le K,$	$P_{(i,k),(Q,K)} = P_{s,k}\cdot B_{K-k}(K-k)\cdot A_{\ge Q-i+\alpha} + kP_{s,k}\cdot \widehat{P}_e\cdot B_{K-k}(K-k)\cdot A_{\ge Q-i} + \widehat{S}_{k+1}\cdot B_{K-k}(K-k)\cdot A_{\ge Q-i};\ 1 \le i \le Q,\ 1 \le k \le K,$
$P_{(i,k),(j,k-1)} = kP_{s,k}\cdot P_e\cdot B_0(K-k)\cdot A_{j-i}1 \le i \le j < Q,\ 1 \le k \le K,$	$P_{(i,k),(Q,k-1)} = kP_{s,k}\cdot P_e\cdot B_0(K-k)\cdot A_{\ge Q-i}1 \le i \le Q,\ 1 \le k \le K.$
Impossible transitions	
$P_{(i,k),(j,k-1)} = 0;\ 1 \le i \le Q,\ j < i,\ 1 \le k \le K,$	$P_{(i,k),(j,l)} = 0;\ F+1 \le i \le Q,\ j < i-F,\ 0 \le k \le l \le K.$
$P_{(i,k),(j,l)} = 0,\ 0 \le i \le j \le Q,\ 2 \le k \le K,\ l \le k-2,$	

and $G = \sum_{i=1}^{Q} \sum_{k=0}^{K} \pi(i,k)$. Similarly, the stationary distribution for the 2D DTMC that defines the operation of the SPT scheme with infinite retransmissions can be readily obtained by configuring $F = 1$.

V. PERFORMANCE PARAMETERS

In this section, we derive expressions for average packet delay, throughput, packet loss probability, average energy consumption per cycle, and energy efficiency for S-MAC operating on both the APT and the SPT schemes. Recall that the 2D and 3D models are developed based on the assumption that the channel is error-free.

A. Average Packet Delay

Let D be the average delay that a packet experiences from its arrival until it is successfully transmitted. Then, D can be determined by applying Little's law,

$$D = \frac{N_{av}}{\gamma_a},\ N_{av} = \sum_{i=0}^{Q} i\pi_i,\ \gamma_a = \sum_{i=0}^{Q} b_i \pi_i, \tag{C.9}$$

where $b_0 = \sum_{q=0}^{Q} q \cdot A_q + Q \cdot A_{\geq Q+1}$ and $b_i = \sum_{q=0}^{Q-i} q \cdot A_q + (Q - i + P_s) A_{\geq Q-i+1}$, $i > 0$. Note that: i) π_i is the stationary probability of finding i packets in the queue of the RN, and is determined by expressions (C.6) or (C.8); ii) N_{av} is the average number of packets in the queue; iii) γ_a is the average number of packets that entered the queue (*accepted*) per cycle; and iv) b_i is the mean number of packets *accepted* per cycle at state i. Note also that the last term of b_i is obtained from $((Q-i+1)P_s + (Q-i)(1-P_s))A_{\geq Q-i+1}$.

B. Throughput

We define the node throughput, η, as the average number of packets successfully delivered by a node in a cycle. For the 3D and 2D DTMCs, η can be determined respectively as follows.

$$\eta = \begin{cases} \sum_{i=1}^{Q} \sum_{k=0}^{K} \sum_{r=0}^{R} \alpha \cdot \pi(i,k,r) \cdot P_{s,k} & \text{for 3D} \\ \sum_{i=1}^{Q} \sum_{k=0}^{K} \alpha \cdot \pi(i,k) \cdot P_{s,k} & \text{for 2D} \end{cases} \tag{C.10}$$

Recall that $\alpha = min(i,F)$. In a network composed of N sensor nodes, the

total network throughput expressed in packets per cycle is given by

$$Th = N \cdot \eta \,. \tag{C.11}$$

C. Packet Loss Probability

Since the channel is assumed to be error-free, two causes might lead to a packet drop: i) it encounters the buffer full upon arrival; i.e., it might be discarded due to buffer overflow; ii) its transmission fails after R retransmissions. Recall that R is the maximum number of retransmissions allowed for a frame. The average number of packets lost per cycle due to buffer overflow is $\lambda T - \gamma_a$, where λT is the mean number of packets that arrived per cycle, and γ_a is the average number of packets accepted in the queue per cycle (C.9).

For the 3D DTMC that models a system with finite retransmissions, let P_L^c denote the packet loss probability due to collisions,

$$P_L^c = \frac{1}{H} \sum_{i=1}^{Q} \sum_{k=0}^{K} \alpha \cdot \pi\,(i,k,R) \cdot P_{f,k}\,, \tag{C.12}$$

where $H = \sum_{i=1}^{Q} \sum_{k=0}^{K} \sum_{r=0}^{R-1} \alpha \cdot \pi\,(i,k,r) \cdot P_{s,k} + \sum_{i=1}^{Q} \sum_{k=0}^{K} \alpha \cdot \pi\,(i,k,R) \cdot P_{sf,k}$. Note that once the packet is in the queue, it will be either successfully transmitted or dropped. Then, P_L^c is the fraction of accepted packets that are discarded after R consecutive unsuccessful retransmissions. Since H is the average number of packets transmitted per cycle successfully or with failure, it must be equal to the average number of packets accepted at the queue per cycle γ_a.

The total packet loss probability, including buffer overflow and packet losses due to collisions in the medium, can be determined by,

$$P_L = 1 - \frac{(1 - P_L^c)\,\gamma_a}{\lambda T}\,. \tag{C.13}$$

Note that in the 2D case, packet loss is only due to buffer overflow since a packet which encounters collisions will be retransmitted until it is successfully received.

D. Average Energy Consumption

As described in Section III, the *active* period of a cycle is further divided

into the *sync* and *data* periods. The energy consumed during the *active* period represents the dominant contribution to the total energy consumption. In this subsection we calculate the energy consumed by the RN in the *sync*, *data* and *sleep* periods. Note that we only study the energy consumed by the radio frequency transceiver. The energy consumed by the sensor nodes due to their event sensing tasks is application dependent and is not included here.

1) Energy Consumption in the* sync *Period: Denote by $T_{sync} = (W - 1) + t_{SYNC} + D_p$ the duration of a *sync* period. Recall that we assume for simplicity that the RN *broadcasts* one *SYNC* packet every N_{sc} cycles, i.e., one packet per *update* super-cycle, and receives one packet per cycle in the remaining $N_{sc} - 1$ cycles. Accordingly, the energy consumed by the RN in the *sync* period is given by,

$$E_{sc} = \frac{1}{N_{sc}} \cdot [(t_{SYNC} \cdot P_{tx} + (T_{sync} - t_{SYNC}) \cdot P_{rx})] + \frac{N_{sc} - 1}{N_{sc}} \cdot (T_{sync} \cdot P_{rx}) \,, \tag{C.14}$$

where P_{tx} and P_{rx} are the transmission and reception power levels respectively. Note that in the transmission of the *SYNC* packet, the RN consumes energy for carrier sensing as well, and this energy consumption is already included in the second part of the first term in (C.14).

2) Energy Consumption in the* data *Period: In the APT scheme, the number of packets aggregated in a frame depends on the number of packets available in the queue at the transmission time. The average size of a frame transmitted by the RN when it contends with other k nodes, f_k, can be obtained by

$$f_k = \begin{cases} \frac{1}{G_k} \sum_{i=1}^{Q} \sum_{r=0}^{R} \alpha \cdot \pi(i,k,r) & \text{for 3D} \\ \frac{1}{G_k} \sum_{i=1}^{Q} \alpha \cdot \pi(i,k) & \text{for 2D} \end{cases} \tag{C.15}$$

where $\alpha = min(i,F)$, $G_k = \sum_{i=1}^{Q} \sum_{r=0}^{R} \pi(i,k,r)$ for the 3D DTMC, and $G_k = \sum_{i=1}^{Q} \pi(i,k)$ for the 2D DTMC, $0 \leq k \leq N-1$, respectively. Note that $f_k = 1$ for the SPT scheme.

In order to calculate the average energy consumed in the *data* period of a cycle, we consider the following constants associated with the RN during: i) a successful transmission when it contends with other k nodes $E_{txs,k} =$

$(t_{RTS} + f_k \cdot t_{DATA}) \cdot P_{tx} + (t_{CTS} + t_{ACK}) \cdot P_{rx}$, ii) a transmission failure (collision) $E_{txf} = t_{RTS} \cdot P_{tx} + t_{CTS} \cdot P_{rx}$, and iii) during overhearing situations $E_{oh} = E_{oh} = t_{RTS} \cdot P_{rx}$, where t_{RTS}, t_{DATA}, t_{CTS} and t_{ACK} are the corresponding packet transmission times. Recall that nodes address their frames to the sink, and that the sink receives but does not transmit. Then, the average energy consumed by the RN during the *data* period of a cycle when it contends with other k nodes, $k \geq 1$, is obtained by

$$\begin{aligned} E_{d,k+1} = {} & q_{1,k} P_{s,k} \cdot \left[E_{txs,k} + \left(4D_p + BT_{s,k} \right) \cdot P_{rx} \right] \\ & + q_{1,k} P_{f,k} \cdot \left[E_{txf} + \left(2D_p + BT_{f,k} \right) \cdot P_{rx} \right] \\ & + q_{2,k} P_{s,k} \left[E_{oh} + \left(D_p + BT_{s,k} \right) \cdot P_{rx} \right] \\ & + q_{3,k} \cdot \left[E_{oh} + \left(D_p + BT_{f,k} \right) \cdot P_{rx} \right] , \end{aligned} \tag{C.16}$$

where D_p is the one-way propagation delay. Conditioned on finding $k+1$ nodes active, $q_{1,k} = (k+1)/N$ is the probability that the RN is active, $q_{2,k} = k q_{1,k} + (k+1)\left(1 - q_{1,k}\right)$ is the average number of active nodes other than the RN, and $q_{3,k} = 1 - q_{2,k} P_{s,k} - q_{1,k} P_{sf,k}$ is the probability that nodes other than the RN transmit a frame with failure. Note that the terms in $E_{d,k+1}$ correspond to the energy consumed by: a frame successfully transmitted, a frame transmitted that collides, overhearing a successful frame transmitted by nodes other than the RN, and overhearing a collision of frames transmitted by nodes other than the RN, respectively. Also, $E_{d,1} = q_{1,0} \cdot [E_{txs,0} + (4D_p + (W-1)/2) \cdot P_{rx}] + q_{2,0} \cdot [E_{oh} + (D_p + (W-1)/2) \cdot P_{rx}]$, and $E_{d,0} = (t_{RTS} + W + D_p) \cdot P_{rx}$.

3) Energy Consumption in the* sleep *Period:

When $k+1$ active nodes contend in a cycle, where $k \geq 1$, the average energy consumed by the RN during the *sleep* period of an *awake* cycle is given by,

$$\begin{aligned} E_{aw,k+1} = {} & q_{1,k} P_{s,k} \cdot \left[\left(T - T_{sync} - T_{d,s,k} \right) \cdot P_{rx} \right] \\ & + q_{1,k} P_{f,k} \cdot \left[\left(T - T_{sync} - T_{d,f,k} \right) \cdot P_{rx} \right] \\ & + q_{2,k} P_{s,k} \left[\left(T - T_{sync} - T_{d,os,k} \right) \cdot P_{rx} \right] \\ & + q_{3,k} \cdot \left[\left(T - T_{sync} - T_{d,of,k} \right) \cdot P_{rx} \right] , \end{aligned} \tag{C.17}$$

where $T_{d,s,k} = t_{RTS} + f_k \cdot t_{DATA} + t_{CTS} + t_{ACK} + 4D_p + BT_{s,k}$, $T_{d,f,k} = t_{RTS} + t_{CTS} + 2D_p + BT_{f,k}$, $T_{d,os,k} = t_{RTS} + D_p + BT_{s,k}$, and $T_{d,of,k} = t_{RTS} + D_p + BT_{f,k}$. These terms represent the duration of the *data* period when the RN contends with other k active nodes and different events happen in the cycle: i) when a successful frame is transmitted by the RN ($T_{d,s,k}$); ii) when a frame transmitted by the RN collides ($T_{d,f,k}$); iii) when the RN overhears a successful frame transmitted by a node different from the RN ($T_{d,os,k}$); and, iv) when the RN overhears a frame transmitted by a node different from the RN that collides ($T_{d,of,k}$). Also, $E_{aw,1} = q_{1,0} \cdot \left[\left(T - T_{sync} - T_{d,s,0}\right) \cdot P_{rx}\right] + q_{2,0} \cdot [(T - T_{sync} - (t_{RTS} + D_p + (W-1)/2)) \cdot P_{rx}]$ and $E_{aw,0} = [(T - T_{sync} - (W + t_{RTS} + D_p)) \cdot P_{rx}]$ where $T_{d,s,0} = t_{RTS} + f_0 \cdot t_{DATA} + t_{CTS} + t_{ACK} + 4D_p + (W-1)/2$, and $T_{d,os,0} = t_{RTS} + D_p + (W-1)/2$. Recall that in cycles where there are not active nodes in the network, the RN has to overhear the medium during the maximum duration of the backoff time, which is W.

Similarly, the energy consumed by the RN during the *sleep* period of a normal cycle, $E_{nr,k}$, can be obtained by replacing the P_{rx} with the sleep power level, P_{sl}, in (C.17).

4) Total Average Energy Consumption per Cycle:

The average energy consumed by the RN during the *data* period of a cycle is given by,

$$E_d = \sum_{k=0}^{N} E_{d,k} \cdot \pi'_k \tag{C.18}$$

where π'_k is the stationary probability of finding k active nodes in the network. For the 3D and 2D DTMCs these probabilities can be respectively determined by,

$$\pi'_k = \begin{cases} \sum_{i=1}^{Q} \sum_{r=0}^{R} \pi(i,k-1,r) + \pi(0,k,0) & \text{for 3D} \\ \sum_{i=1}^{Q} \pi(i,k-1) + \pi(0,k) & \text{for 2D} \end{cases} \tag{C.19}$$

for $1 \leq k \leq N-1$. Also, $\pi'_0 = \pi(0,0,0)$ or $\pi'_0 = \pi(0,0)$, and $\pi'_N = \sum_{i=1}^{Q} \sum_{r=0}^{R} \pi(i,N-1,r)$ or $\pi'_N = \sum_{i=1}^{Q} \pi(i,N-1)$, respectively.

The average energy consumed during the *sleep* period of a *normal* cycle

is obtained by

$$E_{nr} = \sum_{k=0}^{N} E_{nr,k} \cdot \pi'_k \,. \tag{C.20}$$

The average energy consumed during the *sleep* period of a cycle belonging to an *awake* super-cycle where the node is awake is determined by

$$E_{aw} = \sum_{k=0}^{N} E_{aw,k} \cdot \pi'_k \,. \tag{C.21}$$

Then, the average energy consumption during the *sleep* period of a cycle is obtained by

$$E_{sl} = \frac{E_{nr} \cdot N_{sc} \cdot (N_{aw} - 1) + E_{aw} \cdot N_{sc}}{N_{sc} \cdot N_{aw}} \,. \tag{C.22}$$

Finally, the total average energy consumed by the RN in a cycle is obtained by

$$E = E_{sc} + E_d + E_{sl} \,. \tag{C.23}$$

As discussed for the computation of P_s according to (C.5), the accuracy of the energy terms in (C.18), (C.20) and (C.21) improves with the accuracy of the distribution of active nodes in the network.

E. Energy Efficiency

We define the energy efficiency of the RN, ξ, as the ratio between the average number of bytes successfully transmitted per cycle and the total average energy consumed in that cycle. In a network where *DATA* packets have a constant size of S bytes, it can be determined as,

$$\xi = \eta \cdot S/E \,. \tag{C.24}$$

Recall that the number of packets aggregated by a node in consecutive frames changes randomly.

VI. Numerical Results for Error-Free Channels

In this section, we compare the performance of APT against SPT by enabling finite and infinite retransmissions with an error-free channel. The analytical results are obtained based on the developed 3D and 2D DTMC models. The simulation results are obtained by implementing the transmission schemes in a custom-built C based discrete-event simulator.

The developed simulator mimics the physical behavior of the APT and SPT schemes. That is, in each cycle a node receives packets according to a given discrete distribution, contends for channel access with other nodes if it has packets in the buffer, and, if it wins, then transmits a frame (a packet) using APT (SPT). The simulation results are completely independent of those obtained by the analytical models. That is, the calculation of the performance metrics in our simulations is not dependent on the derived mathematical expressions at all, nor are the state transition tables used in these calculations. The performance results reported below are the average values of the measurements made over $5 \cdot 10^6$ cycles and the accuracy of the models is validated later in this section.

Table C.4: Time Parameters (unit: millisecond)

Cycle duration (T)	60	Propagation delay (D_p)	0.001
t_{RTS}, t_{CTS} and t_{ACK}	0.18	t_{SYNC}	0.18
t_{DATA}	1.716	Contention Window (W)	128

Consider a WSN as the one illustrated in Figure C.1. To investigate the performance of our models, the network is configured with the following parameters: number of sensor nodes $N \in \{5,\ldots,30\}$, queue capacity of a node $Q = 10$, *DATA* packet size is $S = 50$ bytes, the APT scheme is configured with a maximum number of packets per frame $F \in \{2,5,10\}$, packet arrival rate $\lambda \in [0.5,4.5]$ packets/s, $N_{sc} = 10$, $N_{aw} = 40$, the transmission, reception and sleep power levels are: $P_{tx} = 52$ mW, $P_{rx} = 59$ mW and $P_{sl} = 3$ μW [23], respectively. The duration of a backoff time slot is configured as 0.1 ms. The time parameters are summarized in Table C.4.

We adopt the term *load* to refer to the offered traffic, i.e., the ratio between the packet arrival rate and the packet service rate. Observe that the packet arrival rate does not depend on the transmission scheme implemented by the

nodes, i.e., APT or SPT. On the other hand, the packet service rate clearly depends on the transmission scheme as, on average, the number of packets transmitted successfully per cycle increases with F. Then, for the same arrival rate, a node, or the network, is more loaded when SPT is deployed than when APT is deployed.

A. APT versus SPT with Finite Retransmissions

Two extreme packet arrival rate conditions are investigated, that correspond to the arrival rates of $\lambda = 0.5$ (light traffic load) and 4.5 packets/s (heavy traffic load), respectively. As a reference to reflect the intensity of the load offered to a node that deploys SPT and has $R = \infty$, the packet loss probabilities due to buffer overflow induced by these two arrival rates are approximately in the order of 10^{-12} and 10^{-1}, respectively.

Clearly, the performance of the APT scheme can be better demonstrated when $\lambda = 4.5$ packets/s. For these evaluation configurations, we define a network of $N = 5$ nodes with a single sink node, and vary the maximum number of retransmissions in the set $R \in \{1, \ldots, 10\}$.

1) Impact of the Maximum Number of Retransmissions: We evaluate the impact that the maximum number of retransmissions, R, has on the total packet loss, i.e., losses due to transmissions that collide plus losses due to buffer overflows, when $\lambda = 4.5$ packets/s. Note that once a packet is accepted in the queue, it might be successfully delivered or dropped. When retransmissions are disabled, the packet is dropped after the first collision. On the other hand, when R is infinite, the packet stays in the queue until it is delivered successfully. When finite retransmissions are enabled, the packet is dropped after R consecutive packet retransmissions that collide.

The variation of the packet loss probability due to unsuccessful retransmissions is illustrated in Figure C.3. In the figure, the curves associated with “DTMC" and “sim" show the results for finite retransmissions obtained by the corresponding 3D DTMC model and simulations respectively. The same notation is adopted in the rest of the figures in this section. Note that the results for zero retransmissions are obtained using the DTMC presented in Table C.3, but by replacing $P_{s,k}$ with $P_{sf,k}$. The results illustrated in Figure C.3 show that a vast majority of packets require at most two retransmissions using either SPT or APT. That is, the packet loss probability due to collisions is negligible for $R \geq 2$. Clearly, the delay, throughput and energy consump-

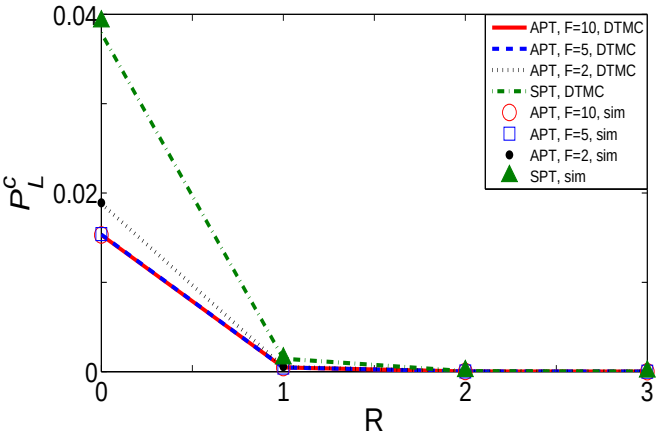

Figure C.3: Variation of the packet loss probability due to collisions, when retransmissions are enabled with $\lambda = 4.5$ packets/s and $N = 5$.

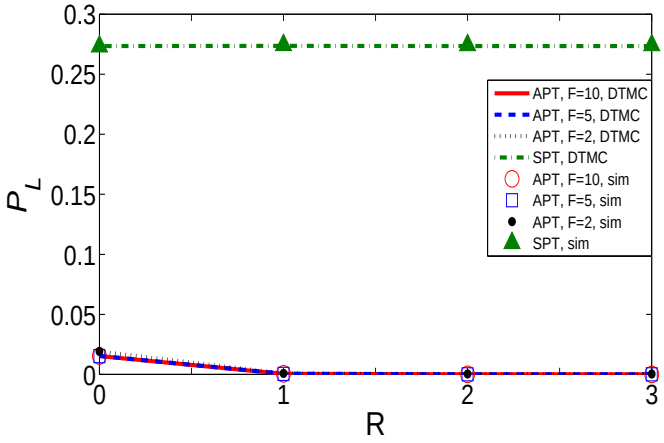

Figure C.4: Variation of the *total* packet loss probability, when retransmissions are enabled with $\lambda = 4.5$ packets/s and $N = 5$.

tion will keep constant for $R \geq 2$. For brevity, these parameters are studied only for $R = \infty$.

Figure C.4 shows the variation of the total packet loss probability, P_L, including losses due to packets discarded after R retransmissions, and buffer overflows, for the APT and SPT schemes. For SPT, $P_L = 27.4\%$ and this value appears to be insensitive to R. As shown in Figure C.3 for SPT, when $R > 2$ the packet drops due to collisions are negligible, then all losses are caused by buffer overflow. When $R = 0$, the SPT scheme will drop packets due to collisions. However, these losses seem to be compensated by having lower buffer overflow.

On the other hand, for the APT scheme and any value of $F \geq 2$, $P_L =$

1.55% for $R = 0$. Observe in Figure C.4 that $P_L \approx 0\%$ for $R \geq 2$ for APT. Clearly, the capability of transmitting multiple packets (a frame) per cycle contributes decisively to reduced queue occupancy, and therefore reduces buffer overflow.

B. APT versus SPT with Infinite Retransmissions

In this subsection we employ the 2D DTMC model to compare the throughput, average packet delay and average energy consumption of APT and SPT. The results are obtained based on two configurations: i) a fixed packet arrival rate of $\lambda = 1.5$ packets/s but different number of nodes $N \in \{5, \ldots, 30\}$; and ii) a fixed network size of $N = 15$ but different arrival rates $\lambda \in [0.5, 4.5]$ packets/s. Since $R = \infty$ in this model, no losses occur due to collisions over the channel, i.e., $P_L^c = 0$.

1) Total Throughput: Figures C.5 and C.7 illustrate the total network throughput Th under these two configurations. In both cases, the achieved throughput increases with the number of nodes, N, or the arrival rate, λ, up to the saturation point. For the SPT scheme, the saturation points occur at $N = 11$ and $\lambda = 1.1$ packets/s, as shown in the corresponding zoomed-in sub-figure of Figures C.5 and C.7 respectively. In the saturation regime, all nodes have packets to send in nearly all cycles, i.e., all nodes are active in nearly all cycles. As a reference, for $N = 15$ the fraction of cycles in which a node is not active is $\pi_0 = 1.18 \cdot 10^{-2}$, while for $N = 20$ it is $\pi_0 = 7.10 \cdot 10^{-4}$.

As shown in these figures, for SPT, Th decreases slightly as N increases beyond $N = 11$. This can be explained since we expect that for $N \geq 11$ all nodes are active in all cycles. Take $N = 15$ as an example. The probability that a node transmits a packet (frame) successfully is $P_{s,14} = 0.063$, while for $N = 30$ it is $P_{s,29} = 0.030$. Recall that $P_{s,k}$ was given by (C.1). That is, for $N = 15$ a node achieves slightly more than 6 successful (frame) transmissions every 100 cycles, while for $N = 30$ it achieves merely 3 successful transmissions every 100 cycles, approximately. Clearly, from (C.11) we have that $Th(N = 30)/Th(N = 15) \approx 2P_{s,29}/P_{s,14} = 0.94$. This explains why Th decays slightly after the saturation point.

As expected, a similar trend is observed for APT, but for larger values of N as F increases. As a reference, when $F = 2$ the saturation occurs approximately at $N = 20$ and $\lambda \geq 2.5$ packets/s. Note that, once the saturation point is reached, any additional load offered to the nodes will be rejected due to

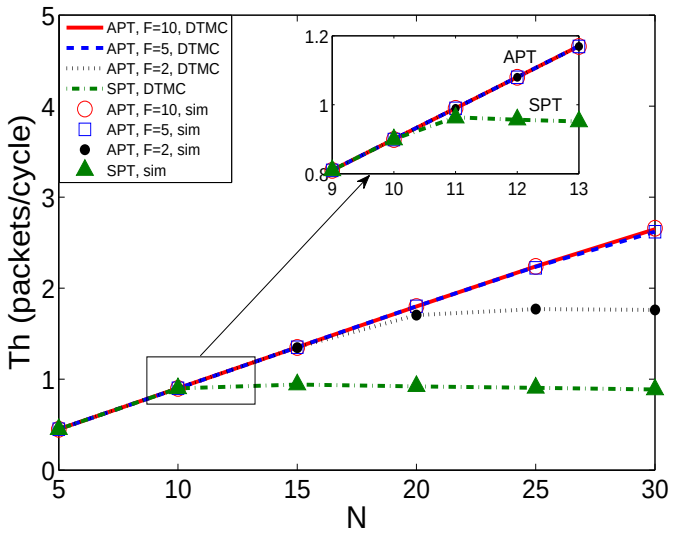

Figure C.5: Total throughput as the number of nodes varies, when $\lambda = 1.5$ packet/s and with infinite retransmissions.

buffer overflow.

2) Average Packet Delay: Figure C.6 displays the variation of the average packet delay with the network size N and with the maximum frame size F, when $\lambda = 1.5$ packets/s. Observe that the delay is almost zero when the number of nodes is small for both the APT and the SPT schemes. The reason is that a network with a small number of nodes has little contention. Then, nodes have immediate access to the channel and can transmit packets as soon as they arrive to the queue. On the other hand, when the number of nodes increases, it takes longer to get channel access due to increased contention. Then, packets have to wait longer time in the queue before being transmitted.

Observe the performance of SPT in Figures C.5 and C.6. We realize that the total throughput Th increases steadily with N up to $N = 11$, while for these network sizes the average packet delay D is very small. For $11 \leq N \leq 15$, Th does not increase but D increases sharply. We can conclude that the knee of the D and Th curves exists at $N = 11$, for the studied configuration. For $N \leq 10$, packets are transmitted as soon as they arrive at the node. Clearly, the number of active nodes per cycle is very small. However, for $N \geq 11$ collisions in the channel and delay both increase.

Figure C.8 depicts the performance of the average packet delay as λ varies, for different F values, when there are $N = 15$ nodes in the network.

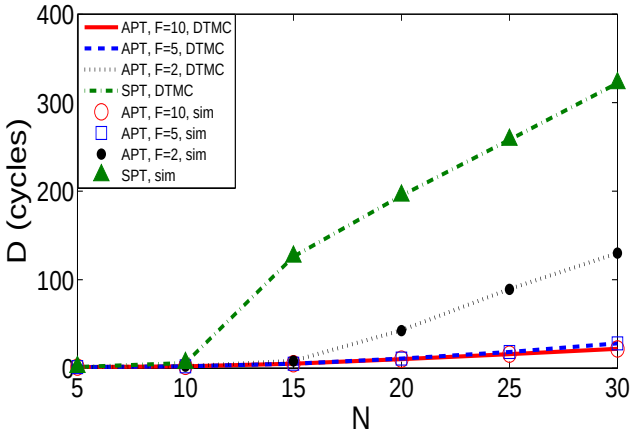

Figure C.6: Average packet delay as the number of nodes varies, when $\lambda = 1.5$ packet/s and with infinite retransmissions.

Similar observation as discussed above applies to this scenario. The delay is almost zero for $\lambda = 0.5$, as this very low arrival rate induces very little contention in the channel. As expected, APT achieves lower average packet delay than SPT does. By simply configuring $F = 2$, a drastic delay reduction is achieved. However, increasing F beyond 5 does not seem to have any significant impact. Recall that when $F = 5$ a frame can fit as much as half of the queue capacity ($Q = 10$).

3) Total Average Energy Consumption: The total average energy consumption per cycle, E, for the SPT and APT schemes is shown in Figures C.9 and C.11 for the two configurations studied. At a first glance it might look counter-intuitive that E is higher when the network is lightly loaded than when it is heavily loaded. This behavior is mainly due to idle listening, which is more acute in light loads. For medium and high loads, a node will go to sleep as soon as it hears an *RTS* or a collision in the channel. Whereas for light load, in many cycles nodes have to listen for the whole backoff window duration to realize that there were no active nodes.

For SPT, we observe that E decreases with the network size N and the arrival rate λ up to a point, approximately $N = 11$ and $\lambda = 1.1$ packets/s. Beyond that point, E decays approximately linearly with N or becomes constant with λ. As discussed above, at $N = 5$, the number of active nodes per cycle is very small, and then the energy consumption due to idle listening contributes significantly to E. For $N \geq 5$, E keeps on decreasing due to the increasing occupancy of the channel, up to the point ($N = 11$) beyond which

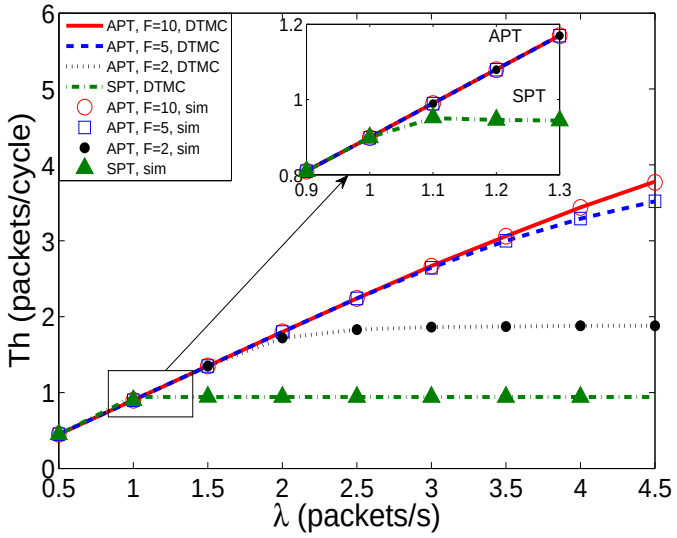

Figure C.7: Total throughput as the data arrival rate varies, when $N = 15$ and with infinite retransmissions.

the channel is busy in all cycles. The evolution of E with λ can be described in similar terms.

For APT, E behaves similarly as in SPT, but the shape of E depends now on the maximum number of packets aggregated per frame F. The total energy consumed by APT is always larger than the total energy consumed by SPT for all N and λ values. As mentioned before, this is due to the fact that as F increases, there will be more cycles with no active nodes, and therefore more energy is wasted by overhearing in those cycles. It is worth noting than the difference between the energy consumed by the APT and SPT schemes reduces drastically as the load increases.

4) Energy Efficiency: Figures C.10 and C.12 illustrate the evolution of the energy efficiency, ξ, with the network size N and the packet arrival rate λ. As shown in the figures, the energy efficiency achieved by APT is substantially higher than the one obtained by SPT, especially at high packet arrival rates and with a large node population. For example, as shown in Figure C.11, at $\lambda = 2.5$ packets/s, the total average energy consumed by a node deploying APT is only marginally higher than the one consumed by a node deploying SPT (0.39% larger for $F = 2$ and 1.65% larger for $F = 5$). On the other hand, with the same arrival rate, the total throughput Th for APT with $F = 2$, expressed as total number of packets successfully transmitted

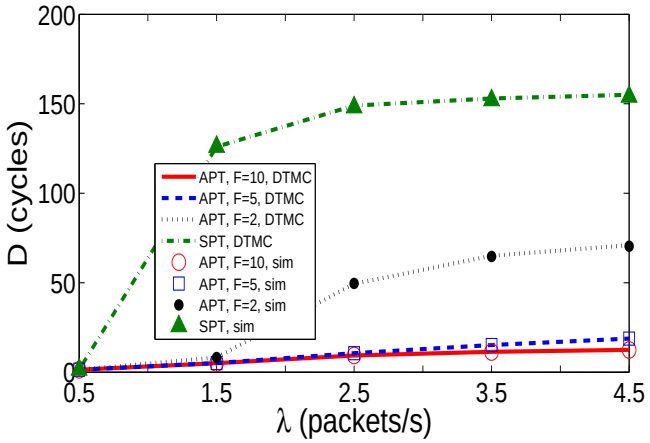

Figure C.8: Average pacekt delay as the data arrival rate varies, when $N = 15$ and with infinite retransmissions.

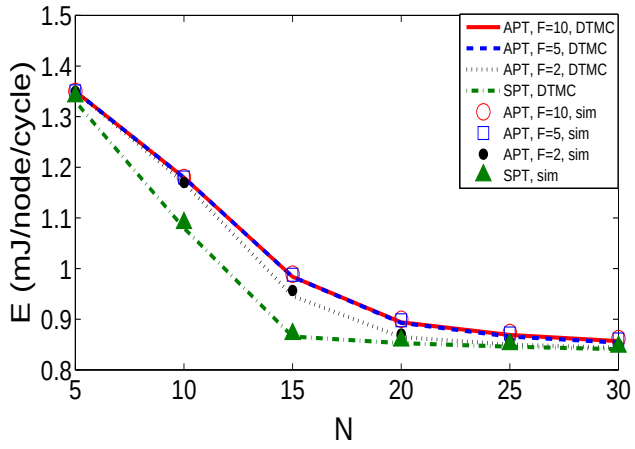

Figure C.9: Total average energy consumed by the RN as the number of nodes varies, when $\lambda = 1.5$ packet/s and with infinite retransmissions.

per cycle, is almost twice as much as Th for SPT, as observed in Figure C.7. Note that node throughput η is equal to Th/N and the same ratio $1/N$ is maintained between Th and η for both APT and SPT.

Accordingly, for a constant packet length of $S = 50$ bytes, Figure C.12 demonstrates that the energy efficiency expressed in transmitted Kbytes (per cycle and node) per consumed energy unit in mJ (per cycle and node) is almost twice as high for APT with $F = 2$ as for SPT. A similar explanation can be formulated for the variation of the energy efficiency with the number of network nodes N.

Moreover, the evolution of ξ with N presents different maximums for different values of F, the maximum number of packets aggregated per frame.

Table C.5: Performance Comparison: Simulation versus 3D DTMC and 2D DTMC

Scheme	Delay (cycles)			E(mJ)			Throughput (packets/cycle)			π_0		
	Sim	3D	2D	Sim	3D	2D	Sim	3D	2D	Sim	3D	2D
SPT	194.8	194.8	194.8	0.859	0.853	0.853	0.92	0.92	0.92	0.00	0.00	0.00
APT, $F = 2$	42.5	42.8	42.8	0.869	0.863	0.863	1.70	1.70	1.70	0.16	0.16	0.16
APT, $F = 5$	10.8	10.8	10.8	0.894	0.889	0.889	1.80	1.80	1.80	0.49	0.49	0.49
APT, $F = 10$	10.2	10.2	10.2	0.896	0.890	0.890	1.80	1.80	1.80	0.51	0.51	0.51

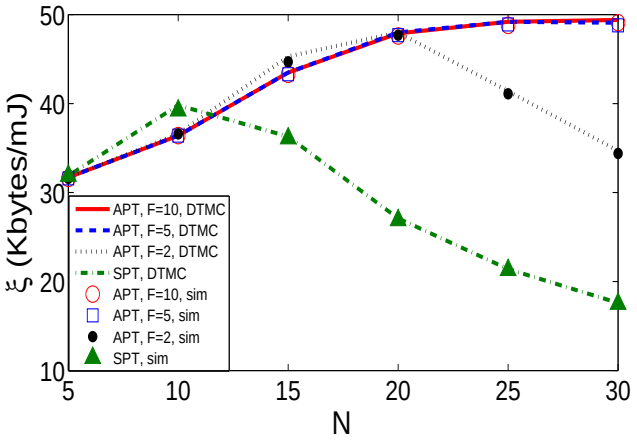

Figure C.10: Energy efficiency as the number of nodes varies, when $\lambda = 1.5$ packet/s and with infinite retransmissions.

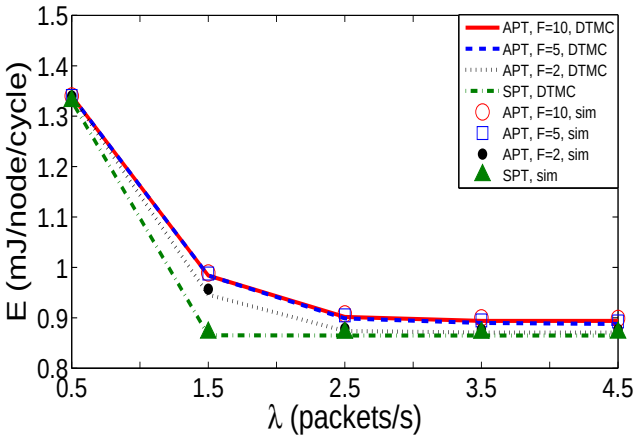

Figure C.11: Total average energy consumed by the RN as the data arrival rate varies, when $N = 15$ and with infinite retransmissions.

For $F = 1$ (SPT) the maximum of ξ is achieved at $N = 10$, while for $F = 2$ it is achieved at $N = 20$. Note that at these network configurations, Th achieves its maximum while D is small. This result suggests that in a network where the number of nodes varies over time and the packet arrival rate per node (λ) remains constant, an adaptive scheme that could adjust the value of F would be beneficial. This optimal F value could keep Th operating in the vicinity of its maximum while maximizing ξ and achieving low D.

When the size of the network N is fixed, the evolution of ξ with λ has a similar behavior as the evolution of Th with λ. In this case, selecting the largest possible F value for any arrival rate could achieve maximum ξ, maximum Th and minimum D. Observe that ξ for $F = 2$ is only marginally higher

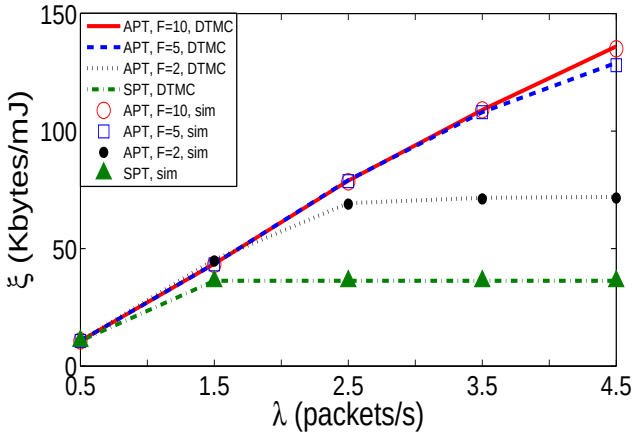

Figure C.12: Energy efficiency as the data arrival rate varies, when $N = 15$ and with infinite retransmissions.

than ξ for $F = 5$ or 10 for $0.5 \leq \lambda \leq 1.5$. Then, selecting the largest value for F would be a very good approximation to the optimal network configuration in this arrival rate interval.

C. Accuracy of the 3D and 2D DTMC Models

In this subsection, we compare the accuracy of the results obtained by the 2D and 3D DTMC models with the results obtained by simulation for the APT and SPT schemes. The results are summarized in Table C.5. The configuration employed for these results is: network size $N = 20$ nodes with a single sink, queue capacity $Q = 10$ packets, and the packet arrival rate to each node $\lambda = 1.5$ packets/s.

Define the relative error of a measure as $|x-y|/y$, where x is the value obtained by the corresponding analytical model and y is the value obtained by simulation. As illustrated in Table C.5, the throughout and delay values obtained from the analytical models and simulations match accurately with each other, being the largest relative error 0.51% for delay in case of $F = 2$. For energy consumption, the relative error for E varies with different configurations but still lower than 0.65% in all cases. Accordingly, we conclude that the relative error of the performance parameters obtained by the analytical models is lower than 1% for all the studied parameters for both 3D and 2D DTMCs.

VII. MODELING APT IN ERROR-PRONE CHANNELS

The 2D and 3D DTMC models presented earlier in this paper were designed with an assumption that the channel was error-free. In this section, as an example of the versatility of the proposed analytical framework, we extend the 3D model to scenarios where wireless channel impairments have an impact on WSN performance.

Our models describe the WSN behavior at the MAC layer. At this layer, channel impairments are revealed via packet (frame) errors. Therefore, we aim at integrating a frame-level error model that characterizes the wireless channel condition into the 3D model. Thus a 4D model is developed. Note that in this approach, bit error rate is neither an input parameter nor an outcome of the model.

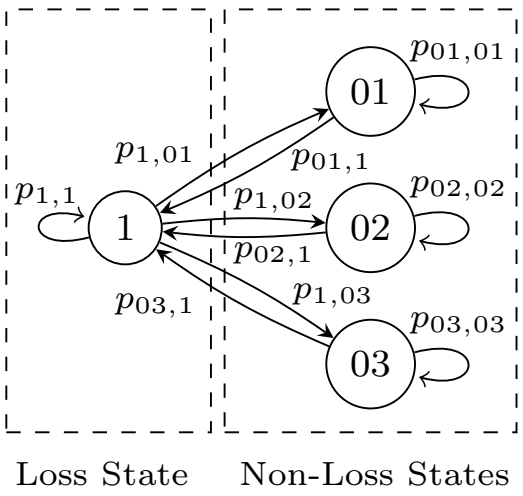

Figure C.13: A frame-level error model for error-prone channels with one state in the *loss* macro-state and three states in the *non-loss* macro-state.

A. An Extended On/Off Model for Frame-Level Errors

Different studies have proposed frame-level error models and shown that their statistical characteristics precisely match those of real packet traces [24, 25, 26]. Typically, the channel condition, with respect to the packets transmitted over it, can be regarded as either On (successful transmission) or Off (transmission failed). That is, packets transmitted without collisions while the channel is in On will be received successfully, while those transmitted while the channel is in Off will be received with errors and discarded.

The extended On/Off model proposed in [24] describes the holding times in the On and Off states by a mixture of geometric distributions. In our error model, the On and Off states are represented by two macro-states rep-

resenting the *loss* and *non-loss* states respectively, where a macro-state is composed of a set of states. This modeling approach captures both first- and second-order statistics with sufficient accuracy, which is considered an adequate characterization of the wireless link for practical scenarios.

Let us represent consecutive cycles in the non-loss and loss states by a sequence of 0s and 1s, respectively. Then, a sequence of consecutive 1s represents an error burst, i.e., a set of consecutive cycles where packets (frames) transmitted will not be received successfully due to channel impairments. The mean frame error rate would be the fraction of 1s in the complete sequence.

For simplicity of configuration, we deploy a single state to describe the *loss* macro-state, and three states to represent the *non-loss* macro-state, as shown in Figure C.13. This model is shown to exhibit a self-similar behavior over a finite but wide enough range of time-scales [27], and can be easily configured. The model has three parameters: H, a and b. The value of H determines the range of time-scales where the process can be considered as self-similar. Once the value of H is decided, the values of a and b are obtained such that they fit respectively the fraction of cycles where the channel produces frame-level errors $\rho_{\text{FE}} = (1-1/b)/(1-1/b^H)$, and the average number of consecutive cycles where the channel produces frame-level errors (average error burst length) $E[B] = \left(\sum_{k=1}^{H-1} a^{-k}\right)^{-1}$.

In the adopted model, we configure $H = 4$. Accordingly, we set $b = 0.4418$ to obtain a frame error rate (FER) of $\rho_{\text{FE}} = 5\%$, and $a = 2$ to obtain a mean frame-error burst length of $E[B] = 1.143$. This is a realistic configuration according to field measurements performed in [25]. However, any other values can be configured in the model.

Denote by $\boldsymbol{P}_{NE}$ the transition matrix that describes the cycles where the channel is in non-loss states. Note that $\boldsymbol{P}_{NE}$ is equal to the transition matrix that defines the 3D DTMC, and that was shown in Table C.2. Also, denote by $\boldsymbol{P}_{E}$ a new transition matrix that describes the cycles where the channel is in loss states and is shown in Table C.6. Then, a new transition matrix which encompasses the transmissions in both macro states needs to be constructed.

The new transition matrix, denoted by $\boldsymbol{P}$, has the following block struc-

Table C.6: Transition Probabilities of the 4D DTMC Model Matrix $\boldsymbol{P_e}$ in the Loss State

No active node exists. Transitions occur due to new arrivals	
$P_{(0,0,0),(j,l,0)} = B_l(K) \cdot A_j;\ 0 \le j < Q,\ 0 \le l \le K,$	$P_{(0,0,0),(Q,l,0)} = B_l(K) \cdot A_{\ge Q};\ 0 \le l \le K.$
No packets in the queue of the RN, i.e., no transmissions by the RN. Transitions are caused by the other k active nodes	
$P_{(0,k,0),(j,l,0)} = B_{l-k}(K-k) \cdot A_j;\ 0 \le j < Q,\ 1 \le k \le l \le K,$	$P_{(0,k,0),(Q,l,0)} = B_{l-k}(K-k) \cdot A_{\ge Q};\ 1 \le k \le l \le K,$
No transmission attempt	
$P_{(i,k,r),(j,l,r)} = \left(1-P_{sf,k}\right) \cdot B_{l-k}(K-k) \cdot A_{j-i};\ 1 \le i \le j < Q,\ 0 \le k \le l \le K,\ 0 \le r \le R,$	$P_{(i,k,r),(Q,l,r)} = \left(1-P_{sf,k}\right) \cdot B_{l-k}(K-k) \cdot A_{\ge Q-i};\ 1 \le i \le Q,\ 0 \le k \le l \le K,\ 0 \le r \le R,$
Failed transmission by the RN due to channel impairments	
$P_{(i,k,r),(j,l,r+1)} = P_{sf,k} \cdot B_{l-k}(K-k) \cdot A_{j-i};\ 1 \le i \le j < Q,\ 0 \le k \le l \le K,\ 0 \le r < R,$	$P_{(i,k,R),(Q,l,0)} = P_{sf,k} \cdot B_{l-k}(K-k) \cdot A_{\ge Q-i};\ 1 \le i \le Q,\ 0 \le k \le l \le K,\ 0 \le r < R.$
$P_{(i,k,R),(j,l,0)} = P_{sf,k} \cdot B_{l-k}(K-k) \cdot A_{j-i+\alpha};\ 1 \le i \le Q,\ i-\alpha \le j < Q,\ 0 \le k \le l \le K,$	$P_{(i,k,r),(Q,l,r+1)} = P_{sf,k} \cdot B_{l-k}(K-k) \cdot A_{\ge Q-i+\alpha};\ 1 \le i \le Q,\ 0 \le k \le l \le K.$

ture:

$$\boldsymbol{P} = \left[\begin{array}{c|ccc} \boldsymbol{A_0} & \boldsymbol{A_1} & \boldsymbol{A_2} & \boldsymbol{A_3} \\ \hline \boldsymbol{B_1} & \boldsymbol{B_4} & \boldsymbol{0} & \boldsymbol{0} \\ \boldsymbol{B_2} & \boldsymbol{0} & \boldsymbol{B_5} & \boldsymbol{0} \\ \boldsymbol{B_3} & \boldsymbol{0} & \boldsymbol{0} & \boldsymbol{B_6} \end{array}\right]. \tag{C.25}$$

where $\boldsymbol{A_0} = p_{1,1}\boldsymbol{P}_E$, $\boldsymbol{A_m} = p_{1,0m}\boldsymbol{P}_E$, $\boldsymbol{B_m} = p_{0m,1}\boldsymbol{P}_{NE}$, $\boldsymbol{B_n} = p_{0m,0m}\boldsymbol{P}_{NE}$, and $m = 1,2,3$. Clearly, matrices $\boldsymbol{A_0}$ to $\boldsymbol{A_3}$ represent the network states in channel error-prone cycles, while matrices $\boldsymbol{B_1}$ to $\boldsymbol{B_6}$ describe the network states in channel error-free cycles. As defined in [27], $p_{1,1} = 1 - \sum_{k=1}^{H-1} 1/a^k$ $p_{1,0m} = 1/a^m$, $p_{0m,1} = (b/a)^m$, and $p_{0m,0m} = 1 - (b/a)^m$, where $m = 1,2,3$.

B. State Description of the 4D DTMC Model

In the 4D DTMC, the state vector is denoted by (i,k,r,e), where i is the number of packets found at the queue of the RN, k keeps track of the number of active nodes in the network, r is the number of retransmissions experienced by the packet at the head of the queue of the RN, and e is a new tuple representing the channel state as presented in Figure C.13. When $e = 1$ a transmitted frame will not be received correctly, whereas when $e = \{01,02,03\}$ the transmitted frames will be received successfully, provided that they did not collide. Note that now a transmission failure happens due to either errors in the channel or contention collision. For further details about the 4D model, like the definition of the transition matrix $\boldsymbol{P}$ and the expressions for the performance parameters, please refer to [28].

C. Numerical Result Example under the 4D Model

Based on the constructed state transition matrix $\boldsymbol{P}$, we are able to obtain the stead state probabilities for each state. Following the same procedure as presented earlier, we deduce the closed-form expressions for the investigated performance parameters.

As an example, we illustrate in Figure C.14 the total throughput under an error-free (E-F) channel and an error-prone (E-P) channel with FER $= 5\%$, obtained from both the 4D analytical model (DTMC) and simulations (sim). The network is configured as in Figure C.5 where $\lambda = 1.1$ packet/s, but with $R = 10$, and N varies from 5 to 30. Again, the analytical results match with the ones obtained from simulations. It is also evident that a slightly lower throughput is achieved in the error-prone channel scenario. However, note

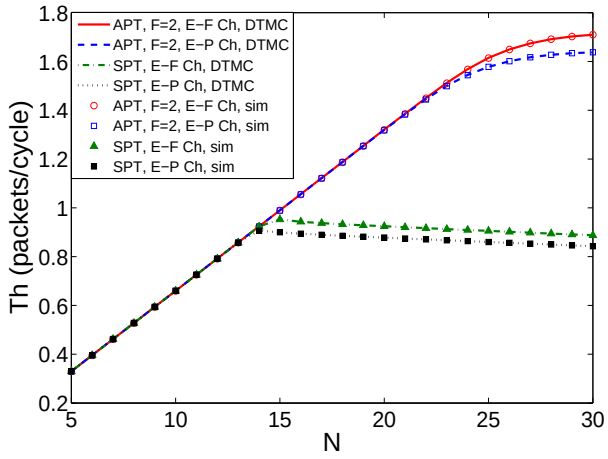

Figure C.14: Total throughput under an error-prone channel as the number of nodes varies, when $\lambda = 1.1$ packet/s, $R = 10$ and FER $= 5\%$.

that the decrease of Th is only marginal, as most of the frames discarded at reception due to errors induced by the channel are recovered by retransmission.

D. Brief Discussion on Model Complexity

Finally, we compare the complexity of the developed models in terms of the number of states in the DTMC models. The number of states in the 2D, 3D, and 4D DTMCs is $N \times (Q+1)$, $N \times (Q+1) \times (R+1)$, and $N \times (Q+1) \times (R+1) \times H$ respectively. The state space cardinality of the DTMC grows very fast as N, Q, R and (or) H increases. This can render the application of simple matrix inversion procedures to determine the stationary distribution infeasible. In such systems, more elaborate iterative and direct methods have been proposed in order to obtain the stationary distribution [29]. For a simple iterative method applicable to moderately large DTMCs, please refer to [30].

VIII. CONCLUSIONS

In this paper, we have proposed an analytical model to evaluate the performance of an aggregated packet transmission (APT) scheme. It operates in WSNs with a synchronous duty-cycled MAC protocol like S-MAC. The model is based on a 3D DTMC. Unlike existing models for duty-cycled MAC protocols, our model integrates the dependence among the nodes by modeling the number of active nodes in the network. In addition, we have also developed a less complex 2D DTMC model for APT in scenarios where packet

loss due to collisions in the channel is negligible, as well as a 4D model which integrates the impact of error-prone channels.

With these models, we obtain closed-form expressions for performance parameters like throughput, average packet delay, packet loss, energy consumption and energy efficiency. The analytical models are validated through extensive discrete-event based simulations. It is shown that they are very accurate, with relative errors below 1%.

The obtained analytical and simulation results show that APT outperforms its single packet transmission (SPT) counterpart in terms of packet loss, average delay and throughput, as more packets can be aggregated per transmitted frame. Therefore, migrating from SPT to APT is a natural choice when the load of the network increases. Even though the total energy consumption required for APT is slightly higher than for SPT, much higher energy efficiency is achieved in terms of the number of bytes transmitted per Joule.

REFERENCES

[1] W. Ye, J. Heidemann, and D. Estrin, “Medium access control with coordinated adaptive sleeping for wireless sensor networks", *IEEE/ACM Trans. Netw.*, vol. 12, no. 3, pp. 493-506, June 2004.

[2] R. Rajagopalan and P. K. Varshney, “Data-aggregation techniques in wireless sensor networks: a survey", *IEEE Commun. Surveys & Tutorials* vol. 8, no. 4, pp. 48-63, 2006.

[3] K. Akkaya, M. Demirbas, and R. S. Aygun, “The impact of data aggregation on the performance of wireless sensor networks", *Wireless Commun. and Mobile Computing*, vol. 8, no. 2, pp. 171-193, Feb. 2008.

[4] M. Bagaa, Y. Challal, A. Ksentini, A. Derhab, and N. Badache, “Data aggregation scheduling algorithms in wireless sensor networks: Solutions and challenges", *IEEE Commun. Surveys & Tutorials* vol. 16, no. 3, pp. 1339-1368, Third Quarter 2014.

[5] G. Bianchi, “Performance analysis of the IEEE 802.11 distributed coordination function", *IEEE J. of Selec. Areas in Commun.*, vol. 18, no. 3, pp. 535-547, Mar. 2000.

[6] R. P. Liu, G. J. Sutton, and I. B. Collings, “A new queuing model for QoS analysis of IEEE 802.11 DCF with finite buffer and load", *IEEE Trans. Wireless Commun.*, vol. 9, no. 8, pp. 2664-2675, Aug. 2010.

[7] O. Yang and W. Heinzelman, “Modeling and performance analysis for duty-cycled MAC protocols in wireless sensor networks", *IEEE Trans. Mobile Computing*, vol. 11, no. 6, pp. 905-921, June 2012.

[8] L. Dai and X. Sun, “A unified analysis of IEEE 802.11 DCF networks: Stability, throughput, and delay," *IEEE Trans. Mobile Comput.*, vol. 12, no. 8, pp. 1558-1572, 2013.

[9] J. Luo, L. Jiang, and C. He, “Performance analysis of synchronous wakeup patterns in contention-based sensor networks using a finite queuing model", in *Proc. IEEE GLOBECOM*, 2007, pp. 1334-1338.

[10] Y. Zhang, C. He, and L. Jiang, “Performance analysis of S-MAC protocol under unsaturated conditions," *IEEE Commun. Lett.*, vol. 12, no. 3, pp. 210-212, Mar. 2008.

[11] O. Yang and W. Heinzelman, “Modeling and throughput analysis for S-MAC with a finite queue capacity," in *Proc. IEEE ISSNIP*, 2009, pp. 409-414.

[12] J. Martinez-Bauset, L. Guntupalli, and F. Y. Li, “Performance analysis of synchronous duty-cycled MAC protocols," *IEEE Wireless Commun. Lett.*, vol. 4, no. 5, pp. 469-472, 2015.

[13] F. Tong, L. Zheng, M. Ahmadi, M. Li, and J. Pan, "Modeling and analyzing duty-cycling, pipelined-scheduling MACs for linear sensor networks," *IEEE Trans. Veh. Technol.*, 2015, early access available in IEEExplore.

[14] S. C.-H. Huang, P.-J. Wan, C. T. Vu, Y. Li, and F. Yao, “Nearly constant approximation for data aggregation scheduling in wireless sensor network," in *Proc. IEEE INFOCOM*, 2007, pp. 366-372.

[15] X. Xu, X. Y. Li, X. Mao, S. Tang, and S. Wang, “A delay-efficient algorithm for data aggregation in multihop wireless sensor networks,"

IEEE Trans. Parallel and Distri. Systems, vol. 22, no. 1, pp. 163-175, Jan. 2011.

[16] L. Galluccio and S. Palazzo, “End-to-end delay and network lifetime analysis in a wireless sensor network performing data aggregation," in *Proc. IEEE GLOBECOM*, 2009, pp. 1-6.

[17] B. Alinia, M. H. Hajiesmaili, and A. Khonsari, “On the construction of maximum-quality aggregation trees in deadline-constrained WSNs," in *Proc. IEEE INFOCOM*, 2015, pp. 1-9.

[18] M. Kamarei, M. Hajimohammadi, A. Patooghy, and M. Fazeli, “An efficient data aggregation method for event-driven WSNs: A modeling and evaluation approach," *Wireless Personal Commun.*, vol. 84, pp. 745-764, 2015.

[19] K. Nguyen, U. Meis, and Y. Ji, “An energy efficient, high throughput mac protocol using packet aggregation," in *Proc. IEEE GLOBECOM Workshops*, 2011, pp. 1236-1240.

[20] Z. Li, Y. Peng, D. Qiao, and W. Zhang, “Joint aggregation and MAC design to prolong sensor network lifetime," in *Proc. IEEE ICNP*, 2013, pp. 1-10.

[21] Y. Sun, O. Gurewitz, and D. Johnson, “RI-MAC: a receiver-initiated asynchronous duty cycle MAC protocol for dynamic traffic loads in wireless sensor networks," in *Proc. ACM SenSys*, 2008, pp. 1-14.

[22] Z. Li, Y. Peng, D. Qiao, and W. Zhang, “LBA: Lifetime balanced data aggregation in low duty cycle sensor networks," in *Proc. IEEE INFOCOM*, 2012, pp. 1844-1852.

[23] `http://edge.rit.edu/edge/P08208/public/Controls_Files/MICaZ-DataSheet.pdf`, 2015.

[24] P. Ji, B. Liu, D. Towsley, Z. Ge, and J. Kurose, “Modeling frame-level errors in GSM wireless channels," *Performance Evaluation*, vol. 55, no. 1, pp. 165-181, 2004.

[25] G. Boggia, P. Camarda, and A. D'Alconzo, "Performance of Markov models for frame-level errors in IEEE 802.11 wireless LANs," *Int. J. Commun. Syst.*, vol. 22, no. 6, pp. 695-718, Jan. 2009.

[26] D. Striccoli, G. Boggia, and A. Grieco, "A Markov model for characterizing IEEE 802.15. 4 MAC layer in noisy environments," *IEEE Trans. Indus. Electron.*, vol. 62, no. 8, pp. 5133-5142, June 2015.

[27] S. Robert and J.-Y. Le Boudec, "New models for pseudo self-similar traffic," *Performance Evaluation*, vol. 30, no. 1, pp. 57-68, 1997.

[28] L. Guntupalli, J. Martinez-Bauset, F. Y. Li, and M. Weitnauer, "Modeling and performance evaluation of synchronous DC MAC protocols in error-prone wireless links," *Tech. Rep.*, [Online]. Available: http://personales.upv.es/jmartine/smac4d.pdf

[29] W. J. Stewart, *Probability, Markov Chains, Queues, and Simulation: The Mathematical Basis of Performance Modeling*. Princeton University Press, 2009.

[30] X. Gelabert, J. PÂŽerez-Romero, O. Sallent, and R. AgustÂŽi, "A Markovian approach to radio access technology selection in heterogeneous multiaccess/multiservice wireless networks," *IEEE Trans. Mobile Comput.*, vol. 7, no. 10, pp. 1257-1270, 2008.

Paper D

Title:	Performance Analysis of Synchronous Duty-Cycled MAC Protocols
Authors:	Jorge Martinez-Bauset‡, Lakshmikanth Guntupalli†, and Frank Y. Li†
Affiliation:	†Dept. of Information and Communication Technology, University of Agder (UiA), N-4898 Grimstad, Norway ‡Dept. of Communications, Universitat Politècnica de València (UPV), 46022 València, Spain
Journal:	*IEEE Wireless Communications Letters (WCL)*, vol. 4, no. 5, pp 469-472, October 2015
Copyright ©:	IEEE

Performance Analysis of Synchronous Duty-Cycled MAC Protocols

Jorge Martinez-Bauset, Lakshmikanth Guntupalli, and Frank Y. Li

***Abstract* —In this letter, we propose an analytical model to evaluate the performance of the S-MAC protocol. The proposed model improves the accuracy of previous models in two aspects. First, it incorporates the dependence among the nodes within a cluster by defining a DTMC that models the number of active nodes, whereas the previous models considered that nodes were mutually independent. Second, it proposes new methods for calculating packet delay and energy consumption. The analytical model is validated through discrete-event based simulations. Numerical results demonstrate that the proposed analytical model and methods yield accurate results under realistic assumptions.**

Keywords—WSNs, duty-cycled MAC protocols, Markov modeling, delay and energy consumption.

I. INTRODUCTION

Duty cycling (DC) appears as a promising solution to reduce energy consumption in wireless sensor networks (WSNs). In the literature, many medium access control (MAC) protocols have been proposed to adopt DC for achieving energy efficiency. Among them, Sensor-MAC (S-MAC) [1] belongs to the category of synchronous duty-cycled MAC protocols in which all nodes in a cluster are coordinated to follow wake-up and sleep cycles simultaneously. Currently, only few analytical models are available to evaluate the performance of the S-MAC protocol. Among them, an M/G/1 based model was proposed in [2], which requires that packet arrivals follow the Poisson process and that each node has an infinite buffer. Recently, a discrete-time Markov chain (DTMC) model was proposed in [3], supporting a more general packet arrival distribution per cycle and zero packet retransmission.

Our work extends the study presented in [3] in three different aspects. First, a DTMC was proposed in [3] to describe the evolution of the number of

packets in the buffer of a node. We refer to it as the *node* DTMC. The solution of their model is based on the assumption that the states of nodes are mutually independent. However, in practice some degree of dependence occurs among nodes. We incorporate this dependence by introducing an additional DTMC, referred to hereafter as the *system* DTMC. It models the number of active nodes in the cluster. As it will be shown later, this new modeling approach substantially improves the model accuracy.

Second, we propose alternative methods to determine two important performance parameters, i.e., delay and energy consumption. The new methods are shown to be more general and accurate than the ones presented in [3].

Third, instead of focusing on zero retransmission, we study scenarios where nodes are allowed to perform infinite retransmissions. S-MAC itself does not specify whether packet retransmission is allowed or not. We consider herein that the operation of S-MAC with zero retransmissions may not be appropriate for certain loss-sensitive applications due to a possibly high number of packet loss. As infinite retransmission is not a feasible mode for node operation, we investigate how many times a packet needs to be retransmitted under various traffic loads in order to achieve zero packet loss. Simulation results show that the vast majority of the packets require only one or two retransmissions, even in a high load scenario. That is, by setting the maximum retransmission counter in the nodes to two, we might achieve close to zero packet loss. This indicates that an infinite retransmission model provides a simpler modeling alternative to the more complex finite retransmission model for systems with negligible packet loss.

II. System Model

Consider a cluster of N nodes consisting of sensors that are one hop away from each other. We focus on this *single-cell cluster* but multiple clusters together may form a larger network. The network employs S-MAC with the CSMA/CA-based RTS/CTS/DATA/ACK handshake, where backoff timers are reset at each cycle initiation. The time is partitioned into cycles, and each cycle is further divided into three parts: synchronization, data transfer and sleep. In S-MAC, a node goes to sleep until the next *data* (*listen*) *period* when: i) it loses the contention (hears a busy medium before its backoff timer

expires); ii) it encounters an RTS collision; and iii) after successful transmission (only one packet sent per cycle).

A homogeneous channel traffic generation is assumed, i.e., the fraction of packets sent from one node to any other node is $1/(N-1)$. For simplicity we assume a renewal arrival process, and characterize the number of packets that arrive to a node per cycle by independent and identically distributed random variables. In each cycle, packets arrive following a general distribution irrespective of where the packets were originated, i.e., internally (as a consequence of its own sensing activity) or externally (arriving from another node). Every node has a queue that can store at most Q packets.

A. Access to the Medium

Consider an arbitrarily selected node as the reference node (RN). Active nodes are those with a non-empty queue, i.e., with packets to send. The active nodes generate a random backoff time selected from $\{0,\ldots,W-1\}$. When the RN is active, it transmits a packet successfully (without collision) if the other contending nodes selected backoff times greater than the one chosen by the RN. A packet transmitted by the RN will fail (collide) when more than one contending nodes select the same backoff time as the RN, and the backoff time is the smallest among all contending nodes. When the backoff time generated by the RN is not the smallest one among those generated by the other contending nodes, two outcomes are possible: either another node is able to transmit successfully, or other nodes collide while transmitting.

Consider a cycle where the RN is active and denote by k, $0 \leq k \leq N-1$, the number of nodes that are also active in the same cycle in addition to the RN. Let $P_{s,k} = \sum_{i=0}^{W-1} (1/W)\,(W-1-i)^k/W^k$, $P_{sf,k} = \sum_{i=0}^{W-1} (1/W)\,(W-i)^k/W^k$, and $P_{f,k} = (1/W)\sum_{i=0}^{W-1}\left[(W-i)^k-(W-1-i)^k\right]/W^k = 1/W$, be the probabilities that the RN transmits a packet successfully, that it transmits (successfully or with failure), and that it transmits with failure, respectively. $P_{s,k}$ is the probability that the RN selects one backoff value from 0 to $W-1$ and the other k nodes choose a larger value. $P_{sf,k}$ and $P_{f,k}$ can be described in similar terms. Note that $P_{sf,k} - P_{s,k} = 1/W = P_{f,k}$ [5].

Conditioned on a successful or unsuccessful packet being transmitted by the RN when contending with other k nodes, the average backoff times are $BT_{s,k} = \left(1/P_{s,k}\right)\sum_{i=0}^{W-1} i\,(1/W)\,(W-1-i)^k/W^k$, or $BT_{f,k} = \sum_{i=0}^{W-1} i\,(W-i)^k/W^k - \sum_{i=0}^{W-1} i\,(W-1-i)^k/W^k$.

B. Node DTMC

Here we model the evolution of the number of packets in the queue (*state*) of the RN over time by a DTMC. At each *data period*, state transition opportunities occur when: i) the RN is active and it transmits a packet (state can decrease); and ii) a packet is received by the RN (state can increase). Consider the homogeneous case where all the nodes behave as the RN does and also support infinite retransmissions.

Let A_i be the probability that i packets arrive to the RN in a cycle of length T. If packets arrive to a node following a Poisson process with rate λ, then $A_i = (\lambda T)^i \cdot e^{-\lambda T}/i!$ and $\widehat{A}_i = 1 - \sum_0^{i-1} A_i$ where $\widehat{A}_i$ denotes the probability that at least i packets arrived during T. Note that our model applies to any other distribution for A_i as well. Let $\boldsymbol{P} = [P_{i,j}]$ be the transition probability matrix of the *node* DTMC, where $P_{i,j}$ is the probability that j packets are found in the queue at cycle $m+1$, conditioned on finding i packets in the queue at cycle m. These transition probabilities are defined by,

$$
\begin{aligned}
&P_{0,i} = A_i\,,\ i \le Q-1\,, \quad P_{0,Q} = \widehat{A}_Q\,,\\
&P_{i,j} = p_s A_{j-i+1} + (1-p_s) A_{j-i}\,,\\
&\qquad i = 0 \ldots Q-1\,,\ j = i \ldots Q-1\,,\\
&P_{i,Q} = p_s \widehat{A}_{Q-i+1} + (1-p_s)\widehat{A}_{Q-i}\,, \quad i = 1 \ldots Q\,,\\
&P_{i,i-1} = p_s A_0\,,\ i = 1 \ldots Q\,, \quad P_{i,j} = 0\,,\ j \le i-2\,.
\end{aligned}
$$

The solution of this DTMC can be obtained by solving the set of linear equations

$$\boldsymbol{\pi} = \boldsymbol{\pi} \boldsymbol{P}\,, \quad \boldsymbol{\pi} \boldsymbol{e} = 1\,, \tag{D.1}$$

where $\boldsymbol{\pi}$ is the stationary distribution vector and $\boldsymbol{e}$ is a column vector of ones. For the *node* DTMC, we adopt the common approximation that the probability of successful transmission, p_s, is independent of the state of the other nodes.

Let $M_k(\pi_0)$ be the probability that k nodes, out of the $N-1$ ones other that the RN, are active, where π_0 is the probability that a node is inactive. Assuming a binomial distribution for the number of active nodes [3], $M_k(\pi_0) = \binom{N-1}{k}(1-\pi_0)^k \pi_0^{N-1-k}$. Then,

$$p_s(\pi_0) = \sum_{k=0}^{N-1} M_k(\pi_0) P_{s,k}\,, \tag{D.2}$$

is the (average) probability that the RN transmits a packet successfully, conditioned on the RN being active.

By solving the set of equations in (D.1), $\pi_0(p_s)$ can be determined for a given p_s. Then, a new $p_s(\pi_0)$ can be obtained from (D.2) for a given π_0. Denote by p_s the solution of this fixed-point equation, i.e., the value of $p_s(\pi_0)$ at the fixed-point. A different approach for determining p_s is proposed in the next subsection using the *system* DTMC, considering that the binomial distribution assumption may not hold.

Note that the *node* DTMC model applies to zero retransmission as well if p_s is replaced by p_{sf} in (D.1). As in [3], the probability that the RN transmits a packet (successfully or with failure), p_{sf}, can be obtained by solving a similar fixed-point equation but with $p_{sf}(\pi_0) = \sum_{k=0}^{N-1} M_k(\pi_0) P_{sf,k}$.

C. System DTMC for Infinite Retransmissions

The system DTMC models the evolution of the number of active nodes in the cluster. Let $\boldsymbol{P'} = \left[P'_{i,j}\right]$ be the transition probability matrix of the DTMC that models the evolution of *the number of active nodes in the system*, where $P'_{i,j}$ is the probability that j nodes are found active at cycle $m+1$, conditioned on finding i active nodes at cycle m. The transition probabilities of the *system* DTMC are:

$$
\begin{aligned}
&P'_{0j} = B_j(N)\ ,\ 0 \le j \le N\,,\\
&P'_{ij} = \left(\widehat{S}_i + S_i\widehat{E}\right) B_{j-i}(N-i) + S_i E B_{j-i+1}(N-i)\ ,\\
&\qquad 1 \le i \le N-1\,,\ i \le j \le N-1\,,\\
&P'_{iN} = \left(\widehat{S}_i + S_i\widehat{E}\right) B_{N-i}(N-i)\ ,\ 1 \le i \le N-1\,,\\
&P'_{NN} = \widehat{S}_N + S_N\widehat{E} = (1 - S_N E)\ ,\\
&P'_{ij} = 0\,,\ 2 \le i \le N\,,\ j < i-1\,,\\
&P'_{ij} = S_i E B_0(N-i)\ ,\ 1 \le i \le N-1\,,\ j = i-1\,,\\
&P'_{NN-1} = S_N E\,,
\end{aligned}
$$

where: i) $B_j(n) = \binom{n}{j}\widehat{A}_1^j A_0^{n-j}$ is the probability that j out of n nodes that have their queues empty receive packets in a cycle, ii) $S_k = kP_{s,k-1}$ and $\widehat{S}_k = 1 - S_k$ are the probabilities that a packet is successfully transmitted in a cycle when k nodes compete, and its complementary $\widehat{S}_k$ is the probability that packets from two or more nodes collide, and iii) $E = p_s A_0 \pi_1 / p_s(1-\pi_0)$ and $\widehat{E} = 1 - E$ are the probabilities that a node's queue becomes empty or remains non-empty when it transmits successfully, respectively. Note that π_0 and π_1

are the stationary probabilities that the queue of a node has '0' and '1' packet, respectively.

The solution of the *system* DTMC can be obtained by solving the set of linear equations in (D.1) but with $\boldsymbol{P'}$. Let $\{\pi'_n\}$ be the stationary distribution of the *system* DTMC. Furthermore, let α'_k be the fraction of cycles where the RN is active, together with other k nodes, and α_k the probability that k nodes other than the RN are active, conditioned on the RN being active. Then, $\alpha'_k = \binom{N-1}{k}\pi'_{k+1}/\binom{N}{k+1} = (k+1)\,\pi'_{k+1}/N$, $\alpha_k(\pi_0) = \alpha'_k/G$, $G = \sum_{k=0}^{N-1}\alpha'_k$, $k = 0,\ldots N-1$.

Finally, $p_s(\pi_0)$ can now be obtained as $p_s(\pi_0) = \sum_{k=0}^{N-1}\alpha_k(\pi_0)\,P_{s,k}$. Clearly, both the *system* and the *node* are one-dimensional DTMCs and they must be solved iteratively to find p_s, the fixed-point equation solution.

III. Delay Analysis

Let D be the average delay that a packet experiences expressed in number of time cycles, i.e., from its arrival until it is transmitted and removed from the buffer. Then, D can be determined by Little's law,

$$D = \frac{N_{av}}{\lambda_a},\; N_{av} = \sum_{n=0}^{Q} n\pi_n,\; \lambda_a = \sum_{n=0}^{Q} b_n\pi_n, \tag{D.3}$$

where $b_0 = \sum_{i=0}^{Q} iA_i + Q\widehat{A}_{Q+1}$ and $b_n = \sum_{i=0}^{Q-n} iA_i + (Q-n+p_s)\,\widehat{A}_{Q-n+1}$, $n > 0$. Note that π_n is the stationary probability of finding n packets in the queue of a node, N_{av} is the average number of packets, λ_a is the average number of packets that entered the queue (*accepted*) per cycle, and that b_n is the mean number of packets *accepted* per cycle at state n. Note also that the last term of b_n is obtained after solving $((Q-n+1)\,p_s + (Q-n)\,(1-p_s))\,\widehat{A}_{Q-n+1}$, where we assume that only one packet can be sent per cycle.

IIV. Energy Consumption Analysis

Define the following constants, where P_{tx} and P_{rx} are the transmission and reception power,

$$\begin{aligned}
E_{txs} &= (t_{RTS} + t_{DATA})\,P_{tx} + (t_{CTS} + t_{ACK})\,P_{rx},\\
E_{rxs} &= (t_{RTS} + t_{DATA})\,P_{rx} + (t_{CTS} + t_{ACK})\,P_{tx},\\
E_{txf} &= t_{RTS}P_{tx} + t_{CTS}P_{rx},\;\; E_{rxf} = t_{RTS}P_{rx}.
\end{aligned}$$

The average energy consumed by the RN during the data transfer part of a cycle when $k+1$, $k \geq 2$, nodes are contending for the channel, is given by

$$\begin{aligned} E_{d,k+1} = {} & q_{1,k}P_{s,k} \cdot \left[E_{txs} + \left(4D_p + BT_{s,k}\right) P_{rx}\right] \\ & + q_{1,k}P_{f,k} \cdot \left[E_{txf} + \left(2D_p + BT_{f,k}\right) P_{rx}\right] \\ & + q_{2,k}P_{s,k}\,\alpha_1 \cdot \left[E_{rxs} + \left(3D_p + BT_{s,k}\right) P_{rx}\right] \\ & + q_{2,k}P_{s,k}\,\alpha_2 \cdot \left[E_{rxf} + \left(D_p + BT_{s,k}\right) P_{rx}\right] \\ & + q_{3,k} \cdot \left[E_{rxf} + \left(D_p + BT_{f,k}\right) P_{rx}\right] . \end{aligned} \tag{D.4}$$

The terms in $E_{d,k+1}$ correspond to the energy consumed by: a packet successfully transmitted, a packet transmitted that collides, a successful packet reception, a successful packet transmitted by nodes other than the RN whose destination is not the RN, and packets transmitted by nodes other than the RN that collide, respectively.

In (D.4) D_p is the one-way propagation delay, $\alpha_1 = 1/(N-1)$ and $\alpha_2 = (N-2)/(N-1)$. Note that α_1 and α_2 might depend on the routing protocol. Moreover, conditioned on finding $k+1$ nodes active, $q_{1,k} = (k+1)/N$ is the probability that the RN is active, $q_{2,k} = kq_{1,k} + (k+1)\left(1 - q_{1,k}\right)$ is the average number of active nodes other than the RN, and $q_{3,k} = q_{1,k}\left[1 - (k+1)P_{s,k} - P_{f,k}\right] + \left(1 - q_{1,k}\right)\left[1 - (k+1)P_{s,k}\right] = 1 - (k+1)P_{s,k} - q_{1,k}P_{f,k}$ is the probability that at least one node different from the RN transmits a packet with failure. Note that when the RN is active (with probability $q_{1,k}$) then $1 - (k+1)P_{s,k} - P_{f,k}$ gives the probability that it does not transmit but the other k nodes collide. However, when the RN is not active (with probability $1 - q_{1,k}$) then it is still listening and reacts to the collisions of the other $k+1$ nodes in the same way.

The expressions for $E_{d,1}$ and $E_{d,2}$ can be easily derived from (D.4), while $E_{d,0} = E_{rxf} + (W + D_p)P_{rx}$. Then, the average energy consumed by the RN during the data transfer part of a cycle is given by

$$E_d = \sum_{n=0}^{N} R_n E_{d,n} , \tag{D.5}$$

where either $R_n = \binom{N}{n}(1-\pi_0)^n \pi_0^{N-n}$ or $R_n = \alpha_n$. In addition to E_d, a node also consumes energy due to the exchange of signaling messages like SYNC. Also, the energy consumed during the *sleep* part of a cycle is not included, as

it is application dependent. Please, refer to [3] for details.

V. NUMERICAL RESULTS

Let $T = T_{SD}/b$ be the duration of a cycle, T_{SD} the duration of the synchronization and data transfer parts, and b the duty cycle fraction. We configure $T_{SD} = 30 \cdot 10^{-3}$ s. Then, for a given duty cycle fraction b, a different cycle duration T is obtained. To run S-MAC we set: backoff tick $= 1$, $t_{RTS} = 1.8$, $t_{CTS} = 1.8$, $t_{DATA} = 17.16$, $t_{ACK} = 1.8$, and $D_p = 2$, where all values are in units of 10^{-4} s. The *reference configuration* is defined by: $N = 5$, $Q = 10$, $W = 128$, $b = 0.5$, $P_{tx} = 52.2$ mW and $P_{rx} = 59.1$ mW. These values are similar to the ones configured in [3].

Three load conditions are considered for the reference configuration, i.e., low load (LL), medium (ML), and high (HL), which correspond to the arrival rates of $\lambda = \{1.5, 3.0, 4.5\}$ packets per second, respectively. As a reference, the packet loss probabilities induced by these loads due to a buffer overflow are approximately in the order of 10^{-12}, 10^{-6} and 10^{-1} respectively. During overflow episodes, some degree of selective packet discarding must occur at the sensors to give priority to the most important information. Once such imperative information is selected, the sensors rely on a loss-free transfer across the network.

We developed a discrete-event simulation model that mimics the physical behavior of the system. The simulation results are therefore completely independent from those obtained by the analytical model. We evaluate first the impact of configuring the nodes with zero retransmissions as presented in [3], versus with infinite retransmissions as proposed in this study.

In the *zero retransmission mode*, packet loss due to collisions in the channel obtained by simulation for the three load levels are: $\{0.435\%, 1.81\%, 3.92\%\}$, respectively. When the infinite retransmission mode is employed, we noted that more than 99.99% of the packets are transmitted after 1 or 2 retransmissions, even in the worst case (in HL). We also determined by simulation the delay and energy consumption when nodes are configured with a finite number of retransmissions. As expected, we observed that the delay and energy consumption when the maximum number of retransmissions was set to 3 or more remain practically identical, and equal to the values obtained for infinite retransmissions. This confirms that an infinite retransmission model

provides a much simpler, yet accurate, alternative to a finite retransmission model for systems with negligible packet loss.

Let us now evaluate the *node* DTMC model in isolation versus the hybrid *node* and *system* DTMC model. Denote by model M1 the model that employs the *node* DTMC alone using the binomial distribution to find p_s, as proposed in [3]. The model that combines the *node* DTMC together with the *system* DTMC to find p_s, as proposed in this letter, is referred to as M2. In both models nodes have retransmissions enabled. Based on the reference configuration and the above mentioned three load levels, we compare the accuracy of these two models using the relative error $|x-y|/y$ as a measure, where x is the value obtained by the corresponding analytical model and y is the value obtained by simulation.

Table D.1: Values and Percentual Relative Errors for π_0

	π_0	M2_err	M1_err
LL	0.88	0.03	0.46
ML	0.51	11.76	23.32
HL	0.008	1.40	1.41

Table D.1 presents the absolute values (π_0) and percentual relative errors (M2_err and M1_err) obtained for π_0. Clearly, the relative error achieved by M1 is much larger, particularly at ML. This is likely due to the fact that the independence assumption of the state of the nodes in the network does not hold. Using M2, the relative error for π_0 is substantially reduced, especially at LL and ML. Note that at the limit of the LL and HL regimes, the distribution of active nodes would be: i) $\pi'_0 \cong 1$ and $\pi'_i \cong 0$, $i \geq 1$; ii) $\pi'_N \cong 1$ and $\pi'_i \cong 0$, $i \leq N-1$, respectively. Then, in these regimes, when a node accesses the channel it always finds the same number of contenders. However, in the ML scenario finding a good distribution of active nodes is crucial to determine p_s, and therefore to solve the node DTMC accurately.

Next, we compare the average packet delay for the reference configuration but with $Q = 5$, in order to highlight the differences with the delay model proposed in [3]. Columns D_{sim} and $E_{d,sim}$ in Tab. D.2 show absolute values obtained from simulation for delay in cycles (units of 60 ms) and energy consumption in units of 10^{-4} J. Columns D, D^*, E_d and E_d^* show relative errors when $\{\pi_n\}$ is obtained by M2. Column D shows the relative errors

obtained using Little's law, as proposed in Sec. III. Column D^* shows the relative errors obtained when expression (15) in [3] is adopted. As observed, the errors in D^* are larger than those in D. This is likely due to the fact that expression (15) in [3] is implicitly based on the application of the arrivals see time averages (ASTA) property. However, ASTA does not hold in this system [4].

Furthermore, using also M2 and the reference configuration, we analyze the energy consumed by the RN during the data transfer part of a cycle. Column E_d in Tab. D.2 lists the relative errors obtained by expression (D.5) proposed in Sec. IV. Column E_d^* shows the relative errors obtained by the energy model in [3]. As observed, the errors in E_d^* are substantially larger than those in E_d for all traffic load levels. This discrepancy is likely due to two facts. First, expression (D.4) above and expression (37) in [3] have different terms. Second, expressions for $BT_{s,k}$ and $BT_{f,k}$ derived in this letter are different from those in [3].

Table D.2: Values and Percentual Relative Errors for M2

	D_{sim}	D	D^*	$E_{d,sim}$	E_d	E_d^*
LL	1.42	0.92	2.15	5.46	0.20	4.94
ML	4.68	20.23	26.78	3.14	4.63	14.56
HL	17.0	0.42	12.34	1.85	0.006	6.19

To further improve the accuracy, we combine both *system* and *node* DTMCs to define a two dimensional DTMC. A state in the new DTMC is represented by (i,m), where i is the number of packets in the queue of the RN, and m is the number of active nodes in the system. With this new model, the relative errors obtained at ML for π_0, delay and energy consumption are 3.20%, 6.05% and 1.85%, respectively. The relative errors obtained under LL and HL are also lower than the ones displayed in Tab. D.2. Details for this integrated model can be found in [5].

VI. CONCLUSIONS

We developed an analytical model for S-MAC operating in an infinite retransmission scenario, which involves the interaction of two one-dimensional DTMCs that model the evolution of the number of packets in the queue and the number of active nodes in a cluster, respectively. The proposed model

is verified by extensive discrete-event based simulations under various traffic load conditions, which show accurate results. We also proposed alternative methods to determine delay and energy consumption, which are more general and accurate than those proposed previously.

REFERENCES

[1] W. Ye, J. Heidemann, and D. Estrin, "Medium access control with coordinated adaptive sleeping for wireless sensor networks," *IEEE/ACM Transactions on Networking*, vol. 13, no. 3, June 2004.

[2] Y. Zhang, C. He and L. Jiang, "Performance analysis of S-MAC protocol under unsaturated conditions," *IEEE Communications Letters*, vol. 12, no. 3, Mar. 2008.

[3] O.Yang and W. B. Heinzelman, "Modeling and performance analysis for duty-cycled MAC protocols with applications to S-MAC and X-MAC," *IEEE Trans. on Mobile Computing*, vol. 11, no. 6, pp. 905–921, June 2012.

[4] B. Melamed and D. Yao, "The ASTA property," *Advances in Queueing: Theory, Methods and Open Problems*, pp. 195–224, 1995.

[5] J. Martinez-Bauset, L. Guntupalli, and F. Y. Li, "Modeling and Performance Evaluation of Synchronous Duty-Cycled MAC Protocols". `http://personales.upv.es/~jmartine/SMAC_2D.pdf`

Paper E

Title:	DTMC Modeling for Performance Evaluation of DW-MAC in Wireless Sensor Networks
Authors:	Lakshmikanth Guntupalli and Frank Y. Li
Affiliation:	Dept. of Information and Communication Technology, University of Agder (UiA), N-4898 Grimstad, Norway
Conference:	*IEEE Wireless Communications and Networking Conference (WCNC)*, April 2016
Copyright ©:	IEEE

DTMC Modeling for Performance Evaluation of DW-MAC in Wireless Sensor Networks

Lakshmikanth Guntupalli and Frank Y. Li

Abstract — **Synchronized duty cycling (DC) aligns sensor nodes to wake up at the same time in order to reduce idle listening for medium access control (MAC) in wireless sensor networks (WSNs). Demand wakeup MAC (DW-MAC) is a popular synchronous DC MAC protocol which allows nodes to compete and transmit multiple packets in one operational cycle. This multiple packet transmission (MPT) feature makes DW-MAC more energy efficient when comparing with other existing single time competition based protocols such as sensor MAC (S-MAC). In the literature, no analytical model exists to evaluate the performance of DW-MAC. In this paper, we develop two associated discrete time Markov chain (DTMC) models and incorporate them with each other for performance evaluation of DW-MAC with MPT. Using the proposed models, energy consumption and network lifetime are calculated. Furthermore, the proposed models are validated through discrete-event simulations.**

I. INTRODUCTION

Energy is a critical resource in battery powered wireless sensor networks (WSNs). When a WSN is deployed for monitoring or detection applications, it is expected to operate uninterruptedly over long duration. On the other hand, network lifetime depends on the battery capacity of a sensor node which is intrinsically limited. Therefore, a medium access control (MAC) protocol which can minimize energy consumption and prolong network lifetime is needed [1]. For instance, extra energy consumption caused by unnecessary actions such as idle listening can be minimized by duty cycling (DC). In DC, nodes can sleep for a while following a predefined schedule. Furthermore, synchronizing the schedules of sending and receiving sensor nodes further reduces idle listening.

In synchronous DC protocols, nodes follow a predefined schedule to wake up and sleep periodically. The combined duration of one *active* period and the

following *sleep* period is regarded as one *cycle*. Synchronization is done in the *sync* period, which is a part of the *active* period. The remaining duration of the *active* period is used for data exchange. Then, nodes wake up at the same schedule in order to exchange data packets. Sensor-MAC (S-MAC) [2] is a benchmark example of synchronous DC protocols. In S-MAC, nodes transmit packets to their neighbors after obtaining channel access. In case that two or more nodes are following the same schedules, they need to compete with each other in order to obtain channel access. The winning node transmits its packet, and the nodes which lost competition go to sleep until the next cycle. If a collision occurs, then all nodes go to sleep and wake up again in the next cycle for competition. Consequently, a packet suffers longer delay in addition to higher node energy consumption.

S-MAC's adaptive listening and routing-enhanced MAC [3] protocols allow nodes to forward packets to more than one hop in the same operational cycle. However, only *one* packet is transmitted in one cycle, meaning that these protocols allow nodes to compete only *once* in a cycle for data transmission. To reduce the latency imposed by single packet transmission, demand wakeup MAC (DW-MAC) [4] protocol introduces sending multiple packets in one cycle besides delivering them over multiple hops. To enable multiple packet transmission (MPT), DW-MAC allows nodes to compete *multiple* times in a cycle. As a result, the channel utilization efficiency for DW-MAC is higher as the channel is occupied for a longer period of time due to transmission of multiple packets. Furthermore, DW-MAC is also considered as a low latency and energy efficient DC MAC protocol. Previously, DW-MAC is evaluated merely through simulations, without enabling MPT. On the other hand, although there exist a few analytical models to evaluate synchronous [5]-[6] or pipelined-scheduling [7] DC MAC protocols including our earlier work [8], these models are valid only for analyzing *single transmission competition* in a cycle. So far in the literature, no mathematical models exist to analyze the MPT supported by DW-MAC.

In this paper, we develop two discrete time Markov chain (DTMC) models for MPT enabled DW-MAC which allows multiple competitions in a single cycle. The first DTMC describes the evolution of the number of packets in the buffer of a node, referred to as the *node* DTMC. The second DTMC models the number of active nodes in the sensing cluster, referred to as the

system DTMC. Then, these two associated analytical models are iteratively solved to calculate the probability of successful transmission for a node in a competing slot of a cycle. Using the obtained stationary probabilities, energy consumption and network lifetime are calculated.

The rest of the paper is organized as follows. In Sec. II, we present the network model and the overview of DW-MAC. Sec. III describes the proposed DTMC models, followed by the energy consumption analysis in Sec. IV. Numerical results from simulations and models are demonstrated in Sec. V, before the paper is concluded in Sec. VI.

II. DW-MAC Highlight and Medium Access

This section presents the overview of DW-MAC and the considered network scenario along with assumptions.

A. DW-MAC Brief and MPT Operation

In typical WSN applications, nodes sense data from the sensing field and transmit them to a sink node in a hop-by-hop fashion with the help of intermediate nodes. Within such a scenario, we consider a cluster of N sensor nodes that generate and send packets by competing with each other towards one *sink* via a relay node, as shown in Fig. E.1. Assume that the relay node forwards packets coming from the source nodes but it is not a traffic generator itself. For analysis convenience, we select one of the N nodes arbitrarily and refer to it as the reference node (RN). Hereafter, *DATA*, *SYNC*, *SCH* and *ACK* represent packets, and t_{DATA}, t_{SYNC}, t_{SCH} and t_{ACK} denote the corresponding packet duration respectively. Similarly, we represent the different parts of a cycle as *active*, *sleep*, *sync*, *data* and their corresponding duration as T_{active}, T_{sleep}, T_{sync} and T_{data} respectively.

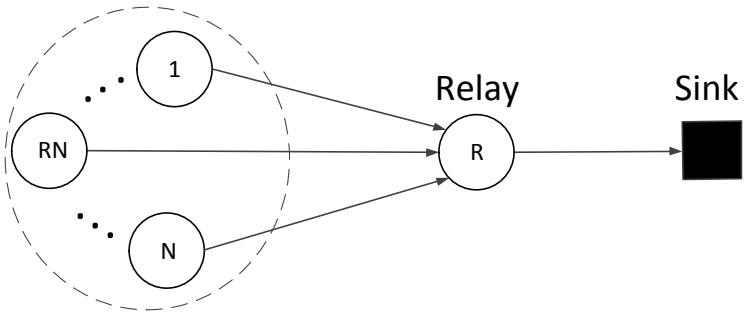

Figure E.1: A 2-hop WSN where a relay forwards traffic to the sink.

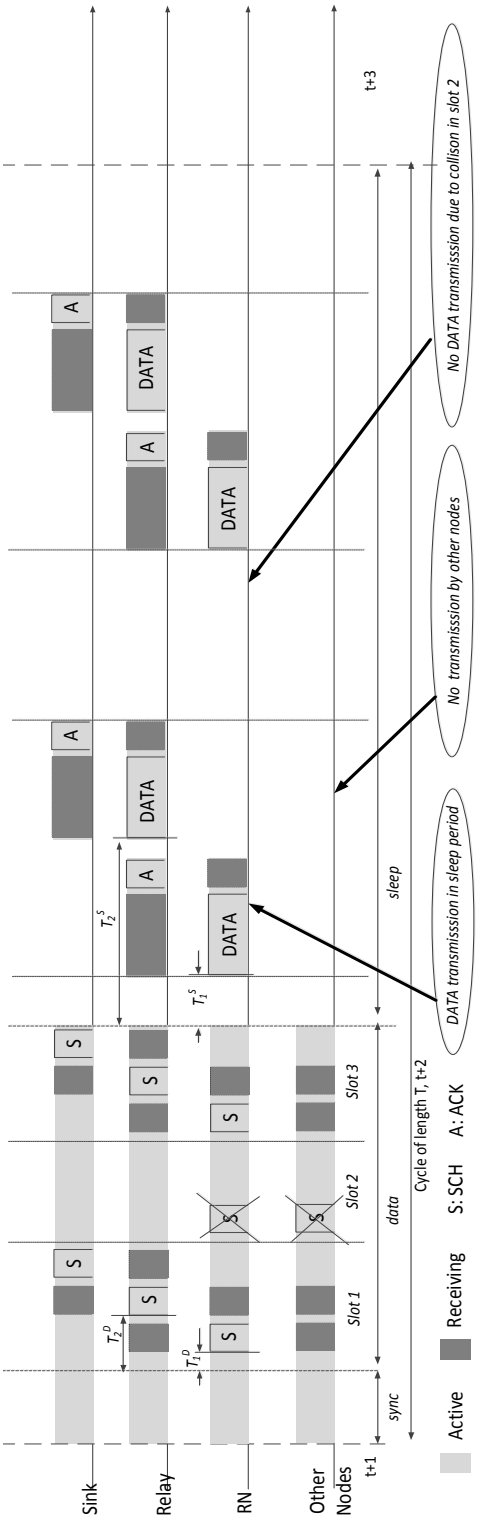

Figure E.2: Operation of multiple packet transmission in DW-MAC where each *active* period consists of n competing slots and a *sync* period. Nodes compete and reserve the channel during the *data* period and *DATA* transmission is performed in the subsequent *sleep* period.

A salient feature of DW-MAC is that it schedules nodes to wake up during the *sleep* period, but not during the *data* period of a cycle as used in other synchronous protocols like S-MAC, in order to exchange multiple *DATA* packets in that cycle. To facilitate MPT, the *data* period of a cycle is divided into multiple time slots. All active nodes compete in each slot to reserve the medium in the subsequent *sleep* period for their *DATA* transmission. The scheduling is done by exchanging an *SCH* message for each slot. Furthermore DW-MAC adopts a proportional mapping function to determine the wakeup time in the *sleep* period, as follows,

$$T_i^{sleep} = T_i^{data} \cdot \frac{T_{sleep}}{T_{data}}, \tag{E.1}$$

where T_i is the time difference between the start of the corresponding period and *the beginning of the* i^{th} *transmission in that slot*. This mapping function assures that any two reservations are not overlapping. Then, upon getting the reservations in all slots, all nodes go to sleep at the end of the *data* period, meaning that the duration of the *data* and *sleep* periods is fixed for a given number of slots. In case of collision in any slot, scheduling is not possible for that slot.

Fig. E.2 illustrates the operation of DW-MAC. In this example, the *data* period is divided into three slots. Assume that the RN is the winner of the contention among N nodes from the same cluster in the first slot. After gaining channel access, the RN transmits an *SCH* to the relay node. Correspondingly, the medium is reserved for the RN in the subsequent *sleep* period based on the mapping function in (E.1). Then the relay forwards the *SCH* message to the sink node and schedules accordingly its wakeup time. Similarly, the scheduling process continues in the third slot with another node as the winner. However, channel is not reserved during the second slot due to a collision. Collision happens when two or more nodes try to transmit *SCH* at the same time. Note that nodes do not go to sleep during the slots in the *data* period but do sleep when no transmission is scheduled in the *sleep* period.

B. Medium Access in DW-MAC

Consider that traffic arrival follows the Poisson distribution and that the channel is error free. Nodes with packets to transmit are *active* nodes. For channel reservation, all the active nodes generate a random backoff from win-

dow $\{0, W-1\}$ in every slot. If the smallest backoff time is selected by only one node, then that node wins channel access and reserves the medium for *DATA* transmission in the corresponding *sleep* period. If a node selects a backoff time which is not the smallest one, it loses the competition and waits until the next slot to compete again. If two or more nodes choose the same smallest backoff time, there will be a collision in that slot.

Consider N active nodes including the RN in a cycle. When the RN is contending with other k, $0 \leq k \leq N-1$ nodes, the probabilities that the RN transmits a frame successfully, $P_{s,k}$, transmits a frame (successfully or collided), $P_{sf,k}$, and failed (collided), $P_{f,k}$, are given by $P_{s,k} = \sum_{i=0}^{W-1} \frac{1}{W} \left(\frac{W-1-i}{W} \right)^k$, $P_{sf,k} = \sum_{i=0}^{W-1} \frac{1}{W} \left(\frac{W-i}{W} \right)^k$, $P_{f,k} = P_{sf,k} - P_{s,k}$ respectively. Here, $P_{s,k}$ is the probability that the RN selects a backoff value from $\{0, W-1\}$ while the other k nodes select a larger value. $P_{sf,k}$ and $P_{f,k}$ can be described in similar terms.

III. DTMC MODELS

This section presents the DTMC models and explains how to integrate them to calculate successful transmission probability.

A. Node DTMC

As mentioned earlier, *node* DTMC models the state of a node's queue, i.e., the evolution of number of packets over time. The state transitions take place based on the number of successful, failed transmissions and packet arrival. Denote the arrival rate as λ. Then the probability of arriving i packets to a node in a cycle of length T is $A_i = (\lambda T)^i \cdot e^{-\lambda T}/i!$ and the probability of arriving i or more packets is $A_{\geq i} = 1 - \sum_{j=0}^{i-1} A_j$. Let $P_{(i,j)}$ be the probability of finding j packets in the queue at cycle $t+1$, conditioned on that i packets are available in the queue at cycle t. Furthermore, denote $V_m(n) = \binom{n}{m} p_s^m (1-p_s)^{n-m}$, as the probability of containing success in m out of n slots and $U_{i-1}(m) = \binom{m}{i-1} p_s^i (1-p_s)^{m-i+1}$ as the probability of having i successful reservations out of $m+1$ slots, where p_s is the successful transmission probability. Then the *node* DTMC's transition probabilities are defined using $V_m(n)$ and $U_{i-1}(m)$ as shown in Table E.1. For example, one of the transition probabilities from State i to State j, $P_{(i,j)} = \sum_{m=0}^{n} V_m(n) \cdot A_{j-i+m}$,

is the sum of the probabilities for having success in m slots when DW-MAC is configured with n competing slots and receiving $j-i+m$ packets in a cycle calculated for $m = 0, ..., n$.

The solution of this DTMC can be obtained by solving the set of linear equations,

$$\boldsymbol{\pi} = \boldsymbol{\pi}\boldsymbol{P}, \quad \boldsymbol{\pi}\boldsymbol{e} = 1, \tag{E.2}$$

where $\boldsymbol{\pi}$ is the stationary distribution vector and $\boldsymbol{e}$ is a column vector of ones.

Table E.1: Transition Probabilities of the *node* DTMC Model for DW-MAC with MPT

The RN is not active	
$P_{(0,j)} = A_j;\ 0 \le j < Q,$	$P_{(0,Q)} = A_{\ge Q}.$
The RN is with 1 packet, $n \ge 1$	
$P_{(1,0)} = \sum_{m=0}^{n-1} U_0(m) \cdot A_j,$ $P_{(1,Q)} = \sum_{m=0}^{n-1} U_0(m) \cdot A_{\ge Q} + (1-P_s)^n \cdot A_{\ge Q-1},$	$P_{(1,j)} = \sum_{m=0}^{n-1} U_0(m) \cdot A_j + (1-P_s)^n \cdot A_{j-1};$ $1 \le j \le Q-1.$
The RN is active, $2 \le i \le n-1$	
$P_{(i,0)} = \sum_{m=i-1}^{n-1} U_{i-1}(m) \cdot A_0,$ $P_{(i,j)} = \sum_{m=i-1}^{n-1} U_{i-1}(m) \cdot A_j$ $+ \sum_{m=0}^{i-1} V_m(n) \cdot A_{j-i+m};\ 1 \le j \le Q-1,$	$P_{(i,j)} = \sum_{m=i-1}^{n-1} U_{i-1}(m) \cdot A_j$ $+ \sum_{m=i-j}^{i-1} V_m(n) \cdot A_{j-i+m};\ 1 \le j \le i-1,$ $P_{(i,Q)} = \sum_{m=i-1}^{n-1} U_{i-1}(m) \cdot A_{\ge Q}$ $+ \sum_{m=i-j}^{i-1} V_m(n) \cdot A_{\ge Q-i+m}.$
The RN is active, $n \le i \le Q-1$	
$P_{(i,j)} = \sum_{m=i-j}^{n} V_m(n) \cdot A_{j-i+m};\ i-n \le j \le i-1,$ $P_{(i,Q)} = \sum_{m=0}^{n} V_m(n) \cdot A_{\ge Q-i+m},$	$P_{(i,j)} = \sum_{m=0}^{n} V_m(n) \cdot A_{j-i+m};\ i \le j \le Q-1,$ $P_{(Q,Q)} = \sum_{m=0}^{n} V_m(n) \cdot A_{\ge m}.$

B. System DTMC

The evolution of number of active nodes in the network is modeled by the *system* DTMC. Denote by $P'_{(k,l)}$ the probability of finding l active nodes in cycle $t+1$, conditioned on that k nodes are already active in cycle t. When k nodes compete in a cycle, the probability of transmitting a packet successfully is $S_k = kP_{s,k-1}$ and for a collision is $\widehat{S}_k = 1 - S_k$. Furthermore, when there is a successful transmission, the probability that a node's queue becomes empty is $E = p_s A_0 \pi_1 / p_s(1-\pi_0)$ and $\widehat{E} = 1 - E$ is the probability that it remains non-empty, where π_0 and π_1 are the stationary probabilities that the node's queue has '0' and '1' packet, respectively. Denote $X_k = S_k E$, $\widehat{X}_k = \widehat{S}_k + S_k \widehat{E}$, and $B_k(l) = \binom{l}{k} \widehat{A}^k A_0^{l-k}$ is the probability that k out of l nodes which have their queues empty receive packets in a cycle, where $\widehat{A} = 1 - A_0$. Then the transition probabilities of the *system* DTMC are defined in Table E.2 using the following set of equations.

$$C_1(k,k-1) = \prod_{r=0}^{k-1} X_{k-r} + \prod_{r=0}^{k-1} X_{k-r} \sum_{v=0}^{k-1} \widehat{X}_{k-v},$$

$$C_2(k,k-1) = C_1(k,k-1) + \prod_{r=0}^{k-1} X_{k-r} \sum_{v=0}^{k-1} [\widehat{X}_{k-v} \sum_{u=v}^{k-1} \widehat{X}_{k-v}],$$

$$C_y(k,k-1) = C_2(k,k-1) + \sum_{y=3}^{n-k} \prod_{r=0}^{k-1} X_{k-r} \sum_{v=0}^{k-1} [\widehat{X}_{k-v}^{(y-1)} \sum_{u=0}^{k-1} \widehat{X}_{k-v}];$$

$$C_1(k,k-2) = \prod_{r=0}^{k-2} X_{k-r} \sum_{v=0}^{k-1} [\widehat{X}_{k-v} \sum_{u=v}^{k-1} \widehat{X}_{k-v}],$$

$$C_{n-k}(k,m) = \prod_{r=0}^{m} X_{k-r} \sum_{v=0}^{m+1} [\widehat{X}_{k-v}^{(n-m-1)} \sum_{u=0}^{m+1} \widehat{X}_{k-v}];$$

$$n-k > 1,\ 0 \le m \le k-2,$$

$$F(k,n-1) = \prod_{r=0}^{n-1} X_{k-r},\ F(k,n-2) = F(k,n-2) \sum_{v=0}^{n-1} \widehat{X}_{k-v},$$

$$F(k,n-3) = F(k,n-3) \sum_{v=0}^{n-2} [\widehat{X}_{k-v} \sum_{u=v}^{n-2} \widehat{X}_{k-v}],$$

$$F(k,m) = F(k,m) \sum_{v=0}^{m+1} [\widehat{X}_{k-v}^{(n-m-1)} \sum_{u=v}^{m+1} \widehat{X}_{k-v}];\ 0 \le m \le n-4.$$

To make the state transitions shown in Table E.2 easier to understand, we explain one of the transition probabilities, $P'_{(k,l)} = \sum_{m=0}^{k-1} C_{n-k}(k,m) \cdot B_{l-k+m+1}(N-k) + \left(\widehat{S}_i + S_i \widehat{E}\right)^n \cdot B_{l-k}(N-k)$, as follows. Consider $n-k=1$ and $m=k-1$, then the first term above becomes $C_1(k,k-1)$. As shown above, X_k is the probability of occurring a state reduction by 1 in the *system* DTMC, i.e., the number of available active nodes for competition in the next slot is $k-1$. Moreover, $\widehat{X}_k$ is the probability of occurring no change in a state. As shown above in the expression for $C_1(k,k-1)$, there are two possible combinations for this term, i.e., *i*) competition succeeded and nodes go empty for all first k slots with the probability of $\prod_{r=0}^{k-1} X_{k-r}$ while the remaining 1 slot is not used; plus *ii*) competition succeeded and nodes go empty in k slots while no state change occurred in the other 1 slot with the probability of $\prod_{r=0}^{k-1} X_{k-r} \sum_{v=0}^{k-1} \widehat{X}_{k-v}$. Furthermore, $B_{l-k+m+1}(N-k)$ is the probability that $l-k+m+1$ out of $(N-k)$ inactive nodes become active. The last term is the probability that the state has not changed in all n slots. Finally, the sum of all the above explained probabilities for $m = 0, \ldots, k-1$ gives the transition probability $P'_{(k,l)}$. Consider $\{\pi'_k\}$ as the stationary distribution of the

Table E.2: Transition Probabilities of the *system* DTMC Model for DW-MAC with MPT

$P'_{(0,l)} = B_l(N)\ ,\ 0 \le l \le N\,;$	For $N=1$, $\quad P'_{(1,0)} = \sum_{m=0}^{n-1} S_i E \cdot \left(\widehat{S}_i + S_i\widehat{E}\right)^m\,;\quad P'_{(1,1)} = \left(\widehat{S}_i + S_i\widehat{E}\right)^n.$
For $2 \le N \le n,\ 1 \le k \le N-1,\ k \le N-k$	
$P'_{(k,l)} = \sum_{m=0}^{k-1} C_{n-k}(k,m) \cdot B_{l-k+m+1}(N-k)\ ;\ 0 \le l \le k-1\,,$	$P'_{(k,N)} = \left(\widehat{S}_k + S_k\widehat{E}\right)^n \cdot B_{N-k}(N-k)\,,$
$P'_{(k,l)} = \sum_{m=0}^{k-1} C_{n-k}(k,m) \cdot B_{l-k+m+1}(N-k)$	$P'_{(k,l)} = \sum_{m=0}^{k-l-1} C_{n-k}(k,m) \cdot B_{l-k+m+1}(N-k)$
$\quad + \left(\widehat{S}_i + S_i\widehat{E}\right)^n \cdot B_{l-k}(N-k)\ ;\ k \le l \le N-k,$	$\quad + \left(\widehat{S}_i + S_i\widehat{E}\right)^n \cdot B_{l-k}(N-k)\ ;\ N-k < l < N.$
For $1 \le N \le n,\ 1 \le k \le N-1,\ k > N-k$	
$P'_{(k,l)} = \sum_{m=k-l-1}^{k-1} C_{n-k}(k,m) \cdot B_{l-k+m+1}(N-k)\ ;\ 0 \le l \le N-k\,,$	$P'_{(k,N)} = \left(\widehat{S}_k + S_k\widehat{E}\right)^n \cdot B_{N-k}(N-k)\,,$
$P'_{(k,l)} = \sum_{m=k-l-1}^{N-l-1} C_{n-k}(k,m) \cdot B_{l-k+m+1}(N-k)\ ;\ N-k < l < k\,,$	$P'_{(k,l)} = \sum_{m=0}^{N-l-1} C_{n-k}(k,m) \cdot B_{l-k+m+1}(N-k)$
$P'_{(N,l)} = C_{n-N}(N, N-l-1)\ ;\ 0 \le l \le N-1\,,$	$\quad + \left(\widehat{S}_i + S_i\widehat{E}\right)^n \cdot B_{l-k}(N-k)\ ;\ k \le l \le N-1\,,$
$P'_{(N,N)} = \left(\widehat{S}_N + S_N\widehat{E}\right)^n.$	
For $N \ge n,\ 1 \le k \le n-1,\ k \le N-k$	
$P'_{(k,l)} = \sum_{m=k-l-1}^{k-1} C_{n-k}(k,m) \cdot B_{l-k+m+1}(N-k)\ ;\ 0 \le l \le k-1\,,$	$P'_{(k,N)} = \left(\widehat{S}_k + S_k\widehat{E}\right)^n \cdot B_{N-k}(N-k)\,,$
$P'_{(k,l)} = \sum_{m=0}^{k-1} C_{n-k}(k,m) \cdot B_{l-k+m+1}(N-k)$	$P'_{(k,l)} = \sum_{m=0}^{N-l-1} C_{n-k}(k,m) \cdot B_{l-k+m+1}(N-k)$
$\quad + \left(\widehat{S}_k + S_k\widehat{E}\right)^n \cdot B_{l-k}(N-k)\ ;\ k \le l \le N-k\,,$	$\quad + \left(\widehat{S}_k + S_k\widehat{E}\right)^n \cdot B_{l-k}(N-k)\ ;\ N-k \le l < N.$
For $N \ge n,\ 1 \le k \le n-1,\ k > N-k$	
$P'_{(k,l)} = \sum_{m=k-l-1}^{k-1} C_{n-k}(k,m) \cdot B_{l-k+m+1}(N-k)\ ;\ 0 \le l \le N-k\,,$	$P'_{(k,N)} = \left(\widehat{S}_k + S_k\widehat{E}\right)^n \cdot B_{N-k}(N-k)\,,$
$P'_{(k,l)} = \sum_{m=k-l-1}^{N-l-1} C_{n-k}(k,m) \cdot B_{l-k+m+1}(N-k)\ ;\ N-k < l < k-1\,,$	$P'_{(k,l)} = \sum_{m=0}^{N-l-1} C_{n-k}(k,m) \cdot B_{l-k+m+1}(N-k)$
	$\quad + \left(\widehat{S}_i + S_i\widehat{E}\right)^n \cdot B_{l-k}(N-k)\ ;\ k \le l \le N-1\,.$
For $N \ge n,\ n \le k \le N-1,\ k \le N-n$	
$P'_{(k,l)} = \sum_{m=k-l-1}^{n-1} F_m(k,m) \cdot B_{l-k+m+1}(N-k)\ ;\ k-n \le l \le k-1\,,$	$P'_{(k,N)} = \left(\widehat{S}_k + S_k\widehat{E}\right)^n \cdot B_{N-k}(N-k)\,,$
$P'_{(k,l)} = \sum_{m=0}^{n-1} C_{n-k}(k,m) \cdot B_{l-k+m+1}(N-k)$	$P'_{(k,l)} = \sum_{m=0}^{N-l-1} C_{n-k}(k,m) \cdot B_{l-k+m+1}(N-k)$
$\quad + \left(\widehat{S}_k + S_k\widehat{E}\right)^n \cdot B_{l-k}(N-k)\ ;\ k \le l \le N-n\,,$	$\quad + \left(\widehat{S}_k + S_k\widehat{E}\right)^n \cdot B_{l-k}(N-k)\ ;\ N-n < l < N.$
For $N \ge n,\ n \le k \le N-1,\ k > N-n$	
$P'_{(k,l)} = \sum_{m=k-l-1}^{n-1} C_{n-k}(k,m) \cdot B_{l-k+m+1}(N-k)\ ;\ k-n < l < N-n\,,$	$P'_{(k,N)} = \left(\widehat{S}_k + S_k\widehat{E}\right)^n \cdot B_{N-k}(N-k)\,,$
$P'_{(k,l)} = \sum_{m=k-l-1}^{N-l-1} C_{n-k}(k,m) \cdot B_{l-k+m+1}(N-k)\ ;\ N-n < l < k\,,$	$P'_{(k,l)} = \sum_{m=0}^{N-l-1} C_{n-k}(k,m) \cdot B_{l-k+m+1}(N-k)$
$P'_{(N,l)} = F_{n-N}(N, N-l-1)\ ;\ 0 \le l < N\,,$	$\quad + \left(\widehat{S}_i + S_i\widehat{E}\right)^n \cdot B_{l-k}(N-k)\ ;\ k \le l < N\,,$
$P'_{(N,N)} = \left(\widehat{S}_N + S_N\widehat{E}\right)^n.$	

system DTMC. This $\{\pi'_k\}$ can be determined by solving (E.2) however with the transition probabilities from Table E.2.

C. The Calculation of p_s

To obtain p_s, we need to solve the equations from both models interactively. By providing an arbitrary p_s value in (E.2) in the *node* DTMC, $\pi_0(p_s)$ can be obtained. Similarly for a given π_0, $p_s(\pi_0)$ can be calculated based on the *system* DTMC, as explained below.

Let α'_k be the fraction of cycles in which the RN and other k nodes are active, and α_k be the probability that k nodes other than the RN are active, conditioned on that the RN is active. Then, we have

$$\alpha'_k = \binom{N-1}{k} \pi'_{k+1} / \binom{N}{k+1} = (k+1)\,\pi'_{k+1}/N$$

$$\alpha_k(\pi_0) = \alpha'_k/G,\;\; G = \sum_{k=0}^{N-1} \alpha'_k,\;\; k = 0,\ldots N-1\,.$$

Now, $p_s(\pi_0)$ can be expressed as

$$p_s(\pi_0) = \sum_{k=0}^{N-1} \alpha_k(\pi_0)\, P_{s,k}\,. \tag{E.3}$$

Clearly, by solving $\pi_0(p_s)$ from the *node* DTMC and $p_s(\pi_0)$ from the *system* DTMC, the value of p_s at the fixed-point can be obtained. Hence, both the *system* and the node *node* DTMCs must be connected and used iteratively until π_0 is converged from an arbitrarily assigned initial value.

IV. Energy Consumption Analysis

For the topology shown in Fig. E.2, the network will be disconnected when the relay node exhausts its battery. In this section, we calculate the energy consumed by the relay node in a cycle and estimate the lifetime of the network.

As described in Sec. II, each cycle contains *sync*, *data* and *sleep* periods. We adopt a synchronization process similar to the one proposed in [5], in which a node transmits one *SYNC* packet every N_{sc} cycles, and receives one

packet per cycle in the remaining $N_{sc}-1$ cycles. Accordingly, the energy consumed by the relay node in the *sync* period is given by,

$$E_{sc} = \frac{1}{N_{sc}} \cdot [(t_{SYNC} \cdot P_{tx} + (T_{sync} - t_{SYNC}) \cdot P_{rx})] + \frac{N_{sc}-1}{N_{sc}} \cdot (T_{sync} \cdot P_{rx}) \,, \tag{E.4}$$

where P_{tx} and P_{rx} are the transmission and reception power levels respectively.

The *data* period of a cycle is further divided into n slots, each with a fixed length. So the duration of *data* is also fixed as $T_{data} = nT_{slot}$. Furthermore, the duration of a *DATA* transmission in one slot during the *sleep* period is $T_{datatx} = T_2^s - T_1^s + t_{DATA} + t_{ACK} + 2D_p$, where D_p is the propagation delay. Correspondingly, the following energy consumption is associated with a successful transmission (E_{txs}), and a failed transmission (due to collision) (E_{txf}),

$$\begin{aligned} E_{txs} &= (t_{SCH} + t_{DATA} + t_{ACK}) \cdot P_{tx} \\ &\quad + (T_{slot} - t_{SCH} + T_{datatx} - t_{DATA} - t_{ACK}) \cdot P_{rx} \,, \\ E_{txf} &= T_{slot} \cdot P_{rx} + T_{datatx} \cdot P_{sl} \,, \end{aligned} \tag{E.5}$$

where P_{sl} is the sleep power level. Then, the average energy consumed by the relay during a *DATA* transfer in a cycle when $k \geq 1$ nodes are active, is obtained by

$$\begin{aligned} E_{d,k+1} &= q_{1,k} P_{s,k} E_{txs} + q_{1,k} P_{f,k} E_{txf} \\ &\quad + q_{2,k} P_{s,k} E_{txs} + q_{3,k} E_{txf} \end{aligned} \tag{E.6}$$

where $q_{1,k} = (k+1)/N$ is the probability that the RN is active, $q_{2,k} = kq_{1,k} + (k+1)\left(1 - q_{1,k}\right)$ is the average number of active nodes other than the RN, and $q_{3,k} = 1 - q_{2,k}P_{s,k} - q_{1,k}P_{sf,k}$ is the probability that nodes other than the RN transmit a packet with failure. Note that the terms in $E_{d,k+1}$ correspond to the energy consumed by the relay when: 1) the RN successfully transmitted a packet; 2) the transmission by the RN collided; 3) a successful transmission by nodes other than the RN; and 4) a collision occurred to the packet sent by the other nodes, respectively. Similarly, $E_{d,1} = [q_{1,0} + q_{2,0}] \cdot P_{s,0} E_{txs}$ and $E_{d,0} = T_{slot} \cdot P_{rx} + T_{datatx} \cdot P_{sl}$. The average energy consumed by the relay

during a *DATA* transfer of a cycle, including the energy consumed during the *data* period for slot based reservations and multiple *DATA* transmissions during the *sleep* period, is given by,

$$E_d = n \cdot \sum_{k=0}^{N} E_{d,k} \cdot \pi'_k \tag{E.7}$$

where π'_k is the stationary probability of finding k active nodes in the network and n is the number slots in the *data* period. Correspondingly, the energy consumed by the relay while really being asleep, i.e., no *DATA* transmission at all, during the *sleep* period of a cycle is given by

$$E_{sl} = (T - T_{sync} - T_{data} - nT_{datarx}) \cdot P_{sl}\,. \tag{E.8}$$

Finally, the total average energy consumed by the relay in a cycle is obtained by

$$E = E_{sc} + E_d + E_{sl}\,. \tag{E.9}$$

Correspondingly, the network lifetime can be determined as

$$LT = \frac{E_{initial}}{E} \text{ cycles}\,. \tag{E.10}$$

V. Simulations and Numerical Results

In this section, we validate the proposed models by comparing the average energy consumption of the relay node and the network lifetime calculated from the models with the results obtained by simulations. The DW-MAC is simulated in a custom C based discrete-event simulator and the performance results are reported as the average values over $5 \cdot 10^6$ cycles.

The MPT enabled DW-MAC is employed in the network illustrated in Fig. E.1. The parameters configured in the network are: number of nodes $N \in (1, 2 \ldots, 5)$; queue length of a node $Q = 5$ with $E_{initial} = 1$ J; the size of the *DATA* packet is 100 bytes; *DATA* arrival rate $\lambda \in [0.5, 1.5 \text{ and } 2.5]$ packets/s; and for the *sync* period, $N_{sc} = 10$. Furthermore, DW-MAC is configured with 5% duty cycle and the number of slots $n \in \{1, 3 \text{ and } 5\}$ per cycle. The other MAC parameters are taken from [4]. The transmission, reception and sleep

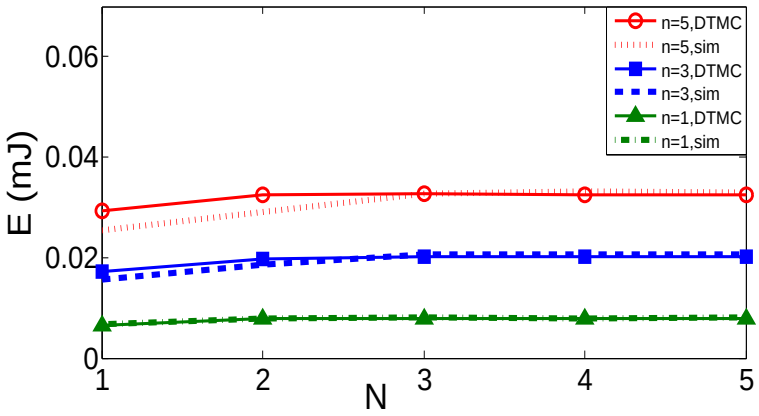

Figure E.3: Average energy consumed by the relay per cycle as the number of nodes varies, given that $\lambda = 1.5$ packet/s.

power levels are, respectively, $P_{tx} = 31.2$ mW, $P_{rx} = 22.2$ mW and $P_{sl} = 3$ μW [9]. The network performance is evaluated by varying the number of nodes N for the following two configurations: 1) different number of slots n with a fixed packet arrival rate $\lambda = 1.5$ packets/s; and 2) different packet arrival rates λ with a fixed number of slots n in a cycle.

A. Energy Consumption and Lifetime

Fig. E.3 depicts the average energy consumed by the relay node per cycle when the number of nodes in the network varies for different number of competing slots. Recall that, in DW-MAC, if there is any successful reservation in a slot, then *DATA* is transmitted. Otherwise, no data transmission is scheduled for that slot. Furthermore, if the number of active nodes is fewer than the number of slots, then some slots may be *idle*, meaning that no competition happens during these idle slots. In both cases, lower energy is consumed by the relay due to fewer number of *DATA* transmissions. With a larger N, more slots are used for competition, which in turn increases the number of *DATA* transmissions. Therefore, the energy consumption becomes higher with a larger N for any number of slots.

If a sufficient number of active nodes or *DATA* packets in the buffer of a node are available in the network, all slots will be occupied. That is, when the network contains more number of active nodes or packets than the number of configured slots, nodes will compete in all slots. Then the number of *DATA* transmissions will be stabilized, and consequently, the energy consumption will be stabilized. That is, the network is saturated. With traditional single packet transmission where only one slot is configured, the network is satur-

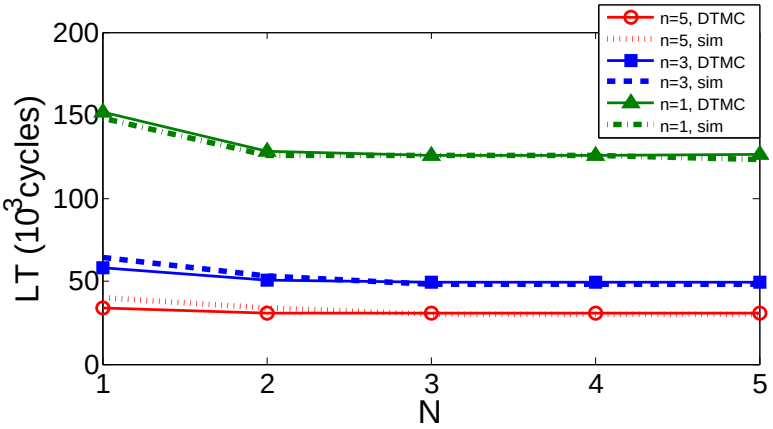

Figure E.4: Network lifetime as the number of nodes varies, given that $\lambda = 1.5$ packet/s.

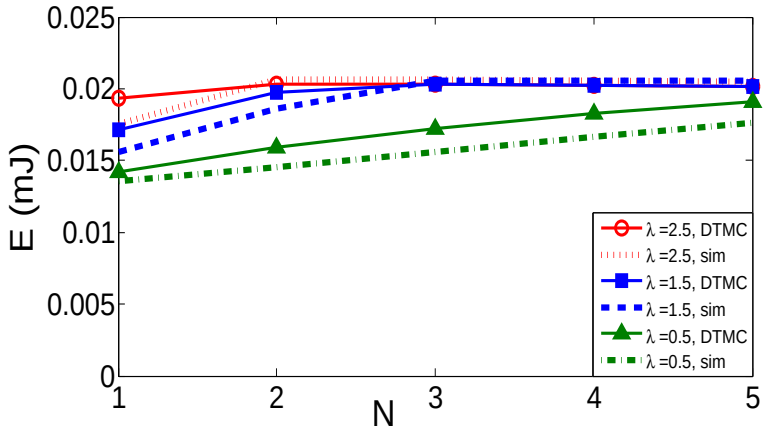

Figure E.5: Average energy consumed by the relay per cycle as the number of nodes varies, given that $n = 3$.

ated at $N = 2$. By employing MPT, however, the saturation point is delayed. As observed in Fig. E.3, the number of nodes required to occupy all the slots is 3 when $n = 3$. In case of $n = 5$, a packet arrival rate of $\lambda = 1.5$ packets/s with this configuration saturates the network with even 3 nodes. Correspondingly, the network lifetime is shown in Fig. E.4. Obviously, the lifetime contains an inverse trend as the energy consumption curve does, i.e., higher energy consumption results in shorter lifetime. When more *DATA* transmissions happen due to a higher number of nodes, the lifetime becomes shorter. However, as observed in this figure, it is also stabilized after the network is saturated.

It is clear that λ affects the network saturation point in DW-MAC. Therefore, we evaluate the performance of DW-MAC with different packet arrival rates in Fig. E.5. With a fixed n, we observe that E increases monotonically

with the network size, N, up to the saturation point. After that point, E becomes constant regardless of N. Fig. E.5 indicates that the injected traffic load at the rate of 0.5 packets/s is too light to saturate the network for the studied range of node population. Given that n is set as 3 in this case, there always exist *idle* slots during the operation of DW-MAC at 0.5 packets/s. However, the network becomes saturated at $N = 3$ if $\lambda = 1.5$. Furthermore, the network is fully occupied at $\lambda = 2.5$ with $N = 2$, meaning that both nodes remain non-empty even though both of them got chance to transmit one packet in one of the first two slots.

B. Accuracy of the Models

From the above figures, we observe that the analytical results match the results obtained from simulations, for all the ranges studied in this paper. At the first glance, it may seem that there is somewhat difference between the results under the non-saturation regime. However, considering that the scale of the *y-axis* is very small for energy consumption, we ascertain that the models are precise enough. This is because that the *system* DTMC can accurately find the distribution of the number of active nodes in the network at each cycle to find p_s. At the same time, using the same p_s the *node* DTMC also correctly estimates the number of packet transmissions at each cycle. To further improve the accuracy, a two dimensional model similar to the one mentioned in [8] could be developed.

VI. CONCLUSIONS

In this paper, a popular synchronous duty cycle MAC protocol in WSNs, DW-MAC, is modeled and evaluated for multiple packet transmissions (MPT). MPT is enabled by competition based reservations in the *data* period and packet transmission in the *sleep* period. By allowing MPT, multiple packets can be accommodated for transmission in a single cycle. We model this procedure by two DTMCs and calculate the transmission probability by interactively solving the equations from the these two DTMCs. Based on the obtained steady state probabilities, we deduce expressions for energy consumption and network lifetime calculations. The discrete-event based simulation results confirm that the behavior of DW-MAC with MPT can be precisely predicted by the developed models.

REFERENCES

[1] T. Kim, I. H. Kim, Y. Sun and Z. Y. Jin, “Physical layer and medium access control design in energy efficient sensor networks: An overview", *IEEE Trans. Ind. Informat.*, vol. 11, no. 1, pp. 2-15, Feb. 2015.

[2] W. Ye, J. Heidemann, and D. Estrin, “Medium access control with coordinated adaptive sleeping for wireless sensor networks", *IEEE/ACM Trans. Netw.*, vol. 12, no. 3, pp. 493-506, June 2004.

[3] S. Du, A. K. Saha, and D. B. Johnson, “RMAC: A routing-enhanced duty-cycle MAC protocol for wireless sensor networks", *in Proc. IEEE INFOCOM* , May 2007.

[4] Y. Sun, S. Du, O. Gurewitz, and D. B. Johnson, “DWMAC: A low latency, energy efficient demand-wakeup MAC protocol for wireless sensor networks", *in Proc. ACM MobiHoc* , 2008.

[5] O. Yang and W. Heinzelman, “Modeling and performance analysis for duty-cycled MAC protocols in wireless sensor networks", *IEEE Trans. Mobile Computing*, vol. 11, no. 6, pp. 905-921, June 2012.

[6] Y. Zhang, C. He, and L. Jiang, “Performance analysis of S-MAC protocol under unsaturated conditions", *IEEE Commun. Lett.*, vol. 12, no. 3, pp. 210-212, Mar. 2008.

[7] F. Tong, L. Zheng, M. Ahmadi, M. Li, and J. Pan, "Modeling and analyzing duty-cycling, pipelined-scheduling MACs for linear sensor networks", *IEEE Trans. Veh. Technol.*, early access available in IEEEXplore, Jan. 2016.

[8] J. Martinez-Bauset, L. Guntupalli, and F. Y. Li, “Performance analysis of synchronous duty-cycled MAC protocols", *IEEE Wireless Commun. Lett.*, vol. 4, no. 5, pp. 469-472, Oct. 2015.

[9] `http://www.ti.com/lit/ds/symlink/cc1000.pdf`, 2015.

Appendix A

Title:	Modeling Cooperative Transmission for Synchronous MAC Protocols in Duty-Cycled WSNs
Authors:	Lakshmikanth Guntupalli†, Jorge Martinez-Bauset‡, and Frank Y. Li†
Affiliation:	†Dept. of Information and Communication Technology, University of Agder (UiA), N-4898 Grimstad, Norway ‡Dept. of Communications, Universitat Politècnica de València (UPV), 46022 València, Spain
Conference:	*IEEE International Conference on Communications (ICC)*, May 2017. To be submitted.

Appendix A

Modeling Cooperative Transmission for Synchronous MAC Protocols in Duty-Cycled WSNs

Abstract — **Energy hole is a phenomenon caused by uneven energy consumption activities among sensor nodes in a wireless sensor network (WSN), and it diminishes network lifetime. Cooperative transmission (CT) promises energy balancing among nodes and extends the lifetime of a network. In this paper, we develop a discrete-time Markov chain (DTMC) model to analyze the performance of CT associated with synchronous CT MAC protocols. For performing CT, we propose a receiver initiated CT MAC protocol, in which the receiving node takes the decision on initiating CT or not. In this way, nodes can avoid idle listening. Using the developed DTMC model, the performance of the protocol is evaluated in terms of energy consumption, energy efficiency and network lifetime. The analytical model is validated through discrete-event simulations. Numerical results demonstrate the accuracy of the model and the effectiveness of CT, in contrast to non-CT, as it leads to balanced energy consumption and a prolonged network lifetime.**

I. INTRODUCTION

Cooperative transmission (CT) [1] appears as a promising technique for energy balancing in wireless sensor networks (WSNs). In CT, neighboring nodes collaborate with a sending node to transmit multiple copies of a packet. Then, the distant destination node recovers the packet by combining these copies of the same packet, exploiting temporal and spatial diversity. CT can be employed in duty cycling (DC) medium access control (MAC) protocols [2] -[4] to mitigate the *energy hole* problem [5] which typically occurs when a forwarding node is exhausted. For instance, the relay node (RLN) in Fig. AppxA.1 depletes its battery earlier than the source nodes since it is involved in more activities. Consequently, the source nodes would be disconnected from the *sink*, resulting in a shorter network lifetime. In a CT enabled network, a source node may, together with its selected neighbors, transmit a packet directly to a distant node bypassing the relay nodes [2]. Consequently, the energy consumption at the relay is reduced. Thus the outbreak of the energy hole is postponed.

In the literature many CT MAC protocols employ a sender initiated CT [2] -[4], where a sending node decides whether or when to perform CT based on the residual energy level of the receiving (i.e., the relay) node. However, this procedure requires to exchange several control packets among the RLN, the cooperating nodes and the destination node before making a decision. During the process, nodes participating in the CT waste energy due to idle listening. Furthermore, these protocols are evaluated merely through simulations.

There exist a few analytical models to evaluate synchronous MAC [6], including our earlier work [7] [8]. These models have however been proposed to analyze only non-CT operations, where energy consumption is not balanced. The energy hole problem was also analyzed from a routing perspective in [5], without considering CT. A Markov decision process was proposed in [9] to optimize the lifetime in a CT network using a combination of routing and MAC mechanisms. However, the adopted traffic model therein is not realistic. To the best of our knowledge, so far no mathematical models exist to analyze CT operations in synchronous DC MAC protocols.

The proposed discrete-time Markov chain (DTMC) model in this study is generic, applicable to other synchronous CT MAC protocols as well. For expression clarity, we focus hereafter on a receiver initiated CT, carrier sensing multiple access/ collision avoidance (CSMA/CA) based MAC (RICT-MAC) protocol, and assess its performance accordingly. The DTMC has two dimensions (2D), one modeling the queue dynamic of a given node, and the other the activity state of the rest of the nodes in the same network. Different from existing one dimensional DTMCs which consider only the number of packets in a queue [6] or obtaining the distribution of active nodes using an auxiliary DTMC [7], the developed model determines the distributions for both the number of packets and the number active nodes using a single 2D DTMC. The solution of this DTMC is used to determine energy consumption, energy efficiency as well as network lifetime considering both CT and non-CT. The model results are validated through discrete-event simulations. For comparison purposes, we evaluate its performance together with the one obtained by the scheduled cooperative transmission MAC (SCT-MAC) [2] and a non-CT protocol, DW-MAC [10].

The rest of the paper is organized as follows. In Sec. II, we present the network model and the RICT-MAC protocol. Sec. III describes the pro-

posed DTMC model and Sec. IV provides the energy consumption analysis. Numerical results from the discrete-event simulations and DTMC model are demonstrated in Sec. V, before the paper is concluded in Sec. VI.

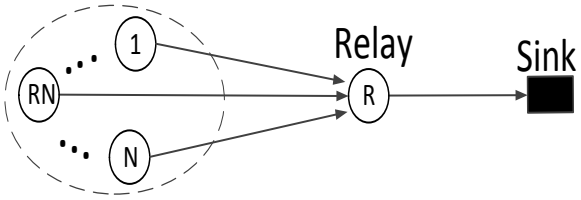

Figure AppxA.1: Illustration of a 2-hop wireless sensor network.

II. RICT-MAC: PRINCIPLE AND OPERATION

Consider a cluster of N sensor nodes that send traffic towards a single *sink*, using one common RLN, as shown in Fig. AppxA.1. For analysis convenience, we select arbitrarily one of the N nodes, and refer to it as the reference node (RN). Hereafter, *DATA*, *SYNC*, *SCH* and *ACK* denote packets, and t_{DATA}, t_{SYNC}, t_{SCH} and t_{ACK} denote the corresponding packet durations respectively. Meanwhile, we represent the different parts of a cycle as *active*, *sleep*, *sync*, *data* and their corresponding durations as T_{active}, T_{sleep}, T_{sync} and T_{data} respectively.

A. RICT-MAC Protocol Overview

When nodes wake up, they synchronize with one another by exchanging schedule messages during a fixed-length *sync* period, followed by a *data* period used to exchange *SCH* packets. After the *data* period, nodes go to sleep. The time elapsed between a node's wake-up moment and the instant it goes to sleep is regarded as an *active* period. Then, the time interval during which nodes sleep is referred to as a *sleep* period. Furthermore, the time interval defined between two wake-up instants is considered as one *cycle*, i.e., a *cycle* contains successively, a *sync*, a *data* and a *sleep* period.

RICT-MAC uses the *data* period only for reserving medium access for its *DATA* transmission in the subsequent *sleep* period. All active nodes (i.e., those with a non-empty queue) compete in the *data* period to transmit a *SCH* packet. The node that successfully transmits (without collision) a *SCH*, occupies the medium in the subsequent *sleep* period for *DATA* transmission. If a collision occurs, *DATA* exchange is not possible in the current cycle, and

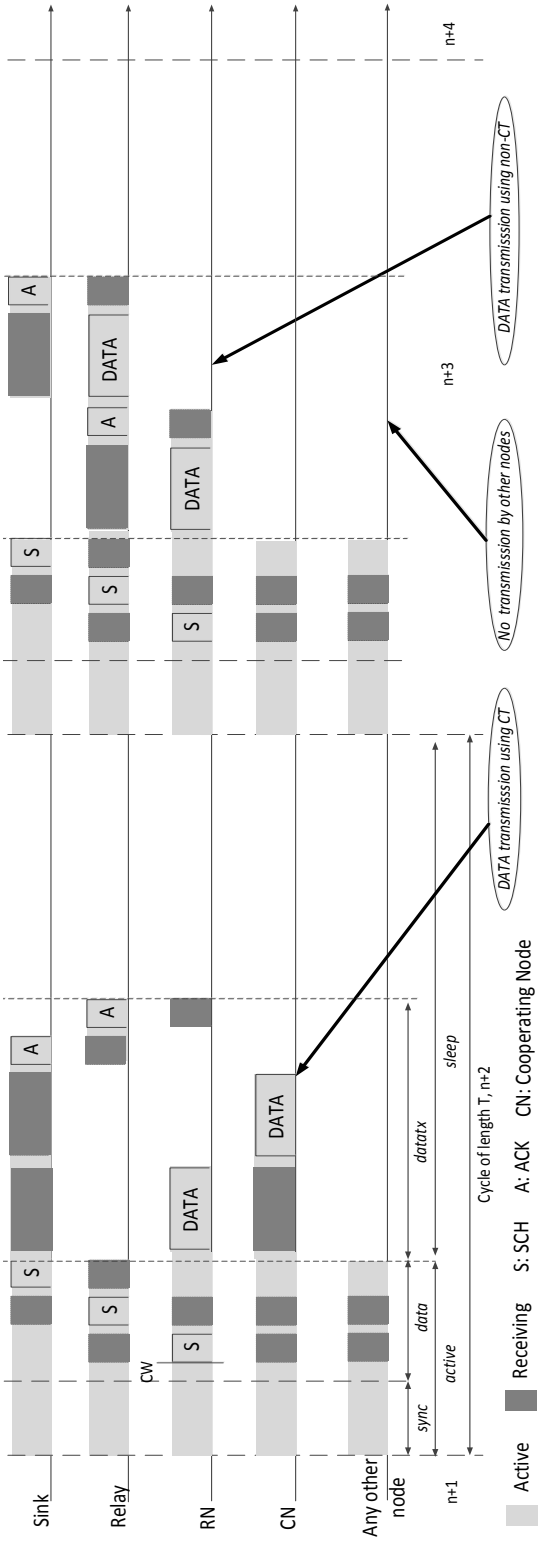

Figure AppxA.2: Illustration of performing CT and non-CT in RICT-MAC.

nodes try again in the next cycle by generating new backoff times. In the studied network, we assume that the channel is error-free and transmission failures occur only due to collisions.

Fig. AppxA.2 illustrates the operation of RICT-MAC. Assume that the RN is the winner of the contention in the *data* period. After gaining channel access, the RN transmits *SCH* to the RLN, reserving the medium along the subsequent *sleep* period. Then, the RLN forwards this message to the *sink* node to inform it about the follow-up *DATA* transmission. In RICT-MAC, the contention among nodes happens only in the *data* period. In other words, no contention occurs during *DATA* exchange. It is worth mentioning that the RICT protocol supports transmitting multiple packets in one cycle similar to DW-MAC [10]. However, for modeling simplicity, only a single packet transmission per cycle is studied in this paper.

After obtaining channel access, two modes are possible for the transmission of a *DATA* packet, as described below.

1) Cooperative Transmission: The RN sends a *SCH* packet to the RLN that includes the residual energy level of the RN, E_{rn}, in addition to the address of the destination node, i.e., the *sink* [10]. The RLN compares E_{rn} with its own energy level, E_f. If $E_f < E_{rn}$, it decides to perform CT by broadcasting a reply *SCH* packet containing the ID(s) of the cooperating node(s) (CN(s)). For the network shown in Fig. AppxA.1, only one CN is enough to transmit the *DATA* to a two-hop away sink node [2]. This reply message is received by the *sink* node as well. Subsequently, the RN, the *sink* and the CN wake up in the subsequent *sleep* period in order to participate in CT. Note that, to save energy, the RLN does not wake up. To perform CT, the RN first broadcasts the *DATA*, and then it goes to sleep. A copy of the same *DATA* is sent to the *sink* again by the CN in a time division CT manner [2], as shown in Fig. AppxA.2. The *sink* combines both copies to decode it properly. Afterwards, the RLN and the RN awake to receive the *ACK* from the *sink*.

In this study we focus on a homogeneous network where all nodes behave in the same way with similar characteristics and have the same initial energy. Then, all nodes have equal probability to be selected as a CN, as we expect an equal energy consumption rate for all source nodes. See Sec. IV.

2) Non-cooperative Transmission: The *DATA* packet is transmitted in a non-CT manner if $E_f \geq E_{rn}$. The RLN replies with a *SCH without any*

ID for the CN. Since there is no ID of any collaborator, nodes follow the non-CT mode. Correspondingly, the RN and the RLN proceed with *DATA* exchange, whereas the *sink* delays its wake-up time by $(t_{DATA} + t_{ACK} + 2D_p)$ where D_p is the one-way propagation delay. Note that the RN goes to sleep after transmitting the *DATA* packet, while the RLN continues to forward the *DATA* packet to the *sink*, as illustrated Fig. AppxA.2.

B. Medium Access in RICT-MAC

Consider that the RN has packets in the queue (is active) and contends with other k, $0 \leq k \leq N-1$ active nodes in a given cycle. All active nodes generate a random backoff time from the set $\{0, W-1\}$ at the beginning of the *data* period. Then the probability that the RN is the only node selecting the smallest backoff time (the winner), and that it transmits a *SCH* successfully (without collision) is given by,

$$P_{s,k} = \sum_{i=0}^{W-1} (1/W)\,(W-1-i)^k / W^k. \qquad \text{(AppxA.1)}$$

Note that the decision on deploying CT is made later. With a probability $P_{sf,k} = \sum_{i=0}^{W-1} (1/W)\,(W-i)^k / W^k$, the RN transmits either successfully or with collision. Otherwise, the RN loses the contention with a probability $(1 - P_{sf,k})$, and it defers access until the next cycle.

III. A DTMC MODEL FOR RICT-MAC

A state in the 2D DTMC is represented by (i,k), where i is the number of packets in the queue of the RN, $i \leq Q$, and k is the number of active nodes other than the RN in the cycle, $k \leq K = N-1$. Assume that packet arrivals follow a Poisson process with rate λ. For cycles of length T, the probability that i (or more) packets arrive to the RN in a cycle is $A_i = (\lambda T)^i \cdot e^{-\lambda T}/i!$ $(A_{\geq i} = 1 - \sum_{j=0}^{i-1} A_j\ )$. Note that the model supports other renewal arrival process as well.

When k nodes compete in a cycle, the probability that any of them transmits a *SCH* packet successfully is $S_k = kP_{s,k-1}$, and the collision probability is $\widehat{S}_k = 1 - S_k$. Furthermore, when a node transmits a *DATA* packet, the prob-

Table AppxA.1: Transition Probabilities of the DTMC Model for RICT-MAC

$P_{(0,0),(j,l)} = B_l(K)\cdot A_j;\ 0 \le j \le Q-1,\ 0 \le l \le K,$	No active nodes. Transitions occur due to new arrivals	$P_{(0,0),(Q,l)} = B_l(K)\cdot A_{\ge Q};\ 0 \le l \le K.$
$P_{(0,k),(j,l)} = S_k \cdot P_e \cdot B_{l-k+1}(K-k)\cdot A_j$ $+S_k \cdot \widehat{P}_e \cdot B_{l-k}(K-k)\cdot A_j;$ $+\widehat{S}_k \cdot B_{l-k}(K-k)\cdot A_j;$ $0 \le j \le Q-1,\ 1 \le k \le l \le K-1,$	RN is a non-active node. Transitions caused by other active nodes	$P_{(0,k),(Q,l)} = S_k \cdot P_e \cdot B_{l-k+1}(K-k)\cdot A_{\ge Q}$ $+S_k \cdot \widehat{P}_e \cdot B_{l-k}(K-k)\cdot A_{\ge Q};$ $+\widehat{S}_k \cdot B_{l-k}(K-k)\cdot A_{\ge Q};$ $1 \le k \le l \le K-1,$
$P_{(0,k),(j,k-1)} = S_k \cdot P_e \cdot B_0(K-k)\cdot A_j;$ $0 \le j \le Q-1,\ 1 \le k \le K,$		$P_{(0,k),(Q,k-1)} = S_k \cdot P_e \cdot B_0(K-k)\cdot A_{\ge Q};\ 1 \le k \le K,$
$P_{(0,k),(j,K)} = S_k \cdot \widehat{P}_e \cdot B_{K-k}(K-k)\cdot A_j;$ $+\widehat{S}_k \cdot B_{K-k}(K-k)\cdot A_j;$ $0 \le j \le Q-1,\ 1 \le k \le K,$		$P_{(0,k),(Q,K)} = S_k \cdot \widehat{P}_e \cdot B_{K-k}(K-k)\cdot A_{\ge Q};$ $+\widehat{S}_k \cdot B_{K-k}(K-k)\cdot A_{\ge Q};$ $1 \le k \le K.$
$P_{(i,k),(j,l)} = P_{s,k}\beta \cdot B_{l-k}(K-k)\cdot A_{j-i+1}$ $+P_{s,k}(1-\beta)\cdot B_{l-k}(K-k)\cdot A_{j-i+1}$ $+kP_{s,k}\cdot P_e \cdot B_{l-k+1}(K-k)\cdot A_{j-i}$ $+kP_{s,k}\cdot \widehat{P}_e \cdot B_{l-k}(K-k)\cdot A_{j-i}$ $+\widehat{S}_{k+1}\cdot B_{l-k}(K-k)\cdot A_{j-i};$ $1 \le i \le j \le Q-1,\ 0 \le k \le l \le K-1,$	Transitions due to multiple contending nodes	$P_{(i,k),(Q,l)} = P_{s,k}\beta \cdot B_{l-k}(K-k)\cdot A_{\ge Q-i+1}$ $+P_{s,k}(1-\beta)\cdot B_{l-k}(K-k)\cdot A_{\ge Q-i+1}$ $+kP_{s,k}\cdot P_e \cdot B_{l-k+1}(K-k)\cdot A_{\ge Q-i}$ $+kP_{s,k}\cdot \widehat{P}_e \cdot B_{l-k}(K-k)\cdot A_{\ge Q-i}$ $+\widehat{S}_{k+1}\cdot B_{l-k}(K-k)\cdot A_{\ge Q-i};$ $1 \le i \le Q,\ 1 \le 0 \le l \le K-1,$
$P_{(i,k),(j,K)} = P_{s,k}\beta \cdot B_{K-k}(K-k)\cdot A_{j-i+1}$ $+P_{s,k}(1-\beta)\cdot B_{K-k}(K-k)\cdot A_{j-i+1}$ $+kP_{s,k}\cdot \widehat{P}_e \cdot B_{K-k}(K-k)\cdot A_{j-i}$ $+\widehat{S}_{k+1}\cdot B_{K-k}(K-k)\cdot A_{j-i};$ $1 \le i \le j \le Q-1,\ 0 \le k \le K,$		$P_{(i,k),(Q,K)} = P_{s,k}\beta \cdot B_{K-k}(K-k)\cdot A_{\ge Q-i+1}$ $+P_{s,k}(1-\beta)\cdot B_{K-k}(K-k)\cdot A_{\ge Q-i+1}$ $+kP_{s,k}\cdot \widehat{P}_e \cdot B_{K-k}(K-k)\cdot A_{\ge Q-i}$ $+\widehat{S}_{k+1}\cdot B_{K-k}(K-k)\cdot A_{\ge Q-i};$ $1 \le i \le Q,\ 0 \le k \le K,$
$P_{(i,k),(j,k-1)} = kP_{s,k}\cdot P_e \cdot B_0(K-k)\cdot A_{j-i}$ $1 \le i \le j \le Q-1,\ 1 \le k \le K,$		$P_{(i,k),(Q,k-1)} = kP_{s,k}\cdot P_e \cdot B_0(K-k)\cdot A_{\ge Q-i}$ $1 \le i \le Q,\ 1 \le k \le K,$
$P_{(i,k),(i-1,l)} = P_{s,k}\beta \cdot B_{l-k}(K-k)\cdot A_0;$ $+P_{s,k}(1-\beta)\cdot B_{l-k}(K-k)\cdot A_0;$ $1 \le i \le Q,\ 0 \le k \le l \le K,$		
$P_{(i,k),(i-1,l)} = 0;\ 1 \le i \le Q,\ 1 \le k \le K,\ l < k,$ $P_{(i,k),(j,l)} = 0,\ 0 \le i \le j \le Q,\ 2 \le k \le K,\ l < k-1,$	Impossible transitions	$P_{(i,k),(j,l)} = 0;\ 2 \le i \le Q,\ j < i-1,\ 0 \le k \le l \le K,$ $P_{(i,k),(j,k-1)} = 0;\ 1 \le i \le Q,\ j < i,\ 1 \le k \le K.$

ability that its queue becomes empty is

$$P_e = P_s A_0 \pi_1 / P_s (1 - \pi_0) , \qquad \text{(AppxA.2)}$$

where P_s is the probability that the RN (or another node) transmits a *SCH* packet successfully in a random cycle, and π_0 and π_1 are the stationary probabilities of finding 0 and 1 packet at the queue of the RN respectively. The probability that it remains non-empty is $\widehat{P}_e = 1 - P_e$. Define also $B_k(l) = \binom{l}{k} \widehat{A}^k A_0^{l-k}$ as the probability that k out of l nodes which have their queues empty receive packets in a cycle, where $\widehat{A} = 1 - A_0$.

Denote by P_{ct} (P_{nct}) the probability that the RN operates in the CT (non-CT) mode in a random cycle. Clearly, $P_s = P_{ct} + P_{nct}$ holds as CT or non-CT can only occur in cycles where the RN has won the contention. Let us define β, where $0 \leq \beta \leq 1$, such that, $P_{ct} = \beta P_s$ and $P_{nct} = (1 - \beta) P_s$. We refer to this parameter as the *CT coefficient*.

In each cycle, a transition in the DTMC might occur based on packet arrivals and departures at the RN, as well as at the other source nodes, as shown in Tab. AppxA.1. Denote further by $P_{(i,k),(j,l)}$ the transition probability from State (i,k) to State (j,l). The terms that compose $P_{(i,k),(j,l)}$ is explained as follows. A transition from (i,k) to (j,l) occurs when: i) the RN transmits a packet successfully in the CT mode with probability $P_{s,k}\beta$; ii) the RN transmits a packet successfully in non-CT with probability $P_{s,k}(1-\beta)$; iii) an active node different from the RN transmits a packet successfully with probability $kP_{s,k}$ and empties its buffer; iv) an active node different from the RN transmits a packet successfully with probability $kP_{s,k}$ and does not empty its buffer; or v) no node is successful with probability $\widehat{S}_{k+1}$. Note that the RN receives $(j-i)$ packets with probability A_{j-i}, except in conditions i) and ii) where it receives $(j-i+1)$ packets. Also, $(l-k)$ out of $(K-k)$ inactive nodes become active with probability $B_{l-k}(K-k)$, except in condition iii) where $(l-k+1)$ nodes become active.

The solution of this 2D DTMC is obtained by solving the following set of linear equations

$$\boldsymbol{\pi P} = \boldsymbol{\pi} , \quad \boldsymbol{\pi e} = 1 , \qquad \text{(AppxA.3)}$$

where $\boldsymbol{\pi}$ is the stationary distribution, $\boldsymbol{P}$ is the transition probability matrix, whose elements are defined in Tab. AppxA.1, and $\boldsymbol{e}$ is a column vector of ones. By solving the set of equations (AppxA.3), $\boldsymbol{\pi}(P_e)$ can be determined for a given P_e. Then, a new $P_e(\boldsymbol{\pi})$ can be obtained from (AppxA.2) for a given $\boldsymbol{\pi}$, where $\pi_i = \sum_{k=0}^{K} \pi(i,k)$. Denote by P_e the solution of this fixed-point equation, i.e., the value of $P_e(\boldsymbol{\pi})$ at the fixed-point.

A. Calculation of P_{ct} as an Optimal Point

The main goal of RICT-MAC is to balance energy consumption in the network through CT. This means that the lifetime of the RLN, the RN and any other source node would converge to the same value. As shown in Fig. AppxA.2, operating in the CT mode continuously wastes the energy of CNs. On the other hand, operating in the non-CT mode would deplete the battery of the RLN earlier. In either case, the network suffers from a limited lifetime, since energy balancing cannot be achieved by running CT or non-CT *alone*.

Therefore, a tradeoff exists between triggering CT and non-CT during network operations. In order to find the optimal probability of deploying CT, we determine the value of β that makes the lifetimes of both the RLN and the RN equal.

IV. Energy Consumption Analysis of RICT-MAC

As explained in Sec. II, each cycle in RICT-MAC contains a *sync*, *data* and *sleep* period. In RICT, one *SYNC* packet is transmitted every N_{sc} cycles, and one packet might be received per cycle in the remaining $N_{sc}-1$ cycles as in [6]. So the energy consumed by a node in the *sync* period is $E_{sc} = [(t_{SYNC} \cdot P_{tx} + (T_{sync} - t_{SYNC}) \cdot P_{rx})] \cdot (1/N_{sc}) + (T_{sync} \cdot P_{rx}) \cdot (N_{sc}-1)/N_{sc}$, where P_{tx} and P_{rx} are the transmission and reception power levels respectively.

As shown in Fig. AppxA.2, *three SCH* packets are required to transfer a *DATA* packet to the sink in the CT mode. Correspondingly, the duration of the *data* period of a cycle is $T_{data} = (W-1)T_B + 3t_{SCH} + 2D_p$, where T_B is the duration of a backoff timer *slottime*. Similarly, the duration of the data transmission part in the *sleep* period is $T_{datatx} = 2(t_{DATA} + t_{ACK} + 2D_p)$.

The amounts of energy consumed per cycle by the RN when it transmits successfully (E_{txs}), either in the CT or non-CT mode, and when it acts as a

cooperating node (E_{cts}) are given respectively by

$$\begin{aligned} E_{txs} &= t_{SCH} \cdot P_{tx} + (T_{data} - t_{SCH}) \cdot P_{rx} \\ &\quad + t_{DATA} \cdot P_{tx} + (t_{ACK} + 3D_p) \cdot P_{rx} \\ &\quad + (T_{datatx} - t_{DATA} - t_{ACK} - 3D_p) \cdot P_{sl}\,, \\ E_{cts} &= T_{data} \cdot P_{rx} + t_{DATA} \cdot P_{tx} + (t_{DATA} + D_p) \cdot P_{rx} \\ &\quad + (T_{datatx} - 2t_{DATA} - D_p) \cdot P_{sl}\,. \end{aligned}$$

Similarly, the amounts of energy consumed per cycle by the RLN in a successful transmission in the CT (E_{ct}) and non-CT (E_{nct}) mode are given respectively by,

$$\begin{aligned} E_{ct} &= t_{SCH} \cdot P_{tx} + (T_{data} - t_{SCH}) \cdot P_{rx} \\ &\quad + t_{ACK} \cdot P_{tx} + (t_{ACK} + 2D_p) \cdot P_{rx} \\ &\quad + (T_{datatx} - 2t_{ACK} - 2D_p) \cdot P_{sl}\,, \\ E_{nct} &= t_{SCH} \cdot P_{tx} + (T_{data} - t_{SCH}) \cdot P_{rx} \\ &\quad + (T_{DATA} + t_{ACK}) \cdot (P_{tx} + P_{rx}) + 2D_p \cdot P_{rx}\,, \\ &\quad + (T_{datatx} - 2t_{DATA} - 2t_{ACK} - 2D_p) \cdot P_{sl}\,, \end{aligned}$$

where P_{sl} is the sleep power level. In case that a collision was caused by other nodes but not by the RN, both the RLN and the RN nodes consume the same energy as $E_{txf} = T_{data} \cdot P_{rx} + T_{datatx} \cdot P_{sl}$. If the RN is a participating node in that collision, then it consumes energy as $E'_{txf} = t_{SCH} \cdot P_{tx} + (T_{data} - t_{SCH}) \cdot P_{rx} + T_{datatx} \cdot P_{sl}$. However the energy consumed by the RLN is E_{txf}.

Consider that the number of active nodes in a cycle is $k+1$. As mentioned in Sec. III, the probability that a successful transmission occurs is S_{k+1} , and a failure is $\widehat{S}_k = 1 - S_k$. Then, the average energy consumed per cycle by the RLN for *DATA* exchange is

$$E_{drl,k+1} = S_{k+1} \left[\beta E_{ct} + (1-\beta) E_{nct}\right] + \widehat{S}_k E_{txf}\,. \qquad \text{(AppxA.4)}$$

Also, the energy consumed per cycle by the RN on average is

$$\begin{aligned} E_{drn,k+1} = {} & q_{1,k} \cdot \left[P_{s,k} E_{txs} + P_{f,k} E'_{txf} \right] \\ & + q_{2,k} P_{s,k} \cdot \left[\beta \alpha_1 E_{cts} + (\beta \alpha_2 + (1-\beta)) E_{txf} \right] \\ & + q_{3,k} E_{txf} \,, \end{aligned} \tag{AppxA.5}$$

where $q_{1,k} = (k+1)/N$ is the probability that the RN is active, $q_{2,k} = kq_{1,k} + (k+1)\left(1 - q_{1,k}\right)$ is the average number of active nodes other than the RN, and $q_{3,k} = 1 - q_{2,k}P_{s,k} - q_{1,k}P_{sf,k}$ is the probability that nodes other than the RN transmit a packet with failure. Moreover, $\alpha_1 = 1/(N-1)$ is the probability of selecting the RN as a cooperating node when CT is triggered by another node, and $\alpha_2 = 1 - \alpha_1$. Recall that for α_1, we assume a homogeneous network. In (AppxA.5), the first term describes RN's actions (in CT, non-CT and collision). The second term describes actions associated to a successful transmission by other nodes different from the RN, where the RN might cooperate in CT. Similarly, the last term represents a collision by the nodes other than the RN. If no node is active, then $E_{drl,0} = E_{drn,0} = T_{data} \cdot P_{rx} + T_{datatx} \cdot P_{sl}$.

In this network, the average energy consumed by the RLN during the *data* period of a cycle is given by,

$$E_{drl} = \sum_{k=0}^{N} E_{drl,k} \cdot \pi'_k \tag{AppxA.6}$$

where $\pi'_k = \sum_{i=1}^{Q} \pi(i, k-1) + \pi(0,k)$ is the stationary probability of finding k active nodes in a cycle. Correspondingly, the energy consumed while nodes sleep in the *sleep* period of a cycle is given by

$$E_{sl} = (T - T_{sync} - T_{data} - T_{datarx}) \cdot P_{sl} \,, \tag{AppxA.7}$$

and the average energy consumed by the RLN in a cycle is

$$E_{rl} = E_{sc} + E_{drl} + E_{sl} \,. \tag{AppxA.8}$$

The lifetime of the network shown in Fig. AppxA.1 depends on the lifetime of the RLN, as the network would be disconnected when RLN's battery is depleted. Accordingly, the network lifetime expressed in cycles is obtained

as

$$LT = (E_{initial}/E_{rl}) \text{ cycles}. \tag{AppxA.9}$$

Furthermore, the average number of successfully transmitted packets by the RN or any sending node in a cycle can be determined as $\eta = \sum_{i=1}^{Q} \sum_{k=0}^{K} \pi(i,k) \cdot P_{s,k}$. Accordingly, the mean number of packets forwarded by the RLN during the total network lifetime is given by,

$$TPT = N \cdot \eta \cdot LT. \tag{AppxA.10}$$

Denote by ξ the energy efficiency of the RLN (network), expressed as the total number of bytes successfully transferred divided by the total amount of consumed energy in the lifetime of the RLN. It is given by

$$\xi = (TPT \cdot S/E_{initial}), \tag{AppxA.11}$$

where S is the size of the *DATA* packet in bytes.

In the same way, the lifetime of the RN can be obtained using the corresponding energy terms calculated from (AppxA.5) and substituting them into (AppxA.6)-(AppxA.9) instead of the RLN related terms. Moreover, the calculations for SCT-MAC can be determined by replacing T_{data} with $(W-1)T_B + 5t_{SCH} + 4D_p$, as SCT needs 4 *SCH*s for channel reservation and 1 *beacon* for disseminating the residual energy information [2]. Likewise, the metrics for DW-MAC are obtained by keeping $P_{ct} = 0$ and $\alpha_1 = 0$.

V. Simulations and Numerical Results

In this section, we validate the proposed analytical model by comparing numerical results obtained from it with the ones obtained from simulations. The RICT-MAC and the other two studied protocols are simulated in a custom C based discrete-event simulator. The behavior of these protocols in the simulator is completely independent of the DTMC model. The results presented in this section are averaged over $5 \cdot 10^6$ cycles, each of 3.2 seconds.

All protocols are studied in the network illustrated in Fig. AppxA.1 with nodes containing a queue length of $Q = 10$. The *DATA* packet size is configured to be of 100 bytes. Packets arrive at a rate of $\lambda = 1.5$ packet/s, and a

node transmits a *SYNC* packet every $N_{sc} = 10$ cycles. Furthermore, we employ a 5% duty cycle while the other MAC parameters are taken from [10]. The transmission, reception and sleep power levels are $P_{tx} = 31.2$ mW, $P_{rx} = 22.2$ mW and $P_{sl} = 3$ μW [11] respectively. The performance metrics are determined by varying the number of nodes N from 2 to 20 at a granularity level 2. All nodes have the same initial energy $E_{initial} = 1$ Joule.

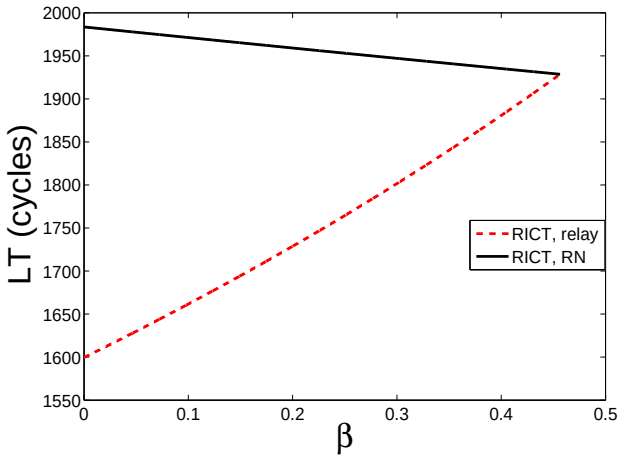

Figure AppxA.3: Optimal CT coefficient β is found to be 0.4565 for $N = 2$.

A. Optimal CT Operation

In order to determine the performance metrics, an optimal P_{ct} needs to be determined first, using the procedure presented in Sec. III. To do so, we calculate the lifetimes of both the RLN and the RN nodes by varying β at a granularity level of 1×10^{-5}. Then, we identify the β with which the lifetimes of both nodes coincide (both deplete their battery at almost the same time). That is, the optimal β is the point where the difference between E_{rl} and E_{rn} is smaller than 1×10^{-5} J. For a given network size N, we determine the optimal β, P_{ct} , P_{nct} , and the other performance metrics for the CT MAC protocols. In Fig. AppxA.3, this approach is applied to the aforementioned scenario with $N = 2$, and the optimal values were found to be $\beta = 0.4565$, and correspondingly $P_{ct} = 0.4565 \times P_s$. Note that this procedure does not apply to DW-MAC since it is a non-CT protocol, i.e., $\beta = 0$.

As observed in Figs. AppxA.4 to AppxA.7, the analytical results precisely match with the simulation results up to $N = 12$. This is because that the CT balanced the energy perfectly among the nodes in the network with few nodes and the modeling approach identified the exact β. Clearly, identifying the

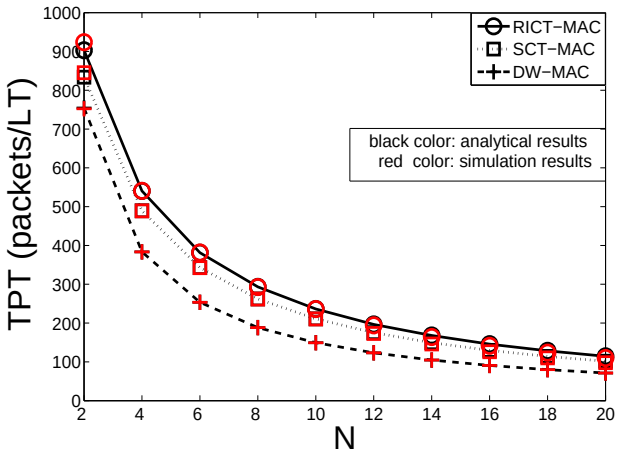

Figure AppxA.4: TPT per cycle for different number of nodes.

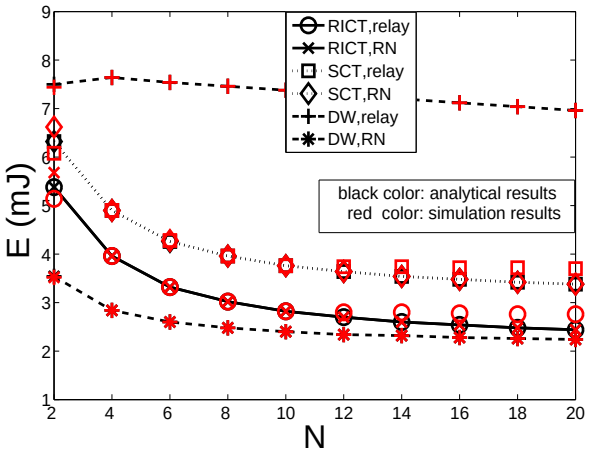

Figure AppxA.5: Energy consumption for different number of nodes.

optimal β is a good approximation for networks of small size.

Recall that the triggering of CT depends on the residual energy levels of the RLN and the source nodes. It is clear that CT is employed in the next cycle only when the winner of the current non-CT cycle obtains channel access again, and this probability, P_{ct}, decreases when N becomes larger. Then, in reality, the RLN consumes slightly higher energy on average when compared with source nodes including the RN. Consequently, the RLN will have slightly shorter lifetime than the RN does as obtained through simulations. On the other hand, the analytical model is based on a determined β which represents the energy balancing point that provides nodes with an equal lifetime and this procedure does not rely on the residual energy level information. Clearly, the analytical approach based on an optimal β leads to the

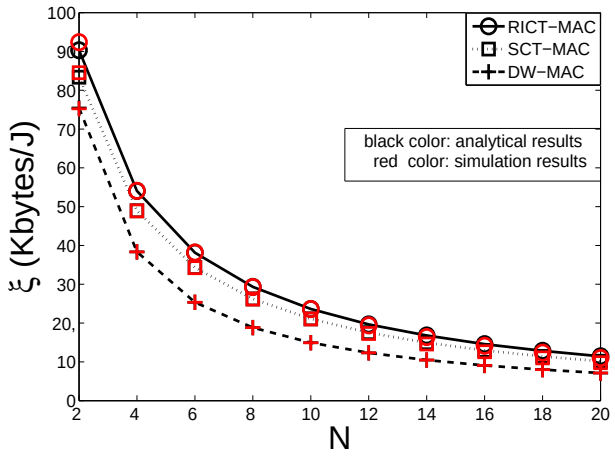

Figure AppxA.6: Energy efficiency for different number of nodes.

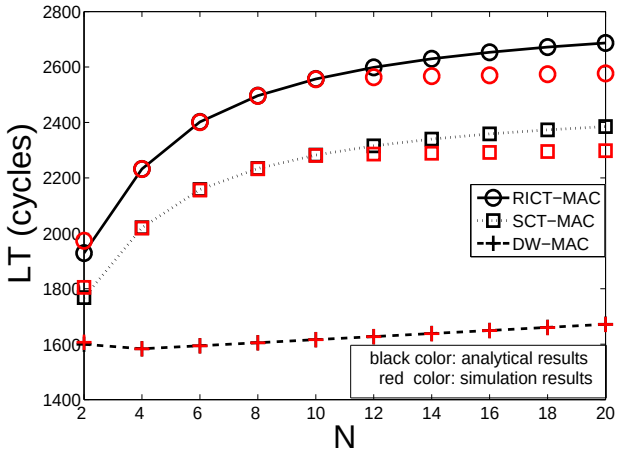

Figure AppxA.7: Network lifetime for different number of nodes.

same lifetime (energy consumption) for both the RLN and the RN whereas the simulations give a slightly shorter lifetime (higher energy consumption) to the RLN. Therefore, in Figs. AppxA.5 and AppxA.7, the discrepancy increases beyond $N = 12$. Anyhow, the deviation beyond $N = 12$ is still below 4% for both CT MAC protocols.

B. Performance Comparison of Three Protocols

Figs. AppxA.4 to AppxA.7 depict the average energy consumed per cycle by the nodes, the network lifetime, the total number of packets transmitted during the lifetime, and the energy efficiency, as the number of nodes in the network varies for all three studied protocols. It is obvious that the probability of getting a successful access is higher when fewer contentions occur (a lower N). Consequently more packets are transmitted, as shown in Fig. AppxA.4.

Accordingly, the highest energy consumed by nodes per cycle is attained at $N = 2$, as depicted in Fig. AppxA.5. Moreover, the highest energy efficiency is obtained at $N = 2$ as shown in Fig. AppxA.6, since ξ depends on TPT and $E_{initial}$ as defined in (AppxA.11). The same trend applies to all three protocols.

More collisions occur when the network size grows. Recall that in case of a collision, no *DATA* transmission occurs. Consequently, with a larger N, lower energy is consumed per node (Fig. AppxA.5), and the energy efficiency decreases (Fig. AppxA.6), as TPT is reduced (Fig. AppxA.4). Beyond $N = 12$, the network is saturated. Then, all nodes have packets in their queues (are active) in almost all cycles. This leads to the stabilization of the network conditions. Consequently, very little performance variation is observed beyond $N = 12$.

The impact of operating CT is clearly visible in Fig. AppxA.5, where the energy consumed by the RLN and the RN is almost equal for both RICT and SCT protocols. However, RICT achieves lower energy consumption (Fig. AppxA.5) and higher energy efficiency. The reason behind this is a shorter *data* period, due to the fact that CT is initiated by the RLN.

In DW-MAC, the RLN consumes much higher energy than in the other two protocols, as a result of the continuous operation in the non-CT mode. As observed in Fig. AppxA.5, the energy consumed by the RN is lower than the one in CT protocols. However, the network lifetime is decided by the lifetime of the RLN. Therefore, the network lifetime in DW-MAC is much shorter, as plotted in Fig. AppxA.7. Observe that the shape of the network lifetime curve is approximately the inverse of the energy consumption curve, as shown in Fig. AppxA.7. For example, RICT achieves 12.04% and 58.2% longer lifetimes at $N = 10$ than in SCT-MAC and DW-MAC respectively.

VI. CONCLUSIONS

In this paper, we modeled cooperative transmission for synchronous duty-cycled MAC protocols by developing a DTMC. We proposed a method to calculate the optimal probability to initiate CT in a cycle, based on the CT coefficient β. Using the developed model, the proposed receiver initiated cooperative transmission MAC protocol is evaluated. The energy consumption by the nodes, the lifetime of the network, the total number of pack-

ets transmitted successfully and the energy efficiency were deduced. It was found that the analytical results precisely matched with those obtained from discrete-event simulations. Moreover, initiating CT by the relaying node in RCT-MAC prolongs the lifetime, when compared with the sender initiated SCT-MAC protocol and non-CT protocols like DW-MAC.

REFERENCES

[1] J. Lin, H. Jung, Y. J. Chang, J. W. Jung, and M. A. Weitnauer, “On cooperative transmission range extension in multi-hop wireless ad-hoc and sensor networks: A review", *Ad Hoc Networks*, vol. 29, pp. 117-134, Jun. 2015.

[2] J. Lin and M. A. Ingram, “SCT-MAC: A scheduling duty cycle MAC protocol for cooperative wireless sensor network", in *Proc. IEEE ICC*, Jun. 2012.

[3] J. Lin and M. A. Ingram, “OSC-MAC: Duty cycle scheduling and cooperation in multi-hop wireless sensor networks", in *Proc. IEEE WCNC*, Apr. 2013.

[4] L. Guntupalli, J. Lin, M. A.Weitnauer, and F. Y. Li, “ACT-MAC: An asynchronous cooperative transmission MAC protocol for WSNs", in *Proc. IEEE ICC Workshops*, Jun. 2014.

[5] J. Ren, Y. Zhang, K. Zhang, A. Liu, J. Chen, and X. Shen, “Lifetime and energy hole evolution analysis in data-gathering wireless sensor networks", *IEEE Trans. Ind. Informat.*, vol. 12, no. 2, pp. 788-800, Apr. 2016.

[6] O. Yang and W. Heinzelman, “Modeling and performance analysis for duty-cycled MAC protocols in wireless sensor networks", *IEEE Trans. Mobile Comput.*, vol. 11, no. 6, pp. 905-921, Jun. 2012.

[7] J. Martinez-Bauset, L. Guntupalli, and F. Y. Li, “Performance analysis of synchronous duty-cycled MAC protocols", *IEEE Wireless Commun. Lett.*, vol. 4, no. 5, pp. 469-472, Oct. 2015.

[8] L. Guntupalli, J. Martinez-Bauset, F. Y. Li, and M. A. Weitnauer, “Aggregated packet transmission in duty-cycled WSNs: Modeling and performance evaluation", *IEEE Trans. Veh. Technol.*, Early access available in IEEEXplore, DOI:10.1109/TVT.2016.2536686, Mar. 2016.

[9] J. Lin and M. A. Weitnauer, “Modeling of multihop wireless sensor networks with MAC, queuing, and cooperation", *Int. J. Distributed Sensor Networks*, vol. 2016, Article ID 5258742, 2016.

[10] Y. Sun, S. Du, O. Gurewitz, and D. B. Johnson, “DWMAC: A low latency, energy efficient demand-wakeup MAC protocol for wireless sensor networks", in *Proc. ACM MobiHoc*, May 2008.

[11] `http://www.ti.com/lit/ds/symlink/cc1000.pdf`, 2016.

Appendix B

Title:	Performance of Duty-Cycled WSN with Aggregated Packet Transmission in Error-Prone Wireless Links
Authors:	Lakshmikanth Guntupalli†, Jorge Martinez-Bauset‡, and Frank Y. Li†
Affiliation:	†Dept. of Information and Communication Technology, University of Agder (UiA), N-4898 Grimstad, Norway ‡Dept. of Communications, Universitat Politècnica de València (UPV), 46022 València, Spain
Journal:	To be decided

Appendix B

Performance of Duty-Cycled WSN with Aggregated Packet Transmission in Error-Prone Wireless Links

Abstract — **Two packet transmission schemes are commonly deployed in duty-cycled wireless sensor networks, i.e., single packet transmission (SPT) and aggregated packet transmission (APT). This paper evaluates the performance of both transmission schemes under error-prone channel conditions, while most of the existing models are based on an error-free channel assumption. We propose a discrete-time Markov chain model to investigate the impact that transmission failures due to channel impairments have on the performance of SPT and APT. Moreover, we analyze packet loss, delay, throughput, energy consumption, and energy efficiency experienced by SPT and APT under error-free and error-prone channel conditions. Numerical results obtained from both analytical model and discrete-event based simulations reveal to which extent channel conditions may affect the performance of such networks. Furthermore, we show that APT outperforms SPT even over error-prone channels.**

I. Introduction

High energy efficiency and short packet delivery delay are salient features for the design of efficient medium access control (MAC) protocols in battery-powered wireless sensor networks (WSNs). A popular approach to reduce energy consumption is to deploy duty-cycling (DC). This mechanism allows to organize the operation of the network in cycles, where sensors wake up for packet transmission or reception, and sleep for the rest of the cycle. In typical duty-cycled WSNs, single packet transmission (SPT) is employed, meaning that only one packet is transmitted per cycle when nodes get access to the medium. On the contrary, when aggregated packet transmission (APT) is used, a node might transmit multiple packets together (forming a *frame*) per cycle. Consequently, APT has the potential to increase energy efficiency and reduce packet delay.

In [1], we proposed an analytical model to evaluate the performance of an APT scheme operating over a synchronous duty-cycled MAC protocol like S-MAC. The developed model therein was a three-dimensional (3D) discrete-

time Markov chain (DTMC), with each dimension representing the number of packets in the queue of a reference node, the number of retransmissions experienced by the packet (SPT) or *frame* (APT) at the head of the queue of the reference node, and the number of active nodes in the network (those with a non-empty queue). Unlike many other existing models for duty-cycled MAC protocols, our 3D model considers also the dependence among the nodes by integrating the time evolution of the number of active nodes in the network into the model. In addition, a simpler two-dimensional (2D) DTMC was also developed in [1] to model scenarios where the vast majority of packet (frame) losses are recovered by retransmissions. However, the 2D and 3D DTMC models developed in our previous work [1] [2], and also those proposed by many other related studies [3] [4] were conceived under the assumption that the channel was error-free.

As SPT is a particular case of APT, where only one packet is inserted into a frame for transmission, we use hereafter a frame instead of a packet when referring to a transmission data unit. In reality, wireless channels are prone to errors and transmission failures may happen due to two reasons, i.e., collisions in the channel as well as poor channel conditions. In what follows, we refer to the first reason as collisions and the second reason as channel errors.

In this paper, we elaborate a four-dimensional (4D) DTMC model, that was briefly introduced in [1], and further investigate in-depth the impact that error-prone channels have on the performance of the SPT and APT schemes in synchronous DC WSNs. To do so, we integrate the 3D DTMC with a frame-level error model that describes the occurrence of errors in the channel as a burst of successful or failed transmission cycles. Based on the proposed 4D model, we develop expressions for throughput, delay, packet loss, energy consumption, and energy efficiency in WSNs operating over error-prone channels.

The rest of this paper is organized as follows. In Section II we develop the 4D DTMC model as an extension of the previous 3D model. The expressions for performance parameters are derived in Section III. In Section IV we present the numerical results obtained by the proposed analytical model and discrete-event simulations. Section V concludes the paper.

II. MODELING SPT/APT IN ERROR-PRONE CHANNELS

Consider a cluster of N source nodes in a DC WSN, where all nodes in the cluster can hear each other. All these nodes have homogeneous characteristics, and transmit frames towards a common destination node (sink) using a CSMA/CA contention-based scheme with RTS/CTS/DATA/ACK handshake for channel access. The buffer of any node can store up to Q packets. We select one of these nodes arbitrarily and refer to it as the a reference node (RN). Once a node wins access competition to the channel, it transmits a *frame* that aggregates up to F packets. If $F = 1$, the transmission is performed based on SPT. For $F > 1$, the APT scheme is adopted. However, a transmitted frame may not be correctly received due to either a collision or channel errors. To recover it, a node might perform up to R retransmissions.

A. Modeling of Frame-level Transmission Errors

As an example, assume that $X_n \in \{0,1\}$ is a discrete binary random process, where for the n-th frame $X_n = 0$ or $X_n = 1$ represents that its transmission was successful or failed, respectively. Then, sequences of consecutive '1s' represent channel error bursts, while sequences of consecutive '0s' represent time intervals of error-free channel operation. In this section we integrate such a channel behavior into the 3D DTMC that we proposed to model a WSN.

Among the different error models proposed to describe channel behavior, the *On*/*Off* model is a pragmatic one [5] [6]. It describes the holding times in the *On* and *Off* macro-states by a mixture of geometric distributions [5]. In the adopted model, *On* and *Off* represent the *loss* and *non-loss* macro-states respectively. By *loss* we refer to operating cycles where a frame transmitted will irremediably fail due to channel error. Whereas by *non-loss* we refer to cycles during which successful transmissions occur, provided that packets do not collide. This modeling approach captures both first- and second-order statistics accurately, and it is considered adequate to characterize wireless channels in practical scenarios [5].

To capture the burstiness of channel behavior, a simple yet effective model was proposed in [7]. There, a single state is used to represent the *loss* macro-state, while the *non-loss* macro-state is defined by multiple states. The model exhibits a self-similar behavior over a configurable (finite) range of time-

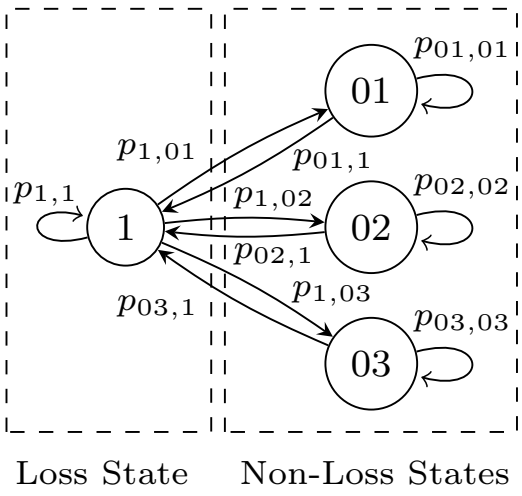

Figure AppxB.1: A frame-level error model for error-prone channels with one state in the *loss* macro-state and three states in the *non-loss* macro-state [1].

scales. It has three parameters, H, a and b. H determines the range of time-scales where the process can be considered as self-similar. Once H is set, the values of b and a are obtained such that they fit the fraction of cycles where the channel produces frame-level errors (frame error rate) $\rho_{\mathrm{FE}} = (1-1/b)/(1-1/b^H)$, and the average number of consecutive cycles where the channel produces frame-level errors (average error burst length) $E[B] = \left(\sum_{k=1}^{H-1} a^{-k}\right)^{-1}$, respectively. Its transition matrix is given by

$$\left[\begin{array}{c|cccc} 1-\sum_{k=1}^{H-1}\alpha^k & \alpha^1 & \alpha^2 & \cdots & \alpha^{H-1} \\ \hline 1-\beta & \beta & & & \\ 1-\beta^2 & & \beta^2 & & \\ \vdots & & & \ddots & \\ 1-\beta^{H-1} & & & & \beta^{H-1} \end{array}\right]. \qquad \text{(AppxB.1)}$$

where $\alpha = 1/a$ and $\beta = 1-(b/a)$. In this study, we consider three states in the *non-loss* macro-state, as shown in Fig. AppxB.1. Then, we have $H = 4$ and correspondingly the transition probabilities are given by, $p_{1,1} = 1 - \sum_{k=1}^{H-1} 1/a^k$ $p_{1,0m} = 1/a^m$, $p_{0m,1} = (b/a)^m$, and $p_{0m,0m} = 1-(b/a)^m$, where $m = 1,2,\ldots,H-1$.

B. A 4D DTMC Model for APT in Error-prone Channels

A state in the 3D DTMC proposed to model the behavior of a WSN is represented by (i,k,r), where i is the number of packets in the queue of the RN, $i \leq Q$, k is the number of active nodes in the network other than the

RN, $k \leq N-1$, and r is the number of retransmissions experienced by the frame at the head of the queue of the RN, $r \leq R$ [1]. In the new 4D DTMC proposed in this paper, the state vector is defined by (i,k,r,e), where the new element e defines the channel state, as described by Fig. AppxB.1. When $e=1$, a transmitted frame will not be received correctly due to channel errors (regardless of a collision occurred or not). Whereas when $e=\{01,02,03\}$, the transmitted frames will be received successfully, provided that they did not collide. For expression simplicity and assuming that $H=4$, we enumerate the e states as $\{1,2,3,4\}$, where states $\{2,3,4\}$ correspond to $\{01,02,03\}$ in Fig. AppxB.1.

Based on the above state definitions, we are able to construct two state transition tables, one that defines the error-free (NE) channel behavior and the another one for the error-prone (E) channel. Due to the page limit, we do not reiterate these tables here. A reader can refer to Table II and Table VI in [1] for the definition of these transition probabilities. Accordingly, we can define two transition matrices, $\boldsymbol{P}_{NE}$ and $\boldsymbol{P}_{E}$, that aggregate these transition probabilities.

Let $\boldsymbol{P}$ be the new transition matrix that defines the behavior of the 4D DTMC. As an example, it has the following block structure for $H=4$

$$\boldsymbol{P}=\left[\begin{array}{c|ccc} \boldsymbol{A_0} & \boldsymbol{A_1} & \boldsymbol{A_2} & \boldsymbol{A_3} \\ \hline \boldsymbol{B_1} & \boldsymbol{B_4} & \boldsymbol{0} & \boldsymbol{0} \\ \boldsymbol{B_2} & \boldsymbol{0} & \boldsymbol{B_5} & \boldsymbol{0} \\ \boldsymbol{B_3} & \boldsymbol{0} & \boldsymbol{0} & \boldsymbol{B_6} \end{array}\right]. \qquad \text{(AppxB.2)}$$

where $\boldsymbol{A_0}=p_{1,1}\boldsymbol{P}_E$, and $\boldsymbol{A_m}=p_{1,0m}\boldsymbol{P}_E$. Similarly, $\boldsymbol{B_m}=p_{0m,1}\boldsymbol{P}_{NE}$, $\boldsymbol{B_n}=p_{0m,0m}\boldsymbol{P}_{NE}$, $m=1,2,3$, $n=m+3$.

The steady-state probabilities $\boldsymbol{\pi}=[\pi(i,k,r,e)]$ can be obtained by solving the set of linear equations $\boldsymbol{\pi P}=\boldsymbol{\pi}$, with $\boldsymbol{\pi e}=\boldsymbol{1}$, where $\boldsymbol{e}$ is a column vector of ones.

III. Performance Expressions under the 4D Model

Once $\boldsymbol{\pi}$ is obtained, we can derive expressions for delay, throughput, packet loss and energy consumption. To do so, we need to determine first the successful transmission probability and the probability that the queue is emptied

after a successful transmission. For additional details about the notation used, please refer to Table I in [1].

A. Successful Transmission Probability

Denote by π_i the stationary probability of finding i packets at the queue of the RN. It is given by,

$$\pi_i = \sum_{k=0}^{K} \sum_{r=0}^{R} \sum_{e=1}^{4} \pi(i,k,r,e)\,. \qquad \text{(AppxB.3)}$$

Let P_s be the average probability that a node transmits a frame successfully in a randomly selected cycle, conditioned on it being active. It is given by,

$$P_s = \frac{1}{G} \sum_{i=1}^{Q} \sum_{k=0}^{K} \sum_{r=0}^{R} \sum_{e=2}^{4} \pi\,(i,k,r,e) \cdot P_{s,k}\,, \qquad \text{(AppxB.4)}$$

where $G = \sum_{i=1}^{Q} \sum_{k=0}^{K} \sum_{r=0}^{R} \sum_{e=1}^{4} \pi\,(i,k,r,e)$ and $P_{s,k}$ is the probability that the RN transmits without collision when contending with the other k active nodes. Recall that when $e = 1$ transmissions will fail due channel errors, even though no collision happened.

Let P_e be the probability that the queue of an active node becomes empty after a successful transmission. Then, $P_e = P_s A_0 \sum_{i=1}^{F} \pi_i / \left[P_s\,(1-\pi_0)\right]$, where A_0 is the probability that no packet arrived during the considered cycle, and F is the maximum number of packets that can be aggregated per *frame*.

Note that transition probabilities in $\boldsymbol{P}_{NE}$ are given as a function of P_e. Then, the steady-state probabilities $\boldsymbol{\pi}$ are obtained as the solution of a fixed-point equation.

B. Queuing Delay

Let us denote by D the average queuing delay of a packet, from its arrival until it is successfully delivered, i.e., it is transmitted without collision and channel error. Then, by Little's law, D (in cycles) is equal to the average number of packets in the queue, N_{av}, divided by the average number of packets that entered the queue per cycle, γ_a ,

$$D = N_{av}/\gamma_a = \sum_{i=0}^{Q} i\pi_i \Big/ \sum_{i=0}^{Q} b_i \pi_i \qquad \text{(AppxB.5)}$$

where b_i is the mean number of packets that entered the queue per cycle at state i, $b_0 = \sum_{q=0}^{Q} q \cdot A_q + Q \cdot A_{\geq Q+1}$, $b_i = \sum_{q=0}^{Q-i} q \cdot A_q + (Q-i+P_s) A_{\geq Q-i+1}$, $i > 0$, and π_i was given in Section III-A. Note that the last term of b_i is obtained from $((Q-i+1)P_s + (Q-i)(1-P_s))A_{\geq Q-i+1}$.

C. Throughput

The throughput a node achieves, denoted by η, is defined as the average number of packets it *successfully* delivers per cycle. Then,

$$\eta = \sum_{i=1}^{Q} \sum_{k=0}^{K} \sum_{r=0}^{R} \sum_{e=2}^{4} \alpha \cdot \pi(i,k,r,e) \cdot P_{s,k} . \qquad \text{(AppxB.6)}$$

given that $\alpha = min(i,F)$ packets can be aggregated in a frame, $1 \leq i \leq Q$, and a successful transmission happens when no collision occurs (with probability $P_{s,k}$) and the channel is in the *non-loss* state ($e > 1$).

With N nodes in the considered cluster, the total network throughput becomes $Th = N \cdot \eta$.

D. Packet Loss Probability

Retransmissions occur due to frame collisions, or failed reception of frames due to channel errors. Moreover, a frame also gets lost (discarded from the buffer) after R consecutive unsuccessful retransmissions. Denote by P_L^c the channel packet loss probability. It is given by,

$$P_L^c = \frac{1}{\gamma_a} \sum_{i=1}^{Q} \sum_{k=0}^{K} \sum_{e=2}^{4} \alpha \cdot \pi(i,k,R,e) \cdot P_{f,k} + \frac{1}{\gamma_a} \sum_{i=1}^{Q} \sum_{k=0}^{K} \alpha \cdot \pi(i,k,R,1) \cdot P_{sf,k} \qquad \text{(AppxB.7)}$$

where γ_a is the average number of packets that entered the queue of a node per cycle, $P_{f,k}$ is the probability that a frame transmitted by the RN collides when contending with the other $k \geq 1$ nodes, and $P_{sf,k}$ is the probability that the RN transmits a frame (with or without collision).

Note that losses can also occur due to buffer overflow. To calculate the total packet loss probability, P_L, overflow losses must be added to P_L^c. Given a packet arrival rate λ and a cycle length T, the mean number of packets lost per cycle (packet loss rate) is $\lambda T - [(1-P_L^c)\gamma_a]$. Then, $P_L = 1 - [(1-P_L^c)\gamma_a / \lambda T]$.

E. Energy Consumption and Energy Efficiency

The average energy consumed by the RN during the data period of a cycle is given by,

$$E_d^* = \sum_{k=0}^{N} E_{d,k} \cdot \pi'_{ne,k} + \widetilde{E}_{d,k} \cdot \pi'_{e,k}, \qquad \text{(AppxB.8)}$$

where $\pi'_{e,k}$ and $\pi'_{ne,k}$ are the stationary probability of finding k active nodes in the network during cycles in the *loss* and *non-loss* macro-states, respectively. They are given by, $\pi'_{e,k} = \sum_{i=1}^{Q}\sum_{r=0}^{R}\pi(i,k-1,r,1) + \pi(0,k,0,1)$, $\pi'_{ne,k} = \sum_{i=1}^{Q}\sum_{r=0}^{R}\sum_{e=2}^{4}\pi(i,k-1,r,e) + \sum_{e=2}^{4}\pi(0,k,0,e)$, for $1 \le k \le N-1$. For $k=0$ and $k=N$, we have $\pi'_{e,0} = \pi(0,0,0,1)$, $\pi'_{ne,0} = \sum_{e=2}^{4}\pi(0,0,0,e)$, $\pi'_{e,N} = \sum_{i=1}^{Q}\sum_{r=0}^{R}\pi(i,N-1,r,1)$, $\pi'_{ne,N} = \sum_{i=1}^{Q}\sum_{r=0}^{R}\sum_{e=2}^{4}\pi(i,N-1,r,e)$.

Let $E_{d,k+1}$ and $\widetilde{E}_{d,k+1}$ be the average energy consumed by the RN when it contends with the other $k \ge 1$ nodes, during the *data* period of cycles in the *non-loss* and *loss* macro-state, respectively. $E_{d,k+1}$ was given in [1] as

$$\begin{aligned} E_{d,k+1} = {} & q_{1,k}P_{s,k} \cdot \left[E_{txs,k} + \left(4D_p + BT_{s,k}\right) \cdot P_{rx}\right] \\ & + q_{1,k}P_{f,k} \cdot \left[E_{txf} + \left(2D_p + BT_{f,k}\right) \cdot P_{rx}\right] \\ & + q_{2,k}P_{s,k}\left[E_{oh} + \left(D_p + BT_{s,k}\right) \cdot P_{rx}\right] \\ & + q_{3,k} \cdot \left[E_{oh} + \left(D_p + BT_{f,k}\right) \cdot P_{rx}\right], \end{aligned} \qquad \text{(AppxB.9)}$$

where D_p is the one-way propagation delay, and $BT_{s,k}$ and $BT_{f,k}$ are the RN average backoff window lengths in cycles where the RN contends with other k nodes and its transmission occurs without and with collision, respectively. Note that $E_{txs,k} = (t_{RTS} + f_k \cdot t_{DATA}) \cdot P_{tx} + (t_{CTS} + t_{ACK}) \cdot P_{rx}$, $E_{txf} = t_{RTS} \cdot P_{tx} + t_{CTS} \cdot P_{rx}$, $\quad E_{oh} = t_{RTS} \cdot P_{rx}$, where t_{RTS}, t_{DATA}, t_{CTS} and t_{ACK}, are the corresponding packet transmission times, P_{tx} (P_{rx}) is the transmission (reception) power, $f_k = (1/G_k)\sum_{i=1}^{Q}\sum_{r=0}^{R}\sum_{e=2}^{4}\alpha \cdot \pi(i,k,r,e)$, $\alpha = min(i,F)$, and $G_k = \sum_{i=1}^{Q}\sum_{r=0}^{R}\sum_{e=2}^{4}\pi(i,k,r,e)$. Clearly f_k is the mean frame length of those frames transmitted in *non-loss* cycles where the RN contends with other k nodes.

On the other hand,

$$\begin{aligned}\widetilde{E}_{d,k+1} = {} & q_{1,k}P_{s,k} \cdot \left[E_{txf} + \left(2D_p + BT_{s,k}\right) \cdot P_{rx}\right] \\ & + q_{1,k}P_{f,k} \cdot \left[E_{txf} + \left(2D_p + BT_{f,k}\right) \cdot P_{rx}\right] \\ & + q_{2,k}P_{s,k} \left[E_{oh} + \left(D_p + BT_{s,k}\right) \cdot P_{rx}\right] \\ & + q_{3,k} \cdot \left[E_{oh} + \left(D_p + BT_{f,k}\right) \cdot P_{rx}\right] . \end{aligned} \tag{AppxB.10}$$

In [1] we explained that nodes need to keep *awake* during the *sleep* period of some cycles in order to avoid missing synchronization messages. Therein, we distinguished between *normal* cycles, where nodes *sleep*, and *awake* cycles. The average energy consumed during the *sleep* period of a cycle when the node is *awake* is determined by

$$E^*_{aw} = \sum_{k=0}^{N} E_{aw,k} \cdot \pi'_{ne,k} + \widetilde{E}_{aw,k} \cdot \pi'_{e,k} , \tag{AppxB.11}$$

where $E_{aw,k+1}$ and $\widetilde{E}_{aw,k+1}$ are the average energy consumed by the RN in cycles with other $k \geq 1$ active nodes, during the *sleep* period of *awake* cycles in the *non-loss* and *loss* macro-state, respectively. $E_{aw,k+1}$ was given in [1], while

$$\begin{aligned}\widetilde{E}_{aw,k+1} = {} & q_{1,k}P_{s,k} \cdot \left[\left(T_{cycle} - T_{sync} - T_{de,s,k}\right) \cdot P_{rx}\right] \\ & + q_{1,k}P_{f,k} \cdot \left[\left(T_{cycle} - T_{sync} - T_{d,f,k}\right) \cdot P_{rx}\right] \\ & + q_{2,k}P_{s,k} \left[\left(T_{cycle} - T_{sync} - T_{d,os,k}\right) \cdot P_{rx}\right] \\ & + q_{3,k} \cdot \left[\left(T_{cycle} - T_{sync} - T_{d,of,k}\right) \cdot P_{rx}\right] , \end{aligned} \tag{AppxB.12}$$

where $T_{de,s,k} = t_{RTS} + t_{CTS} + 2D_p + BT_{s,k}$, $T_{d,f,k} = t_{RTS} + t_{CTS} + 2D_p + BT_{f,k}$, $T_{d,os,k} = t_{RTS} + D_p + BT_{s,k}$, and $T_{d,of,k} = t_{RTS} + D_p + BT_{f,k}$. These terms define the duration of the data period for different cycle configurations, when the RN contends with other k nodes.

Also, $\widetilde{E}_{aw,1} = q_{1,0} \cdot \left[\left(T_{cycle} - T_{sync} - T_{de,0}\right) \cdot P_{rx}\right] + q_{2,0} \left[\left(T_{cycle} - T_{sync} - T_{oh,0}\right) \cdot P_{rx}\right]$, and $\widetilde{E}_{aw,0} = \left[\left(T_{cycle} - T_{sync} - T_{oh,idle}\right) \cdot P_{rx}\right]$, where $T_{de,0} = t_{RTS} + t_{CTS} + 2D_p + (W-1)/2$, $T_{oh,0} = t_{RTS} + D_p + (W-1)/2$, and $T_{oh,idle} = W + t_{RTS} + D_p$. Note that a node has to overhear the medium during the whole backoff window (W) in cycles in which there are no active nodes in the net-

work.

Similarly, the average energy consumed during the *sleep* period of a cycle in *normal* cycles is given by

$$E^*_{nr} = \sum_{k=0}^{N} E_{nr,k} \cdot \pi'_{ne,k} + \widetilde{E}_{nr,k} \cdot \pi'_{e,k}\,, \qquad \text{(AppxB.13)}$$

where, conditioned on cycles in which the RN and other $k \geq 1$ nodes are active, $E_{nr,k+1}$ and $\widetilde{E}_{nr,k+1}$ are the average energy consumed by the RN during the *sleep* period of a *normal* cycle under the *non-loss* and *loss* macro-state, respectively. $E_{nr,k+1}$ was given in [1], while $\widetilde{E}_{nr,k}$ can be obtained by replacing P_{rx} with the sleep power level, P_{sl} , in (AppxB.12) .

Then, the average energy consumption during the *sleep* period of a cycle is obtained by

$$E^*_{sl} = \frac{E^*_{nr} \cdot N_{sc} \cdot (N_{aw} - 1) + E^*_{aw} \cdot N_{sc}}{N_{sc} \cdot N_{aw}}\,. \qquad \text{(AppxB.14)}$$

Consequently, the total average energy consumed by the RN in a cycle is obtained by

$$E^* = E_{sc} + E^*_d + E^*_{sl}\,. \qquad \text{(AppxB.15)}$$

where E_{sc} is the energy consumed during the *sync* period of a cycle, and was given in [1].

Finally, the energy efficiency, ξ, expressed as the number of bytes successfully transmitted in a cycle per energy unit consumed in a cycle, is given by $\xi = \eta \cdot S/E^*$, where S is the packet size.

IV. Simulations and Numerical Results

Consider a network with $N = 15$ nodes, each with a queue capacity of $Q = 10$ packets, and with a maximum number of $R = 10$ allowed retransmissions. The packet arrival rate varies from $\lambda = 0.5$ to $\lambda = 2.5$ packets/s. The other network and MAC parameters are configured as in [1], unless otherwise stated. To investigate the impact of channel impairment on network performance, we set $H = 4$ and consider two frame error rates (FERs), $\rho_{\text{FE}} = 5\%$ and 15% . Correspondingly, the other parameters for the frame-error model

are configured as: i) $a = 2$ and $b = 0.4418$ to obtain $E[B] = 1.143$ (for FER $= 5\%$); and ii) $a = 2.92$ and $b = 0.7388$ to obtain $E[B] = 2.003$ (for FER $= 15\%$).

A. Model Validation and Performance over Wireless Links

To assess the preciseness of the developed model, we plot in all figures both the analytical results obtained from the solution of the 4D DTMC model, and the results obtained from discrete-event based simulations. Evidently, these two sets of results match very well with each other, confirming that the analytical model is sufficiently accurate.

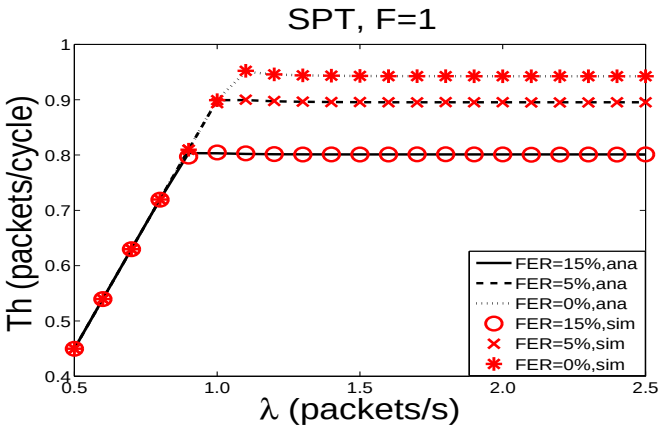

Figure AppxB.2: Total throughput for SPT ($F = 1$) under different FERs.

Clearly, as the FER increases, the number of cycles required to successfully transmit a packet increases, and therefore the service rate decreases. This effect has two important consequences. First, the higher the FER, the lower the throughput, as observed in Fig. AppxB.2 where the SPT scheme is deployed. Second, given an equal arrival rate, decreasing the service rate (a higher FER) leads to a higher offered load, inducing earlier network saturation. For example in Fig. AppxB.2, it saturates at $\lambda = 0.9$ packet/s when FER $= 15\%$, whereas in an error-free channel the saturation point is reached at 1.1 packet/s .

Fig. AppxB.3 shows the mean energy consumed per cycle by a node deploying SPT under different channel conditions. Clearly, two distinguishable operation zones can be observed: unsaturated and saturated network. In the unsaturated part, the packet arrival rate λ is low and there are no active nodes in many cycles. This leads to frequent occurrences of idle listening cycles, where nodes have to listen for the whole backoff window before they realize

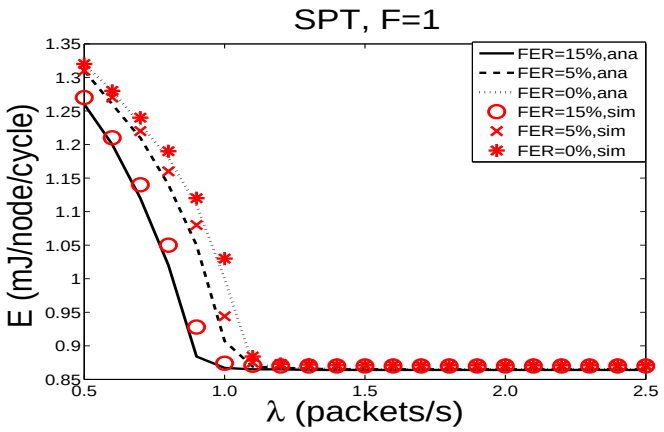

Figure AppxB.3: Mean energy consumption per node and cycle for SPT ($F = 1$) under different FERs.

that there were no nodes intending to transmit, and this procedure wastes energy. As the network load increases, the energy consumption decreases, since idle listening cycles diminish. When the network saturates, the consumed energy level stabilizes, as most of the nodes are active in every cycle. Note that for a fixed λ, the energy consumption decreases as the FER increases, as more active nodes are found per cycle.

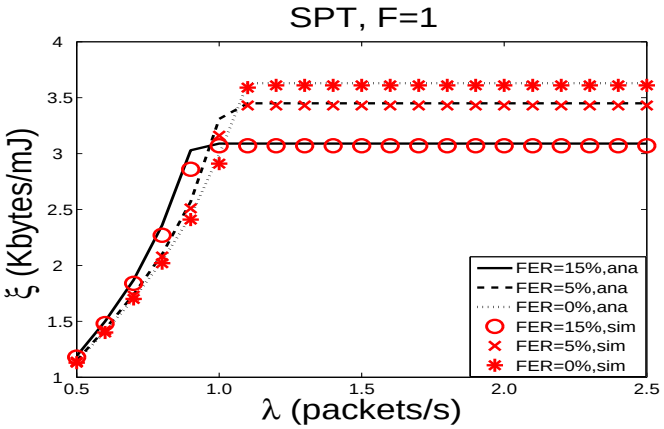

Figure AppxB.4: Energy efficiency for SPT ($F = 1$) under different FERs.

The energy efficiency is shown in Fig. AppxB.4. We observe here again the same two distinct operation zones that appeared for the consumed energy shown in Fig. AppxB.3. In the unsaturated part, the efficiency increases with the FER. Clearly, in this zone, the impact of idle listening is more severe than the impact of the energy consumed due to retransmissions. Whereas in the saturated part, an opposite trend is observed.

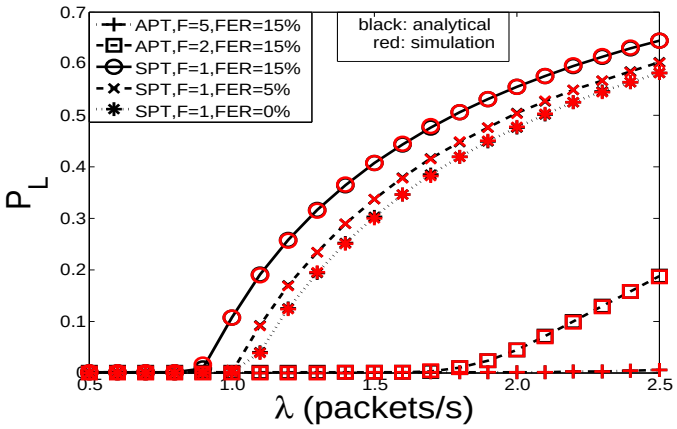

Figure AppxB.5: Total packet loss probability for different values of F and FER.

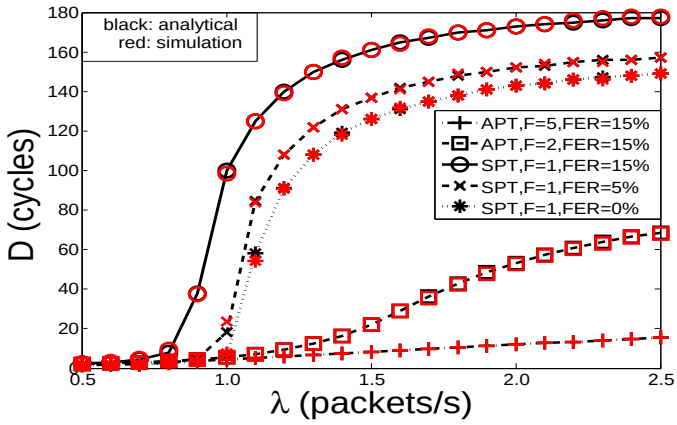

Figure AppxB.6: Mean packet delay for different values of F and FER.

B. Performance Comparison: APT versus SPT

When comparing the performance of both transmission schemes, APT exhibits its superiority in terms of throughput, packet loss, delay and energy efficiency. For a fixed λ, the mean number of packets in the queue and the mean packet delay, in general increase with the FER. However, under the same channel condition, better performance is achieved with a larger F, as shown in Figs. AppxB.5, AppxB.6, and AppxB.7. Then, provided that the maximum frame size is within the limit allowed by layer 2, the larger the F, the lower the total packet loss (mainly due to buffer overflow) and the shorter the delay. At the same time, higher energy efficiency is achieved by deploying APT (increasing F). For a given F, better channel condition would result in lower packet loss and shorter delay.

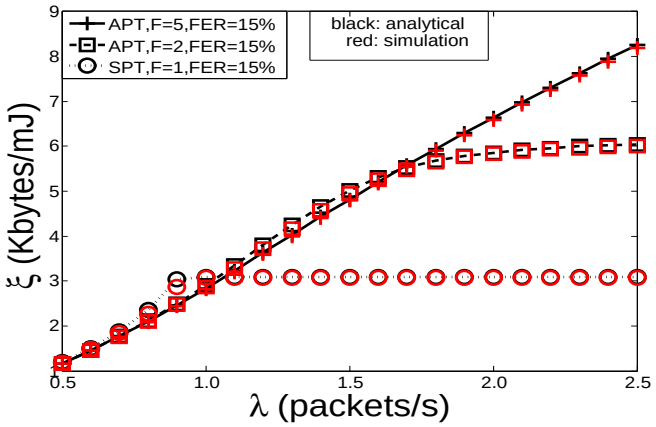

Figure AppxB.7: Energy efficiency for different values of F and FER.

V. Conclusions

In this paper, we developed a 4D DTMC to model the behavior of synchronous duty-cycled MAC protocols for WSNs with error-prone wireless channels. In addition to tracking the number of active nodes in the network, the queue length, and the number of retransmissions, we integrate a macro-state frame-error channel model into the DTMC to reflect the effect of transmission failures due to poor channel conditions. Furthermore, closed-form expressions for throughput, average queuing delay, packet loss, energy consumption and energy efficiency are derived. The numerical results based on both analysis and simulations confirm the accuracy of the model and reveal the impact that transmission errors have on network performance, as well as the benefits brought by the APT scheme in both error-free and error-prone environments.

References

[1] L. Guntupalli, J. Martinez-Bauset, F. Y. Li, and M. A. Weitnauer, “Aggregated packet transmission in duty-cycled WSNs: Modeling and performance evaluation," *IEEE Trans. Veh. Technol.*, Early access available in IEEEXplore, DOI:10.1109/TVT.2016.2536686, Mar. 2016.

[2] J. Martinez-Bauset, L. Guntupalli, and F. Y. Li, “Performance analysis of synchronous duty-cycled MAC protocols," *IEEE Wireless Commun. Lett.*, vol. 4, no. 5, pp. 469-472, Oct. 2015.

[3] O. Yang and W. Heinzelman, “Modeling and performance analysis for duty-cycled MAC protocols in wireless sensor networks," *IEEE Trans. Mobile Comput.*, vol. 11, no. 6, pp. 905-921, Jun. 2012.

[4] F. Tong, L. Zheng, M. Ahmadi, M. Li, and J. Pan, “Modeling and analyzing duty-cycling, pipelined-scheduling MACs for linear sensor networks," *IEEE Trans. Veh. Technol.*, vol. 65, no. 4, pp. 2608-2620, Apr. 2016.

[5] P. Ji, B. Liu, D. Towsley, Z. Ge, and J. Kurose, “Modeling frame-level errors in GSM wireless channels," *Perform. Eval.*, vol. 55, no. 1, pp. 165-181, Jan. 2004.

[6] D. Striccoli, G. Boggia, and A. Grieco, “A Markov model for characterizing IEEE 802.15. 4 MAC layer in noisy environments," *IEEE Trans. Ind. Electron.*, vol. 62, no. 8, pp. 5133-5142, Jun. 2015.

[7] S. Robert and J.-Y. Le Boudec, “New models for pseudo self-similar traffic," *Perform. Eval.*, vol. 30, no. 1, pp. 57-68, Jul. 1997.